MECHANISMS OF ACID INFLUX IN THE CAROTID BODY TYPE I CELL

KE - LI TSAI

Keble College

Thesis submitted for the degree of Doctor of Philosophy

University of Oxford

University Laboratory of Physiology

Trinity Term 2003



ABSTRACT

Mechanisms of Acid Influx in the Carotid Body Type I Cell

KE-LI TSAI

Keble College

A thesis submitted for the degree of Doctor of Philosophy at Oxford University

Trinity Term 2003

Type I cells of the carotid body play a major role in acid chemoreception. Extracellular acidosis causes membrane depolarisation, Ca^{2+} influx and neurosecretion in the type I cell. A previous study has shown that pH_i in the type I cell is very sensitive to changes of pH_o, and intracellular acidification is a key step in the signalling pathway for acid chemoreception. This thesis investigates the mechanism responsible for mediating acid influx during isocapnic extracellular acidosis.

Type I cells were enzymically isolated from carotid bodies obtained from neonatal rats. pH_i was determined by microspectrofluorimetry, using pH-sensitive fluorescent dye carboxy-SNARF-1. My results show that there are two acid influx pathways. At resting pH_i, Cl^--HCO_3^- exchange accounts for over 70% of acid influx in response to extracellular acidosis. The remaining 30% of acid influx is mediated by an unidentified mechanism, which does not require either Cl^- or HCO_3^-. I have also demonstrated that, the second pathway is an acid loading mechanism enhanced by a fall in pH_o, rather than an existing background acid loading unmasked by the inhibition of acid extruder.

Although 200 μM DIDS inhibited Cl^-_o-free induced acid efflux mediated by reversed mode of Cl^--HCO_3^- exchange as well as the acid influx induced by alkali load, it had no effect on the acid influx in response to acid challenge. The difference in DIDS effect to block acid influx is probably due to difference in Cl^--HCO_3^- exchangers. I proposed that the Cl^--HCO_3^- exchange system in the type I cell comprises two distinct exchanger populations. One of them is DIDS sensitive and activated by high pH_i, while the other is DIDS insensitive and activated by low pH_o.

The pH_i and pH_o sensitivity of both acid influx pathways have also been characterised. It is found that the unidentified HCO_3^--independent acid loading mechanism is activated by H_o^+ while virtually pH_i-independent. In addition, the activity of Cl^--HCO_3^- exchange system is very sensitive to pH_i and pH_o, with pK_a^i and pK_a^o values close to resting pH_i and pH_o. Thus any shift of pH_i or pH_o from the normal resting range will produce significant changes in exchange activity, leading to changes in acid flux into the cell. In this way, the Cl^--HCO_3^- exchange system serves as a link for transducing acidic pH_o into parallel acidification in pH_i in the type I cell.

Acknowledgement

Foremost I would like to express my sincere gratitude to my supervisors, Professor Richard Vaughan-Jones and Dr. Keith Buckler, both gave me patient support and invaluable advice during the course of this study. Their expertise and experience enabled me to establish a broad and solid basis of knowledge in the field of cell physiology.

I would like to give thanks to Dr. Mei-Lin Wu for her encouragement and for recommending me to pursue DPhil degree in Oxford. To Dr. Shih-Hurng Loh for his hospitality while he was in Oxford. Also to Mr. John Halfacree, who helped me on the manuscript and gave me much friendship.

Of course, a very special tribute must go to my parents. Without their long term emotional and financial support, I could not have finished my study. I am indebted to my wife, for her persistent inspiration and appreciation. She has been my mainstay over these years. I also thank my sister for her encouraging international phone calls.

To all members of the "Professor Vaughan-Jones group" and "Dr. Buckler group", I was delighted to have you around. Many thanks to Mr. Pawel Swietach for his companionship and humour, which gave me a lot of emotional uplift. To Dr. Beatrice Williams and Dr. Chris Wyatt for their help in cell isolation. To Dr. Andrew Stewart for his guidance on the use of the set-up when I first came to the lab. In addition, past and present co-workers in both groups, particularly Anna, Ruth, Emma, Darren, Neelam, Max and Alessandra all deserve big thanks.

Finally, friends from Oxford University Taiwanese Students' Society were an important source of support in my life in Oxford. I thank you all.

The present work was funded by Overseas Research Student (ORS) Awards Scheme and Oxford Bursaries.

Contents

Abstract

Acknowledgement

Contents *i*

List of Figures *viii*

List of Tables *x*

Abbreviations *xi*

Chapter 1

General Introduction *1*

Part A: Respiratory chemoreceptors: an overview *1*

1. Central chemoreceptor *3*
2. Carotid chemoreceptor *3*
3. Aortic chemoreceptor *4*

Part B: Type I Cells Are Principal Chemoreceptor Cells in the Carotid Body *5*

Anatomy and Histology of Carotid Body *5*

Carotid Body Type I Cells Are Chemoreceptor Cells *9*

1. Acetylcholine hypothesis *10*
2. Dopamine hypothesis *11*
3. ATP hypothesis *12*

Part C. The Signalling Pathways for Chemoreception in Type I Cells *14*

Common signalling pathway for hypoxia and acidosis *14*

Oxygen Chemoreception in Type I Cells *14*

1. Metabolic hypothesis *15*
2. Reactive oxygen species hypothesis *15*

3. K^+ channel hypothesis *17*

Acid Chemoreception in Type I Cells *17*

1. Na^+-Ca^{2+} exchanger hypothesis *17*
2. Membrane depolarisation hypothesis *17*

Part D. The Relationship between pH_i and pH_o in Type I Cells *20*

The pH_o sensitivity of pH_i in type I cells *25*

Dynamic Balance of pH_i *28*

Part E. Acid-equivalent Transport Systems and Their Roles in Type I Cells *29*

General Introduction to Acid-equivalent Transport Systems *29*

1. Na^+-H^+ exchange (NHE) *30*
2. Cl^--HCO_3^- exchange (AE) *32*
3. Na^+-dependent Cl^--HCO_3^- exchange (NCBE) *35*
4. Na^+-HCO_3^- cotransport (NBC) *36*
5. HCO_3^- channel *40*
6. H^+ channel *40*
7. K^+-H^+ transporter *41*
8. V-type H^+ ATPase *42*
9. Other acid-equivalent transporters *43*

Acid-equivalent Transport Systems in Type I Cells *43*

1. Na^+-H^+ exchange *43*
2. Cl^--HCO_3^- exchange *44*
3. Na^+-dependent Cl^--HCO_3^- exchange *44*
4. HCO_3^- channel *44*
5. K^+-H^+ exchanger *45*

Summary of Introduction *46*

The Aims of this Thesis *47*

Chapter 2

Materials and Methods *48*

Cell Isolation *48*

Solutions *50*

Drugs *52*

Superfusion Apparatus *52*

Measurement of Intracellular pH *53*

Microspectrofluorimetry *53*

Loading carboxy-SNARF-1 into type I cells *54*

Microspectrofluorimetry set-up *55*

In situ calibration of pH_i measurements *56*

Decontamination of the superfusion apparatus *57*

Experimental Alteration of pH_i *58*

Production of intracellular acidosis by ammonium pre-pulse technique *58*

Production of intracellular alkalosis by acetate pre-pulse technique *59*

Analyses of Net Acid Fluxes *60*

Statistics *62*

Chapter 3

The Dual Acid Influx Pathways in the Carotid Body Type I Cell *63*

Introduction *63*

Methods *65*

General Methods *65*

Solutions *65*

Cell Membrane Depolarisation by High K^+_o Treatment *70*

Drugs *70*

Results *71*

I. HCO_3^--dependent and Cl^--dependent acid influx pathway: Cl^--HCO_3^- exchange *71*

Acid loading induced by isocapnic acidosis *71*

HCO_3^--dependence of acid loading *71*

Cl^--dependence of acid loading *72*

The major acid loading mechanism is both HCO_3^--dependent and Cl^--dependent *73*

Acid loading mechanism is Na^+-independent *74*

Does HCO_3^- channel play a significant role in acid influx? *74*

The major acid influx pathway: Cl^--HCO_3^- exchange *75*

II. HCO_3^--independent and Cl^--independent acid influx pathway: an unknown mechanism *75*

Discussion *78*

I. HCO_3^--dependent and Cl^--dependent acid influx pathway: Cl^--HCO_3^- exchange *79*

II. HCO_3^--independent and Cl^--independent acid influx pathway: an unknown mechanism *82*

1. H^+ channel *83*
2. Ca^{2+}-ATPase *84*

Chapter 4

The Effect of DIDS upon Cl^--HCO_3^- Exchange in the Carotid Body Type I Cell *85*

Introduction *85*

Methods *87*

General Methods *87*

Solutions *87*

Drugs *87*

Results *88*

Alkalosis induced by Cl^-_o-removal is inhibited by DIDS *88*

Acid loading is insensitive to DIDS *88*

DIDS insensitivity of acid loading is not caused by acidic pH_o *90*

DIDS insensitivity of acid loading is not caused by the presence of Cl^-_o *90*

DIDS insensitivity of acid loading is not caused by combined high H^+_o and normal Cl^-_o *92*

The rate of pH_i recovery from alkali load is reduced by DIDS *93*

Cl^--free induced alkalosis is still present under HCO_3^--free conditions *94*

Discussion *94*

DIDS insensitivity of acid loading *94*

DIDS inhibition of Cl^-_o-induced alkalosis is irreversible *95*

DIDS insensitivity of acid influx on the Cl^--HCO_3^- exchanger *96*

Possible explanations for the DIDS insensitivity of acid influx *97*

1. Two distinct exchanger populations *97*
2. Unidirectional inhibition of DIDS *97*

Hypothesis: two distinct Cl^--HCO_3^- exchangers with different DIDS and pH sensitivity *98*

Chapter 5

Characterisation of pH_i and pH_o Sensitivity of Acid Influx in the Carotid Body Type I Cell *101*

Introduction *101*

Methods *102*

General Methods *102*

Solutions *103*

Determination of Acid Influx at Different pH_i During Acid Loading *103*

Curve Fitting and Data Handling *103*

Results *104*

Effect of pH_o on acid loading in CO_2/HCO_3^--buffered solution *104*

Effect of pH_o upon acid loading in HEPES-buffered solution *105*

Effect of pH_o upon Cl^--HCO_3^- exchange-mediated acid loading *106*

pH_i and pH_o sensitivity of Cl^--HCO_3^- exchange activity *106*

pH_i and pH_o sensitivity of HCO_3^--independent acid loading *107*

Discussion *109*

Determination of acid influx rates *109*

pH_i and pH_o sensitivity of Cl^--HCO_3^- exchange system in type I cells *111*

pH_i and pH_o sensitivity of Cl^--HCO_3^- exchange in other cell types *112*

pK_a^i and pK_a^o for Cl^--HCO_3^- exchanger and its physiological significance *114*

pH_i and pH_o sensitivity of HCO_3^--independent acid influx pathway in the type I cell *115*

Modelling acid fluxes during acid loading *115*

Chapter 6

General Discussion *117*

The major acid influx pathway: Cl^--HCO_3^- exchanger *117*

DIDS insensitivity of acid influx *118*

Two types of Cl^--HCO_3^- exchanger in the type I cell *120*

The minor acid influx pathway: an unknown mechanism *122*

1. H^+ channel *123*
2. Ca^{2+}-ATPase *123*

Integrated kinetic model for pH_i-pH_o relationship in the type I cell *124*

Comparison with other acid sensing cells *125*

Future directions of investigation *126*

Appendix I

Effect of Hoe694 on Na^+-H^+ Exchanger in the Carotid Body Type I Cell *128*

Introduction *128*

Methods *129*

General Methods *129*

Solutions *129*

Drugs *130*

Curve Fitting and Data Handling *130*

Results *130*

Dose-dependent inhibition of Na^+-H^+ exchanger by Hoe694 *130*

Does NHE operate in reverse mode in when Na^+_o is removed? *132*

Discussion *133*

Appendix II

Ca^{2+}_o-dependent Intracellular Acidosis Induced by High K^+_o in the Carotid Body Type I Cell *135*

Introduction *135*

Methods *136*

General Methods *136*

Solutions *136*

Drugs *137*

Results *138*

High K^+_o-induced acid loading *138*

Ca^{2+}_o dependency of High K^+_o-induced acid loading *138*

Discussion *139*

References *143*

List of Figures

Figure 1. 1 Diagrammatic representation of the carotid body (A) and its glomoid (B)

Figure 1. 2 Membrane depolarisation model of acid chemosensing pathway

Figure 1. 3 Schematic representation showing the concept of dynamic balance of pH_i

Figure 1. 4 Schematic representation showing HCO_3^- ion efflux has an equivalent effect on pH_i as H^+ ion influx

Figure 1. 5 Schematic diagram of the principle acid-equivalent transport systems found in animal cells

Figure 1. 6 Membrane topology of Cl^--HCO_3^- exchanger AE1

Figure 1. 7 Schematic diagram of acid-equivalent transport systems proposed to exist in carotid body type I cell

Figure 2. 1 Photograph of the experimental equipment used in the present study

Figure 2. 2 Schematic representation showing how the two-way tap works

Figure 2. 3 Uncorrected emission spectra for carboxy-SNARF-1 excited at 540nm

Figure 2. 4 Schematic diagram of the equipment used for recording carboxy-SNARF-1 fluorescence from carotid body type I cells

Figure 2. 5 Inducing acid load by ammonium pre-pulse technique (A) and inducing alkali load by acetate pre-pulse technique (B)

Figure 3. 1 Effect of changing pH_o upon pH_i in CO_2/HCO_3^--buffered solution

Figure 3. 2 Effect of HCO_3^- upon acid loading

Figure 3. 3 Effect of Cl^-_o removal upon acid loading in CO_2/HCO_3^--buffered solution

Figure 3. 4 Effect of Cl^-_o removal upon acid loading in HEPES-buffered solution

Figure 3. 5 Comparison of Cl^--independent acid influx in CO_2/HCO_3^--buffered solution and acid influx in HEPES-buffered solution

Figure 3. 6 Effect of Na^+_o removal upon acid loading in CO_2/HCO_3^--buffered solution

Figure 3. 7 Effect of high K^+_o upon acid loading in CO_2/HCO_3^--buffered solution

Figure 3. 8 Effect of high K^+_o treatment upon pH_i at pH_o 7.7 in CO_2/HCO_3^--buffered solution

Figure 3. 9 Comparison of acid influx rates in response to pH_o 6.4 acid challenge, Hoe694 and pH_o 6.4 acid challenge plus Hoe694 in HEPES-buffered solution

Figure 3.10 Comparison of acid influx rates in response to pH_o 6.4 acid challenge, Na^+-free and pH_o 6.4 acid challenge plus Na^+-free in HEPES-buffered solution

Figure 3.11 Schematic diagram illustrates the dual acid influx in the type I cell

Figure 3.12 Schematic diagram showing the analysis of respective contribution from different acid loading mechanisms

Figure 4. 1 Effect of Cl^-_o removal upon pH_i in CO_2/HCO_3^--buffered solution

Figure 4. 2 Effect of DIDS upon acid loading in CO_2/HCO_3^--buffered solution

Figure 4. 3 Effect of DIDS upon Cl^--independent acid loading in CO_2/HCO_3^--buffered solution

Figure 4. 4 Effect of DBDS upon acid loading in CO_2/HCO_3^--buffered solution

List of Figures

Figure 4. 5 Effect of pH_o 6.4 upon DIDS inhibition of Cl^--free induced alkalosis in CO_2/HCO_3^--buffered solution

Figure 4. 6 Effect of DIDS upon pH_i recovery from Cl^--free induced alkalosis in CO_2/HCO_3^--buffered solution

Figure 4. 7 Effect of DIDS upon acid loading after a period of Cl^--free pre-treatment in CO_2/HCO_3^--buffered solution

Figure 4. 8 Effect of DIDS upon Cl^--free induced alkalosis after a period of Cl^--free pre-treatment in CO_2/HCO_3^--buffered solution

Figure 4. 9 Combined effect of pH_o 6.4 and Cl^-_o upon DIDS inhibition of Cl^--free induced alkalosis in CO_2/HCO_3^--buffered solution

Figure 4.10 Effect of DIDS upon pH_i recovery from acetate prepusle in CO_2/HCO_3^--buffered solution

Figure 4.11 Effect of Cl^-_o removal upon pH_i, in the presence and absence of HCO_3^- ion

Figure 4.12 Two possible explanations for the failure of DIDS to block acid influx via Cl^--HCO_3^- exchange

Figure 4.13 Hypothesis for DIDS-sensitive and DIDS-insensitive acid influx via Cl^--HCO_3^- exchange

Figure 5. 1 Effect of varying pH_o on acid loading in CO_2/HCO_3^--buffered solution

Figure 5. 2 pH_i dependence of total acid influx at different pH_o measured in CO_2/HCO_3^--buffered solution

Figure 5. 3 Effect of varying pH_o on acid loading in HEPES-buffered solution

Figure 5. 4 pH_i dependence of HCO_3^--independent acid influx at different pH_o measured in HEPES-buffered solution

Figure 5. 5 pH_i dependence of HCO_3^--dependent acid influx at different pH_o

Figure 5. 6 pH_o dependence of HCO_3^--dependent acid influx at different pH_i

Figure 5. 7 Analysis of pH_i (A) and pH_o (B) dependence of HCO_3^--dependent acid influx

Figure 5. 8 pH_o dependence of HCO_3^--independent acid influx at different pH_i

Figure 5. 9 Analysis of pH_i (A) and pH_o (B) dependence of normalised HCO_3^--independent acid influx

Figure 5.10 Schematic diagram showing the pH_i and pH_o sensitivity of acid influx mechanism in the type I cell

Figure 5.11 Modelling HCO_3^--dependent and HCO_3^--independent acid influxes during acid loading

Figure 6. 1 Schematic diagram showing the summary of conclusions

Figure 6. 2 A proposed integrated model for the pH_o-pH_i relationship in the carotid body type I cell

Figure Ai.1 Effects of different doses of Hoe694 upon Na^+-H^+ exchanger activity measured from pH_i recovery rate from acid load

Figure Ai.2 Effects of different doses of Hoe694 upon Na^+-H^+ exchanger activity measured from acid extrusion rates after the re-addition of Na^+_o

Figure Ai.3 Effect of Hoe694 on Na^+-free induced intracellular acidification

Figure Aii.1 Effect of high K^+ treatment upon acid influx in HEPES-buffered solution

Figure Aii.2 Effect of high K^+ treatment upon acid influx in Ca^{2+}-free HEPES-buffered solution

Figure Aii.3 Effect of Ca^{2+}_o upon acid influx in high K^+ HEPES-buffered solution

List of Tables

Table 1.1	Comparison of hypercapnic acidosis, isocapic acidosis and isohydric hypercapnia
Table 1.2	Cellular metabolic activities producing or consuming acid
Table 4.1	Summary of DIDS sensitivity of Cl^--HCO_3^- exchange under various conditions
Table 5.1	Non-linear regression analysis of pH_i and pH_o dependency of HCO_3^--dependent acid influx
Table 5.2	Linear regression analysis of pH_i and pH_o dependency of HCO_3^--independent acid influx
Table 5.3	Linear regression analysis of pH_i and pH_o dependency of normalised HCO_3^--independent acid influx

Abbreviations

α	solubility of CO_2 gas
4-AP	4-aminopyridine
9-AC	anthracene-9-carboxylic acid
AE	anion exchanger (Cl^--HCO_3^- exchange)
ATP	adenosine triphosphate
ATPase	adenosine triphosphatase
β	buffering power
β_{CO2}	CO_2-dependent buffering power
β_i	intrinsic buffering power
β_{tot}	total buffering power
Bay K 8644	1,4-dihydro-2,6-dimethyl-3-nitro-4-(2-trifluoromethylphenyl) -pyridine-5-carboxylic acid methyl ester
Ca^{2+}_i	intracellular Ca^{2+}
Ca^{2+}_o	extracellular Ca^{2+}
$[Ca^{2+}]_i$	intracellular Ca^{2+} concentration
$[Ca^{2+}]_o$	extracellular Ca^{2+} concentration
cAMP	cyclic adenosine monophosphate
CAPSO	3-cyclohexamino-2-hydroxy-1-propane sulphonic acid
Carboxy-SNARF-1	carboxyseminapthorhodafluor-1
cDNA	complementary DNA
Cl^-_i	intracellular Cl^-
Cl^-_o	extracellular Cl^-
$[Cl^-]_i$	intracellular Cl^- concentration
$[Cl^-]_o$	extracellular Cl^- concentration
CSN	carotid sinus nerve
Ctx	charybdotoxin
Δ	change of amount
$\Delta\mu$	change in Gibb's free energy
$\Delta pH_i / \Delta pH_o$	ratio of change in intracellular pH to change in extracellular pH
D600	methoxyverapamil
DBDS	4,4'-dibenzoyl stibene-2,2'-disulphonic acid
DIDS	4,4'-diisothiocyano dihydrostilbene-2,2'-disulphonic acid
DMSO	dimethyl sulphoxide
DNA	deoxyribonucleic acid
DNP	2,4-dinitrophenol
dpH_i/dt	rate of change of intracellular pH
DPhil	Doctor of Philosophy
DRA	down-regulated in adenoma protein
DRG	dorsal respiratory group
EGTA	ethyleneglycol-bis-(b-aminoethylether) *N,N,N ,,N,*-tetraacetic acid
E_H	equilibrium potential for H^+
E_{HCO3}	equilibrium potential for HCO_3^-
E_K	equilibrium potential for K^+
E_m	membrane potential
Eqn	equation
F	Faraday's constant (96485 C mol^{-1})

Abbreviations

Fig	figure
g_{HCO3}	electrical conductance for HCO_3^-
GABA	γ-aminobutyric acid
h	Hill coefficient
H_2DIDS	4,4'-diisothiocyanatodihydrostilbene-2,2'-disulphonic acid
H^+_i	intracellular H^+
H^+_o	extracellular H^+
$[H^+]_i$	intracellular H^+ concentration
$[H^+]_o$	extracellular H^+ concentration
$HCO_3^-{}_i$	intracellular HCO_3^-
$HCO_3^-{}_o$	extracellular HCO_3^-
$[HCO_3^-]_i$	intracellular HCO_3^- concentration
$[HCO_3^-]_o$	extracellular HCO_3^- concentration
HEPES	*N*-2-hydroxyethylpiperazine-*N*,-2-ethanesulphonic acid
Hoe694	3-methylsulphonyl-4-piperidinobenzoyl guanidine methanesulphonate
IC_{50}	drug concentration giving half-maximal inhibition
I_{HCO3}	HCO_3^- current
J_H	H^+ (or acid-equivalent) flux
J_{HCO3}	HCO_3^- flux
K_{2P}	two-pore-domain K^+ channel
K_a	dissociation constant of acid
K_i	inhibition constant
K_M	Michaelis-Menten constant
$K_{0.5}$	substrate concentration at which flux rate is half-maximal
K^+_i	intracellular K^+
K^+_o	extracellular K^+
$[K^+]_i$	intracellular K^+ concentration
$[K^+]_o$	extracellular K^+ concentration
log	common logarithm ($\log_{10}$)
ln	natural logarithm ($\log_e$)
MES	2-(N-morpholino) ethane sulphonic acid
mRNA	messenger RNA
Na^+_i	intracellular Na^+
Na^+_o	extracellular Na^+
$[Na^+]_i$	intracellular Na^+ concentration
$[Na^+]_o$	extracellular Na^+ concentration
NADPH	nicotinamide–adenine dinucleotide phosphate (reduced form)
NBC	Na^+-HCO_3 cotransport
NCBE	Na^+-dependent Cl^--HCO_3^- exchange
$[NH_3]_i$	intracellular NH_3 concentration
$[NH_3]_o$	extracellular NH_3 concentration
$[NH_4^+]_i$	intracellular NH_4^+ concentration
$[NH_4^+]_o$	extracellular NH_4^+ concentration
NHE	Na^+-H^+ exchange
NMDG	N-methy-D-glucamine
NTS	nucleus tractus solitarius
P_{Cl}	permeability for Cl^-
P_{HCO3}	permeability for HCO_3^-
P_{CO2}	partial pressure of CO_2
P_{O2}	partial pressure of O_2
Pa_{CO2}	partial pressure of CO_2 in arterial blood
Pa_{O2}	partial pressure of O_2 in arterial blood
PDS	Pendred syndrome protein (pendrin)

Abbreviations

pH	$-\log[H^+]$
pHa	pH in arterial blood
pH_i	intracellular pH
pH_o	extracellular pH
PIPES	1,4-piperazinediethane sulphonic acid
pK_a	$-\log K_a$
PPADS	pyridoxalphosphate-6-azophenyl-2,,4,-disulphonic acid
R	ideal gas constant (8.31 J K^{-1} mol^{-1})
R^2	square of correlation coefficient
RNA	ribonucleic acid
SDS	sodium dodecyl sulphate-polyacrylamide
S.E.M	standard error of mean
SITS	4-acetamido-4,-isothiocyanatostilbene-2,2,-disulphonic acid
SNARF	carboxyseminapthorhoda-fluor-1
SLC	solute linked carrier
T	absolute thermodynamic temperature (K)
TASK	TWIK-related acid-sensitive K^+ channel
TEA	tetraethylammonium
TWIK	tandem of P domains in weak inward rectifier K^+ channel

CHAPTER 1

General Introduction

This thesis is concerned with a physiologically important function: the link between arterial acidosis and increased ventilation. This link is acid chemoreception. Under resting conditions, about 20-30% of the link depends on the activation of the carotid body. In this thesis, I attempt to elucidate the cellular ionic mechanism linking intracellular pH (pH_i) in carotid body type I cells to changes in extracellular pH (pH_o). This introductory chapter provides background information for the rest of this thesis. It is divided into four parts:

A. Respiratory chemoreceptors: an overview

B. Type I cells are principal chemoreceptor cells in the carotid body

C. The signalling pathways for chemoreception in type I cells

D. The relationship between pH_i and pH_o in type I cells

E. Acid-equivalent transport systems and their roles in type I cells

Part A: Respiratory chemoreceptors: an overview

Breathing is a very complicated process although it has a simple ultimate aim for all animals: to supply oxygen to the cells to oxidise nutrients for chemical energy, and to remove the by-product, carbon dioxide. To meet an animal's metabolic demand, the controlling link between ventilation rate and aerobic metabolism is vital. This control is so precise that in healthy individuals the partial pressure of arterial CO_2 (Pa_{CO2})

remains remarkably constant over a wide range of metabolic rates. During episodes of increased metabolism, more CO_2 is released and acid is accumulated in the blood. By sensing the increased amount of acid, chemoreceptors initiate a chemoreflex to enhance ventilation and optimise the removal of CO_2. As a result, the amount of CO_2 and acid in the blood is reduced to the normal level, and homeostasis is maintained.

Since the 19th century it has been known that the chemical composition of blood, such as the partial pressure of oxygen (P_{O2}), carbon dioxide (P_{CO2}) and pH, influence ventilation: a decrease in P_{O2} (hypoxia) and pH (acidosis) as well as an increase in P_{CO2} (hypercapnia) all increase ventilation. Nevertheless, for many years it was thought that the hyperventilation associated with hypoxia and hypercapnia resulted from direct stimulation of elements solely located within the so-called "respiratory centre" in the brain (Haldane & Priestley, 1905). This concept was revised following the discovery of the chemosensing function of carotid body (Heymans, Bouckaert & Dautrebande, 1930, 1931). It was then proved that these peripheral chemoreceptors are responsible for the immediate increase in ventilation during hypoxia and hypercapnia (for historical account of early research on chemoreception, see Fitzgerald & Lahiri, 1996).

There are three types of chemoreceptor responsible for detecting changes in partial pressure of arterial CO_2 (Pa_{CO2}), O_2 (Pa_{O2}) and arterial pH (pHa) (reviewed by O'Regan, 1982; Cunningham, Robbins & Wolff, 1986; Fitzgerald & Lahiri, 1986; Honda & Tani, 1999):

1. **Central chemoreceptor**: Located in the ventrolateral surface of the medulla oblongata, the central chemoreceptors are stimulated by hypercapnia and are responsible for up to 80% of the subsequent ventilatory response. They are, however, insensitive to hypoxia (Mitchell, Loeschcke, Massion & Severinghaus, 1963; Mitchell, 1966; see Loeschcke, 1982; Nattie, 1999; Ballantyne & Scheid, 2000 for review). Recent studies suggested a wider distribution of chemoreceptors outside the medulla. For example, neurons in locus coeruleus of dorsal pone have been reported to be sensitive to hypercapnia (Pineda & Aghajanian, 1997; Filosa, Dean & Putnam, 2002).
2. **Carotid chemoreceptor**: The carotid bodies are located near the external carotid artery. Of the three chemoreceptors, carotid bodies are the most sensitive to variations in Pa_{O2}, but they only contribute a small proportion to the steady-state ventilatory response to hypercapnia (see Fidone & González, 1986; González, Almaraz, Obeso & Rigual, 1994b for review). Based on studies carried out on human subjects whose carotid bodies have been resected, all the ventilatory response to acute hypoxia, plus 30% of the response to hypercapnia and nearly all the response to acute metabolic acidosis are lost (Guz, Noble, Widdicombe, Trenchard, & Mushin, 1966; Honda *et al.* 1979). There is no absolute physiological threshold for initiation of carotid chemoreceptor activity. Even at a Pa_{O2} of 600 mmHg, there is still some carotid sinus nerve discharge. Nerve discharge rises abruptly as Pa_{O2} is reduced to about 75 mmHg and reaches maximum activity at a Pa_{O2} of 10-20 mmHg (Biscoe, Purves & Sampson, 1970). In addition, when hypoxia and hypercapnia are present simultaneously, a multiplied increase in nerve discharge is observed, suggesting a synergy between the two stimuli (Lahiri & Delaney, 1975).

3. **Aortic chemoreceptor**: Aortic bodies are scattered over the aortic arch (Comroe, 1939). They are not as sensitive as the carotid bodies to hypoxia, hypercapnia and acidity (Paintal & Riley, 1966; Lahiri, Mokashi, Mulligan & Nishino, 1981; Fitzgerald & Dehghani 1982). Their main role seems to be related to cardiovascular reflexes (Lahiri, Nishno, Mokashi & Mulligan, 1980a; Jones & Daly, 1997).

Although traditional views hold that the carotid body is only responsible for up to 30% of acid chemoreception while the central chemoreceptor plays the major part (O'Regan, 1982; Honda & Tani, 1999), its importance during acute metabolic (isocapnic) acidosis can not be ignored. In fact, central chemoreceptors are only slightly stimulated by acute increases in pHa with a constant Pa_{CO2}, due to the presence of the blood-brain barrier which greatly restricts movements of H^+, OH^- and HCO_3 ions (Mitchell, 1966; Teppema, Barts, Folgering & Evers, 1983; Voipio & Ballanyi, 1997). Therefore, most of the changes of pHa associated with acute metabolic acidosis are not transferred to the brain cerebrospinal fluid. In this case, the carotid body is better positioned to regulate ventilatory responses in order to counteract acute metabolic acid-base imbalance than the central chemoreceptors (Wasserman, Whipp, Koyal & Cleary, 1975; Oren, Whipp & Wasserman, 1982; Rausch, Whipp, Wasserman & Huszczuk, 1991; Vovk, Duffin, Kowalchuk, Paterson & Cunningham, 2000).

This thesis will focus on acid chemoreception by the carotid body.

Part B: Type I Cells Are Principal Chemoreceptor Cells in the Carotid Body

Anatomy and Histology of Carotid Body

The carotid bodies are small organs weighing no more than 50 mg in neonatal rats. They are located near the bifurcation of the common carotid arteries, lying on the internal carotid artery (**Fig 1.1A**). The intraglomic tissue is perfused at a rate of 15 mL/g/min, which is 15 times greater than human cerebral blood flow. According to Whalen & Nair (1983), the O_2 consumption rate of this tissue is about 1.3 mL/100mg/min.

In the 1920s De Castro demonstrated that the carotid body was innervated by sensory fibres of the carotid sinus nerve, which have their cell bodies located mostly in the petrosal ganglion of the IX^{th} (glossopharyngeal) cranial nerve (De Castro, 1926; De Castro, 1928). He postulated that chemoreceptor cells in the carotid body activate the sensory nerve endings. Although the sensory nature of these nerve endings was once challenged (Biscoe, Lall & Sampson, 1970), later investigations tracing axonal transport using radiolabeled amino acids supported De Castro's original findings (Fidone, Zapata & Stensaas, 1977). Single unit carotid sinus nerve recordings *in vivo* revealed that the carotid body chemoreceptor could be activated by an increase in Pa_{CO2} as well as a decrease in pHa and Pa_{O2} (Eyzaguirre & Koyano, 1965a; Biscoe, Purves & Sampson, 1970; Vidruk, Olson, Ling & Mitchell, 2001).

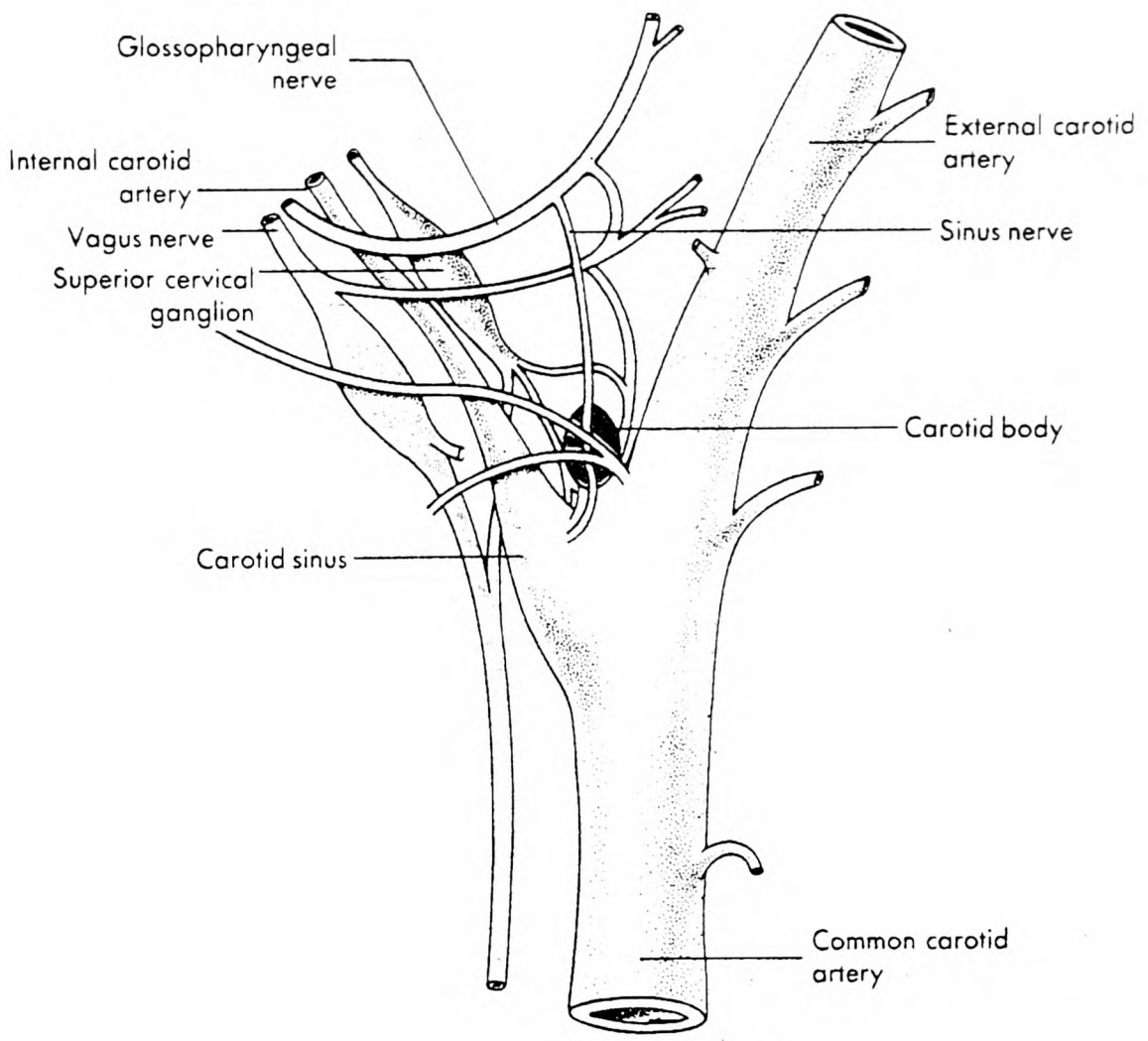


Figure 1.1

A, Diagrammatic representation of the carotid body and its innervation (reproduced from Adams, 1958). ***B***, Diagrammatic representation of a glomoid of carotid body: glomus cells or type I cells (g.c.); sustentacular cells or type II cells (S.C.); carotid sinus nerve terminals (S.n.t); capillary (C) (reproduced from Eyzaguirre & Zapata, 1984).

After leaving the carotid body, some afferent fibres from the carotid sinus nerve project to the nucleus tractus solitarius (NTS) in the medulla via the IXth cranial nerve (Finley & Katz, 1992). The NTS can be regarded as a major relay of carotid body afferent fibres, with neural pathways linking to other respiratory neurones (Davies & Edwards, 1975; Chitravanshi, Kachroo & Sapru, 1994; reviewed by Gozal, Gozal, & Simakajornboon, 2000). In this way, chemosensing signals from the carotid body are integrated in the medulla to control ventilation (Morris, Arata, Shannon & Lindsey, 1996) (for general review on central control of respiration, see Feldman & Smith, 1994; Bianchi, Denavit-Saubie, & Champagnat, 1995).

The parenchymal cells of the carotid body are grouped into cell lobules (also referred to as glomoids), innervated by afferent fibre bundles and surrounded by capillaries (**Fig 1.1B**; for a review on the histology of the carotid body, see McDonald, 1981). Based on differences in shape, size and density, Gómez (1908) classified parenchymal cells into two types: (1) specialised preneural glomus cell or type I cells, and (2) sustentacular cell or type II cells. In the cell lobules, type I cells are usually enveloped by processes from the type II cells. These two cell types were investigated in further detail by De Kock and Dunn (1966). It is estimated that, in the carotid body, type I cells are about five times more abundant than type II cells. The type I cells appear ovoid with a diameter of 8-12 μm and contain numerous dense core granules when examined with an electron microscope (Lever & Boyd, 1957). In addition, these studies confirmed De Castro's earlier observations that sinus nerve endings appose on type I cells to form sensory synapse (De Castro, 1951; Lever, Lewis & Boyd, 1959; Hess & Zapata, 1972). In contrast, neither dense core granules nor synaptic structures can be seen in type II cells. Type II cells also lack the extensive Golgi complex

present in type I cells (De Kock & Dunn, 1966). Generally, the type II cells resemble glial or Schwann cells in the peripheral nervous system. Immunocytochemical studies demonstrated that type I cells contain a neuron-specific enolase, while the glial marker protein S-100 is found in type II cells (Kondo, 1975; Kondo, Iwanaga & Nakajima. 1982). Le Douarin and colleagues removed cells from the neural crest of quail embryo and transplanted them to the neural crest of chicks. After birth, the carotid body of the operated chicks had type I cells with characteristic quail-type nuclei. Therefore, it may be concluded that carotid body cells originate from the neural crest during embryogenesis, like adrenal chromaffin cells (Le Lièvre, & Le Douarin, 1975; Kameda, Nishimaki, Takeichi & Chisaka, 2002).

Neurochemical studies suggested that the dense core granules present in type I cells are secretory granules that are released during exocytosis (Lishajko, 1970; Gronblad, Akerman & Eranko, 1979). Catecholamines including dopamine, adrenaline and noradrenaline were the first neurotransmitters to be found in these dense core granules (Chiocchio, Biscardi & Tramezzani, 1966; Fidone & González, 1982). In addition, other neurotransmitters such as acetylcholine (Eyzaguirre, Koyano & Taylor, 1965), ATP (Bock, 1980), serotonin (Chiocchio, Biscardi & Tramezzani, 1967) and substance P (Cuello & McQueen, 1980) have also been identified in type I cells.

In the early 1970s, several research groups recorded intracellular membrane potential in type I cells. They reported a membrane potential less negative than that seen in most other cell types and observed that both hypoxia and hypercapnia failed to induce depolarisation (Eyzaguirre, Leitner, Nishi & Fidone, 1970; Goodman, & McCloskey, 1972). On the basis of these observations it was assumed that type I cells are not

excitable. These results are not reliable, however, due to the possibility for cell injury by conventional microelectrode recording, and the lack of identity of the impaled elements (González *et al.* 1994b). The true electrophysiological properties of type I cells were not clarified until the realisation of two techniques: primary culture of isolated type I cells and patch clamp recording techniques (Fishman, Greene & Platika, 1985; Duchen, Caddy, Kirby, Patterson, Ponte, & Biscoe, 1988).

Subsequent studies using these new techniques demonstrated the type I cells are indeed excitable, while type II cells are almost electrically silent (Duchen *et al.* 1988; López-Barneo, López-López, Urena & González, 1988). Duchen and colleagues found that most rabbit carotid body type I cells have a resting membrane potential around –55 mV. Upon depolarisation, type I cells are able to generate action potentials, which are composed of a fast, inactivating tetrodotoxin-sensitive Na^+ current in rabbit type I cells and a high threshold voltage-dependent Ca^{2+} current in rabbit and rat type I cells (Duchen *et al.* 1988; Urena, López-López, González & López-Barneo, 1989; Buckler & Vaughan-Jones, 1994a,b). Later studies revealed that the Ca^{2+} current in type I cells is mainly carried by L-type Ca^{2+} channels (Fieber & McCleskey, 1993), although N-type Ca^{2+} and P-type Ca^{2+} channels are also probably involved (e Silva & Lewis, 1995; Overholt & Prabhakar, 1997). K^+ channels in type I cells have greater diversity than other channels and will be introduced below. Gap junctions have also been found between adjacent type I cells, suggesting that they may be electrically coupled (Monti-Bloch, Abudara & Eyzaguirre, 1993).

Carotid Body Type I Cells Are Chemoreceptor Cells

Based on the observation that sensory nerve endings appose on type I cells, De Castro was the first to propose that type I cells are the actual chemoreceptor cells (De Castro, 1928; De Castro, 1951), a model later supported by Eyzaguirre (see Eyzaguirre & Zapata, 1984 for review).[1] Eyzaguirre and colleagues determined the carotid chemoreceptor response to hypoxia, hypercapnia and acidosis using *in vitro* superfusion, in order to avoid complications caused by blood circulation (Eyzaguirre & Lewin, 1961, Eyzaguirre & Koyano, 1965a). Their results showed that nerve impulses were probably initiated by neurotransmitters released from type I cells (Eyzaguirre & Koyano, 1965b). Verna, Roumy & Leitner (1975) demonstrated that, after destruction of type I cells, the carotid body response to chemostimuli was lost. Therefore, the present consensus is that type I cells are the principal chemoreceptor cells in carotid body.

If the type I cell is the primary site of chemoreception, which neurotransmitters are involved in the excitation of afferent nerve endings? This issue has been disputed for decades (Eyzaguirre & Fidone, 1980; Fitzgerald, 2000). Three candidate hypothesis have been suggested:

---

[1] By contrast, Paintal (1966) suggested that type II cells play the chemosensing role via a mechanical transmission mechanism. In addition, another "small nerve ending" model was postulated by Mills & Jobsis (1972). In the last model, hypoxia stimulates type II cells to release potassium (K^+) ions and depolarise the enclosed sensory nerve endings. However, no strong evidence supports the latter two hypotheses.

1. **Acetylcholine hypothesis**: In the 1930s it was proposed that acetylcholine was the excitatory neurotransmitter in the carotid chemosensory synapse, since exogenous acetylcholine stimulated carotid sinus nerve activity, and acetylcholinesterase blockers enhanced this effect (Schweitzer & Wright, 1938). Eyzaguirre and colleagues later showed that acetylcholine produced a dose-dependent chemosensory excitation *in situ* and *in vitro*, and the excitatory effects of exogenous acetylcholine were blocked by various cholinergic antagonists (Eyzaguirre, Koyano & Taylor, 1965; Eyzaguirre & Zapata, 1968b). They demonstrated that if superfusing fluid was perfused from one carotid body to another, the sensory discharge of the "downstream" carotid body increased when the "upstream" carotid body was electrically stimulated. The "downstream" response could be amplified in the presence of the cholinesterase blocker eserine, while it was abolished in the presence of acetylcholinesterase. The hypoxia-evoked carotid sinus nerve activity was also augmented by a cholinesterase inhibitor (von Euler, Liljestrand & Zotterman, 1939). Metz determined the amount of acetylcholine released from the *in vivo* dog carotid body and found an increased release in response to hypoxia and hypercapnia (Metz, 1969). It was later confirmed that the type I cell synthesizes acetylcholine (Fidone, Weintraub & Stavinoha, 1976), and both nicotinic and muscarinic receptors are found on sensory afferent fibres abutting on the type I cell (Shirahata, Ishizawa, Rudisill, Schofield, Fitzgerald, 1998). More recent studies on co-cultures of rat petrosal neurons and type I cells confirmed that nicotinic receptor antagonists (100 μM hexamethonium or 1 mM mecamylamine) reduced hypoxia-induced chemoreceptor responses (Zhong, Zhang & Nurse, 1997; Zhang, Zhong, Vollmer, & Nurse, 2000). However, in these experiments some response remained even in

the presence of these nicotinic antagonists, suggesting other neurotransmitter may be also involved (see below).

Since the emergence of this hypothesis, investigators have been intrigued by the observation that, although cholinergic antagonists block the increased nerve activity induced by exogenous acetylcholine, they do not affect the response induced by natural stimuli (hypoxia and hypercapnia) to the same extent. Furthermore, for those results which did show reduced nerve activity, there is also a wide variability in the extent of reduction reported by different research groups (Douglas, 1952; Eyzaguirre, & Koyano, 1965b; Eyzaguirre & Zapata, 1968a,b; Sampson, 1971; McQueen, 1977). Based on this discrepancy, some investigators argued that acetylcholine is not involved in the neurotransmission during normal chemoreception. Nevertheless, the aforementioned observation does not necessarily mean acetylcholine is not an endogenous neurotransmitter. Alternatively, this difference could be due to endogenous release of acetylcholine by type I cells so close to postsynaptic neurons, that very high concentrations of the neurotransmitter gain access to the receptors in the synaptic cleft despite the presence of cholinergic antagonist (reviewed by Fitzgerald, Shirahata & Ide, 1997; Fitzgerald, 2000).

2. **Dopamine hypothesis**: Another neuroactive agent, dopamine, has also been proposed as the candidate neurotransmitter (for review see González, Almaraz, Obeso & Rigual, 1994b). González and his colleagues found both hypoxia and acidosis stimulate the secretion of dopamine from rabbit type I cells, which is correlated with increased carotid sinus nerve activity (González & Fidone, 1977;

Fidone & González, 1982; Fidone, González & Yoshizaki, 1982; Rigual, López-López & González, 1991). However, many studies have shown that exogenous dopamine produces an inhibitory effect on carotid sinus nerve activity (Sampson, Aminoff, Jaffe, & Vidruk, 1976; Docherty & McQueen, 1978). Blockade of dopaminergic receptors actually enhances the chemosensory response to hypoxia (Zapata, 1975; Lahiri, Nishino, Mokashi & Mulligan, 1980b). In rat carotid body, the magnitude of dopamine release was shown to be not proportional to sinus nerve activity (Doyle & Donnelly, 1994). Furthermore, in their co-cultures of type I cells and petrosal neurons, Nurse and colleagues demonstrated that the dopamine D2 receptor blocker spiperone failed to block neurotransmission between co-cultured type I cells and petrosal neurons (Zhong, Zhang & Nurse, 1997).

3. **ATP hypothesis**: The excitatory effect of exogenous ATP on the chemosensory synapse has been recognised since the 1950s (Jarisch, Landgren, Neil & Zotterman, 1952; Spergel & Lahiri, 1993). Recently, Nurse and colleagues showed that the purinoceptor P2X blocker, suramin, inhibited chemosensory response induced by hypoxia and hypercapnia. They also identified mRNA for both P2X2 and P2X3 purinoceptor subunits in petrosal ganglion neurones that convey afferent chemosensory information from carotid body (Zhang, Zhong, Vollmer, & Nurse, 2000; Prasad, Fearon, Zhang, Laing, Vollmer & Nurse, 2001). Additionally, Kumar and co-workers reported that suramin reduced ventilatory CO_2 sensitivity of carotid body in rat, and PPADS (another purinoceptor antagonist) also partially inhibited carbonic monoxide-mediated discharges in carotid sinus nerve (Al-Hashem, Barbe & Kumar, 2001; Barbé, Al-Hashem, Conway, Dubuis, Vandier & Kumar, 2002).

Combining all the evidence, the emerging consensus is that ATP and acetylcholine are co-released by type I cells during chemosensory response. This view is also supported by the observation that, hexamethonium and suramin partially inhibited the discharges of carotid sinus nerve when applied separately, while joint application of both eliminated chemosensory response completely (Zhang *et al.* 2000; Varas, Alcayaga & Iturriaga, 2003). In addition, possibly other neuroactive agents, including dopamine, also have modulatory effects upon neurotransmission.

Like neurosecretion in other synapses, hypoxia-induced neurotransmitter release from type I cells is dependent upon extracellular Ca^{2+} (Gronblad *et al.* 1979). Fidone *et al.* (1982) proposed that hypoxia-induced Ca^{2+} influx leads to neurotransmitter secretion, which in turn initiates action potentials in the carotid sinus nerve. Similarly, acidosis-induced neurosecretion is also dependent upon extracellular Ca^{2+} (Rigual, López-López & González, 1991).

In summary, the type I cell is the major chemoreceptor in carotid body. This cell responds to hypoxic and acidic stimuli with a Ca^{2+} influx and neurosecretion, which in turn activates afferent fibres of the carotid sinus nerve.

Part C. The Signalling Pathways for Chemoreception in Type I Cells

Common signalling pathway for hypoxia and acidosis

The forgoing results concluded that chemostimuli cause Ca^{2+}-dependent neurosecretion. The next question is: how do both acidosis and hypoxia induce Ca^{2+} influx in type I cells? I will discuss each case separately.

Oxygen Chemoreception in Type I Cells

Since oxygen is required for the synthesis of ATP in mitochondria, it may seem straightforward that the deficiency of ATP during hypoxia triggers chemoreception in type I cells. However, ATP contents in carotid body do not change significantly during modest hypoxia (P_{O2} ~60 mmHg) (Verna, Talib, Roumy & Pradet, 1990). In fact, in most tissue, cytochrome c oxidase (the enzyme reduces oxygen in electron transport chain of mitochondria) has high affinity for oxygen such that oxidative phosphorylation remains independent of P_{O2} down to 2 mmHg (Wilson, Rumsey, Green & Vanderkooi, 1988). Thus a more specific mechanism for sensing modest hypoxia must be present in carotid body. Currently there are several hypotheses for oxygen chemoreception in type I cells, they can be generally grouped into three major categories (reviewed by Prabhakar, 2000):

1. **Metabolic hypothesis**: This hypothesis suggests that a haeme and/or a redox-sensitive enzyme serve as the oxygen sensor, and a metabolic event associated with the enzyme triggers the signalling pathway (Anichcov & Belen'kii, 1963; Lahiri, 1980). It has been known that inhibitors of electron transport chain including cyanide, antimycin A and oligomycin stimulate carotid chemoreflex (Heymans & Neil, 1958; Mulligan, Lahiri & Storey, 1981). Since haeme groups of mitochondrial cytochromes bind to oxygen, it was proposed that one of these cytochromes with unusually low affinity to oxygen serve as an oxygen sensor (Mills & Jösis, 1972). However, such low affinity oxygen sensor has not been discovered. Biscoe and colleagues measured the mitochondrial potential and found that hypoxia causes mitochondrial depolarisation (Biscoe, Duchen, Eisner, O'Neill, & Valdeolmillos, 1989; Duchen & Biscoe, 1992). They hypothesised that such depolarisation could lead to increased $[Ca^{2+}]_i$, although the detailed mechanism is still not clear.

2. **Reactive oxygen species hypothesis**: Another candidate of oxygen sensor is NADPH oxidase, a haeme-linked enzyme utilising oxygen to produce reactive oxygen species such as superoxide ion (O_2^{-}·). After they identified NADPH oxidase in the carotid body, Acker and colleagues proposed that the production of reactive oxygen species by NADPH oxidase is inhibited during hypoxia, leading to chemoreception (Acker, Dufau, Huber & Sylvester, 1989; Kummer & Acker, 1995). Nevertheless, this possibility has recently been discounted because specific inhibitors of NADPH oxidase fail to block neurosecretion induced by hypoxia (Wyatt, Weir & Peers, 1994; Obeso, Gómez-Niño & González, 1999).

3. **K^+ channel hypothesis**: Lately, there is growing evidence that hypoxia decreases K^+ current in type I cells, and different types of K^+ channels have been found to be inhibited by hypoxia (López-Barneo, López-Lopez, Urena & González, 1988; Peers, 1990; Buckler, 1997; see below for further details). Since the resting membrane potential in type I cells is mainly mediated by K^+ channels, inhibition of them induces, sequentially, membrane depolarisation, activation of voltage-gated Ca^{2+} channel and Ca^{2+} influx. It has been shown that two of these K^+ channels (K_{O2} channel and K_{Ca} channel, see below) are inhibited by hypoxia in a membrane-delimited manner (Ganfornina & López-Barneo, 1991; Riesco-Fagundo, Pérez-García, González & López-López, 2001). Based on these findings, López-Barneo suggests the channel molecule *per se* may sense P_{O2}, or is tightly attached to an oxygen-sensitive subunit (for review, see López-Barneo, 1996). However, it is not clear whether hypoxia actually induces neurosecretion in the type I cell by directly modulating these K^+ channels.

At present, the exact mechanism of oxygen chemosensing in type I cells remains to be clarified. It should be noted that the metabolic and K^+ channel hypothesis are not mutually exclusive. Instead, it is very likely that each mechanism plays a part in the signalling pathway. A currently attractive model combines the two hypotheses and indicates that certain haeme-containing proteins, possibly aforementioned mitochondrial cytochromes, serve as the oxygen sensor in type I cells. During hypoxia, the oxygen sensor triggers a change of redox status and/or of the amount of reactive oxygen species, leading to inhibition of cell membrane P_{O2}-sensitive K^+ channels. Recently, Wyatt & Buckler (2000) showed that mitochondrial electron transport inhibitors (cyanide, rotenone and oligomycin) mimic the response of

hypoxia in inhibiting background K^+ current. Although the link between mitochondrial metabolism and membrane K^+ channel remains elusive, these findings suggest that metabolic hypothesis demands closer scrutiny. However, since this thesis is focused on acid chemoreception, aspects specifically relating to oxygen chemosensing pathway will not be discussed further.

Acid Chemoreception in Type I Cells

Regarding to the acid chemosensing pathway, two mechanisms linking acidosis to extracellular Ca^{2+} entry have been proposed:

1. **Na^+-Ca^{2+} exchanger hypothesis**: González and co-workers proposed the following mechanism for Ca^{2+} influx (Rocher *et al.* 1991; González *et al.* 1992): initially, acidic stimuli induce a fall in pH_i. This acidification activates Na^+-dependent acid extruders such as Na^+-H^+ exchange, then the increase in $[Na^+]_i$ promotes reverse mode of Na^+-Ca^{2+} exchange, leading to Ca^{2+} influx (summarised in González, Almaraz, Obeso & Rigual, 1994a). Their model was based on the following observation using proton ionophore 2,4-dinitrophenol (DNP) as the putative acid stimulus: (1) DNP increased dopamine secretion, (2) the DNP-induced dopamine secretion is abolished in Na^+-free solutions and can be blocked by ouabain (a Na^+-K^+ ATPase inhibitor).

2. **Membrane depolarisation hypothesis**: This hypothesis indicates that, some K^+ channels in type I cells are inhibited by acidosis, resulting in membrane depolarisation and Ca^{2+} entry through voltage-gated Ca^{2+} channels. Buckler &

Vaughan-Jones (1994b) provided evidence of direct link between acidosis and voltage-gated Ca^{2+} entry: (1) the hypercapnic acidosis-induced Ca^{2+} response is partially inhibited by the specific L-type Ca^{2+} channel antagonists, nicardipine and methoxyverapamil (D600), (2) acidosis promotes membrane depolarisation and electrical activity, (3) Ca^{2+} influx can be abolished by voltage-clamp using the perforated patch technique.

There are doubts relating to the Na^+-Ca^{2+} exchanger hypothesis. Buckler & Vaughan-Jones (1994b) were able to demonstrate that the acidosis-induced Ca^{2+} response was inhibited in Na^+-free solutions. Their electrophysiological studies, however, revealed that this was due to membrane hyperpolarisation caused by removal of Na^+_o, not via inhibition of Na^+-H^+ exchange. Most importantly, later they showed that DNP was not purely acting as an acidic stimulus. In fact, DNP inhibits a background K^+ conductance and induces a small inward current. As a result, the membrane potential is depolarised, leading to voltage-gated Ca^{2+} entry (Buckler & Vaughan-Jones, 1998). This explains why DNP increased dopamine secretion in previous studies (Rocher *et al.* 1991).

Several K^+ channels have been proposed as the candidate acid sensor. As indicated above, López-Barneo *et al.* (1988) found that low P_{O2} blocked a K^+ channel (later denoted as K_{O2}), leading to inhibition of K^+ currents. This K_{O2} channel was also inhibited by low pH and tetraethylammonium (TEA). According to their proposal, inhibition of the transient K^+ current is the initial event in the chemotransducing cascade. Similarly, Peers (1990) found another K^+ current in rat type I cells which is also inhibited by both acidosis and hypoxia. The outwardly rectifying K^+ current was

enhanced by Bay K 8644 and intracellular Ca^{2+} and can be blocked by charybdotoxin (Ctx), thus presumed to be carried through a BK_{Ca} channel.

Although both the K_{O2} channel and K_{Ca} channel have been claimed to be able to produce depolarisation when they are inhibited by chemostimuli (López-López *et al.* 1989; Peers, 1990), it should be noted that both are voltage-gated K^+ channels which are not activated at resting membrane potential (about -50 mV). They might play a modulatory role in maintaining the chemosensing response, but it is hard to postulate how they can initiate depolarisation from the resting membrane potential. In addition, 20 nM Ctx (an inhibitor of BK_{Ca} channel), 5 mM 4-aminopyridine (4-AP) and 10 mM TEA, all failed to evoke a significant membrane depolarisation and Ca^{2+} influx under resting pH conditions. Taking these lines of evidence together, there seemed to be a severe flaw in the membrane depolarisation hypothesis (Lahiri, Roy, Rozanov & Mokashi, 1998).

Recently, Buckler and colleagues showed that a novel background K^+ current in the type I cell is inhibited by both acidosis and hypoxia (Buckler, 1997; Buckler & Vaughan-Jones, 1998; Buckler, 1999; Buckler, Williams & Honoré, 2000). It is very different from the K_{O2} channel or K_{Ca} channel found earlier, in that it is responsible for the "leak current" under resting conditions and it is not voltage-gated. It is also resistant to BK_{Ca} and K_{O2} channel blockers such as Ctx, 4-AP and TEA. Later studies showed that its biophysical properties are very similar to those of a newly cloned K^+

channel, TASK-1[2]. TASK-1 is also inhibited by acidic pH, but stimulated by anaesthetics such as halothane (Duprat, Lesage, Fink, Reyes, Heurteaux & Lazdunski, 1997; Buckler, Williams & Honoré, 2000). It belongs a new two-pore-domain K^+ (K_{2P}) channel family (also named as KCNK family), in which the channel subunit has 4 transmembrane domain and two pore domains (for general review on K_{2P} channels, see Lesage & Lazdunski, 2000; Goldstein, Bockenhauer, O'Kelly & Zilberberg, 2001). Due to its activity at the resting membrane potential and its sensitivity to pH, this novel K^+ channel is likely to play a key role in the initial step of the acid signalling pathway, to transduce acidosis stimuli into Ca^{2+} response in type I cells (for review on the role of background K^+ current in carotid body chemoreception, see Buckler, 1998).

Part D. The Relationship between pH_i and pH_o in Type I Cells

In the preceding section, it has been established that acidosis inhibits K^+ channel activity in the type I cell, leading to membrane depolarisation and neurosecretion. Since acidosis could occur extracellularly or intracellularly, the next step is to analyse the respective roles of pH_o and pH_i in acid chemoreception. It is first necessary to distinguish different kinds of acidosis observed under physiological conditions.

---

[2] "TASK" stands for TWIK-related Acid-Sensitive K^+ channels. TWIK-1 (for Tandem of P domains in Weak Inward rectifier K^+ channels) was the first K_{2P} channel cloned (Lesage *et al.* 1996).

As a result of cellular metabolism, CO_2 is continuously produced and dissolved in most of the body fluids. Dissolved CO_2 combines with H_2O and dissociates according to the following equation (Pauling, 1970):

$$\underset{\text{①}}{CO_2 + H_2O} \leftrightarrows \underset{\text{②}}{H_2CO_3} \leftrightarrows \underset{\text{③}}{HCO_3^- + H^+} \leftrightarrows CO_3^{2-} + H^+ \qquad \textbf{[Eqn. 1.1]}$$

The first step (①) in the above reaction, i.e. the hydration of CO_2 into carbonic acid (H_2CO_3), is catalysed by carbonic anhydrase. The enzyme accelerates the reaction rate up to 20000-fold (Edsall, 1969). Once H_2CO_3 is formed, the second step (②) reaches equilibrium almost instantaneously. In the physiological pH range, the secondary dissociation shown in the third step (③) can be ignored.

The first two steps of the above reaction can be combined and rearranged into the Handerson-Hasselbalch equation (Henderson, 1908; Hasselbalch, 1916):

$$pH = pK_a' + \log\frac{[HCO_3^-]}{\alpha \cdot P_{CO2}} \qquad \textbf{[Eqn. 1.2]}$$

The apparent acid dissociation constant (pK_a') has a value of 6.10 in human plasma at 37°C, and the CO_2 solubility coefficient α is 0.03253 mM/mmHg (Putnam & Roos, 1991).

Therefore, an arterial acidosis is the result of a decrease in the ratio of $[HCO_3^-]$ to the amount of dissolved CO_2 ($\alpha \cdot P_{CO2}$) (**Equation 1.2**). This could be achieved by

increasing the retention of CO_2 (respiratory acidosis), or reducing the plasma level of HCO_3^- ions (metabolic acidosis), or, a combination of the two. In physiological experiments, respiratory acidosis and metabolic acidosis are often mimicked by changing either P_{CO2} or $[HCO_3^-]$ of the extracellular fluid while keeping the other factor constant, in order to reduce the ratio of the two. Hence these two kinds of acidosis are called "hypercapnic acidosis" and "isocapic acidosis", respectively. The pH value of isohydric hypercapnia, however, does not change, because there is a proportional increase in both P_{CO2} and $[HCO_3^-]$ (see **Table 1.1**).

Table 1.1

Comparison of hypercapnic acidosis, isocapic acidosis and isohydric hypercapnia

	Hypercapnic acidosis (respiratory acidosis)	Isocapnic acidosis (metabolic acidosis)	Isohydric hypercapnia
P_{CO2}	Increase	Constant	Increase
$[HCO_3^-]$	Constant	Decrease	Increase
$[HCO_3^-] / (\alpha \cdot P_{CO2})$	Decrease	Decrease	Constant
pH	Decrease	Decrease	Constant

It was once believed that CO_2 *per se* activates the chemoreceptor (Torrance, 1968; Torrance, 1974). Subsequently, investigators observed that hypercapnic acidosis and isocapnic acidosis both stimulate carotid body chemoreceptor cells and increase the discharge frequency in carotid sinus nerve (Eyzaguirre & Koyano, 1965a; Biscoe, Purves & Sampson, 1970), while isohydric hypercapnia did not produce a sustained response, but only a transient one (Gray, 1968). Since the only common feature of hypercapnic acidosis and isocapnic acidosis (both induce acid chemosensing response) is a reduction in pH_o, while in isohydric hypercapnia pH_o remains constant

although CO_2 is raised, Gray concluded that CO_2 stimulates chemoreceptors by producing H^+ in the perfusing solution. Thus it is pH, rather than CO_2 itself, that stimulates the chemoreceptor.

Gray's view was challenged later by Torrance, who suggested pH_i is probably more important than pH_o (Torrance, 1977). The idea that pH_i might play a key role in acid chemosensing gained support when Torrance and colleagues found the membrane-permeant carbonic anhydrase inhibitor, acetazolamide, slowed the onset of increased nerve discharge response to hypercapnic acidosis (Hanson, Nye & Torrance, 1971), while membrane impermeant carbonic anhydrase inhibitors did not. Combined with the observation that carbonic anhydrase is present in the type I cell (Gray, 1971; Ridderstrale & Hanson, 1984), their results suggested that the increased CO_2 needs to cross the cell membrane then hydrate, producing H^+ ions intracellularly to induce a chemosensing response. Another line of evidence came when Thomas (1976) observed a transient pH_i change in response to isohydric hypercapnia in snail neurones. In light of Thomas's observation, Hanson noticed a similar transient increase of carotid sinus nerve activity induced by isohydric hypercapnia in Gray's original experiments. Based on the similarity between nerve response and probable pH_i changes, they suggested the carotid body chemoreceptor responds to pH_i rather than pH_o.

Due to the lack of convincing pH_i measurement in carotid body type I cells, the aforementioned theories had not been further examined until Buckler *et al.* measured pH_i in type I cells tested with different kinds of acidosis listed in **Table 1.1** (Buckler, Vaughan-Jones, Peers & Nye, 1991b). Their results showed that both hypercapnic

acidosis and isocapnic acidosis induced steady-state intracellular acidification, while isohydric hypercapnia initially caused pH_i to fall it then returned to basal levels within 4 minutes. All these results are strikingly similar to the pattern of carotid sinus nerve discharge recorded by Gray (1968). Furthermore, they also observed that acetazolamide significantly slowed the pH_i response following extracellular hypercapnic acidosis, which is also consistent with the nerve activity results reported by Hanson *et al.* (1971). Buckler & Vaughan-Jones (1993) further determined the relationship between intracellular acidification and change in intracellular calcium concentration $[Ca^{2+}]_i$. They reported that both hypercapnic acidosis and isocapnic acidosis induce an increase in steady-state $[Ca^{2+}]_i$ in CO_2/HCO_3^--buffered saline, while in isohydric hypercapnia there was no sustained $[Ca^{2+}]_i$ increase but only a transient one (reviewed in Buckler & Vaughan-Jones, 1994c).

The foregoing observations seem to indicate that pH_i rather than pH_o is the initial signal implicating in acid chemosensing. However, recent studies revealed that this matter is more complicated and probably both pH_o and pH_i are involved. Buckler *et al.* (2000) showed that isocapnic acidosis induces membrane depolarisation by inhibiting TASK-1-like current within 20s. This rapid response is faster than the subsequent, slower reduction in pH_i (see Chapter 3), suggesting the initial effect of acidosis is likely mediated by the fall in pH_o *per se*. In addition, Kim and colleagues demonstrated that a decrease in pH_o from 7.2 to 6.4 reduces the open probability of TASK-1 channel by 81%, whereas a similar decrease in pH_i reduces the open probability by 47%. They concluded that acidic pH_o is twice as effective than acidic pH_i in blocking TASK-1 current (Kim, Bang & Kim, 1999). Nevertheless, the importance of pH_i must not be disregarded, as it has been known that pH_i also

regulates the activity of K_{Ca} channel (Peers & Green, 1991), which may play a significant modulatory role after the initiation of depolarisation (see above). Therefore, it is most appropriate to conclude that both pH_o and pH_i are key factors in mediating acid stimulus. A revised model of acid chemosensing pathway is summarised in **Fig 1.2**.

The pH_o sensitivity of pH_i in type I cells

As concluded above, a fall in pH_i in response to isocapic acidosis plays an important role in the acid chemosensing pathway in type I cells. It follows logically that pH_i in type I cells must therefore respond to changes in pH_o. We can define the proportionality coefficient as changes in pH_i in respect to changes in pH_o:

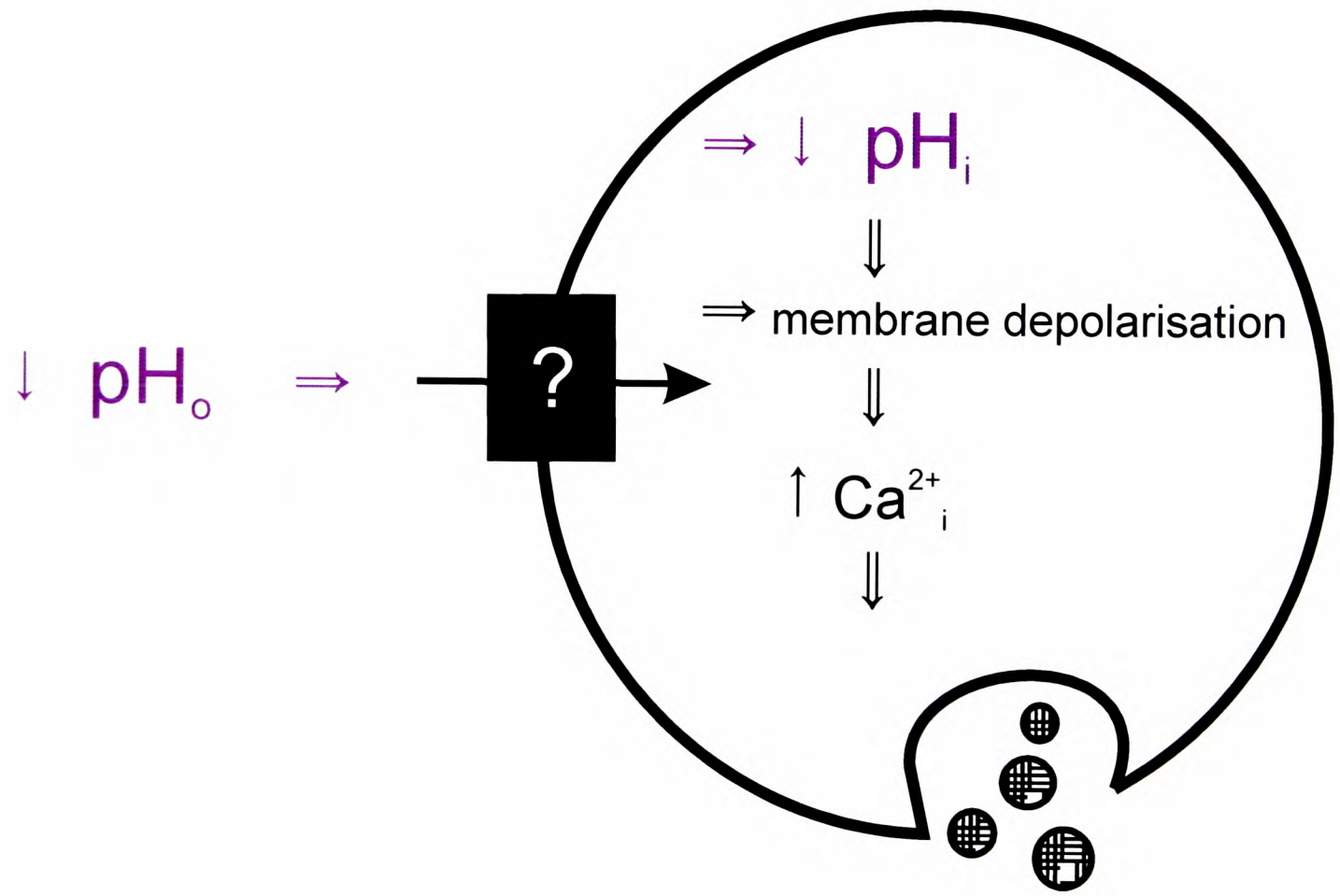
$$\frac{\Delta pH_i}{\Delta pH_o} = \frac{pH_i^2 - pH_i^1}{pH_o^2 - pH_o^1} \qquad \textbf{[Eqn. 1.3]}$$

Where pH_i^2 : the final steady-state pH_i ; pH_i^1 : the initial steady-state pH_i ; pH_o^2 : the final steady-state pH_o ; pH_o^1 : the initial steady-state pH_o.

It should be stressed here it is the "steady-state pH_i" that is concerned. The value of this ratio can be used to estimate and compare the sensitivity of pH_i to pH_o among different cell types.

The ratio of $\Delta pH_i/\Delta pH_o$ is normally 0.2-0.3 in mammalian cardiac Purkinje fibre (Vaughan-Jones, 1986), 0.3 in skeletal muscle (Aickin & Thomas, 1977), 0.2 in rat dorsal root ganglion cells (Tolkovsky & Richards, 1987) and 0.35 in guinea-pig vas

A



B

↓ pH$_o$ / ↓ pH$_i$

⇓

↓ K$^+$ channel activity

⇓

membrane depolarisation

⇓

↑ voltage-gated Ca^{2+} channel activity

⇓

Ca^{2+} influx

⇓

↑ cytosolic Ca^{2+}

⇓

neurosecretion

Figure 1.2

The membrane deplorisation model of acid chemosensing pathway (modified from Buckler & Vaughan-Jones, 1994). ***A***, Schematic diagram. ***B***, Flow diagram.

deferens (Aickin, 1984). Surprisingly, Buckler *et al.* (1991b) reported the ratio of $\Delta pH_i/\Delta pH_o$ in rat carotid body type I cells to be 0.6-0.7, while Wilding *et al.* (1992) reported an even higher value of 0.82. He, Wei & Eyzaguirre (1991) also observed a close relationship between pH_i and pH_o in the rabbit type I cells. In comparison with other cell types, therefore, these ratio values are exceptionally high. In fact, there are very few cell types with a ratio of $\Delta pH_i/\Delta pH_o$ as high as type I cells. A high sensitivity of pH_i to pH_o change has however, been found in other chemosensitive cells. For example, in chemosensitive neurones from ventrolateral medulla and locus coeruleus, $\Delta pH_i/\Delta pH_o$ is 0.6-0.8 and 0.5, respectively (Ritucci, Chambers-Kersh, Dean & Putnam, 1998; Filosa, Dean, & Putnam, 2002). DeSimone and co-workers reported a ratio of 0.8-1.2 in the rat taste reporter cell of taste bud (Lyall, Feldman, Heck & DeSimone, 1997).

Buckler *et al.* (1991b) also found that both hypercapnic acidosis and isocapnic acidosis produce very similar pH_i *versus* pH_o relationships and have the same $\Delta pH_i/\Delta pH_o$ ratio, although during isocapnic acidosis it takes 2-3 minutes longer to reach a final steady-state pH_i than in hypercapnic acidosis (also see Buckler, Nye, Peers & Vaughan-Jones, 1990). This is an intriguing observation: because the plasma membrane is much more permeable to CO_2 than to H^+ and HCO_3^- ions, so it is expected that hypercapnic acidosis would produce more rapid pH_i changes. However, such a difference in permeability does not influence the final steady-state pH_i achieved by either acidosis protocol (i.e. hypercapnic or isocapnic). Two inferences can be drawn from their observation: (1) the steady-state pH_i achieved is only dependent upon pH_o, irrespective of the P_{CO2} or $[HCO_3^-]_i$ used; (2) H^+ and/or HCO_3^- ions are able to move across type I cell plasma membrane in some way.

It might be expected that, because pH_i in type I cell is very sensitive to changes in pH_o, the distribution of H^+ ions across the plasma membrane is at electrochemical equilibrium, which is defined by the Nearnst equation:

$$E_H = \frac{RT}{F} \times \ln \frac{[H^+]_o}{[H^+]_i} \approx \frac{2.3RT}{F} \times \log \frac{[H^+]_o}{[H^+]_i} \qquad \textbf{[Eqn. 1.4]}$$

Where E_H is the electrochemical equilibrium potential for H^+, R is ideal gas constant, T is absolute thermodynamic temperature and F is Faraday's constant.

The above equation can be rearranged into:

$$pH_i = pH_o + \frac{F}{2.3RT} \times E_H \qquad \textbf{[Eqn. 1.5]}$$

At resting conditions pH_o = 7.4 assuming $E_H = E_m$ = -50 mV (Buckler & Vaughan-Jones, 1998), according to **Equation 1.5** it can be calculated that the pH_i at equilibrium is about 6.5. This predicted equilibrium pH_i value, of course, is far more acidic than the real pH_i value of 7.2-7.3 in type I cells perfusing with pH_o 7.4 solution (Buckler *et al.* 1991b; Wilding *et al.* 1992). This calculation suggests that the steady-state pH_i of type I cells is a result of an active regulation rather than transmembrane passive equilibrium of H^+ ion, despite the high value of $\Delta pH_i/\Delta pH_o$. Furthermore, the regulation of steady-state pH_i must be tightly determined by pH_o.

Dynamic Balance of pH_i

A steady-state pH_i is maintained when the rate of acid loaded into the cytoplasm equals the rate of acid removed from the cytoplasm. The cellular processes responsible for acid loading and acid removal can be summarised as the following three processes (**Fig 1.3**):

1. Intracellular acid production and consumption
2. Transmembrane acid influx
3. Transmembrane acid efflux

In process 1, acid is either produced or consumed by cellular metabolic activity. Some important cellular metabolic activities producing or consuming acid are listed in **Table 1.2**. Under normal conditions the overall combined effect of these activities is a net accumulation of acid, referred to as "intracellular background acid loading" or "*de novo* acid production" (Gevers, 1977; Hochachka & Mommsen, 1983; reviewed by Putnam, 1998).

In the last two processes, acid (or base) is transported into or out of the cell. Process 2 leads to accumulation of intracellular acid (acid loading), while process 3 results in elimination of intracellular acid (acid removal). Since process 1 is relatively constant under resting conditions, the large part of pH_i regulation is controlled by process 2 and 3, that is, influx or efflux of acid and/or base (see below).

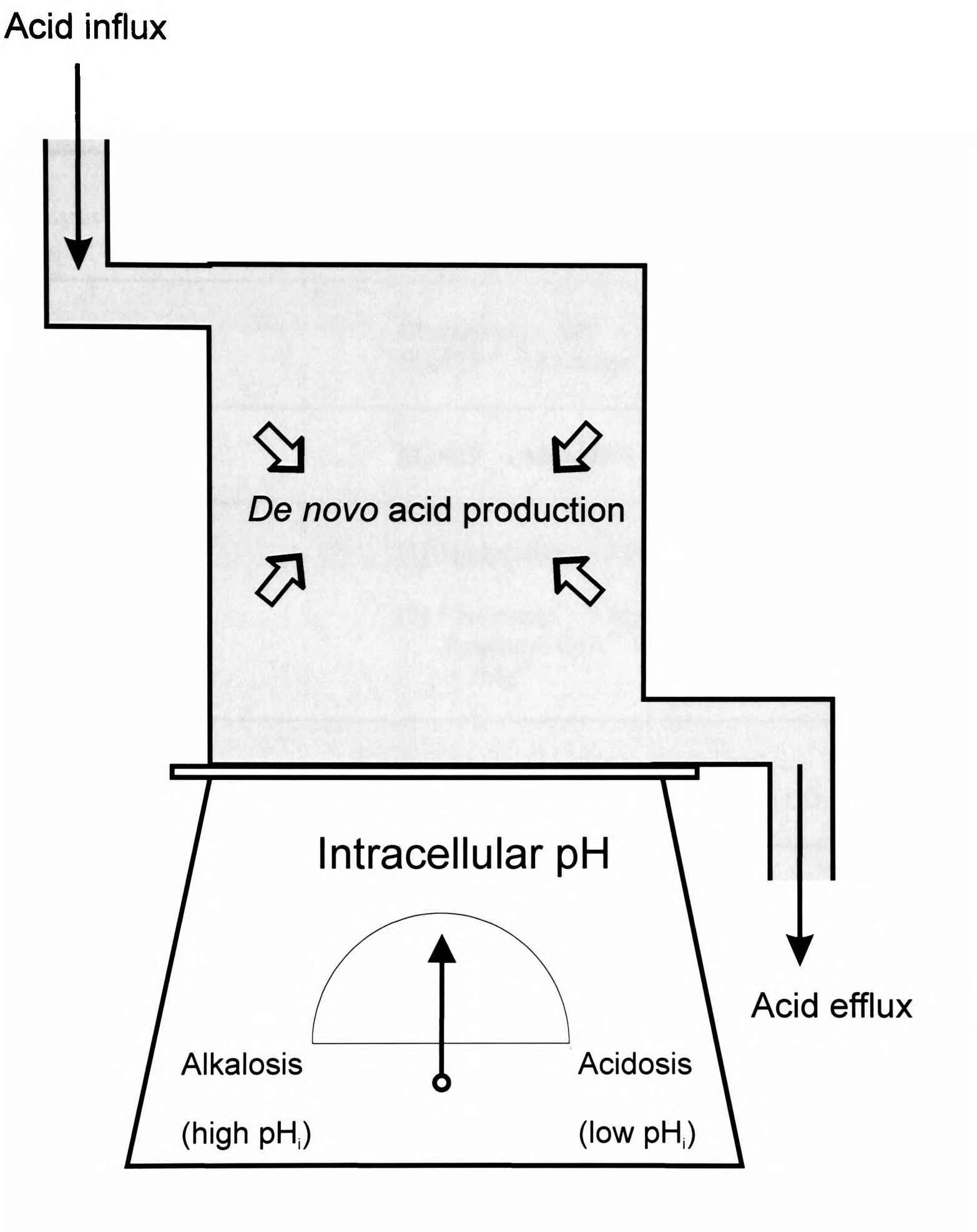


Figure 1.3

Schematic representation showing the concept of dynamic balance of pH_i. pHi reflects the balance between acid loading (transmembrane acid influx plus de novo acid production) and acid removal (transmembrane acid efflux). When the rate of acid loading equals that of acid removal, a steady-state pH_i is maintained.

Table 1.2

Cellular metabolic activities producing or consuming acid.

Glycolysis*	$Glucose + 2\ MgADP^- + 2\ P_i^{2-} \rightarrow 2\ Lactate^- + 2\ MgATP^{2-}$
Glycogenolysis*	$Glycogen_{(N)} + 3\ P_i^{2-} + 3\ MgADP^- + H^+ \rightarrow 3\ MgATP^{2-} + 2\ Lactate^- + Glycogen_{(N-1)}$
ATP hydrolysis	$MgATP \rightarrow MgADP + 2\ P_i^{2-} + 2\ H^+$
Lipolysis	(1) $Triglyceride \rightarrow 3\ Palmitate^- + 3\ H^+$ (2) $3\ Palmitate^- + 3\ MgATP^{2-} + 3\ CoA^{4-} \rightarrow 3\ Palmitoyl\text{-}CoA^{4-} + 3\ AMP^{2-} + 6\ P_i^{2-} + 3\ H^+ + 3Mg^{2+}$
Hexose monophosphate shunt	$Glucose\text{-}6\text{-}phosphate^- + 12\ NADP^+ + 6\ H_2O \rightarrow NADPH + P_i^- + 12\ H^+ + 6\ CO_2$

*For these processes, the net H^+ production or consumption is dependent on intracellular pH, the most likely result at physiological pH is shown here.

Part E. Acid-equivalent Transport Systems and Their Roles in Type I Cells

General Introduction to Acid-equivalent Transport Systems

In response to gain or loss of intracellular H^+, the cellular buffering system plays a major role in opposing the immediate changes in pH_i. There are two distinct components of cellular buffering: (1) intrinsic buffering, which includes cytosolic protein, intracellular weak acids and weak bases, and organelles which sequester H^+ ions; (2) extrinsic buffering, provided by CO_2 and HCO_3^-. The latter plays a major role in cellular buffering under physiological conditions, when cells are superfused in CO_2 / HCO_3^--buffered blood or saline (see Roos & Boron, 1981 for review).

Acid influx can be mediated by H^+ influx, OH^- efflux or HCO_3^- efflux, provided CO_2 moves across cell membrane freely and the cell behaves like an open system. In this case efflux of OH^- or HCO_3 ions leaves behind an extra H^+ ion due to the dissociation of water or H_2CO_3 (cf. **Equation 1.1** and **Fig 1.4**). The net results are the same: $[H^+]_i$ increases (pH_i decreases). Conversely, acid efflux can be achieved when H^+ ions directly move out of the cell, or when OH^- or HCO_3^- ions move into the cell, so $[H^+]_i$ decreases (pH_i increases). Collectively therefore, H^+, OH^- and HCO_3 ions can all be regarded as "acid-equivalent" where pH_i regulation is concerned. Transport of acid-equivalents across plasma membrane is mediated via membrane transporters and channels. In general, acid-equivalent transport systems can be classified into two

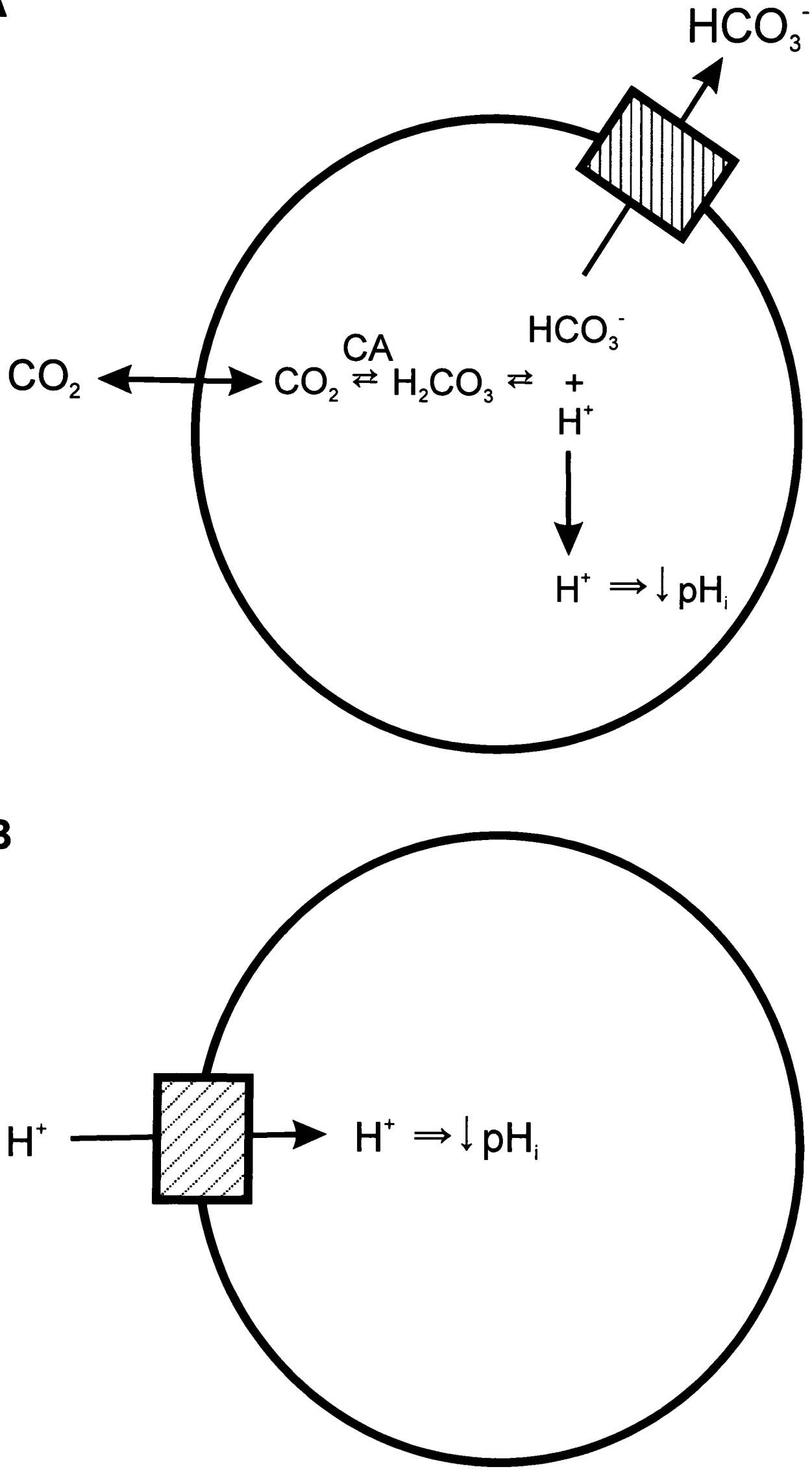


Figure 1.4

Schematic representation showing HCO_3^- ion efflux has an equivalent effect on pH_i as H^+ ion influx. ***A***, Moving 1 HCO_3^- ion out of the cell leaves 1 H^+ ion inside the cell, since CO_2 enters the cell readily and dissociates into H^+ and HCO_3^- ions. This reaction is catalysed by carbonic anhydrase (CA). So the net effect of ***A*** is equivalent to moving 1 H^+ ion into the cell, as shown in ***B***.

functional groups: "acid loader" (for those involving acid influx) and "acid extruder" (for those involving acid efflux).

A large number of acid-equivalent transport systems have been described in animal cells, they include Na^+-H^+ exchange, Cl^--HCO_3^- exchange, Na^+-dependent Cl^--HCO_3^- exchange, Na^+-HCO_3^- cotransport, K^+-H^+ exchange and anion channels which are HCO_3^- permeable (for general review, see Putnam, 1998; Pucéat, 1999). This section gives a general background of these acid-equivalent transport systems, the operative models of individual transport systems are illustrated in **Fig 1.5**.

1. **Na^+-H^+ exchange** (NHE): NHE appears to be a ubiquitous membrane transporter among vertebrate cells (see Wakabayashi, Shigekawa & Pouyssegur, 1997; Counillon & Pouyssegur, 2000 for review). Pitts and co-workers first proposed exchange of Na^+ for H^+ as a mechanism for renal tubular acidification (Pitts, Ayer & Schiess, 1949), but it was not experimentally identified until 1976 in vesicles prepared from brush border membranes of kidney tubules (Murer, Hopfer & Kinne, 1976). The operational mode of NHE was further investigated by Aronson *et al.* (Kinsella & Aronson, 1980; Kinsella & Aronson, 1981; Aronson, Shum & Nee, 1983; Aronson, 1985): its activity is driven by transmembrane chemical gradient of Na^+ and H^+ ions with a 1:1 stoichiometry under normal physiological conditions, functioning as acid extruder. It is electrically neutral and insensitive to changes of membrane potential (Kinsella & Aronson, 1980; Grinstein, Cohen, & Rothstein, 1984). NHE activity is pH_i-dependent, being enhanced as pH_i falls, while inhibited as pH_i increases (Aronson, Suhm & Nee, 1983), suggesting the presence of an allosteric modulation site for intracellular protons in addition to the

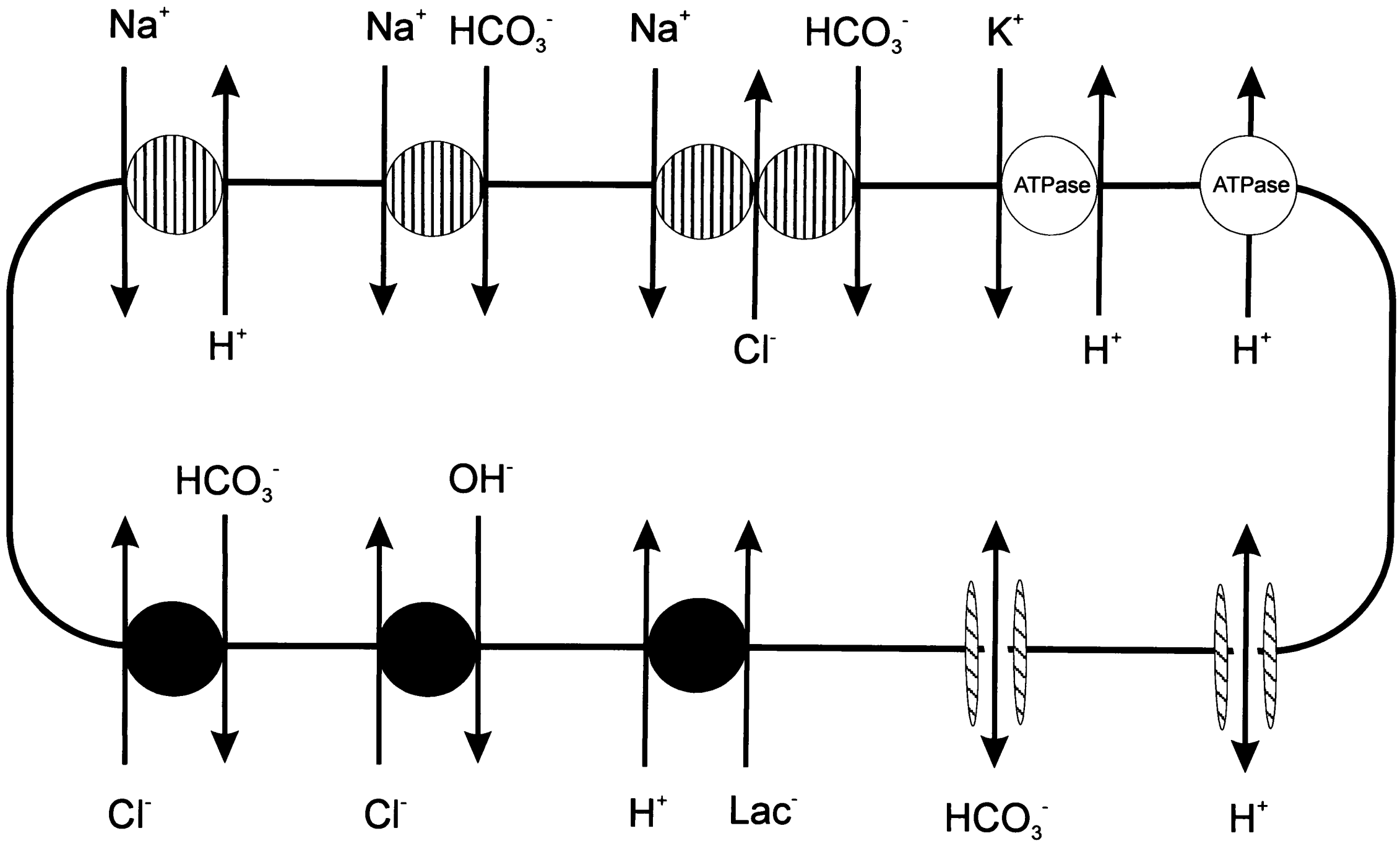


Figure 1.5

Schematic diagram of the principle acid-equivalent transport systems found in animal cells.

intracellular "transport" site (Aronson, Nee & Suhm, 1982; Aronson, 1985). Conversely, NHE activity is inhibited as pH_o falls and enhanced as pH_o increases (Aronson, Suhm & Nee, 1983; Vaughan-Jones & Wu, 1990).

Pouyssegur and colleagues pioneered a molecular biological study of NHE (Sardet, Franchi, & Pouyssegur, 1989). Their results and subsequent studies by other groups have shown that at least six isoforms of this gene family exist in the plasma membrane of mammalian cells, i.e. NHE1-5 (Orlowski, Kandasamy & Shull, 1992; Collins *et al.* 1993; Klanke *et al.* 1995) and NHE8 (Goyal, Vanden Heuvel & Aronson, 2003). The amino acid sequence deduced from all of these NHE cDNAs showed similar membrane spanning domains, but with low homology in the cytosolic C-terminus region, which contains several regulatory domains. The NHE1 isoform is expressed widely in most cell types, thus is believed to function as a "housekeeper" responsible for normal pH_i regulation. The NHE2, NHE3 and NHE4 isoforms are mainly found in epithelial tissues, where they are probably involved in the transepithelial Na^+ transport (Collins *et al.* 1993; Orlowski, 1993). Klanke *et al.* (1995) and Baird *et al.* (1999) cloned the NHE5 isoform and showed that NHE5 protein can be detected in multiple regions of the brain. The novel NHE8 isoform is expressed in the proximal tubule of kidney (Goyal, Vanden Heuvel & Aronson, 2003). In addition to the aforementioned six isoforms found on plasma membrane, isoforms NHE6 and NHE7 have been identified on subcellular membranes recently. NHE6 is found in recycling endosomes, where it may regulate endosomal pH and volume (Numata, Petrecca, Lake & Orlowski, 1998; Brett, Wei, Donowitz & Rao, 2002).

Immunocytological analyses showed NHE7 is predominately localised in the trans-Golgi network (Numata & Orlowski, 2001).

2. **Cl^--HCO_3^- exchange (AE)**: In 1878, Nasse discovered that exposing erythrocytes to CO_2 caused a loss of Cl^- from the serum, a phenomenon referred to as the "chloride shift". This was the first evidence of the existence of Cl^--HCO_3^- exchange. This exchanger was also known as the "band 3 protein", which relates to its purification from erythrocyte by SDS gel electrophoresis (Fairbanks, Steck, & Wallach, 1971). Band 3 protein is abundantly expressed in the erythrocyte where it allows efficient transmembrane passage of HCO_3^- ions. In this way, it is estimated that the Cl^--HCO_3^- exchanger promotes the transport capacity of CO_2 in blood up to 4-5 fold (see Jennings, 1989 and Geers & Gros, 2000 for review). The Cl^--HCO_3^- exchanger is an electroneutral carrier, inhibited by stilbene derivatives such as SITS (4-acetamido-4'-isothiocyano-2,2'-disulphonic stilbene) and DIDS (4,4'-diisothiocyanatostilbene-2,2'-disulphonic acid) (Cabantchik & Rothstein, 1974; Lambert & Lowe, 1978). Kinetics studies showed Cl^--HCO_3^- exchange mediated by band 3 protein proceeds via a ping-pong mechanism (Falke & Chan, 1985; Falke, Kanes & Chan, 1985). Under physiological conditions the transmembrane gradients favour Cl^- influx and HCO_3^- efflux, that is, the exchanger act as an *acid loader*. This is referred to as the "forward transport mode". A similar Cl^--HCO_3^- exchange has also been found to act as an acid loader in many other tissues such as cardiac Purkinje fibre (Vaughan-Jones, 1979), bladder epithelium (Fischer, Husted & Steinmetz, 1983), smooth muscle (Aickin & Brading, 1984) and liver cells (Meier, Knickelbein, Moseley, Dobbins & Boyer, 1985). Only in cells with very elevated $[Cl]_i$ could the exchanger theoretically

function as an acid extruder. Cl^--HCO_3^- exchange also plays a role in cell volume regulation (Mason, Smith, Gracia-Soto & Grinstein, 1989) and intracellular Cl^- regulation (Vaughan-Jones, 1979; 1982; Aickin & Brading, 1984).

Band 3 protein belongs to SLC4 (for Solute Linked Carrier 4) transporter superfamily, which also comprises other HCO_3^- dependent transporters, including NCBE and NBC (see below). Kopito & Lodish (1985) cloned and sequenced the 100 kDa band 3 protein and named it AE1 (for Anion Exchanger 1). Molecular cloning studies subsequently demonstrated the existence of four AE genes, referred to as AE1-4 (also named SLC4A1-3 and SLC4A9, respectively) (see Alper, 1991; Alper, Darman, Chernova & Dahl, 2002, for review). Through alternative splicing each gene can encode more than one protein product. So far, at least 11 functional AE proteins have been found in mammalian cells, with different postulated physiological roles. Members of all AE proteins share an amino acid sequence identity of 80% in the membrane-associated transport domain. AE proteins are predicted to form 12 membrane-spanning helices with both N-terminus and C-terminus oriented intracellularly, and contain two lysine residues as DIDS covalent binding sites (Pucéat, 1999). The topological structure of AE1 is shown in **Fig 1.6.** eAE1 is the band 3 protein originally found in erythrocytes mediating chloride shift. The alternative splicing product kAE1 (also known as AE1b) lacks the first 79 amino acids present in eAE1 near N-terminus and is found on the basolateral plasma membrane of the acid-secreting Type A intercalated cells (Sabolic, Brown, Gluck & Alper, 1997). AE2 proteins are widely expressed and appear to be involved in pH_i regulation (Demuth *et al.* 1986; Alper, Kopito, Libresco, & Lodish, 1988), showing lower sensitivity to DIDS than AE1

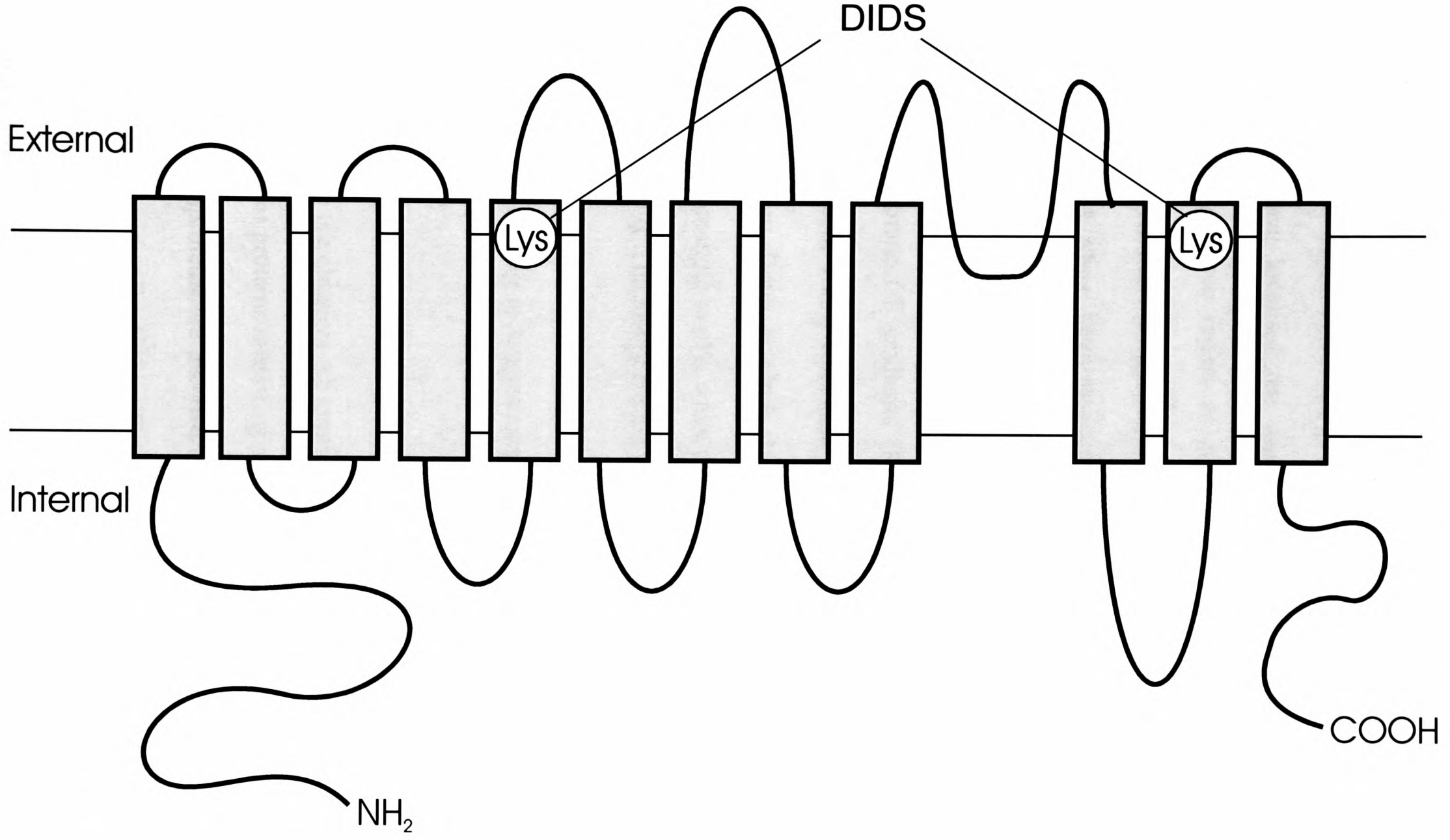


Figure 1.6

Membrane topology of Cl^--HCO_3^- exchanger AE1 (modified from Pucéat, 1999). The AE protein exhibit 12 transmembrane domains. Covalent binding sites of DIDS have been localised to two lysine residues in the 5^{th} and 11^{th} transmembrane domain of AE1.

and AE3 (Lee, Gunn & Kopito, 1991). Furthermore, recombinant AE2 protein is inhibited by intracellular acidosis, consistent with its postulated role in recovery from alkaline load (Humphreys, Jiang, Chernova, Alper, 1994). Alper and colleagues have localised the region responsible for pH_i sensitivity in NH_2-terminal cytoplasmic region of AE2 molecule using sequential NH_2-terminal deletion and chimeric polypeptides of AE1 and AE2 (Zhang, Chernova, Stuart-Tilley, Jiang & Alper, 1996; Stewart, Chernova, Kunes & Alper, 2001). bAE3 and cAE3 are splicing variant proteins encoded by AE3 gene, predominantly found in brain and heart, respectively. Their function may involve maintenance of pH_i and plasma membrane Cl^- gradients (Kopito, Lee, Simmons, Lindsey, Morgans & Schneider, 1989; Linn, Kudrycki & Shull, 1992; Yannoukakos, Stuart-Tilley, Fernandez, Fey, Duyk & Alper, 1994). Lee *et al.* (1990) showed evidence that AE3 is also sensitive to pH_i, while there is a report claiming the contrary (Sterling & Casey, 1999). The newly cloned AE4 is not sensitive to DIDS (Tsuganezawa *et al.* 2001). Its amino acid sequence is highly homologous to that of Na^+-dependent transporters, leading to suggestions that AE4 is probably another NBC isoform (see below).

In addition to the classical AE proteins listed above, recent studies have identified a new group of proteins mediating anion exchange (reviewed by Everett & Green, 1999). These proteins are encoded by SLC26 (for Solute Linked Carrier 26) gene family and structurally distinct from the aforementioned AE transporter proteins. They were originally believed to mediate sulfate/formate/oxalate transport in renal and intestinal tissue. However, at least five of them (SLC26A2-4 and SLC26A6-7) have been shown to function as Cl^--HCO_3^- exchanger under physiological

conditions (Satoh, Susaki, Shukunami, Iyama, Negoro & Hiraki, 1998; Melvin, Park, Richardson, Schultheis & Shull, 1999; Lohi *et al.* 2000; Soleimani *et al.* 2001; Petrovic *et al.* 2003).

It should be added that, another anion exchanger, Cl^--OH^- exchanger, has also been found in cardiomyocyte (Sun, Leem & Vaughan-Jones, 1996; Leem & Vaughan-Jones, 1997). At present the molecular identity of Cl^--OH^- exchanger has not been determined, therefore it is not known whether the Cl^--OH^- exchanger is encoded by any of the genes mentioned above.

3. **Na^+-dependent Cl^--HCO_3^- exchange (NCBE)**: Thomas (1976) and Russell & Boron (1976) observed that pH_i recovery from intracellular acidosis in the snail neurone and squid giant axon, respectively, could be stimulated in HCO_3^-/CO_2–buffered solution and inhibited by stilbene derivatives. This recovery in the snail neurone is also Na^+-dependent and electroneutral (Thomas, 1977). Thomas proposed a model (the so-called '4-ion carrier model') stating that this exchange involves influx of Na^+ and HCO_3^- ions coupled to efflux of Cl^- and H^+ ions. Alternatively, Boron (1985) proposed an "ion pair" model, in which the influx of the ion pair $NaCO_3^-$ is coupled to the efflux of one Cl^- ion. The exact nature of its transport cycle is still unknown. As there is no direct evidence for the involvement of H^+ ions, it will be referred to as "Na^+-dependent Cl^--HCO_3 exchange". Like AE, NCBE is also inhibited by DIDS. Since the work of Boron and Thomas, several Na^+-dependent Cl^--HCO_3^- exchangers have been identified in vertebrate cells, including embryonic chick heart cells (Liu, Piwinca-Worms & Lieberman, 1990), astrocytes (Shrode & Putnam, 1994), hippocampal neurones (Schwiening

& Boron, 1994), sperm (Zeng, Oberdorf & Florman, 1996), and vascular endothelial cells (Sun, Vaughan-Jones & Kambayashi, 1999). It has also been reported to play a role in cell volume regulation, particularly during osmotic activation (Reusch, Lowe & Ives, 1995).

Recently, Na^+-dependent Cl^--HCO_3^- exchanger has been cloned from mouse insulinoma MIN6 cell line and *Drosophila* embryo, separately (Wang, Yano, Nagashima & Seino, 2000; Romero *et al.* 2000). Boron and colleagues also identified a similar protein in human brain, testis and kidney (Grichtchenko, Choi, Zhong, Bray-Ward, Russell & Boron, 2001)[3]. Like AE, hydropathy analysis predicts that NCBE has 12 putative membrane-spanning segments. Comparison of the amino acid sequences between NCBE and other bicarbonate-dependent transporters shows that the cloned mouse NCBE shares over 70% and 30% amino acid identity with human NBC (see below) and mouse AE, respectively.

4. **Na^+-HCO_3^- cotransport (NBC)**: Na^+-HCO_3 cotransport was first described by Boron and his colleagues in proximal renal tubule of salamander (Boron & Boulpaep, 1983). Their experiment showed this cotransporter to be electrogenic, with an estimated Na^+ : HCO_3 stoichiometric ratio of 1:3. It normally mediates Na^+ and HCO_3 efflux across the basolateral membrane of proximal tubule, thus is proposed to be responsible for Na^+ and HCO_3^- reabsorption. A similar cotransporter was subsequently identified in mammalian corneal endothelia (Jentsch, Keller, Koch, & Wiederholt, 1984), renal proximal tubule (Yoshitomi,

[3] Na^+-dependent Cl^--HCO_3 exchanger genes cloned from different tissue and species are given different names. Those cloned from mouse MIN6 cell line, *Drosophila* embryo and human brain are named NCBE, NDAE1 and NDCBE1, respectively.

Burckhardt & Fromter, 1985) and hepatocytes (Fitz, Persico & Scharschmidt, 1989). Electrogenic Na^+-HCO_3^- cotransporter was also found in the glial cell of leech central nervous system by Deitmer and colleagues (Deitmer & Schlue, 1989). However, its Na^+ : HCO_3^- stoichiometric ratio was determined to be 1: 2, suggesting that this cotransporter operates as an acid extruder during membrane depolarisation, and an acid loader during hyperpolarisation (Deitmer & Szatkowski, 1990; Deitmer & Schneider, 1995). Neuronal activity in leech central nervous system is accompanied by an alkalisation in the extracellular space, probably resulting from H^+ influx into neurones via glutamate receptor. In addition, $[K^+]_o$ is also increased. High $[K^+]_o$ induces membrane depolarisation in the adjacent glial cells, leading to HCO_3^- influx (i.e. acid-equivalent efflux) on electrogenic Na^+-HCO_3^- cotransporter. In this way, the cotransporter modulates stimulus-evoked pH_o transients and reduces extracellular alkalisation produced by neuronal activity (Rose & Deitmer, 1995a; 1995b; reviewed in Deitmer & Rose, 1996). Later studies revealed similar cotransporters in pancreas (Ishiguro, Steward, Lindsay & Case, 1996) and astrocytes (Bevensee, Apkon & Boron, 1997), both with 1 Na^+ : 2 HCO_3^- stoichiometry. In some tissues like colon and parotid however, the stoichiometry is not well defined yet (for review, see Boron & Boulpape, 1989; Romero & Boron, 1999). The coupling ratio of Na^+ : HCO_3^- is physiologically significant, since at resting membrane potential, an electrogenic cotransporter with a 1:2 stoichiometry would mediate Na^+ and HCO_3^- influx in most mammalian cells, while that with a 1:3 stoichiometry can only mediate efflux. It has recently been reported that the electrogenic Na^+-HCO_3 cotransporter can alter its stoichiometry from 1:3 to 1:2, depending on cellular conditions (Planelles, Thomas & Anagnostopoulos, 1993; Gross *et al.* 2000).

Four NBC isoforms (NBC1-4) have been cloned so far (for review, see Romero & Boron, 1999; Soleimani, 2002). Human NBC1 shows a high level of expression in kidney (particularly proximal tubule) and pancreas. Originally cloned from salamander proximal tubules, the kidney NBC1 (denoted as kNBC1) has 1035 amino acids and 10 deduced transmembrane domains, sharing 30-35% identity to AE1-AE3 at the amino acid level (Romero, Hediger, Boulpaep & Boron, 1997). Pancreatic NBC1 (pNBC1) is a splice variant of kNBC1, and shares 93% amino acid identity with kNBC1 (Abuladze *et al.* 1998). In addition, Schmitt *et al.* (2000) detected significant levels of NBC1 mRNA and protein in glia and neurones of rat brain. Ishibashi, Sasaki & Marumo (1998) cloned NBC2 isoform from human retina, where it is presumably responsible for the light-induced extracellular alkalisation. It has highest expression in testis and spleen, and a moderate one in colon and muscle. Subsequent studies revealed that NBC2 is almost identical to NBCn1, which encodes electroneutral Na^+-HCO_3^- cotransporter (see below). The NBC3 isoform was cloned from human neuroepithelial NT-2 cell line (Amlal, Burnham & Soleimani, 1999). NBC3 is also referred to as NDCBE1 (see above) by Boron and colleagues, suggesting it functions as Na^+-dependent Cl^--HCO_3^- exchanger (Grichtchenko *et al.* 2001). However, the Cl^-_i dependency was not observed in the original report by Amlal *et al.* NBC3 has been found to be highly expressed in central nervous system, where it probably plays a role in pH_i regulation in neurones. NBC3 shows 72% identity with NBC2 and 53% identity with NBC1. The novel isoform NBC4 was cloned from human heart, encoding a protein of 1074 residues. It has the highest expression levels in liver, testes and spleen (Pushkin *et al.* 2000). Functional studies showed that NBC4 protein is an

electrogenic Na^+-HCO_3^- cotransporter (Virkki, Wilson, Vaughan-Jones & Boron, 2002).

Vaughan-Jones and colleagues reported an electroneutral Na^+-HCO_3^- cotransport in mammalian cardiomyocyte, with a Na^+ : HCO_3^- stoichiometry of 1:1 (Dart & Vaughan-Jones, 1992; Lagadic-Gossmann, Buckler & Vaughan-Jones, 1992), since they found no membrane potential dependence of the fluxes mediated by the cotransporter. This electroneutral cotransporter mediates HCO_3^- ions influx and acts as an acid extruder. A similar electroneutral cotransport has also been reported in smooth muscle cells (Aickin, 1994). In contrast, Cingolani and co-workers proposed an electrogenic cotransport in heart, based on the observation that in cat papillary muscle, the Na^+-dependent and DIDS-sensitive HCO_3^- influx is reversibly increased in high K^+_o solution (Camilion de Hurtado, Perez & Cingolani, 1995). Recently, Boron and his colleagues cloned an electrogenic Na^+-HCO_3^- cotransporter from human heart (designated hhNBC) and another electroneutral Na^+-HCO_3^- cotransporter from rat vascular smooth muscle (designated NBCn1), respectively (Choi, Romero, Khandoudi, Bril & Boron, 1999; Choi, Aalkjaer, Boulpaep & Boron, 2000). hhNBC is identical to human kNBC1, except for the first 85 amino acids in amino terminus. For NBCn1 (alternatively named NBC2) protein, it has 1218 amino acids and shares 55-57% identity with electrogenic NBC and 33-43% identity with AE. Although other NBC proteins are sensitive to DIDS inhibition, NBCn1 is not. Furthermore, a Northern blot of rat heart tissue also shows hybridisation to NBCn1 cDNA probe. This finding suggests that electrogenic and electroneutral Na^+-HCO_3^- cotransporter may co-exist in heart.

5. **HCO_3^- permeable channel**: Kaila and colleagues have shown that the activated $GABA_A$ receptor anion channels are also permeable to HCO_3^- ions, with a selectivity ratio (P_{HCO3}/P_{Cl}) of 0.34 and 0.18 in crayfish muscle and neurone (Kaila & Voipio, 1987; Kaila, Saarikoski & Voipio, 1990; Kaila, Voipio, Paalasmaa, Pasternack & Deisz, 1993). HCO_3 fluxes through this ligand-gated anion channel could therefore be important in regulating neuronal pH_i and pH_o. Moreover, the depolarisation during neuronal activity may reverse HCO_3^- flux, resulting in pH_o acidification, which may lead to neuronal inhibition (Chesler & Kaila, 1992). A similar mechanism was also observed in rat medullary ventral respiratory group neurones, in which glycine evoked a fall in pH_i due to HCO_3^- efflux through glycine receptor anion channels (Lückermann, Trapp & Ballanyi, 1997). Such a mechanism could also play an important role in mediating central acid chemoreception.

6. **H^+ channel**: The H^+ channel was discovered in snail neurones (Thomas & Meech, 1982). Subsequently, it has been described in amphibian (*Ambystoma*) oocytes (Barish & Baud, 1984), rat alveolar epithelial cells (DeCoursey, 1991), macrophages (Kapus, Romanek, Qu, Rotstein & Grinstein, 1993) and neutrophils (DeCoursey & Cherny, 1993). The H^+ channel is gated by membrane potential and opens upon depolarisation. It is also activated by low pH_i while inhibited by low pH_o. The result of this regulation is that the H^+ channel opens only at potentials positive to the equilibrium potential of H^+ (E_H) and therefore conducts only outward H^+ current. These properties seem ideally suited for the H^+ channel to function as an acid extrusion mechanism during membrane depolarisation, while precluding acid influx at resting potentials (reviewed by Lukacs, Kapus, Nanda,

Romanek, & Grinstein, 1993; DeCoursey & Cherny 2000). There is also evidence that another H^+ channel is associated with NADPH oxidase (the enzyme responsible for producing O_2^-.) in phagocytes (Schrenzel *et al.* 1998; Bánfi *et al.* 2000), where it serves to eliminate the excess positive charge caused by the secretion of O_2^-. during respiratory burst (Henderson, Chappell & Jones, 1987). The H^+ channel is blocked by transition metals Zn^{2+} and Cd^{2+} at micromolar concentrations (Cherny & DeCoursey, 1999).

7. **K^+-H^+ transporter**: Two different classes of K^+-H^+ electroneutral transporter have been proposed so far: a primary active K^+-H^+ ATPase and a secondary active K^+-H^+ exchanger. The K^+-H^+ ATPase requires ATP hydrolysis as an energy source. It was originally found in parietal cells of gastric membrane, where it is responsible for gastric acid secretion (Sachs, Chang, Rabon, Schackman, Lewin & Saccomani, 1976; see Munson, Lambrecht, Shin & Sachs, 2000 for review). This gastric K^+-H^+ ATPase is inhibited by benzimidazole derivatives such as omeprazole (a gastric acid control drug) (Keeling, Fallowfield & Underwood, 1987) and SCH 28080 (Wallmark *et al.* 1987; Hofer & Machen, 1992). Subsequent studies identified other closely related K^+-H^+ ATPases in colon and kidney (Cougnon, Planelles, Crowson, Shull, Rossier & Jaisser, 1996; Silver & Soleimani, 1999). Structural research revealed that these K^+-H^+ ATPases and Na^+-K^+ ATPase (also known as Na^+-K^+ pump) are related members of the P-type ion motive ATPase family (reviewed by Jaisser & Beggah, 1999).

Unlike K^+-H^+ ATPase, K^+-H^+ exchanger mediates K^+ efflux in exchange for H^+ influx under normal physiological conditions. Its presence has been proposed in

corneal epithelium (Bonanno, 1991) and renal epithelial cells (Graber & Pastoriza-Munoz, 1993), where it is suggested to be involved in acid loading and cell volume regulation. However, speculations have been raised that the K^+-H^+ exchange activity described in these cell types could be due to nigericin contamination introduced accidentally during the calibration of pH-sensitive fluoroprobe (Richmond & Vaughan-Jones, 1997; see below).

8. **V-type H^+ ATPase**: Kirshner (1962) demonstrated the accumulation of catecholamines into chromaffin granules is driven by an ATP-dependent H^+ gradient. Subsequently, it was found that the H^+ gradient is maintained by an electrogenic H^+ ATPase, which pumps H^+ into the granule (Cidon & Nelson, 1983). Other investigators showed that a similar H^+ ATPase is also present in vacuoles of plant and fungi cells (Kakinuma, Ohsumi & Anraku, 1981), hence it is named V-type H^+ ATPase (V for vacuole) (for review, see Wieczorek, Brown, Grinstein, Ehrenfeld & Harvey, 1999). Gene analysis revealed that the V-type H^+ ATPase is closely related to F-type H^+ ATPase (Bowman, Tenney & Bowman, 1988; Nelson & Nelson, 1989), although in eukaryotic cells the latter only functions as an ATP synthase, utilizing the H^+ gradient to make ATP (Mitchell, 1961). Gluck and colleagues showed that, V-type H^+ ATPase is also present on the apical membrane of Type A intercalated cells in vertebrate kidney, where it is responsible for acid secretion (Gluck & Al-Awqati, 1984; Brown, Gluck & Hartwig, 1987). Mutations in these genes are linked to recessive distal renal tubular acidosis (dRTA). Additionally, V-type H^+ ATPase expressed in osteoclasts is involved in bone resorption (Chatterjee *et al.* 1992).

9. **Other acid-equivalent transporters**: In addition to the transport systems listed above, which might be recognised as "primary acid-equivalent transporter", there are other weak acid transporters that may also influence pH_i. For example, H^+-Lac^- transporter, a member of monocarboxylate transporter (MCT) family, transports one H^+ ion with one lactate anion molecule (Fafournoux, Demigne & Remesy, 1985; Poole & Halestrap, 1993; see Halestrap & Price, 1999 for review). However, I will not introduce them in further detail.

Acid-equivalent Transport Systems in Type I Cells

Thus far, there have been few studies of the pH_i regulation in type I cells. The results of these studies are summarised below:

1. **Na^+-H^+ exchange**: As in other cells, Na^+-H^+ exchange activity is found in type I cells. It is activated as pH_i falls, therefore is responsible for acid extrusion during intracellular acidosis. So far, this is the only HCO_3^--independent acid-equivalent transporter found in type I cells (Buckler, Vaughan-Jones, Peers, Lagadic-Gossmann & Nye, 1991a). It is inhibited by EIPA and amiloride, both are common drugs used to inhibit Na^+-H^+ exchange activity in other cell types. However, the molecular isoform of NHE in type I cells remains unknown.

2. **Cl^--HCO_3^- exchange**: Buckler *et al.* (1991a) showed in Cl^--free solutions, the reverse transport mode of Cl^--HCO_3 exchange is inhibited by DIDS. Cl^--HCO_3^- exchange also promotes acid loading during intracellular alkalosis (Richmond,

1993). Although there is speculation that the Cl^--HCO_3^- exchanger operates as an acid loader at resting pH_i, it has never been proved.

3. **Na^+-dependent Cl^--HCO_3^- exchange**: Earlier studies proposed a role of Na^+-dependent and HCO_3^--dependent transporter in mediating acid efflux, but it was not clear whether it is Na^+-dependent Cl^--HCO_3^- exchange or Na^+-HCO_3^- co-transporter (Buckler *et al.* 1991a). Richmond (1993) subsequently provided evidence that the Na^+-dependent and HCO_3^--dependent acid efflux is also Cl^--dependent, suggesting the involvement of Na^+-dependent Cl^--HCO_3^- exchange. It was therefore concluded that Na^+-dependent Cl^--HCO_3^- exchange is also responsible for acid extrusion in responding to intracellular acidosis.

4. **HCO_3^- channel**: Stea & Nurse (1989) reported a Cl^- channel which is also permeable to HCO_3^- ions in rat carotid body type I cells. It has a selectivity ratio (P_{HCO3}/P_{Cl}) of 0.71, and a relatively large conductance of 296 pS. It is blocked by typical Cl^- channel blockers such as anthracene-9-carboxylic acid (9-AC) and NPPB, but, in general, it is insensitive to stilbene derivatives. The electrochemical equilibrium potential of HCO_3^- ions (E_{HCO3}) can be estimated from the following equation assuming an open system for CO_2:

$$E_{HCO3} = \frac{2.3RT}{F} \times (pH_i - pH_o) \qquad \textbf{[Eqn. 1.6]}$$

It follows that under resting conditions, E_{HCO3} = -18 mV. So it would be expected that such anion channel would mediate HCO_3^- ion efflux (i.e. acid influx) when

pH_o is reduced. In this way, it may play a role in acid loading in type I cells. The identity of this anion channel is still not clarified since its lack of voltage sensitivity is remarkably distinct from the ClC channel family (Jentsch, Gunther, Pusch & Schwappach, 1995). Carpenter & Peers (1997) described a swelling- and cAMP-activated Cl^- current in type I cells, which may serve a candidate for the HCO_3^- ion permeant channel. However, it is different from the HCO_3^- channel previously reported by Stea & Nurse in terms of DIDS and cAMP sensitivity, and rectification properties.

5. **K^+-H^+ exchanger**: Wilding *et al.* observed a marked alkalisation under high K^+ conditions (Wilding, Cheng & Roos, 1992). They proposed that in type I cells, K^+-H^+ exchanger plays a major role in pH_i regulation, therefore, it would be responsible for the high $\Delta pH_i/\Delta pH_o$ ratio. Richmond & Vaughan-Jones (1997), however, have recently concluded that K^+-H^+ exchanger is not native to the carotid body type-1 cell. They argued that the previously reported K^+-H^+ exchange was an artefact caused by nigericin (a microbial K^+-H^+ exchanger) contamination, due to inadequate cleaning of experimental apparatus after post-experimental *in situ* calibration of the pH-sensitive fluoroprobe by nigericin (see Chapter 2). Despite this artefact, Richmond (1993) confirmed the high sensitivity of pH_i to changes in pH_o in type I cells is genuine, even after rigorous cleansing of the experimental set up.

In summary, at the moment the following acid-equivalent transport systems are known to exist in carotid body type I cells: Na^+-H^+ exchange, Na^+-dependent Cl^--HCO_3^-

exchange (both have been shown as acid extruders), Cl^--HCO_3^- exchange, and a putative HCO_3^- channel, which has not been investigated (**Fig 1.7**).

Summary of Introduction

So far, this Introduction has reviewed the basic anatomy and physiology of the carotid body, particularly on acid chemoreception by type I cells. In brief, changes in Pa_{CO2}, pHa and Pa_{O2} elicit electrical activity in the type I cell, resulting in synaptic activation of the carotid sinus nerve, sending chemosensory signals to the medulla to regulate ventilation. It has been shown that both pH_i and pH_o are key factors in the acid signalling pathway in type I cells. To serve as a chemoreceptor, pH_i in the type I cell is very sensitive to changes in pH_o. However, one intriguing feature of the type I cell is that it still possesses several effective acid-equivalent transport systems, and is able to regulate its pH_i efficiently. Therefore, the high $\Delta pH_i/\Delta pH_o$ ratio in the type I cell must be a result of dynamic balance between acid influx, acid efflux and intracellular background acid loading.

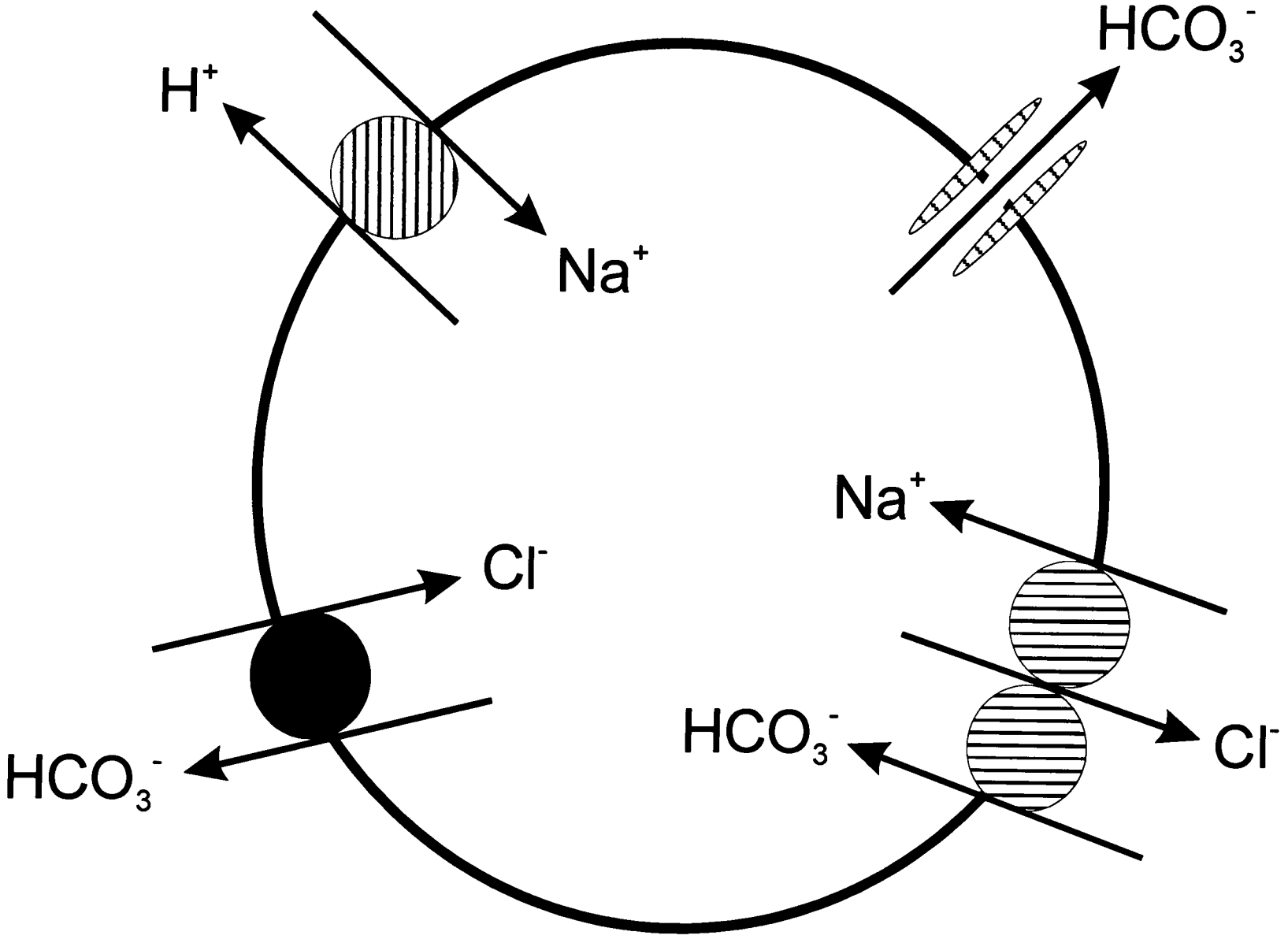


Figure 1.7

Schematic diagram of acid-equivalent transport systems proposed to exist in carotid body type I cell: Na^+-H^+ exchange, Na^+-dependent Cl^--HCO_3^- exchange, Cl^--HCO_3^- exchange, and a putative HCO_3^- channel.

The Aims of this Thesis

In light of the pivotal importance of pH_i and its dependence on pH_o in type I cells, this thesis aims to investigate the following topics:

1. The mechanisms responsible for acid influx in type I cells.
2. The relative contribution of each mechanism to acid influx.
3. The pharmacological and kinetic properties of those mechanisms involved.
4. Based on above results, to provide a preliminary model for the pH_i *versus* pH_o relationship in type I cells.

CHAPTER 2

Materials and Methods

Cell Isolation

Carotid type I cells were isolated from 10 to 16-day-old neonatal Sprague-Dawley rats (*Rattus norvegicus*). Rat pups were anaesthetized by inhaling 4% halothane (ICI) in O_2 through a facemask at approximately 0.4 (l/min). The skin between the clavicle and lower jaw was cut, adipose tissue and salivary glands were removed. Muscles running alongside the trachea were parted to reveal the carotid artery, and this was traced upwards to the carotid bifurcation. The connective tissue covering the bifurcation was removed, and the hypoglossal nerve was severed by forceps. The carotid body lies just above the bifurcation. Its appearance is as a pearly white lump. The occipital artery was broken and reflected. Both of the carotid bodies were removed with fine forceps and placed into ice-cold Dulbecco's phosphate-buffered saline (Sigma) with 900 μM $CaCl_2$ and 490 μM $MgCl_2$. This phosphate-buffered saline was previously equilibrated with O_2. The residual nerve and connective tissue was then removed from carotid bodies by forceps under a dissecting microscope. Afterwards, the carotid bodies were dissociated by incubation in approximately 2 ml enzyme solution for 23 min at 37 °C. The enzyme solution contains 0.5 mg/mL collagenase (Worthington Chemical Co.) and 0.2 mg/mL trypsin (Sigma) in low calcium phosphate-buffered saline. 9 ml of Ca-free and Mg-free phosphate-buffered saline was mixed with 0.65 ml of standard $CaCl_2$ and $MgCl_2$ phosphate-buffered saline, giving 60 μM $CaCl_2$ and 33 μM $MgCl_2$ as final concentrations. The enzyme

solution was filtered through a sterilised filter (pore diameter 0.2 μm) before use. After 23 min, the enzyme solution containing the carotid bodies was removed from the incubator and the carotid bodies were gently teased apart and cleaned under dissecting microscope with forceps. The carotid bodies were then incubated in the enzyme solution for a further 7 min before finally being transferred to a centrifuge tube. The cell suspension solution was centrifuged at 1000 rpm for 5 min. After the centrifugation, supernatant was decanted carefully. The enzyme solution was then replaced with approximately 2 ml 23 mM HCO_3^--buffered Ham's F-12 culture medium, containing insulin (84 U/L), penicillin (100 IU/mL), streptomycin (100 μg/mL) and 10% fetal calf serum. The culture medium was also filtered through a sterilised filter (pore diameter 0.2 μm) before use. The pellet was resuspended and triturated gently. Then the cell suspension was recentrifuged again at 1000 rpm for 5 min. This was followed by further trituration to disperse remaining tissue fragments. The cell suspension was then carefully placed onto poly-L-lysine-coated, 6 mm diameter cover slips. Finally, all the cells were maintained in 5% CO_2 / 95% air at 37 °C for 2-12 hrs before being used. Type I cells were identified by the appearance under phase contrast microscope as being near spherical and a phase bright appearance with a diameter of approximate 10 μm.

Solutions

(1) Standard CO_2/HCO_3^--buffered solution

Composition	Concentration (mM)
NaCl	117
KCl	4.5
NaHCO3	23
$MgCl_2$	1
$CaCl_2$	2.5
Glucose	11
Equilibrated with 5% CO_2 / 95% air, final pH 7.4 at 37 °C	

(2) pH 6.4 CO_2/HCO_3^--buffered solution

In the presence of CO_2/HCO_3^- buffer, a simulated metabolic acidosis was achieved by decreasing $NaHCO_3$ concentration to 2.3 mM with osmotic compensation of NaCl.

Composition	Concentration (mM)
NaCl	137.7
KCl	4.5
$NaHCO_3$	2.3
$MgCl_2$	1
$CaCl_2$	2.5
Glucose	11
Equilibrated with 5% CO_2 / 95% air, final pH 6.4 at 37 °C	

(3) pH 7.7 CO_2/HCO_3^--buffered solution

In the presence of CO_2/HCO_3^- buffer, a simulated metabolic alkalosis was achieved by increasing $NaHCO_3$ concentration to 46 mM with osmotic compensation of NaCl.

Composition	Concentration (mM)
NaCl	94
KCl	4.5
$NaHCO_3$	46
$MgCl_2$	1
$CaCl_2$	2.5
Glucose	11
Equilibrated with 5% CO_2 / 95% air, final pH 7.7 at 37 °C	

(4) HEPES-buffered HCO_3^--free standard Tyrode solution

Composition	Concentration (mM)
NaCl	140
KCl	4.5
$MgCl_2$	1
$CaCl_2$	2.5
HEPES	20
Glucose	11
Adjust pH with NaOH to 7.4 at 37 °C	

(5) pH 6.4 PIPES-buffered HCO_3^--free Tyrode solution

Composition	Concentration (mM)
NaCl	140
KCl	4.5
$MgCl_2$	1
$CaCl_2$	2.5
PIPES	20
Glucose	11
Adjust pH with NaOH to 6.4 at 37 °C	

For 20 mM ammonium chloride (NH_4Cl) or sodium acetate (CH_3COONa) solutions used in acid loading / alkali loading (see below), an equivalent concentration of NaCl was substituted by NH_4Cl or CH_3COONa, respectively, to maintain osmolality.

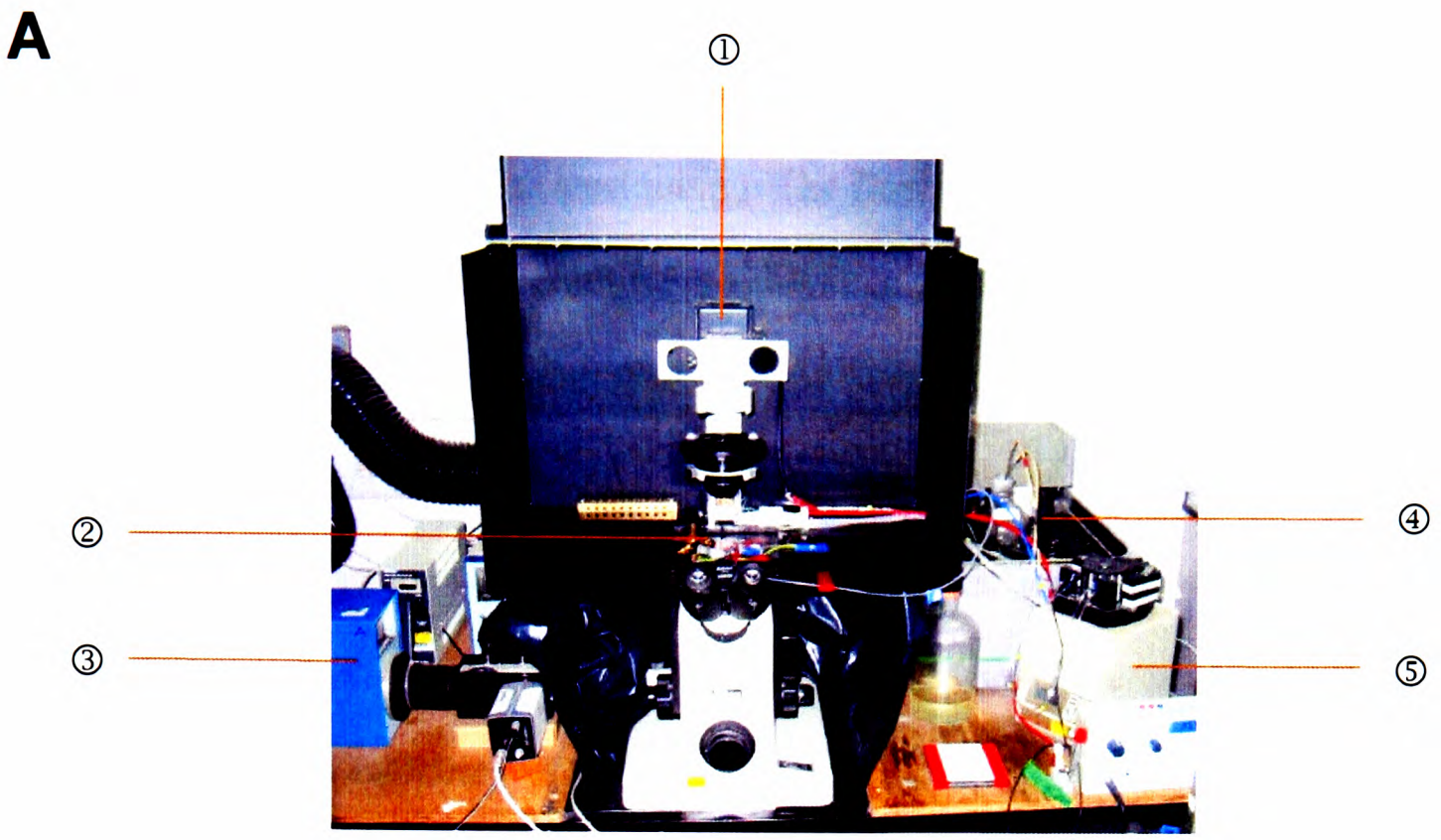
Nigericin calibration solutions contained (in mM): KCl 140; $MgCl_2$, 1; and nigericin, 10 μM; buffered with one of the following buffers and adjusted to respective pH at 37 °C: MES, 20 (pH 5.5); HEPES, 20 (pH 7.5); CAPSO, 20 (pH 9.5).

Drugs

All chemicals used in the solutions were from Sigma Chemical Co. (Poole, UK), unless stated otherwise. The composition of other solutions and the use of specific drugs are given in the chapters to which they are relevant.

Superfusion Apparatus

Fig 2.1 shows the experimental equipment used in the present study. Coverslips with cells attached were placed in a perfusion chamber with a volume of approximately 75 μl, of which the sides were made of perspex, while the bottom surface was sealed with



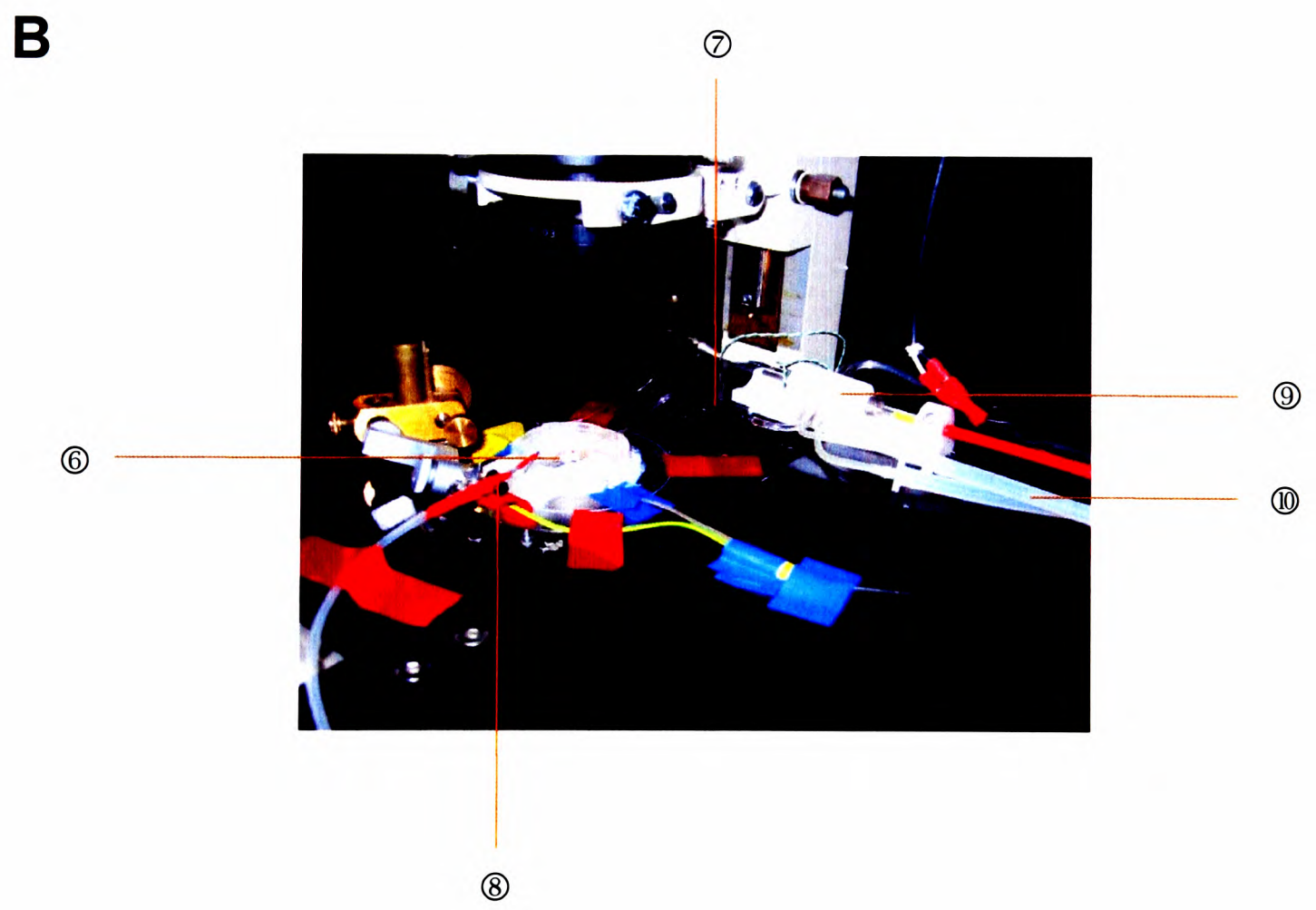


Figure 2.1

Photograph of the experimental equipment used in the present study. ***A***, Overview: ① headlight of microscope ② stage of microscope (see ***B*** for details) ③ photomultiplier tube ④ solutions in water bath ⑤ peristaltic pump. ***B***, Close-up view of the stage of microscope: ⑥ perfusion chamber ⑦ heating coil ⑧ suction tube ⑨ two-way tap ⑩ solution tubes.

a large cover-glass (see **Fig 2.1B**). A peristaltic pump was used to force solution into the chamber through stainless steel tubing. The flow rate was about 2 ml/min. During the experiment two lines of solution were simultaneously pumped through a specially designed two-way tap composed of plastic and perspex, as shown in **Fig 2.2**. This tap was used to switch these two input solution lines between a chamber output and a waste line. This was to ensure rapid and smooth changes from one solution to another. The tap was mechanically coupled to a lever outside the enclosed apparatus, permitting remote switching.

Solutions were preheated in a water bath, and reheated immediately prior to entering the chamber, by a heating coil linked to a thermistor that recorded the temperature in the chamber. In this way the temperature of solutions was maintained at 36±1 °C. Perfusate was sucked out from the chamber through a syringe needle coupled to a vacuum water-pump. The half-time for solution exchange in the chamber was about 3 s (Buckler & Vaughan-Jones, 1990).

Measurement of Intracellular pH

Microspectrofluorimetry

Microspectrofluorimetry was used to measure intracellular pH (pH_i) (Buckler & Vaughan-Jones, 1990). The pH-sensitive, dual-emmision fluorescent dye, carboxyseminapthorhoda-fluor-1 (carboxy-SNARF-1 or SNARF, briefly) was used as the fluoroprobe. The emission spectra of SNARF are shown in **Fig 2.3**, in which the SNARF samples were excited at 540±12 nm. This emission spectrum is shifted by

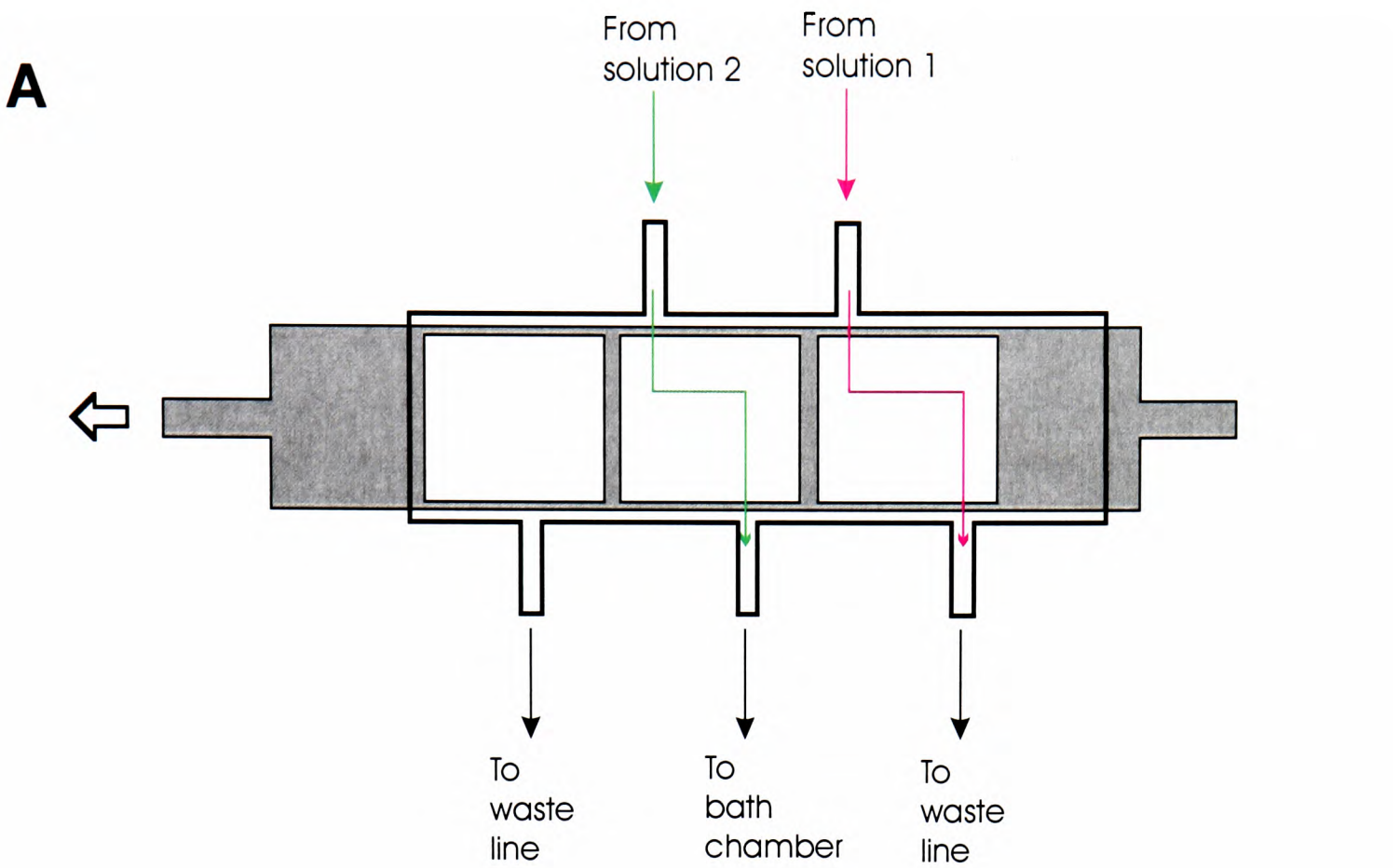


Figure 2.2

Schematic representation showing how the two-way tap works. ***A***, Solution 1 flows into the bath chamber, solution 2 enters the waste line. ***B***, After the lever connected to the tap is swithced, now solution 2 perfuses the bath chamber, while solution 1 entering the waste line.

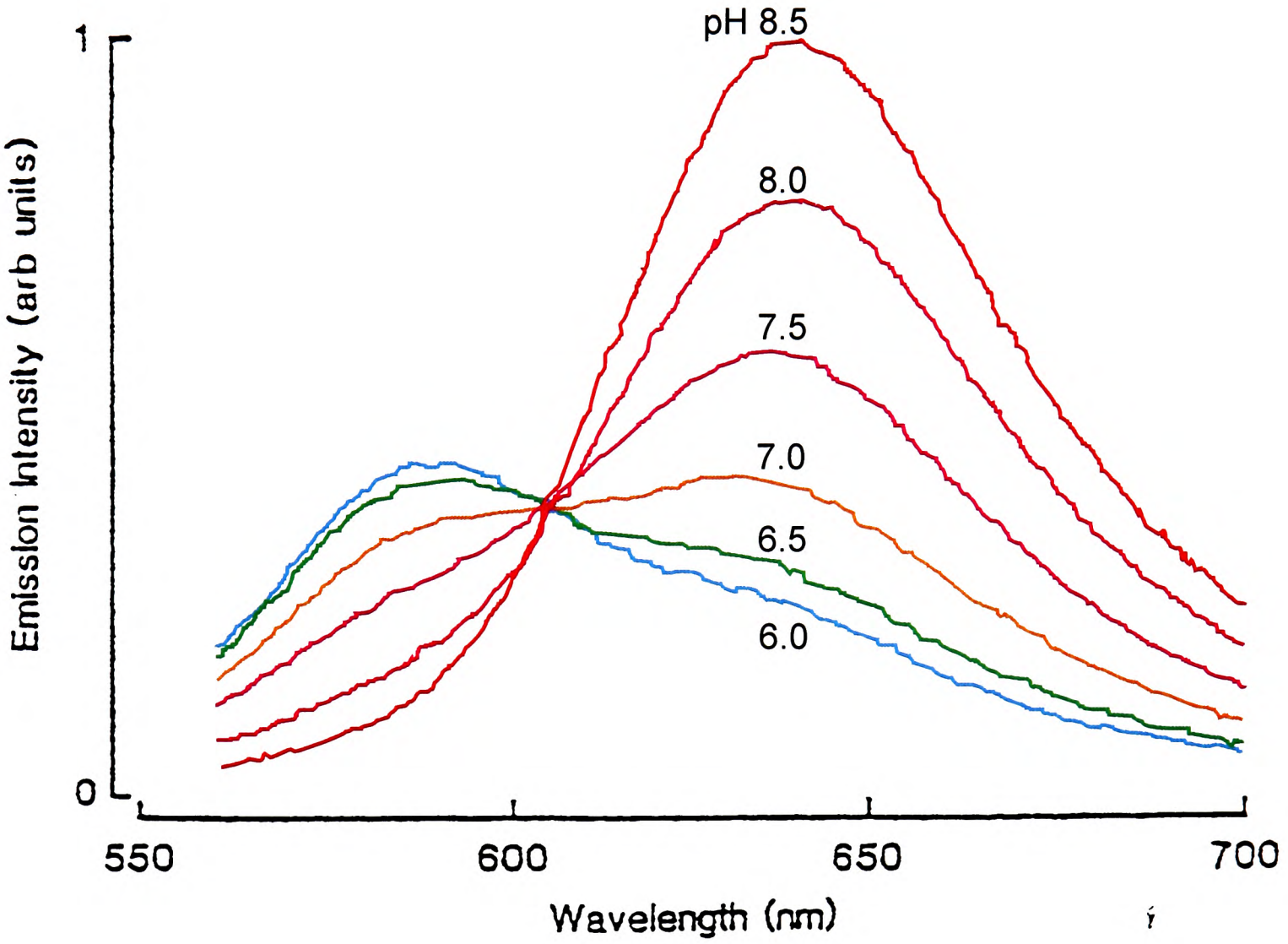


Figure 2.3

Uncorrected emission spectra for 25 μM carboxy-SNARF-1 excited at 540±12 nm, recorded in a spectrofluorimeter (Applied Photophysics, London, UK), emission slit width 2.5 nm, path length 1 cm. Solutions contained 140 mM KCl, 1 mM $MgCl_2$, 10 mM HEPES or 10 mM PIPES. PH was adjusted to 6.0, 7.0, 7.5, 8.0 and 8.5 with NaOH at room temperature. Reproduced from Buckler & Vaughan-Jones (1990).

protonation: the protonated form has an emission maximum at 588 nm and the unprotonated form has maximum at 638 nm, respectively. Thus, as pH increases, the emission intensity measured at 590 nm (mainly from protonated form) decreases, while that measured at 640 nm (mainly from unprotonated form) increases inversely. This feature allows SNARF to be a sensitive pH fluoroprobe, since it responds to a small pH change with large differences between the ratios (R) of emitted fluorescence intensity measured at 590 nm (F_{590}) to 640 nm (F_{640}).

$$R = \frac{F_{590}}{F_{640}} \qquad \textbf{[Eqn. 2.1]}$$

The ratio (R) was then transformed into pH according to the following relationship:

$$pH = pK_a + \log\frac{(R_{max} - R)}{(R - R_{min})} + \log F640_{min/max} \qquad \textbf{[Eqn. 2.2]}$$

The derivation of this formula is based on the principle suggested by Grynkiewicz, Poenie & Tsien (1985). By using this ratiometric approach the measurement of pH is independent of total dye concentration, optical path length and absolute sensitivity of the instrument. Moreover, the choice of SNARF as fluoroprobe has another advantage, since its pK_a is around 7.5 to 7.8, it is particularly suitable for use within the physiological range of pH_i.

Loading carboxy-SNARF-1 into type I cells

Cell membrane-permeable carboxy-SNARF-1-acetoxy-methyl ester (SNARF-1-AM) (Molecular Probes, Eugene, Oregon, USA) was used in fluorescent dye loading. In its

esterified form SNARF-1-AM is highly membrane-permeable, so cells can take up the fluoroprobe very quickly. Once it enters the cell, intracellular esterases hydrolyse the ester bond releasing the charged and membrane-impermeable, carboxylic acid SNARF-1. Thus SNARF-1 becomes trapped in the cytoplasm. SNARF-1-AM was dissolved in dimethyl sulphoxide at a concentration of 1mg/ml and stored at –70 °C in 50 µl aliquots. Before use, one aliquot was defrosted and diluted with cell culture medium to a final concentration of around 5 µM SNARF-1-AM. Cover slips with attached type I cells were incubated in this solution for 10-15 min at room temperature.

Microspectrofluorimetry set-up

The basic design of the microspectrofluorimetry set-up is outlined in **Fig 2.4**. SNARF-loaded cells were placed in the perfusion chamber, which, in turn, was mounted on the stage of an inverted microscope (Nikon) designed for epifluorescence measurements. During the experiment, a carotid body type I cell was firstly chosen, the microscope was focused, and then the cell was illuminated. The excitation light was provided by a 75 W Xenon lamp, then filtered at a 540±12 nm (interference filter). This light beam again was diverted by a 560 nm long-pass dichoric mirror, and focused onto the target cell through the X40 objective (Fluor 40/1.30 oil Ph4DL). After the excitation beam excited the SNARF inside the cell, the fluorescence beam emitted from the cell was split by a 610 nm long-pass dichroic mirror into two, and filtered at 590±5 nm and 640±5 nm, individually. Both of the beams were respectively detected by two trialkali S20 photomultiplier tubes (Thorn EMI, UK), which were air-cooled to around –20 °C to reduce dark currents and increase the signal-to-noise ratio. The current from the photomultiplier tubes was converted to voltage by a current/voltage (I/V) converter

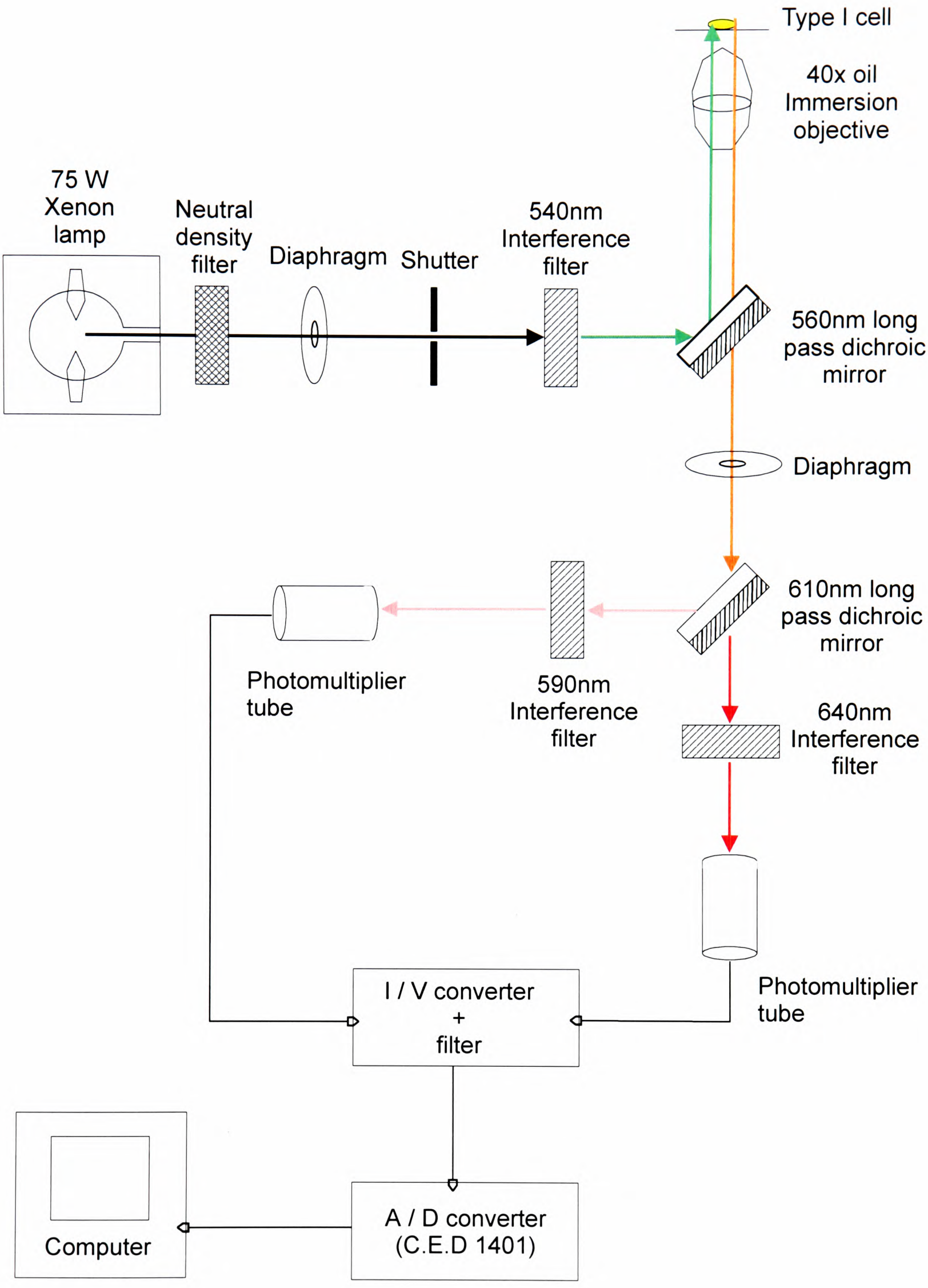


Figure 2.4

Schematic diagram of the equipment used for recording carboxy-SNARF-1 fluorescence from carotid body type I cells (after Buckler & Vaughan-Jones, 1990).

and filtered at 10 Hz. The filtered signals were then passed to an analogue-digital converter (CED 1401, Cambridge Electronic Design) sampling the signals at 0.5 kHz. The digitised signals were then passed to a microcomputer (Dan Computer), which integrated both individual wavelength signals over 0.5 s and stored the integrated data onto the computer hard disk. The ratio of signals were also calculated and displayed on line. After the completion of the experiment, the data on the computer were analysed off line. Ratio recordings were transformed into pH_i values (see below).

In situ calibration of pH_i measurements

To calibrate the ratiometric recordings of SNARF fluorescence, the standard *in situ* nigericin calibration technique was used (Thomas, Bushsbaum & Racker, 1979). Prior to recording from the cell, the background signal was electronically subtracted by the I/V converter to eliminate noise. Based on **Equation 2.2**, in order to obtain real pH_i from emission ratio (R), we need to determine R_{max}, R_{min}, pK_a and $F640_{min/max}$. Accordingly, the emission ratio is measured at pH 5.5 (R_{max}), 9.5 (R_{min}) and 7.5 ($R_{7.5}$), as well as the maximal ($F640_{max}$, at pH 9.5) and minimal ($F640_{min}$, at pH 5.5) emission fluorescence intensity measured at 640 nm.

It has been shown that the nigericin K^+-H^+ exchanger produces net K^+ and H^+ movements across the membrane until it reaches equilibrium, whereupon:

$$\frac{[K^+]_o}{[K^+]_i} = \frac{[H^+]_o}{[H^+]_i}$$

Since intracellular K^+ is approximately 140 mM, raising extracellular K^+ concentration to 140 mM thus forces the pH_i at equilibrium to equal to pH_o. Thus, pH_i can be clamped to the value of pH_o.

Because now $pH_i = pH_o$, pK_a can be easily worked out. By doing so, six to eight sets of pK_a, R_{max}, R_{min} and log $F640_{min/max}$ values were obtained. Finally, mean values of pK_a, R_{max}, R_{min} and $F640_{min/max}$ were used as default values in the subsequent experiments, to derive pH_i directly from the ratio of SNARF emission fluorescence (R). However, since the optical path length and the settings on the photomultiplier tube were occasionally changed, new sets of calibration parameters were obtained every three to six months, which were then used to calibrate pH_i recordings in subsequent experiments. The superfusion system was decontaminated after each calibration.

Decontamination of the superfusion apparatus

Richmond & Vaughan-Jones (1997) reported that nigericin used in the calibration procedure could cause contamination of the superfusion apparatus, thus affecting the accuracy of pH_i measurement. Therefore, after the calibration procedure was completed, all the superfusion tubes, the experiment chamber and the switching tap were perfused continuously with 100 ml 2% bovine albumin (Sigma) solution at 37 °C, then with 2 l 20% solution of detergent Decon 75 (Decon Laboratories Ltd) at 60 °C. This was followed by flushing with 100 ml ethanol, then 3 l of distilled water at room temperature. This whole procedure was to ensure minimal residual nigericin in the superfusion apparatus.

Experimental Alteration of pH_i

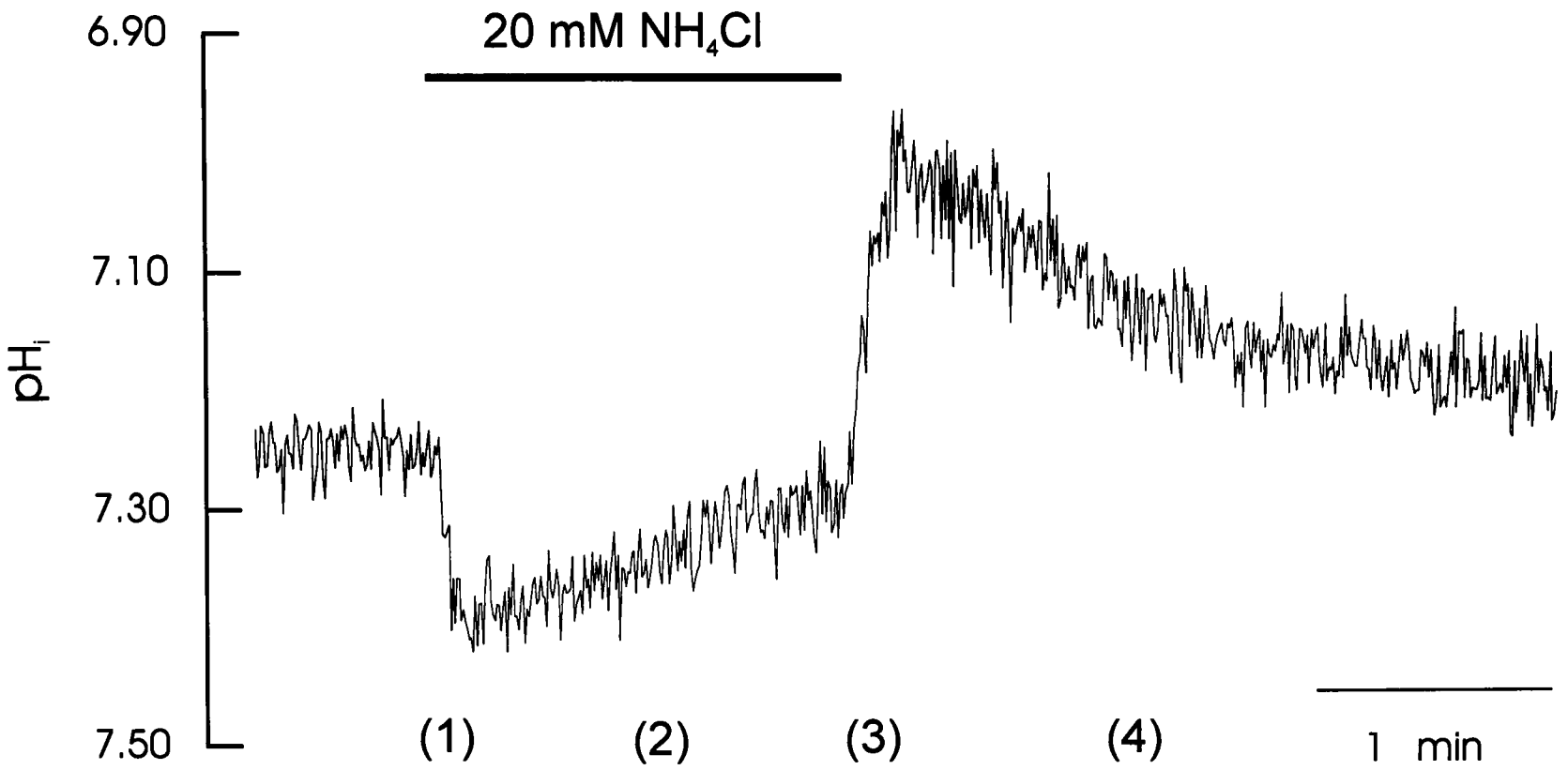
This thesis is aimed at investigating the relationship between pH_i and pH_o in type I cells. Therefore it is necessary to alter pH_i in the absence of a pH_o change, so that acid influx or efflux can be observed at different pH_i values while keeping pH_o constant. This was accomplished by inducing intracellular acid loading (for reducing pH_i) or intracellular alkali loading (for increasing pH_i) via the weak base pre-pulse technique (for acid loading) or weak acid pre-pulse technique (for alkali loading) (Thomas, 1984).

The most commonly used salts of weak acid and base were sodium acetate (CH_3COONa) and ammonium chloride (NH_4Cl). The principle of the technique is based on the fact that, weak acids/bases are incompletely dissociated in the solution, thus both charged (e.g. NH_4^+ or CH_3COO^-) and uncharged (e.g. NH_3 or CH_3COOH) species coexist. The uncharged species are able to permeate the cell membrane rapidly, whereas, the charged species permeate much more slowly.

Production of intracellular acidosis by ammonium pre-pulse technique

20 mM NH_4Cl was usually used to induce an intracellular acid load (**Fig 2.5A**).

(1) Phase 1: The addition of NH_4Cl to the superfusate initially causes rapid alkalosis. This is due to the entry of uncharged NH_3 and its subsequent protonation, thus raising pH_i.



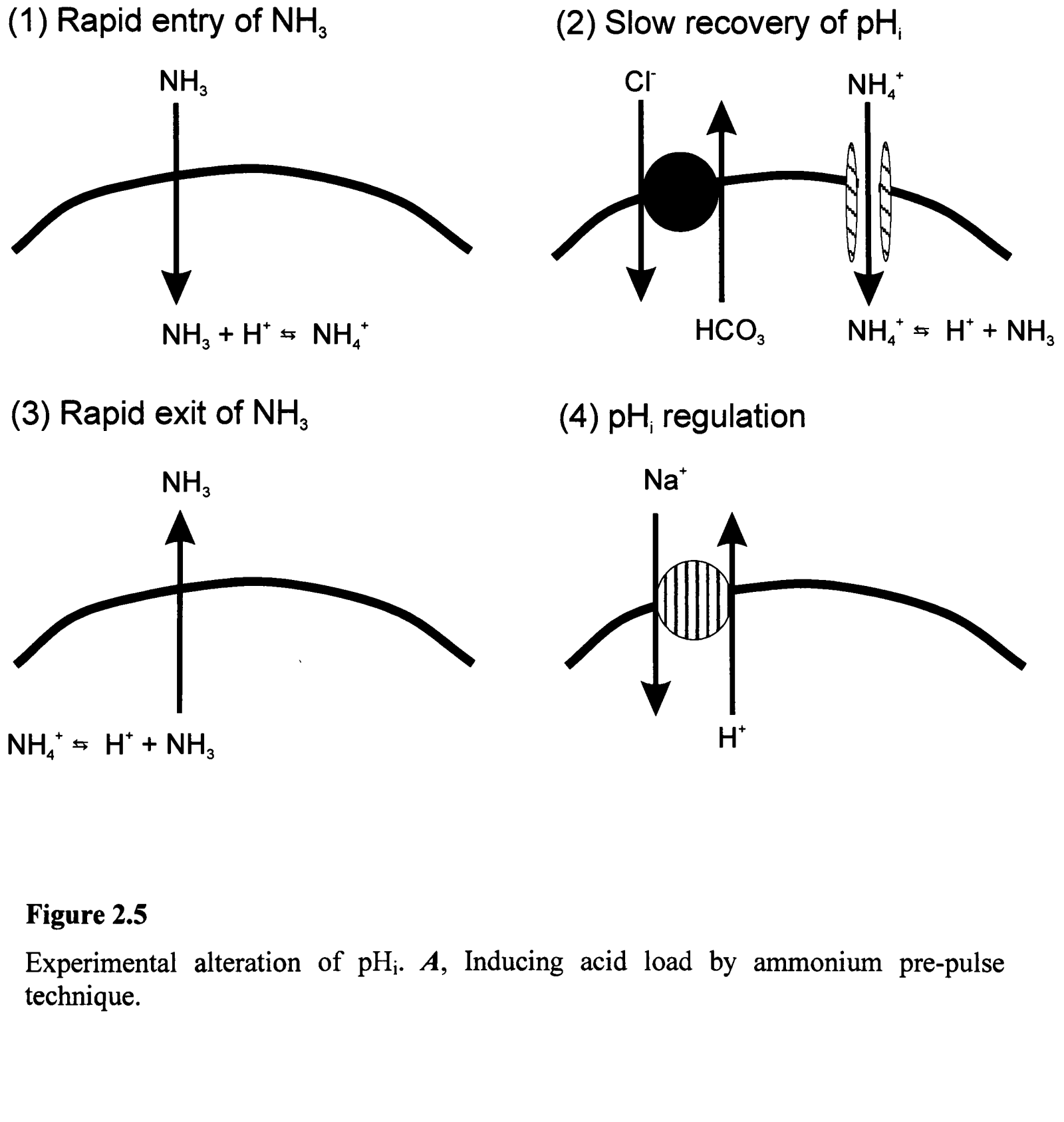


Figure 2.5

Experimental alteration of pH_i. ***A***, Inducing acid load by ammonium pre-pulse technique.

(2) Phase 2: The charged species NH_4^+ gradually enters the cell possibly via K^+ channels, then dissociates into NH_3 and H^+, reducing pH_i from the initial alkalosis. Other cellular pH_i regulation mechanisms, such as Cl^--HCO_3^- exchanger, may also contribute to the slow recovery in this phase. Due to these processes, the amount of intracellular NH_4^+ ($[NH_4^+]_i$) is now more than that in phase 1.

(3) Phase 3: The removal of NH_4Cl from the superfusate causes rapid acidosis. Intracellular NH_3 readily exits the cell, causing the remaining intracellular NH_4^+ to dissociate into NH_3 and H^+. However, the H^+ generated in this reaction cannot permeate the cell membrane rapidly, so an intracellular *acid load* is produced. The more intracellular NH_4^+ that has accumulated in phase 2, the greater acid load is produced after the removal of NH_4Cl.

(4) Phase 4: The cell recovers from the acid load due to activation of acid extruders, such as Na^+-H^+ exchanger.

Production of intracellular alkalosis by acetate pre-pulse technique

20 mM CH_3COONa was usually used to induce an intracellular alkali load (**Fig 2.5B**).

(1) Phase 1: The addition of CH_3COONa to the superfusate initially causes rapid acidosis. This is due to the entry of uncharged CH_3COOH and its subsequent dissociation, thus reducing pH_i.

(2) Phase 2: Normally, the charged species CH_3COO^- does not enter the cell. However, due to the activation of cellular pH_i regulation mechanisms, such as Na^+-H^+ exchange, excess H^+ is extruded from the cell. Hence there is a slow pH_i

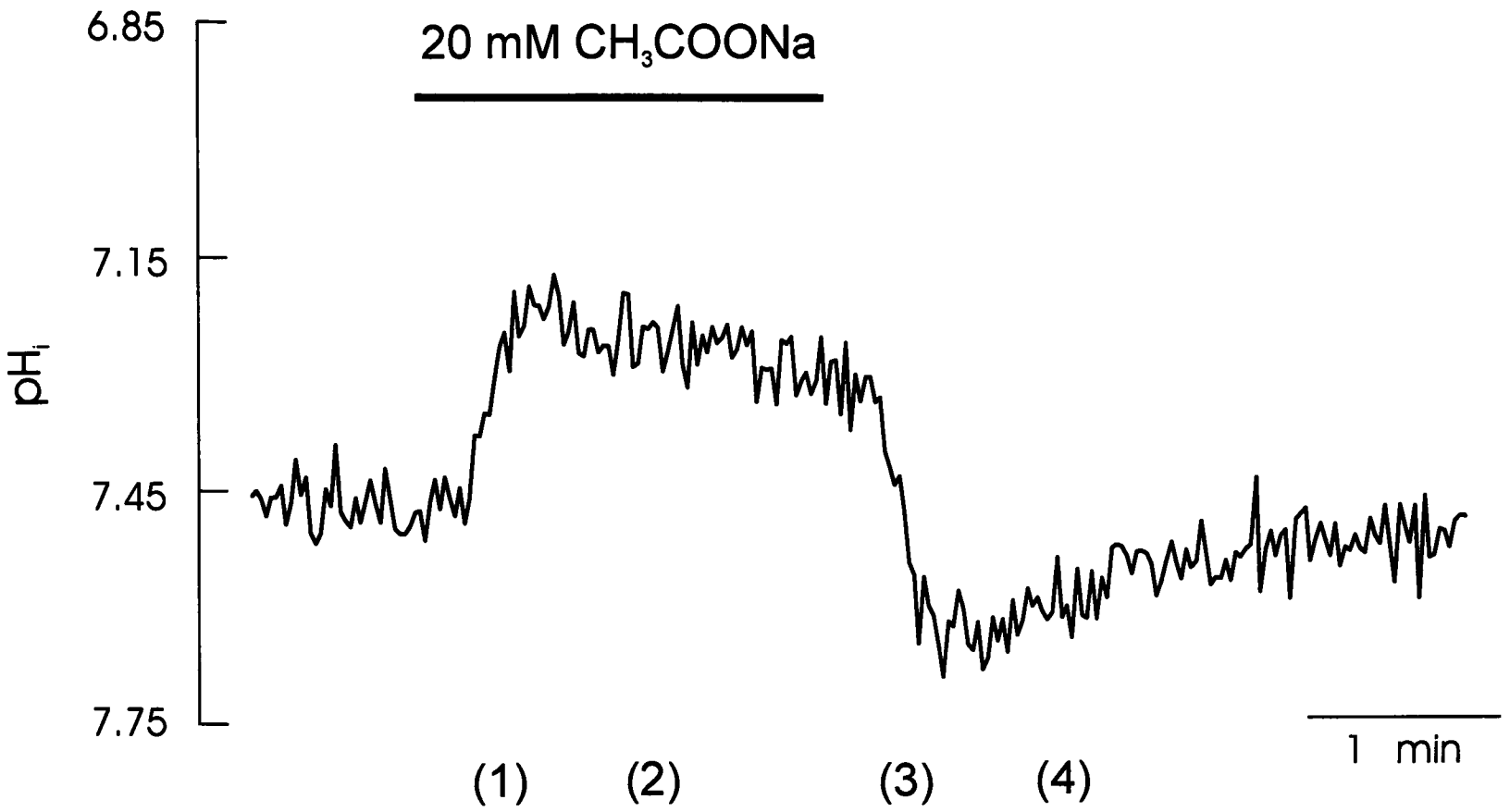


Figure 2.5 (continued)

B, Inducing alkali load by acetate pre-pulse technique. HA = CH_3COOH; A^- = CH_3COO^-.

increase from the initial acidosis. Due to this process, the amount of intracellular CH_3COO^- ($[CH_3COO^-]_i$) is now more than that in phase 1.

(3) Phase 3: The removal of CH_3COONa from the superfusate causes rapid alkalosis. Because CH_3COOH readily exits the cell, thus the remaining intracellular CH_3COO^- is protonated to CH_3COOH, which also leaves the cell. H^+ is consumed in this reaction, so an intracellular *alkali load* is produced. The more intracellular CH_3COO^- that has accumulated in phase 2, the greater alkali load is produced after the removal of CH_3COONa.

(4) Phase 4: The cell recovers from the alkaline load due to activation of an acid loader, such as Cl^--HCO_3^- exchanger.

Analyses of Net Acid Fluxes

To quantify the plasmalemmal acid fluxes in type I cells, the *net* acid flux (J_H) is defined as the amount of *net* hydrogen ion added to or removed from the intracellular compartment per unit time:

$$J_H = (\text{added or removed } H^+) / \Delta t$$

This is expressed as mmoles of acid-equivalent per litre of cytoplasm per minute (mequiv l^{-1} min^{-1}).

The total hydrogen ion buffering power (β_{tot}) in the cells is defined as the amount of strong acid (or base) needed to produce 1 pH unit change in 1 litre of cytoplasm (Roos & Boron, 1981):

$$\beta_{tot} = -(\text{added } H^+) / \Delta pH_i = (\text{added } OH^-) / \Delta pH_i \qquad \textbf{[Eqn. 2.3]}$$

It follows that:

$$J_H = \beta_{tot} \times \Delta pH_i / \Delta t \qquad \textbf{[Eqn. 2.4]}$$

β_{tot}, in turn, is the sum of β_i (intrinsic buffering power) and β_{co2} (CO_2/HCO_3^--induced buffering power) (see Chapter 1):

$$\beta_{tot} = \beta_i + \beta_{co2} \qquad \textbf{[Eqn. 2.5]}$$

Here β_i can be estimated from the empirical equation obtained in type I cells (Buckler *et al.* 1991a):

$$\beta_i = 127.6 - 16.04 \times pH_i \qquad \textbf{[Eqn. 2.6]}$$

β_{co2}, on the other hand, is determined by the following equation:

$$\beta_{CO2} = 2.3 \times [HCO_3^-]_i \qquad \textbf{[Eqn. 2.7]}$$

where

$$[HCO_3^-]_i = [HCO_3^-]_o / 10^{(pHo-pHi)} \qquad \textbf{[Eqn. 2.8]}$$

assuming the cell behaves as an open system (Van Slyke, 1922; Burton, 1975).

Statistics

Average values are all expressed as mean±standard error of mean (S.E.M.), followed by the number of experiments, n. Average values were examined for significant differences using student's *t*-test, setting a P value of 0.05 or less as the criteria of significance. Both the control and test responses were obtained from the same cell if possible, and a comparison was made using a two-tailed paired *t*-test. Otherwise, if such a manoeuvre was not feasible, a two-tailed unpaired *t*-test was used instead.

CHAPTER 3

The Dual Acid Influx Pathways in the Carotid Body Type I Cell

Introduction

As described in Chapter 1, the carotid body type I cell detects changes in arterial pH and P_{CO2}. It transduces the stimulus of extracellular acidosis into a membrane depolarisation, leading to Ca^{2+} influx and finally neurotransmitter secretion. Previous studies have shown that intracellular pH (pH_i) in the type I cell is very sensitive to extracellular pH (pH_o) change, thus a fall in pH_o induces a parallel fall in pH_i. The reported ratio of $\Delta pH_i/\Delta pH_o$ is around 0.6 or even higher (Buckler *et al.* 1991b; Wilding *et al.* 1992). A fall in extracellular pH (pH_o) could be a result of reducing HCO_3^- ion concentration at constant P_{CO2} (isocapnic acidosis or metabolic acidosis) or increasing P_{CO2} (hypercapinc acidosis or respiratory acidosis). Buckler *et al.* (1991b) also demonstrated that both kinds of acidosis in pH_o induce a similar decrease of steady state pH_i. In this thesis I will focus on the pH_i response stimulated by the isocapnic acidosis.

pH_i is determined by a dynamic balance between acid influx, acid efflux and intracellular background loading. Therefore a fall in pH_i in response to extracellular acidosis could be a result of increased acid influx or decreased acid efflux (and thus

the *unmasking* of intracellular background acid loading), or a combination of both. The aim of the present studies was to identify the mechanisms responsible for mediating acid loading in type I cells when stimulated by isocapnic acidosis. Therefore the possibility of an increase in acid influx and a decrease in acid efflux is considered.

The most likely candidates involving this acid loading are those acid-equivalent transport systems mediating transmembrane acid fluxes. The following acid-equivalent transporters are known to exist in carotid body type I cells: Na^+-H^+ exchange, Na^+-dependent Cl^--HCO_3^- exchange and Cl^--HCO_3^- exchange. There is evidence that Na^+-H^+ exchange and Na^+-dependent Cl^--HCO_3^- exchange both operate as acid extruders in type I cells (Buckler *et al.* 1991a). Cl^--HCO_3^- exchange is proposed to operate as an acid loader, although this has not yet been proved in the type I cell. In addition, a putative HCO_3^- channel has also been proposed by Stea & Nurse (1989). The possible involvement of these acid-equivalent transport systems in the acid loading has been tested in the present work.

In this chapter, it is shown that the fall of pH_i in the type I cell when stimulated by extracellular acidosis is predominantly a result of increased acid influx rather than a decrease in acid efflux. The majority of acid influx is mediated by a HCO_3^--dependent and Cl^--dependent mechanism, probably a Cl^--HCO_3^- exchange. The results are separated into two sections: a HCO_3^--dependent and Cl^--dependent pathway is investigated in the first section, while the second section deals with a HCO_3^--independent and Cl^--independent pathway. The possible contribution of the HCO_3^- channel in the acid influx is also considered.

Methods

General Methods

pH_i was recorded in isolated type I cells from the neonatal rats using carboxy-SNARF-1, as described in Chapter 2.

Solutions

Standard CO_2/HCO_3^--buffered solution, pH 6.4 CO_2/HCO_3^--buffered solution, HEPES-buffered HCO_3^--free standard Tyrode solution and pH 6.4 PIPES-buffered solution were prepared as described in Chapter 2.

For Cl^--free solutions (CO_2/HCO_3^--buffered and HEPES-buffered), Cl^- ions were substituted by gluconate. Ca^{2+} was elevated from 2.5 to 12 mM to compensate its binding with gluconate (see Kenyon & Gibbons, 1977). For Na^+-free solutions (CO_2/HCO_3^--buffered and HEPES-buffered), Na^+ ions were substituted by N-methy-D-glucamine (NMDG).

(1) Cl^--free CO_2/HCO_3^--buffered solution

Composition	Concentration (mM)
Na-gluconate	117
K-gluconate	4.5
$NaHCO_3$	23
Mg-gluconate	1
Ca-gluconate	12
Glucose	11
Equilibrated with 5% CO_2 / 95% air, final pH 7.4 at 37 °C	

(2) Cl^-–free HEPES-buffered solution

Composition	Concentration (mM)
Na-gluconate	135
K-gluconate	4.5
Mg-gluconate	1
Ca-gluconate	12
HEPES	20
Glucose	11
Adjust pH with NaOH to 7.4 at 37 °C	

(3) pH 6.4 Cl^-–free PIPES-buffered solution

Composition	Concentration (mM)
Na-gluconate	135
K-gluconate	4.5
Mg-gluconate	1
Ca-gluconate	12
PIPES	20
Glucose	11
Adjust pH with NaOH to 6.4 at 37 °C	

(4) Na^+-free CO_2/HCO_3^--buffered solution

Composition	Concentration (mM)
NMDG	117
KCl	4.5
$MgCl_2$	1
$CaCl_2$	2.5
Glucose	11
Adjust pH with HCl to around 7.0 then add 23 mM NMDG. Equilibrated with 5% CO_2 / 95% air, final pH 7.4 at 37 °C	

(5) pH 6.4 Na^+-free CO_2/HCO_3^--buffered solution

Composition	Concentration (mM)
NMDG	138
KCl	4.5
$MgCl_2$	1
$CaCl_2$	2.5
Glucose	11
Adjust pH with HCl to around 6.0 then add 2.3 mM NMDG. Equilibrated with 5% CO_2 / 95% air, final pH 6.4 at 37 °C	

For pH 7.7 solution, add 94 mM NMDG first. Adjust pH with HCl to around 7.4 then add 46 mM NMDG. Equilibrated with 5% CO_2 / 95% air, final pH 7.7 at 37 °C

(6) Na^+-free HEPES-buffered solution

Composition	Concentration (mM)
NMDG	140
KCl	4.5
$MgCl_2$	1
$CaCl_2$	2.5
HEPES	20
Glucose	11
Adjust pH with 2N HCl to 7.4 at 37 °C	

For pH 6.4 solution, replace HEPES with PIPES and adjust pH to 6.4 at 37 °C.

(7) Na^+-free high K^+ CO_2/HCO_3^--buffered solution

Composition	Concentration (mM)
KCl	121.5
$KHCO_3$	23
$MgCl_2$	1
$CaCl_2$	2.5
Glucose	11
Equilibrated with 5% CO_2 / 95% air, final pH 7.4 at 37 °C	

For pH 6.4 and 7.7 solutions, change $KHCO_3$ concentrations to those of $NaHCO_3$ in normal pH 6.4 and 7.7 CO_2/HCO_3 -buffered solution described in Chapter 2, with osmotic compensation of KCl.

(8) pH 7.7 low Na^+ CO_2/HCO_3^--buffered solution

Composition	Concentration (mM)
NMDG	94
KCl	4.5
$NaHCO_3$	23
$MgCl_2$	1
$CaCl_2$	2.5
Glucose	11
Adjust pH to around 7.4 then add 23 mM NMDG. Equilibrated with 5% CO_2 / 95% air, final pH 7.7 at 37 °C	

For pH 6.4 solution, change $NaHCO_3$ concentration to 2.3 mM with osmotic compensation of 20.7 mM NaCl. Adjust pH to around 6.0 then add 23 mM NMDG. Equilibrated with 5% CO_2 / 95% air, final pH 6.4 at 37 °C

(9) pH 7.7 low Na^+ high K^+ CO_2/HCO_3 -buffered solution

Composition	Concentration (mM)
KCl	98.5
$KHCO_3$	23
$NaHCO_3$	23
$MgCl_2$	1
$CaCl_2$	2.5
Glucose	11
Equilibrated with 5% CO_2 / 95% air, final pH 7.7 at 37 °C	

Cell Membrane Depolarisation by High K^+_o Treatment

Because of the large K^+ conductance in the membrane of the type I cell, its membrane potential (E_m) is largely dependent on the equilibrium potential for K^+ ions, E_K (Buckler, 1997). According to the Nernst equation,

$$E_K = \frac{RT}{F} \times \ln \frac{[K^+]_o}{[K^+]_i} \qquad \textbf{[Eqn. 3.1]}$$

Where R is the ideal gas constant, T is absolute thermodynamic temperature and F is Faraday's constant.

raising $[K^+]_o$ results in a more positive E_K (hence a more depolarised E_m). So the application of high K^+_o in solution was used as a tool to depolarize E_m.

The intracellular K^+ concentration in the type I cell is assumed to be 140 mM. For the two high K^+ solutions used in this study, the membrane potential will be depolarised to approximately 0 mV in Na^+-free high K^+ solution ($[K^+]_o$=144.5 mM), and around -10 mV in low Na^+ high K^+ solution ($[Na^+]_o$=23 mM, $[K^+]_o$=121.5 mM), respectively.

Drugs

3-methylsulphonyl-4-piperidinobenzoyl guanidine methanesulphonate (Hoe694) was a gift from Hoechst Pharmaceuticals (Germany). Drug was added as solid to the solutions shortly before use. As Hoe694 is light-sensitive, containers in which solutions of the drug kept were covered with aluminum foil.

Results

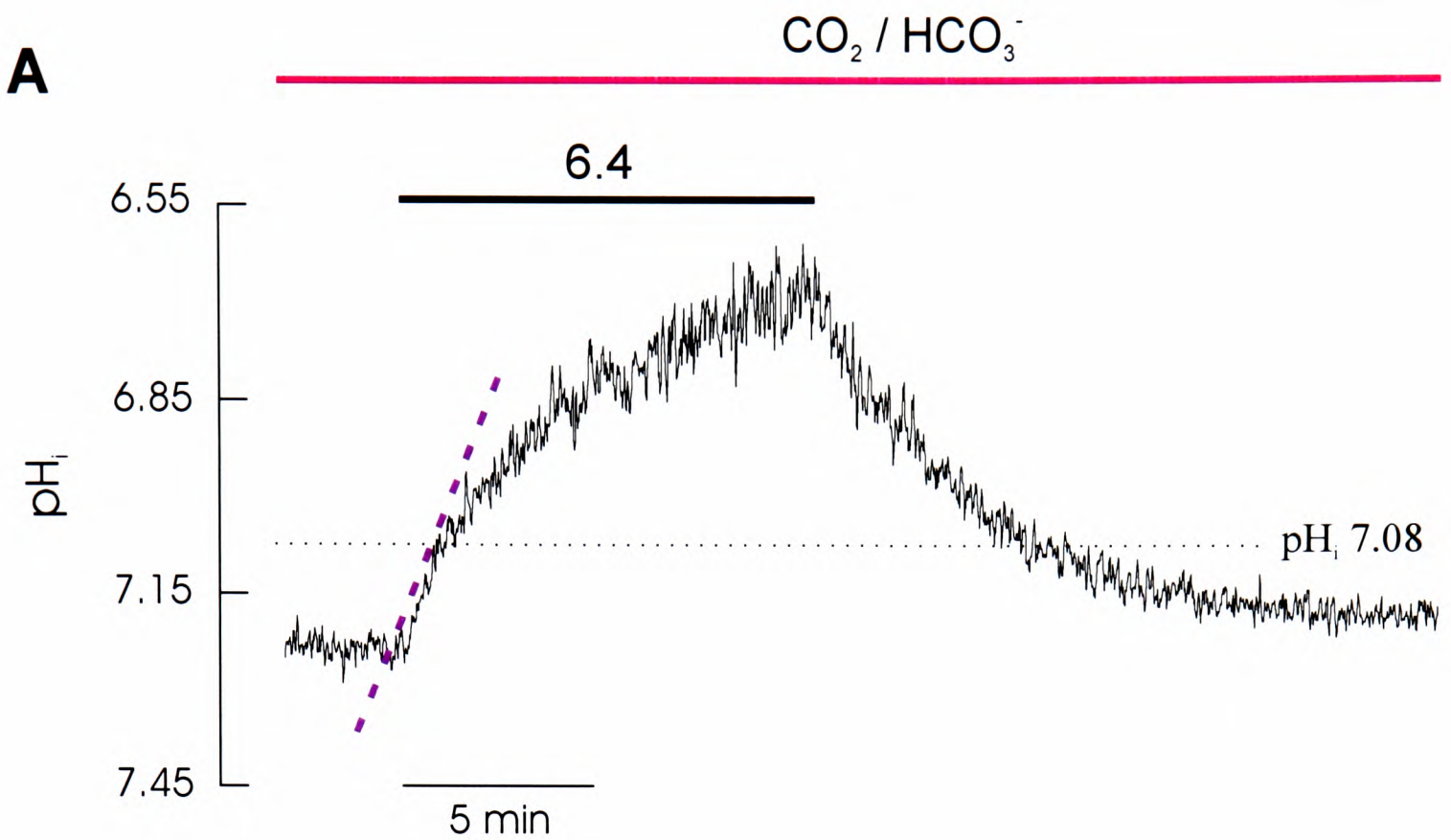
I. HCO_3^--dependent and Cl^--dependent acid influx pathway: Cl^--HCO_3^- exchange

Acid loading induced by isocapnic acidosis

Fig 3.1A shows the typical response of carotid body type I cells when stimulated by extracellular isocapic acidosis. The type I cell was initially superfused with 5% CO_2/23 mM HCO_3^--buffered standard Tyrode solution (pH_o 7.4), with its resting pH_i 7.25±0.15 (n=6). When pH_o was decreased from 7.4 to 6.4 by a reduction of $[HCO_3^-]_o$ to 2.3 mM at constant P_{CO2}, there was a related fall of pH_i by 0.57±0.13 pH unit (n=6). The initial net acid influx rate (J_H) was 6.88±1.23 mequiv l^{-1} min^{-1}, at pH_i 7.26±0.01 (n=5). An example of calculating the net acid influx (J_H) from the rate of pH_i change (dpH_i/dt) and total intracellular buffering power (β_{tot}) is also illustrated (for details see **Equation 2.5-2.7** in Chapter 2). This response was reversible and repeatable. When the isocapnic acid challenge was tested for a second time, its response remained virtually the same. On average, as shown in **Fig 3.1B**, an acid flux of 91% of the original response was observed (n=5, no significant difference).

HCO_3^--dependence of acid loading

To test the whether this acid loading was HCO_3^--dependent, a similar protocol was repeated in nominally HCO_3^--free HEPES-buffered Tyrode solution. In **Fig 3.2A**, following the control response in normal HCO_3^--buffered Tyrode solution like that in **Fig 3.1**, the superfusate was changed to HEPES-buffered Tyrode solution (both pH_o



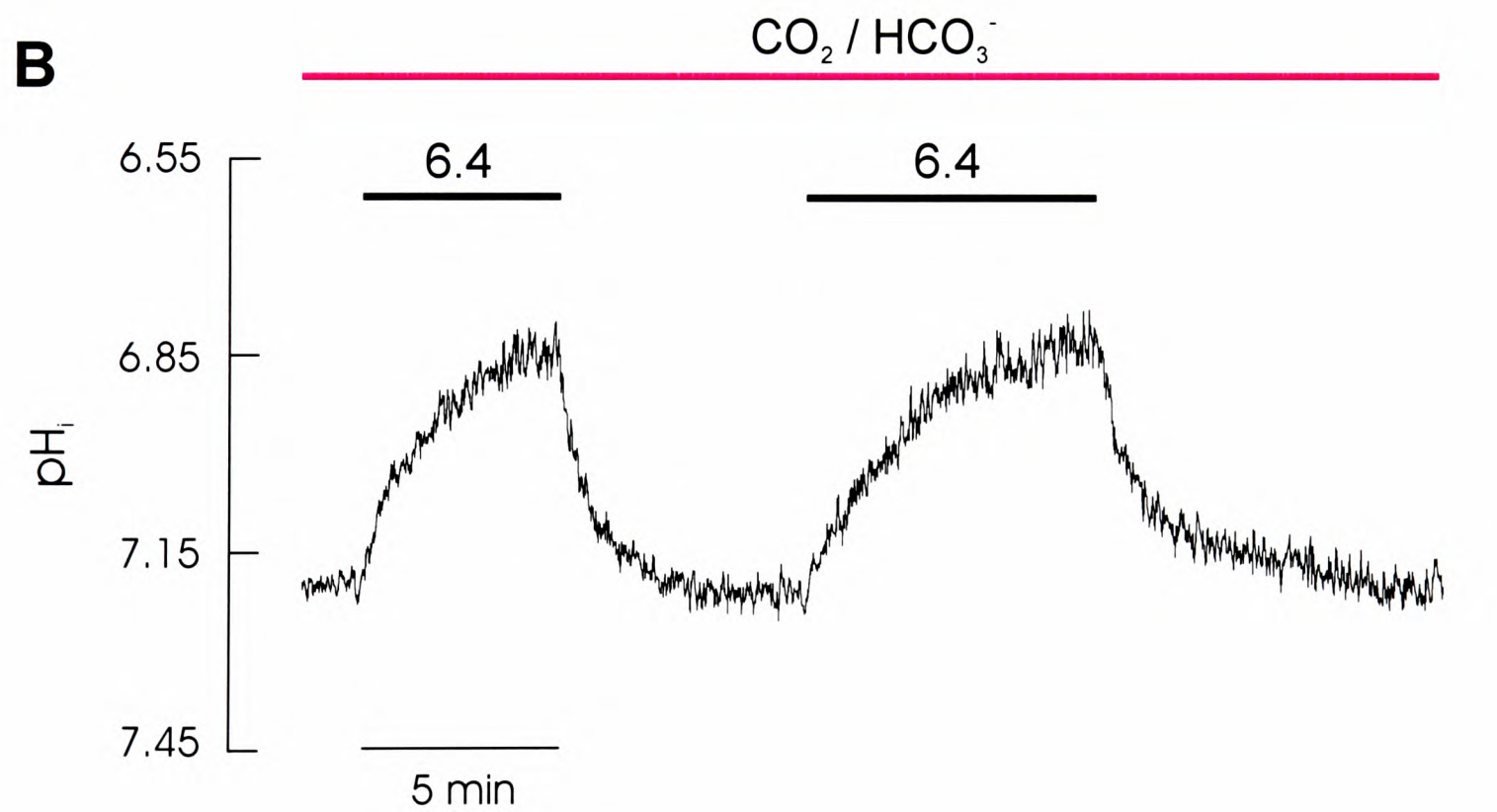


Figure 3.1

A, Effect of pH_o upon pH_i in carotid type I cell perfused with 5%CO_2/23mM HCO_3^--buffered solution. pH_i is very sensitive to changes in pH_o, as a change of pH_o from 7.4 to 6.4 caused a change of pH_i by approximately 0.5 pH unit. The general method used to determine initial net acid influx (J_H) is also demonstrated. ***B***, The response is reversible, and repeatable.

were 7.4). The abrupt alkalisation during the transition is due to rapid exit of intracellular CO_2, thus removing intracellular H^+ ions. The steady-state pH_i under this HCO_3^--free condition is 7.63±0.05 (n=5). Afterwards, the acid challenge (pH_o 6.4) was applied under this nominal HCO_3 -free condition, resulting in an apparently similar fall of intracellular pH. To compare acid influx under different conditions, acid influx rate has to be measured at the same pH_i (cf. point ***a*** and point ***b*** shown in **Fig 3.2A**). It should be noted, however, that the total intracellular buffering power (β_{total}) is much greater in the presence of CO_2/HCO_3^- buffer system than in its absence. Net acid influx rate is much smaller in the absence of HCO_3^-: the net acid influx (J_H) was 6.09±0.79 mequiv l^{-1} min^{-1} in HCO_3^--buffered solution and 1.32±0.37 mequiv l^{-1} min^{-1} in HEPES-buffered solution, at pH_i=7.26±0.01 (n=6; P<0.001) (**Fig 3.2B**). This result clearly showed that, compared with the response observed in HCO_3^--buffered solution, only 22% of acid influx remained in the absence of HCO_3^-. Therefore, under physiological conditions, 78% of acid influx is HCO_3 -dependent.

Cl^--dependence of acid loading

To test the involvement of any Cl^-_o-dependent mechanism (for example, Cl^--HCO_3^- exchange or Cl^--OH^- exchange) in the acid loading, an acid challenge experiment was repeated under Cl^--free conditions. In HCO_3^--buffered Cl^--free solution (external Cl^- substituted by gluconate), acid influx rate was reduced to 2.30±0.28 mequiv l^{-1} min^{-1}, 34% of the control value, 6.65±0.91 mequiv l^{-1} min^{-1} (pH_i=7.26±0.01; n=7, P<0.01), suggesting 66% of total acid influx requires Cl^-_o under physiological conditions (**Fig 3.3**).

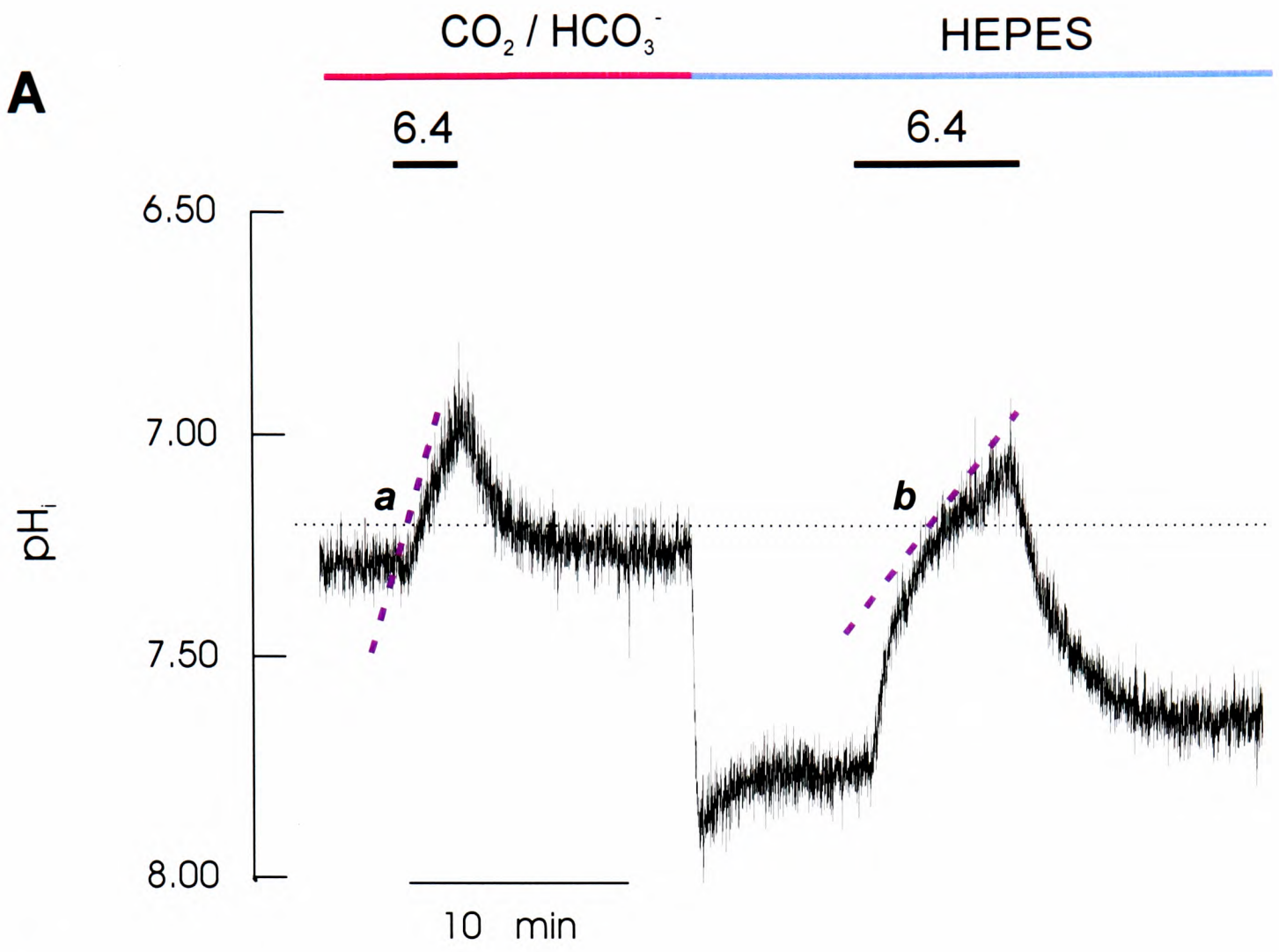


Figure 3.2

A, Effect of HCO_3^- upon acid loading. Cells were initially perfused with HCO_3^--buffered solution, then replaced by HEPES-buffered Tyrode solution. The acid influx rate was decreased by 80% in latter case. Note the buffering capacity in HCO_3^--buffered solution is much larger than that in nominal HCO_3^--free HEPES-buffered Tyrode solution. Therefore for two similar rates of pH_i change measured in HCO_3^--buffered solution (point ***a***) and HEPES-buffered solution (point ***b***), the former actually has much higher acid influx rate. ***B***, Histogram shows mean acid influx rate measured at pH_i 7.26±0.01 using data from 6 experiments similar to that shown in ***A***. Columns represent mean±S.E.M. *** significant difference, P<0.001.

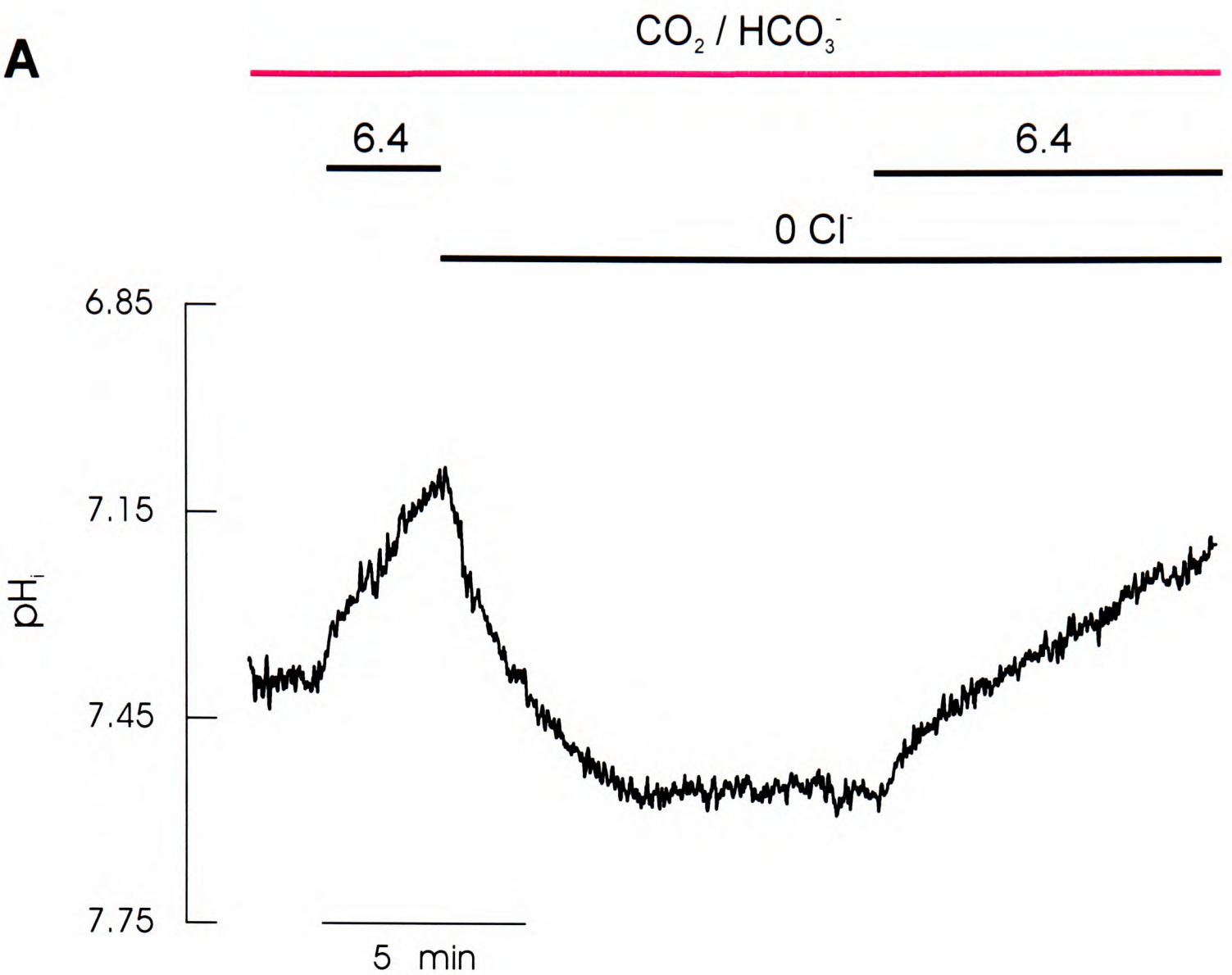


Figure 3.3

A, Effect of Cl^-_o removal upon acid loading. In the absence of external Cl^- ions, the acid influx rate was decreased by 66% when challenged with pH_o 6.4 solution ($P<0.01$). This result suggests the majority of acid loading is Cl^--dependent. ***B***, Histogram shows mean acid influx rate measured at pH_i 7.20±0.09 using data from 7 experiments similar to that shown in ***A***. Columns represent mean±S.E.M. ** significant difference, $P<0.01$.

The major acid loading mechanism is both HCO_3^--dependent and Cl^--dependent

The results shown in **Fig 3.2** and **Fig 3.3** reveal that about 80% and 70% of acid loading is HCO_3^--dependent and Cl^--dependent, respectively. This suggests the majority of acid loading must be mediated via a mechanism that requires both HCO_3^- and Cl^- ions. To clarify the relative contributions of the HCO_3^--dependent and Cl^--dependent components of acid loading, the following experiments were carried out.

The Cl^--dependency of acid influx in the absence of HCO_3^- was examined in **Fig 3.4**. Acid influx rate in the presence and absence of Cl^-_o in HEPES-buffered solutions was 1.90±0.36 mequiv l^{-1} min^{-1}, and 1.15±0.28 mequiv l^{-1} min^{-1}, respectively (J_H measured at pH_i 7.46±0.05; n=6). Although there seems to be a slightly slower flux rate under Cl^--free condition, the difference was not statistically significant, suggesting there is little or no Cl^--dependent acid influx in the absence of HCO_3^-. This experiment indicates that, the HCO_3^--independent acid loading mechanism is also Cl^--independent.

The evidence obtained so far strongly implies that, nearly *all* of the HCO_3^--dependent acid loading mechanism is also Cl^--dependent. To confirm this, in the experiment shown in **Fig 3.5A**, by measuring acid influx rates in CO_2/HCO_3^--buffered Cl^--free solution and in HEPES-buffered solution (containing Cl^-) in the *same* type I cell, I was able to compare directly the Cl^--independent acid influx with the HCO_3^--independent acid influx. There was no significant difference between these two fluxes (1.99±0.51 mequiv l^{-1} min^{-1} and 2.19±0.53 mequiv l^{-1} min^{-1}, respectively, at pH_i 7.24±0.03; n=6).

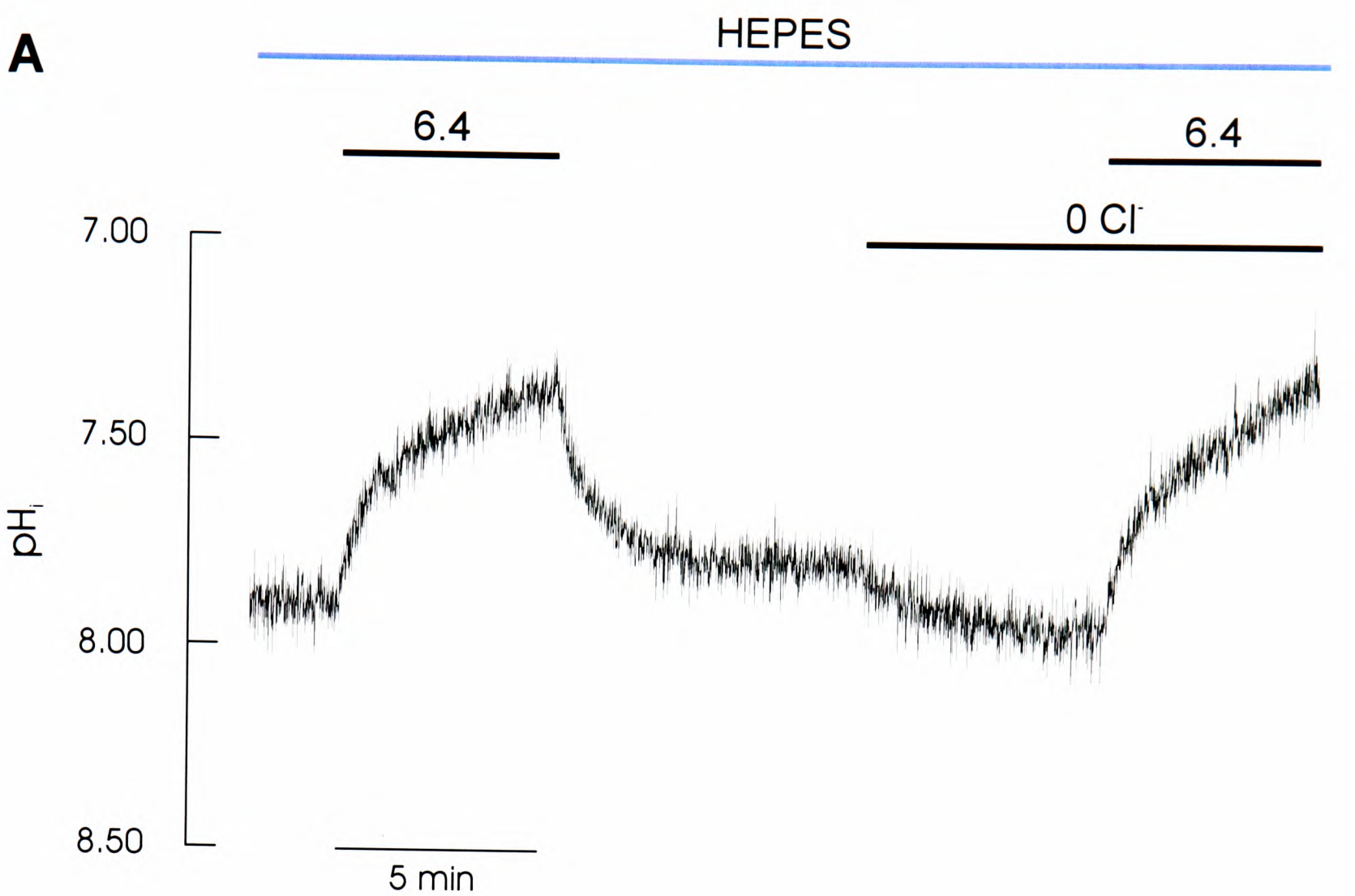


Figure 3.4

A, Effect of Cl^-_o removal upon acid loading in HEPES-buffered solution. In the absence of HCO_3^- (i.e. HEPES-buffered solution), the acid influx rate was not affected by removing Cl^-_o, suggesting the HCO_3^--independent acid loader is also Cl^--independent. ***B***, Histogram shows mean acid influx rate measured at pH_i 7.46±0.05 using data from 6 experiments similar to that shown in ***A***. Columns represent mean±S.E.M.

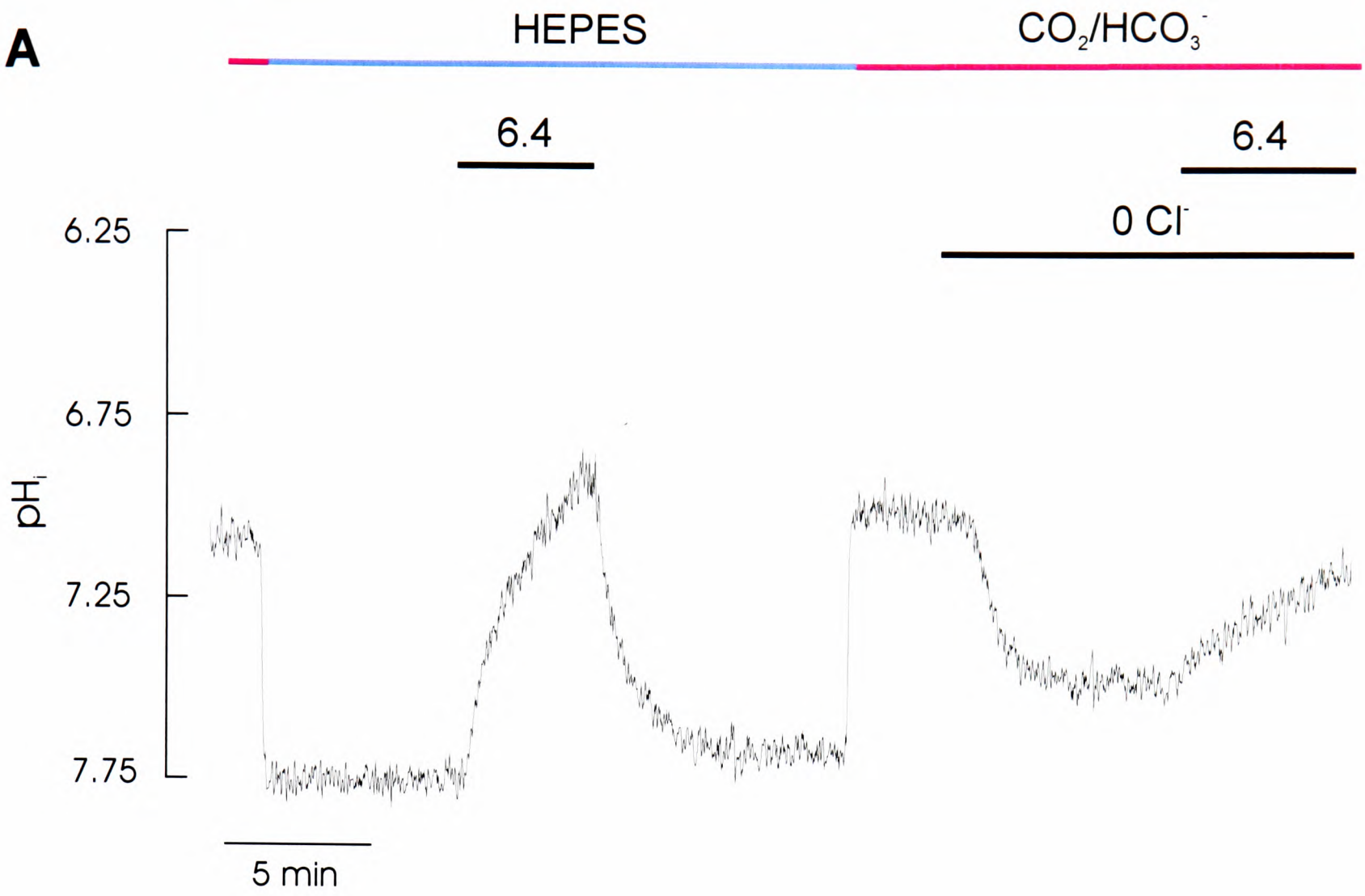


Figure 3.5

A, Comparison between Cl^--independent acid influx in CO_2/HCO_3^--buffered solution and acid influx in HEPES-buffered Tyrode solution. This result suggests that Cl^--independent acid influx is equal to HCO_3^--independent acid influx. ***B***, Histogram shows mean acid influx rate measured at pH_i 7.24±0.03 using data from 6 experiments similar to that shown in ***A***. Columns represent mean±S.E.M.

Acid loading mechanism is Na^+-independent

By combining the results of these experiments, one may conclude that up to 70% of acid loading must be mediated by a mechanism that is both Cl^- and HCO_3^- dependent. The most likely candidates for this mechanism are Na^+-dependent Cl^--HCO_3^- exchange and Cl^--HCO_3^- exchange, and both have been shown to exist in type I cells (Buckler *et al.* 1991a; Richmond, 1993). Therefore, the next experiment was to test whether this acid loading process also requires Na^+_o. In **Fig 3.6A**, cells were perfused with CO_2/HCO_3^--buffered Na^+-free solution. The net acid influx rate in Na^+-free condition (5.17±0.58 mequiv l^{-1} min^{-1}) was not statistically different from that in control condition (6.22±0.17 mequiv l^{-1} min^{-1}; n=5) at pH_i 7.24±0.03. Therefore, the contribution of Na^+-dependent Cl^--HCO_3^- exchange can be ruled out. Moreover, we can conclude that the acid influx had no obligatory requirement for Na^+.

Does HCO_3^- channel play a significant role in acid influx?

To test whether a HCO_3^- channel is also involved in the acid influx process, the acid challenge was repeated in Na^+-free high K^+ CO_2/HCO_3^--buffered solution, in which all Na^+ was replaced by K^+ ($[K^+]_o$ 144.5 mM) (**Fig 3.7A**). This treatment would cause membrane potential depolarise to about 0 mV. If a HCO_3^- channel were responsible for the acid loading, the HCO_3^- efflux (i.e. acid influx) might be expected to decrease significantly in Na^+-free high K^+ solution, because the electrochemical driving force for HCO_3 efflux is almost halved (see **Equation 1.6** and Discussion). However, the results clearly showed that the acid influx rate in Na^+-free high K^+ solution (5.43±1.74 mequiv l^{-1} min^{-1}) was not different from that measured under control conditions (4.76±1.25 mequiv l^{-1} min^{-1}; n=5 at pH_i 7.24±0.04). In fact, there was a slight increase

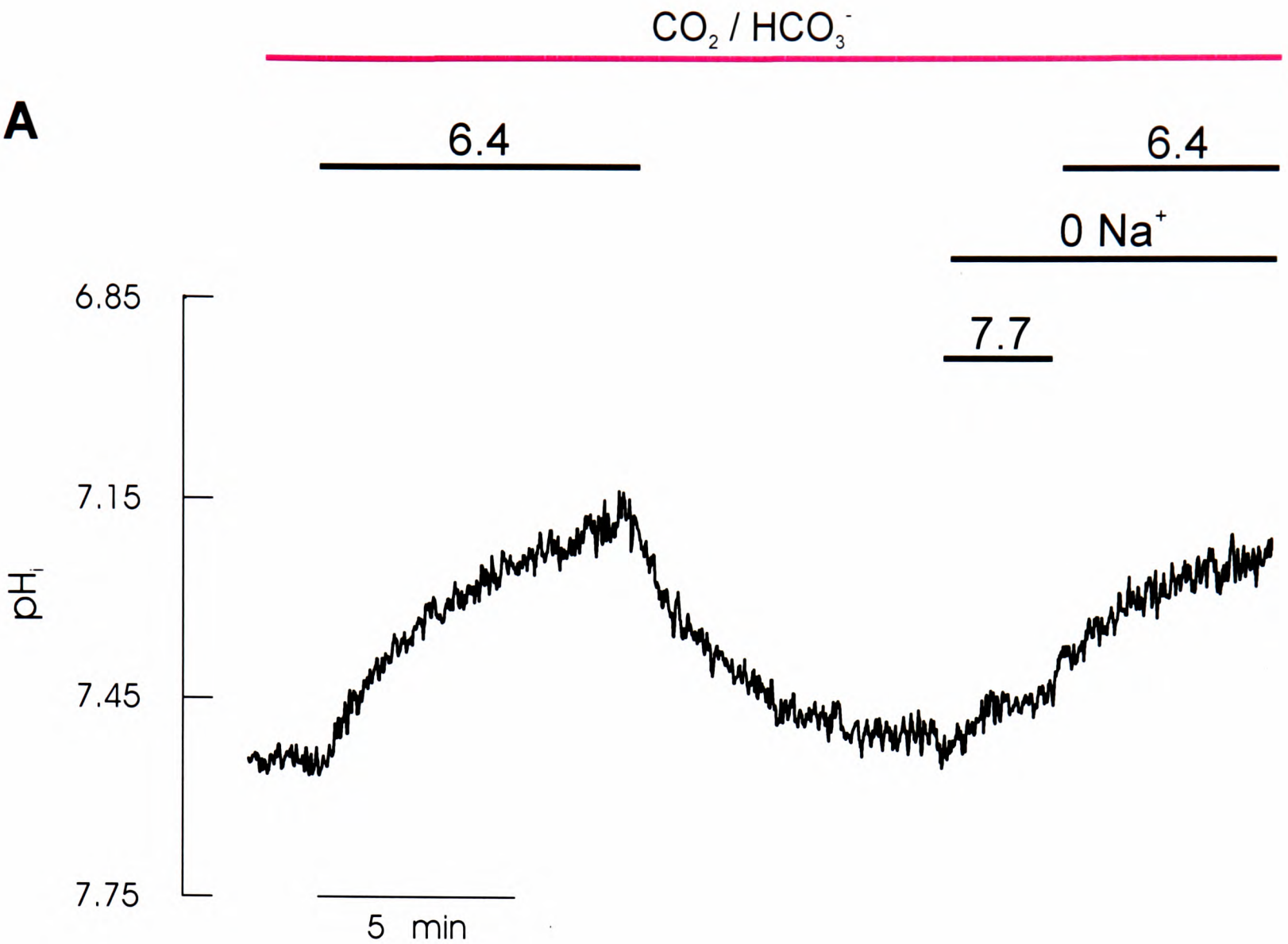


Figure 3.6

A, Effect of Na^+_o removal upon acid loading. In the absence of external Na^+ ions, the acid influx rate was not changed, suggesting the acid loading process is not Na^+-dependent. Cells were perfused with 5%CO_2/23mM HCO_3^--buffered solution. ***B***, Histogram shows mean acid influx rate measured at pH_i 7.35±0.04 using data from 5 experiments similar to that shown in ***A***. Columns represent mean±S.E.M.

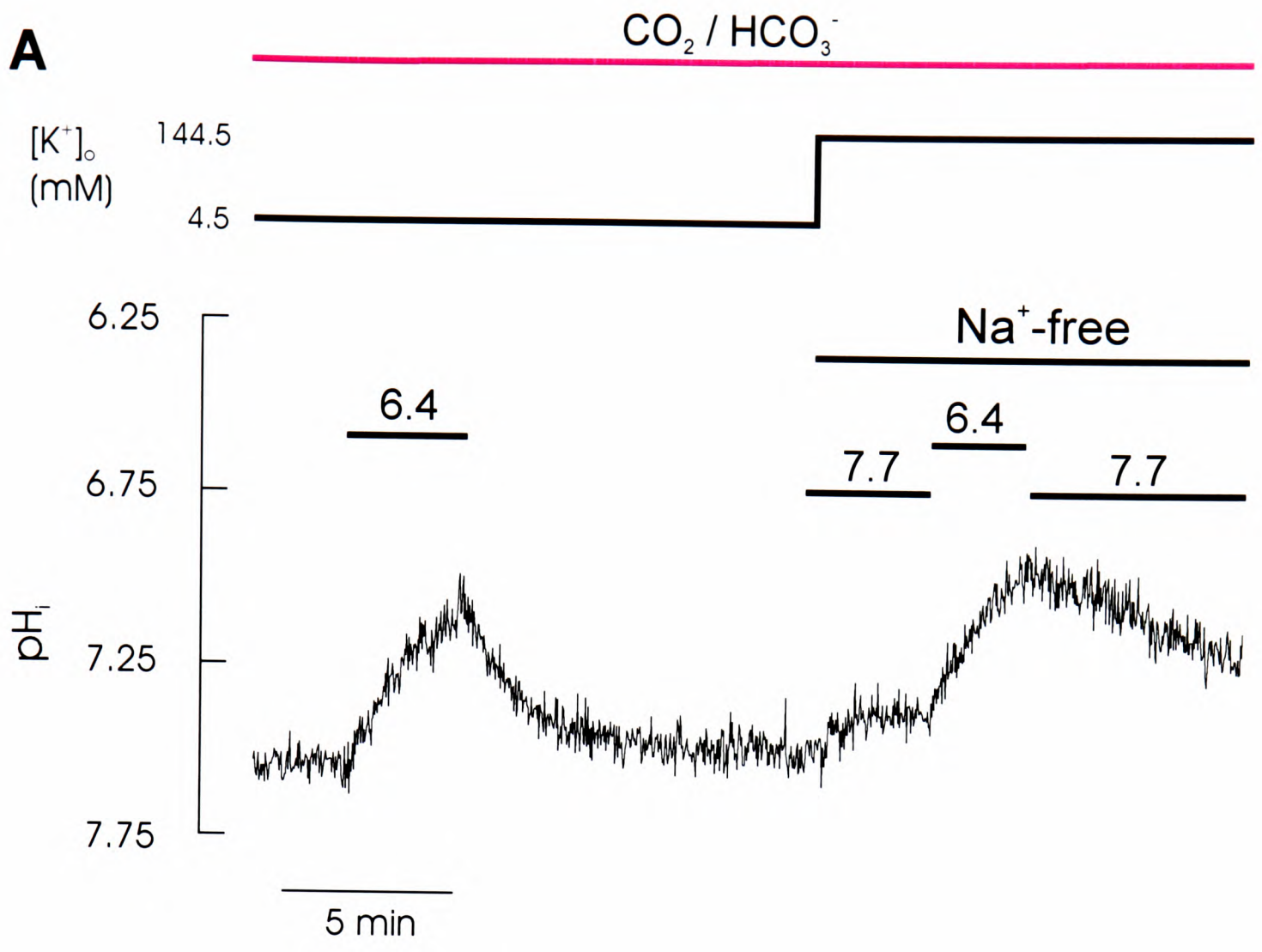


Figure 3.7

A, Effect of high K^+_o upon acid loading. For Na^+-free high K^+ treatment, pH_o 7.7 solution was initially perfused to prevent significant acidosis. In Na^+-free high K^+ pH_o 6.4 solution, the acid influx rate was not changed, suggesting the acid loading process is not electrogenic. Cells were perfused with 5%CO_2/23mM HCO_3^--buffered solution. ***B***, Histogram shows mean acid influx rate measured at pH_i 7.24±0.04 using data from 5 experiments similar to that shown in ***A***. Columns represent mean±S.E.M.

in acid influx, although this was not statistically significant. Similar results were obtained in low Na^+ high K^+ solution ($[Na^+]_o$=23 mM, $[K^+]_o$=121.5 mM), with an acid influx rate of 5.84±1.05 mequiv l^{-1} min^{-1}, compared with the control value of 4.41±0.58 mequiv l^{-1} min^{-1} (n=4 at pH_i 7.30±0.01; P>0.1) (data not shown).

The possible contribution of a HCO_3 channel to background acid loading was also tested at a more alkaline pH_o. As shown in **Fig 3.8**, after the control acid challenge, the cell was perfused with low Na^+ pH_o 7.7 solution ($[Na^+]_o$ = 23 mM, in which 23 mM Na^+ was kept in the solution to prevent the inhibition of other Na^+_o-dependent acid transporters). Then the superfuate was changed to low Na^+ pH_o 7.7 high K^+ solution ($[Na^+]_o$ = 23 mM, $[K^+]_o$ =121.5 mM). Under these conditions, the equilibrium potential for HCO_3^- was around –30 mV. The high K^+ treatment would therefore be expected to induce a HCO_3^- influx (i.e. acid efflux, hence leading to an increase in pH_o), if a HCO_3^- channel were operational. Increased K^+_o had no effect on pH_i. pH_i virtually did not change (0.42±0.02 mequiv l^{-1} min^{-1}; n=5) from its resting level (7.23±0.06). It is thus concluded that a HCO_3 channel does not play a significant role in the acid loading process.

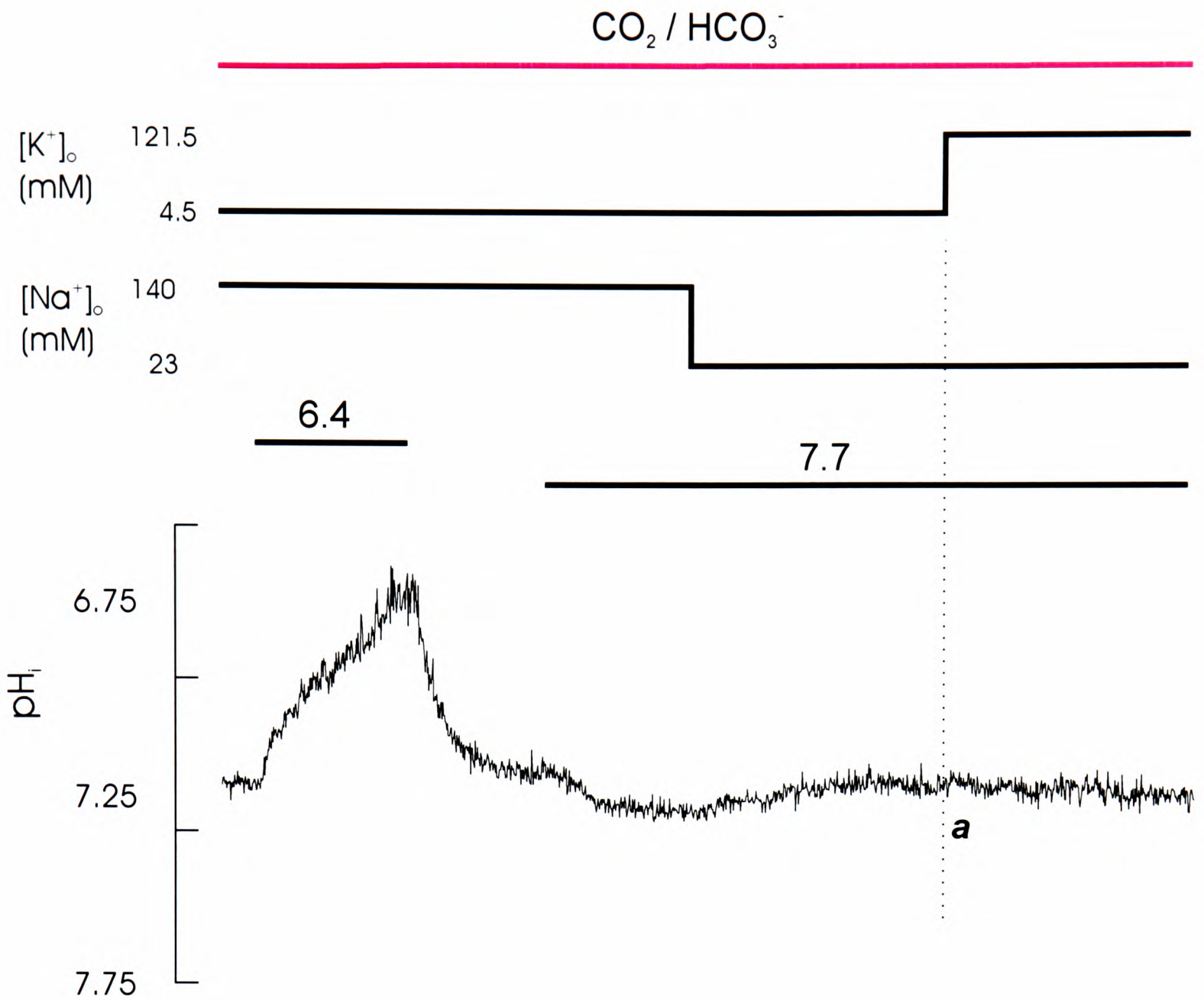


Figure 3.8

Effect of high K^+_o treatment upon pH_i at pH_o 7.7. When the superfusate was changed from low Na^+ solution to low Na^+, high K^+ solution (point ***a***), there was almost no HCO_3^- influx (hence alkalosis), suggesting HCO_3^- conductance is not significant under this condition.

The major acid influx pathway: Cl^--HCO_3^- exchange

Taking the aforementioned results together, I conclude that the main acid loading mechanism under physiological conditions is a Cl^--HCO_3^- exchange, which contributes more than 70% of the total acid influx into the type I cell during a pH_o 6.4 acid challenge.

II. HCO_3^--independent and Cl^--independent acid influx pathway: an unknown mechanism

Data presented in the previous section suggest that a HCO_3 -independent and Cl^--independent acid influx pathway accounts for about 30% of total acid influx in HCO_3^- -buffered solution. In order to examine the properties of this unknown mechanism, experiments in this section were all carried out in HEPES-buffered solution.

An inhibitory effect of extracellular H^+ ions on Na^+-H^+ exchanger has been reported (Aronson, Suhm & Nee, 1983; Vaughan-Jones & Wu, 1990). It is possible that the acid influx induced by external acid challenge in HEPES-buffered solution (see **Fig 3.2A**) is actually the background acid loading unveiled after the Na^+-H^+ exchanger is inhibited by reducing pH_o from 7.4 to 6.4. In this hypothesis, the HCO_3^--independent and Cl^--independent acid influx is simply an unmasked background acid loading, rather than an additional acid influx. I tested this hypothesis in the following two experiments.

In **Fig 3.9A**, acid influx rates were measured during 3 different treatments: pH_o 6.4, 50 μM Hoe694 and 50 μM Hoe694 plus pH_o 6.4. Hoe694 is a highly selective inhibitor of

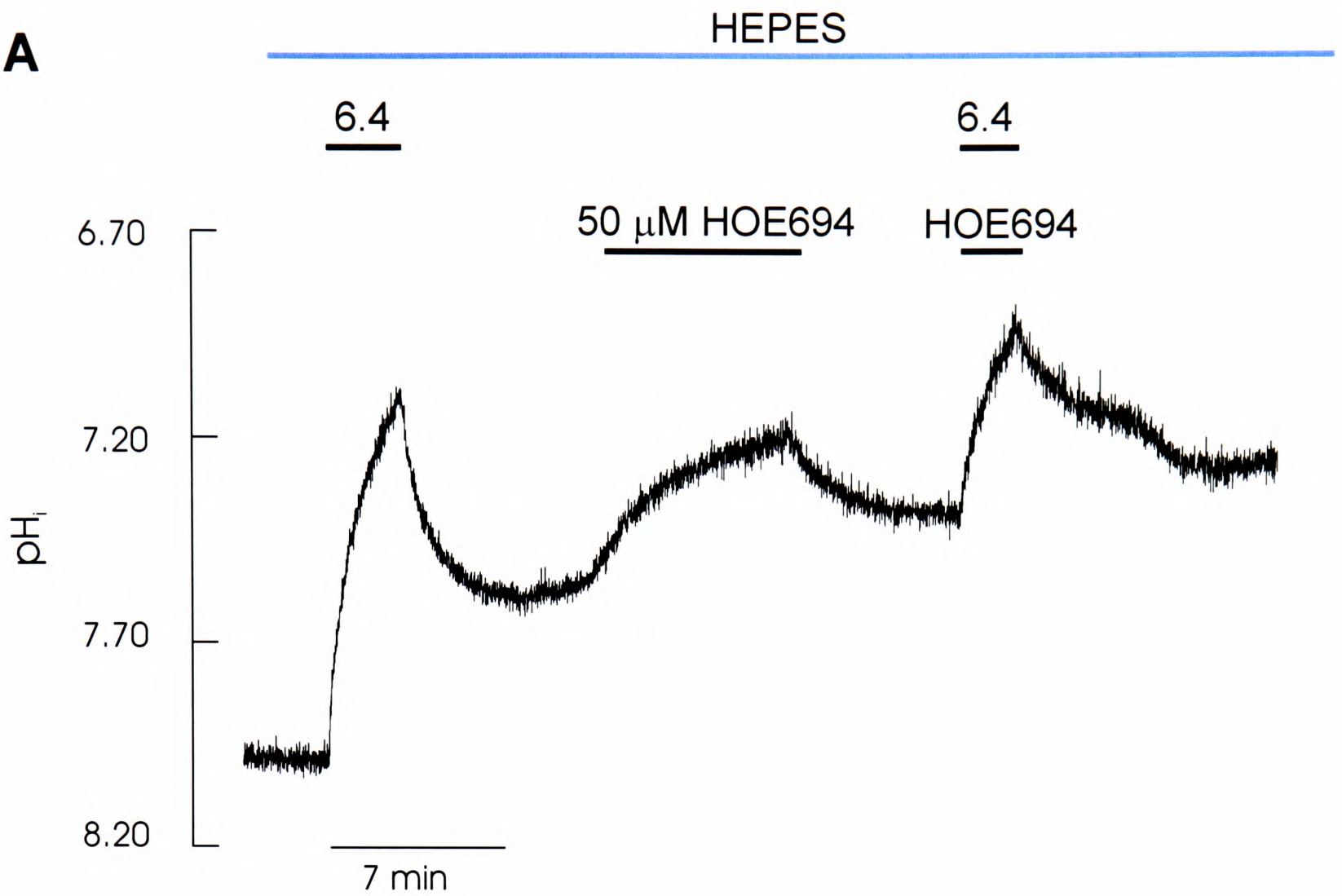


Figure 3.9

A, Comparison of acid influx rates during 3 treatments: pH_o 6.4 acid challenge, 50 μM Hoe694 and pH_o 6.4 acid challenge plus 50 μM Hoe694. There was no difference between the acid influx rates during the pH_o 6.4 and pH_o 6.4 plus Hoe694 treatments. But the influx during pH_o 6.4 plus Hoe694 treatment is significantly faster than that during Hoe694 treament alone. Cells were perfused with HEPES-buffered solution. ***B***, Histogram shows mean acid influx rate measured at pH_i 7.30±0.07 using data from 5 experiments similar to that shown in ***A***. Columns represent mean±S.E.M. * significant difference, $P<0.05$.

NHE1 (Counillon, Scholz, Lang & Pouyssengur, 1993). At this concentration (50 μM), Hoe694 inhibited almost all Na^+-H^+ exchanger activity in the type I cell (see Appendix 1). Therefore the acid influx measured in the presence of 50 μM Hoe694 (0.79±0.05 mequiv l^{-1} min^{-1}; n=5 at pH_i 7.17±0.07) can be regarded as reflecting the resting background acid loading in HEPES-buffered solution. **Fig 3.9B** shows that application of Hoe694 did not significantly change the net acid influx induced by acid challenge (2.28±0.12 mequiv l^{-1} min^{-1} and 1.99±0.39 mequiv l^{-1} min^{-1}, in the absence and presence of Hoe694, respectively; P>0.1). This suggests that, the Na^+-H^+ exchanger activity must be completely inhibited under pH_o 6.4 conditions. Therefore when Hoe694 was applied in addition to pH_o 6.4 treatment, there was no further acidification due to additional inhibition. However, the acid influx in the presence of Hoe694 plus pH_o 6.4 was considerably larger than that seen with Hoe694 alone (1.99±0.39 mequiv l^{-1} min^{-1} and 0.79±0.05 mequiv l^{-1} min^{-1}, respectively; P<0.05). This indicates that there is an extra acid influx stimulated at pH_o 6.4, in addition to the background acid loading exposed by the inhibition of Na^+-H^+ exchanger. The acid loading seen in pH_o 6.4 HEPES-buffered solutions must therefore due to two causes: the stimulation of an acid influx pathway and the inhibition of Na^+-H^+ exchanger.

In **Fig 3.10** I applied an experimental protocol similar to that shown in **Fig 3.9**, but using Na^+-free treatment instead of Hoe694 addition. **Fig 3.10A** shows the acid influx during 3 different treatments: pH_o 6.4, Na^+-free and Na^+-free plus pH_o 6.4. The acid influx rate in response to Na^+-free plus pH_o 6.4 treatment (2.09±0.22 mequiv l^{-1} min^{-1}) is not different from the control response (1.74±0.32 mequiv $^{-1}$ min^{-1}; n=6; P>0.1) at pH_i = 7.29±0.02, but it is significantly faster than that in Na^+-free solution alone

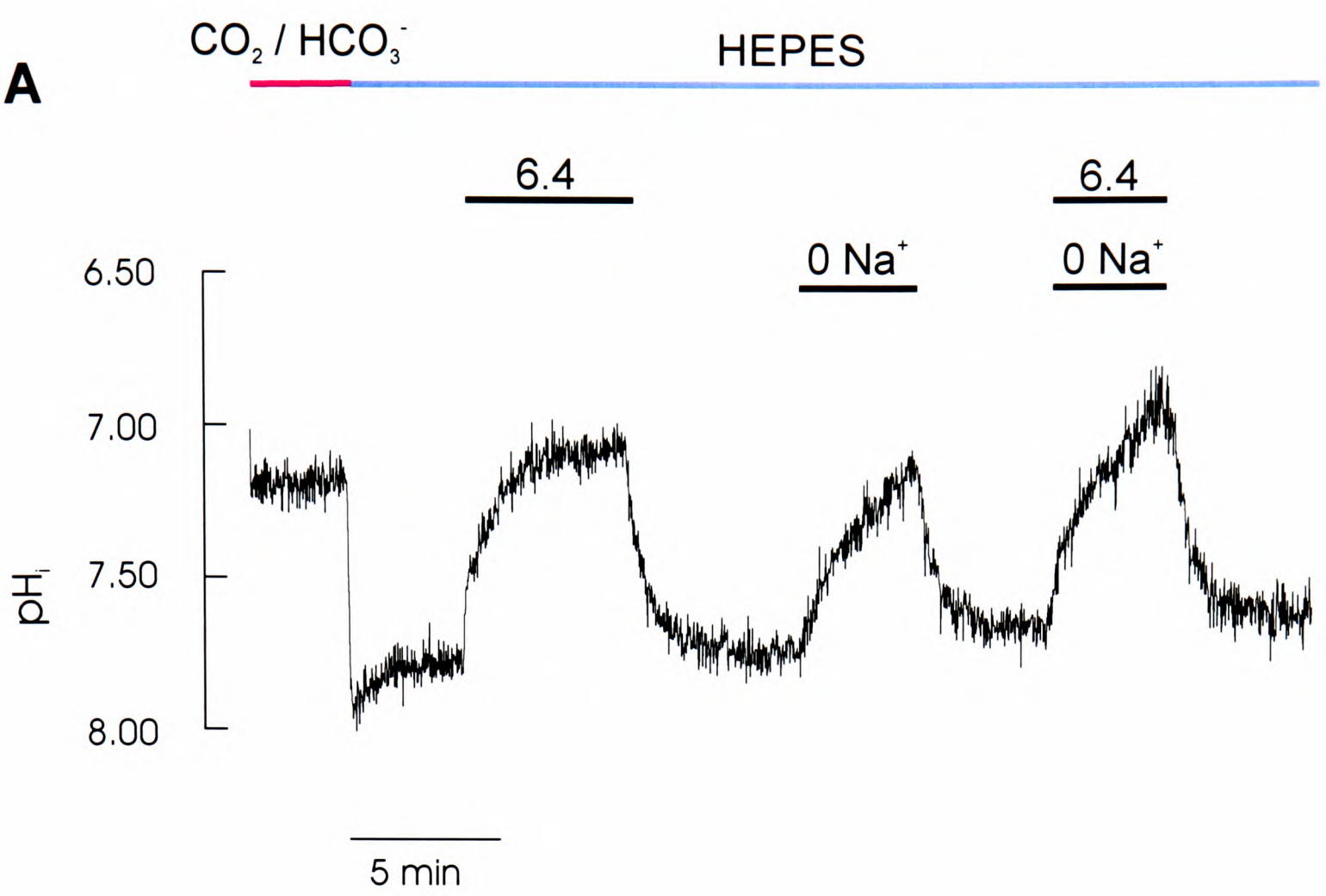


Figure 3.10

A, Comparison of acid influx rates during 3 treatments: pH_o 6.4 acid challenge, Na^+-free and pH_o 6.4 acid challenge plus Na^+-free. There was no difference between the acid influx rates during the pH_o 6.4 and pH_o 6.4 plus Na^+-free treatments. But the influx during pH_o 6.4 plus Na^+-free treatment is significantly faster than that during Na^+-free treament alone. Cells were perfused with HEPES-buffered solution. ***B***, Histogram shows mean acid influx rate measured at pH_i 7.29±0.02 using data from 5 experiments similar to that shown in ***A***. Columns represent mean±S.E.M. ** significant difference, $P<0.01$.

(1.15±0.27 mequiv $^{-1}$ min^{-1}; n=6; P<0.01). This result further strengthens the previous conclusion taken from **Fig 3.9**, that in HEPES-buffered solution, an acid challenge induces an increase in acid influx, in addition to the inhibition of Na^+-H^+ exchanger by low pH_o.

The identity of HCO_3^--independent acid loading pathway remains unknown. Some candidates for this mechanism will be considered below.

Discussion

In this study, I have investigated the mechanism for acid influx in response to an isocapnic external acidosis in carotid body type I cells. My results show that in type I cells there are dual acid influx pathways, as summarised in **Fig 3.11**. Cl^--HCO_3 exchange is responsible for approximately 70% of acid influx induced by pH_o 6.4 acid challenge in physiological conditions (i.e. in the presence of CO_2/HCO_3^-). In addition to Cl^--HCO_3 exchange, a second acid loading pathway has been detected. This pathway, which contributes about 30 % of the total acid loading at resting pH_i, is independent of both extracellular Cl^- and HCO_3^-. For this minor pathway, my results suggest that it is an increased acid influx induced by external acidosis. The possible candidates for this acid influx pathway are discussed.

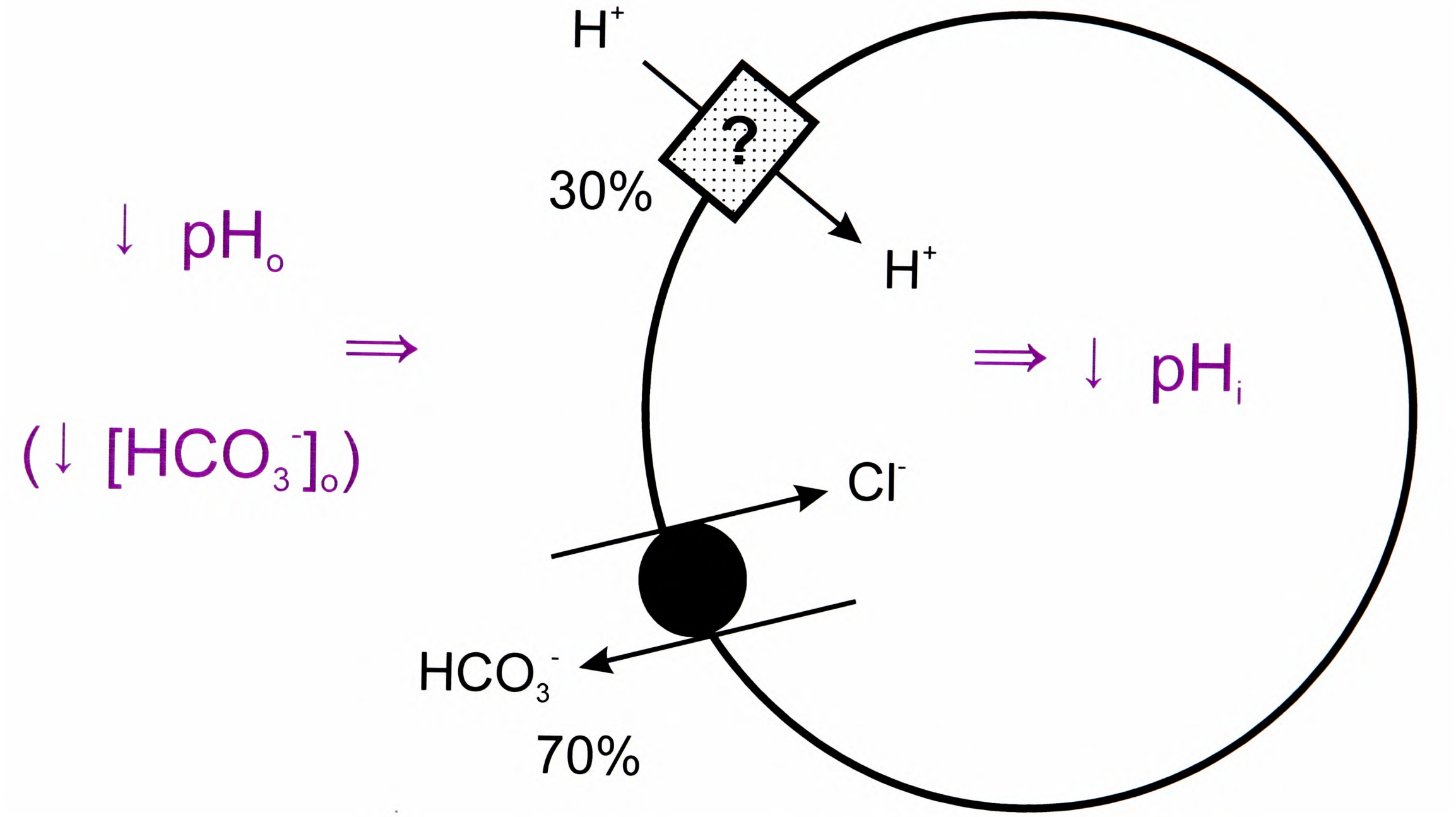


Figure 3.11

This schematic diagram illustrates the dual acid influx in the type I cell: a Cl^--HCO_3^- exchanger and an unknown H^+_o-activated HCO_3^--independent mechanism. Under physiological conditions (in the presence of CO_2/HCO_3^-), Cl^--HCO_3^- exchanger is responsible for 70% of total acid influx induced by isocapnic acidosis, while the unknown H^+_o-activated mechanism mediates the remaining 30% of acid influx.

I. HCO_3^--dependent and Cl^--dependent acid influx pathway: Cl^--HCO_3^- exchange

As shown in **Fig 3.1**, intracellular acidification is induced by extracellular isocapnic acidosis, resulting in a $\Delta pH_i/\Delta pH_o$ value of 0.57, which is exceptionally high when compared with other cell types (see Chapter 1). This value is consistent with that reported by Buckler *et al.* (1991a). Although Wilding *et al.* (1992) reported an even higher value of 0.82, it is now regarded that the extra high value was probably an artefact, caused by cell contamination with nigericin, a K^+-H^+ exchange ionophore used for the *in situ* calibration procedure (Richmond & Vaughan-Jones, 1996).

The experimental results shown in **Fig 3.2-Fig 3.6** are summarised in **Fig 3.12**: it has been revealed that the HCO_3^--dependent mechanism comprises 78% of total acid influx (see **Fig 3.2**), while **Fig 3.3** shows that the Cl^--dependent mechanism contributes 66% of the total acid influx. So it can be deduced that at least 44% of total acid loading requires both HCO_3 and Cl^-, which is represented by the minimal overlapping portion of the two components (**Fig 3.12A**). To clarify the exact relationship between the HCO_3^--dependent and Cl^--dependent mechanism, results shown in **Fig 3.4** and **Fig 3.5** are further considered. **Fig 3.4** suggests that there is no HCO_3^--independent and Cl^--dependent mechanism, so the relative contribution of the two components should be rearranged as illustrated in **Fig 3.12B**. **Fig 3.5** further confirms that the HCO_3 -independent acid influx virtually equals Cl^--independent acid influx. Therefore, it is concluded that about 70% of acid influx is mediated by a mechanism dependent on both HCO_3^- and Cl^-, as shown in **Fig 3.12C**. As it is clear that there is no Na^+_o requirement for the acid influx, the involvement of Na^+-

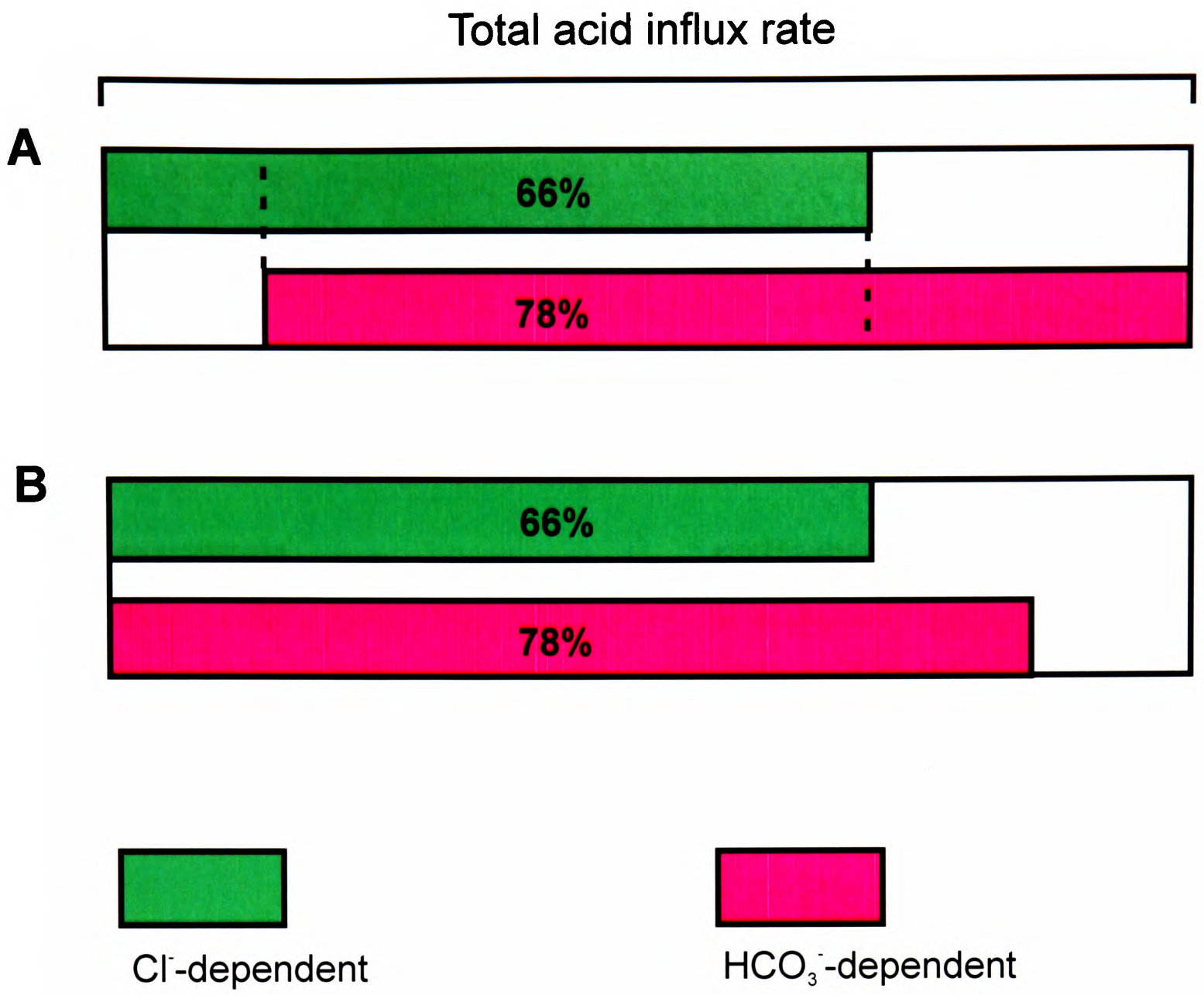
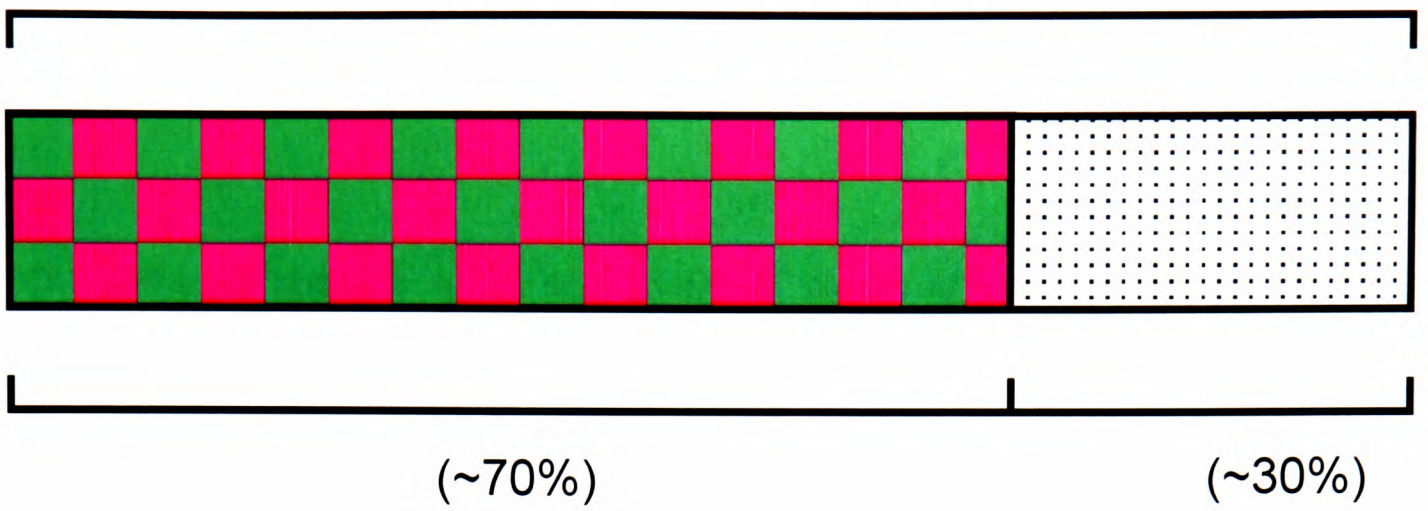


Figure 3.12

A schematic diagram showing the analysis of respective contribution from different acid loading mechanisms. ***A***, Based on data obtained in **Fig 3.2** and **Fig 3.3**, at least 44% of total acid loading requires both HCO_3^- and Cl^-. ***B***, **Fig 3.4** shows that HCO_3^--independent mechanism does not require Cl^-. **Fig 3.5** confirms HCO_3^--independent acid influx equals Cl^--independent acid influx in the same cell.

C



D

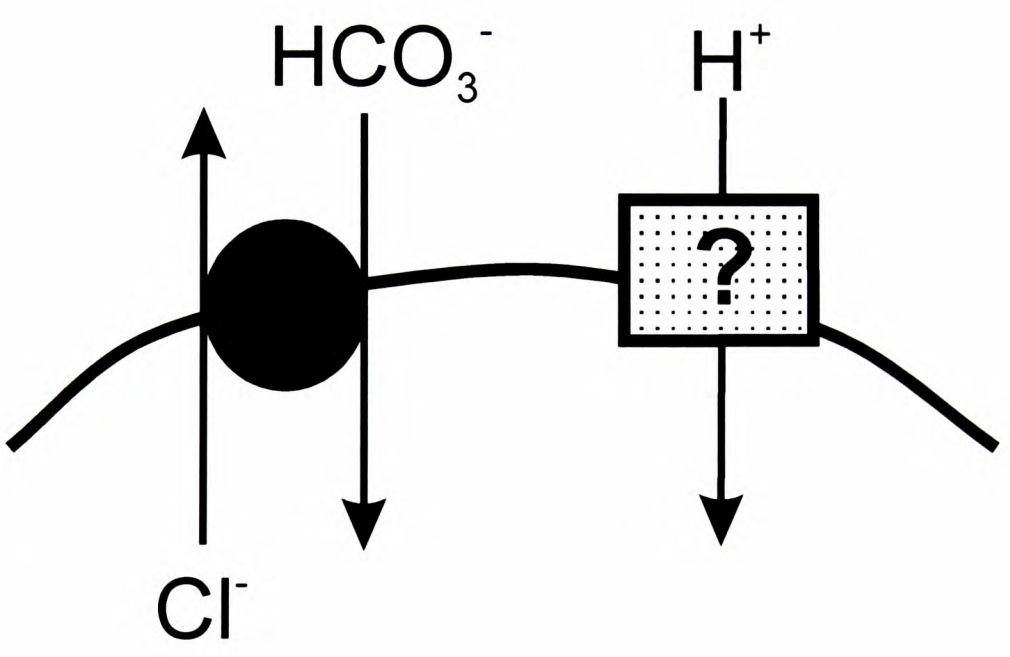


Figure 3.12 (continued)

C, Combining all the evidence, it is suggested that the HCO_3^--dependent mechanism and the Cl^--dependent mechanism are the same. In summary, about 70% of acid loading is mediated via a mechanism dependent on both HCO_3^- and Cl^-. The remaining 30% does not require either HCO_3^- or Cl^-. ***D***, As shown in **Fig 3.6**, Na^+_o is not required in the acid loading. It is concluded the major acid influx pathway is Cl^--HCO_3^- exchanger. The unidentified HCO_3^--independent mechanism is activated by H^+_o.

dependent Cl^--HCO_3^- exchange can be excluded (**Fig 3.6**). In conclusion, the majority of acid influx is probably mediated by Cl^--HCO_3^- exchange (**Fig 3.12D**).

Cl^--HCO_3 exchange operates as an acid loader in many other cell types, including cardiomyocytes (Vaughan-Jones, 1979), smooth muscle (Aickin & Brading, 1984), and liver cells (Meier, Knickelbein, Moseley, Dobbins & Boyer, 1985). Thermodynamics predicts that, the change in Gibb's free energy ($\Delta\mu$) for Cl^--HCO_3 exchange operating in forward transport mode (i.e. as acid loader) is:

$$\Delta\mu = 2.3RT \times \{\log\frac{[Cl^-]_i}{[Cl^-]_o} + \log\frac{[HCO_3^-]_o}{[HCO_3^-]_i}\}$$
$$= 2.3RT \times \{\log\frac{[Cl^-]_i}{[Cl^-]_o} + (pH_o - pH_i)\} \qquad \textbf{[Eqn. 3.2]}$$

(assuming an open system for CO_2)

Taking the intracellular Cl^- concentration ($[Cl^-]_i$) in the type I cell to be 45 mM (Oyama, Walker & Eyzaguirre, 1986), it can be seen that during acid challenge, at resting pH_i 7.2 and pH_o 6.4, $[Cl^-]_o$ = 142.5 mM, Cl^--HCO_3^- exchange in type I cells can act as acid loader, with a free energy change of –7.76 kJ/mol (negative $\Delta\mu$ value represents thermodynamically spontaneous process). The kinetics of this exchange will be further examined in Chapter 5.

Stea and Nurse (1989, 1991) reported that a Cl^- channel in type I cells can also display a high HCO_3 conductance of 210 pS. At pH_i 7.2-7.3 and pH_o 6.4, the equilibrium potential of HCO_3 ion (E_{HCO3}) is about 50 mV, since E_{HCO3}= 2.3 RT/F (pH_i-pH_o) (**Equation 1.6**). As the resting membrane potential of type I cell is around –50 mV

(Buckler & Vaughan-Jones, 1998), a net HCO_3^- efflux would be expected when the anion channel is opened. It follows that under this condition (pH_o 6.4 CO_2/HCO_3^- solution), the putative HCO_3^- channel could be responsible for mediating the acid influx. Intracellular acidification produced by HCO_3^- efflux through an anion channel has been recorded in crayfish muscle by Kaila *et al.* (1990). However, my results in the type I cell clearly show that there is no significant contribution to acid influx from a HCO_3^--dependent mechanism that does not require Cl^-, such as a HCO_3^- channel (see summary in **Fig 3.12C**). To further confirm this, I investigated directly whether a HCO_3^- channel is involved in the acid influx.

By applying 144.5 mM K^+_o in the superfusate, the membrane potential of type I cell would be depolarised from –50 mM to around 0 mV. According to Ohm's law:

$$I_{HCO3} = g_{HCO3} \times (E_m - E_{HCO3}) \qquad \textbf{[Eqn. 3.3]}$$

Where I_{HCO3} is HCO_3^- current, g_{HCO3} is HCO_3^- conductance.

Such a depolarisation would significantly reduce the electrochemical driving force acting on HCO_3^- ions to about 50% of the original value, since the value of (E_m - E_{HCO3}) is halved. One would expect to see a significant decrease in acid influx. The lack of such a decrease in **Fig 3.7** suggests a HCO_3^- channel does not play any major role in acid influx.

The magnitude of the possible HCO_3^- flux through an anion channel was also assessed at pH_i 7.2-7.3 and pH_o 7.7. Under such conditions, E_{HCO3} = -30 mV, which would mediate HCO_3^- efflux if a HCO_3^- channel is open. By depolarising the membrane

potential from –50 mV to around -10 mV in low Na^+, high K^+ solution, the direction of HCO_3^- flux should be expected to reverse from efflux to influx, causing intracellular alkalosis. However, there is no significant pH_i response (**Fig 3.8**). It is therefore concluded that a HCO_3^- channel is not mediating significant HCO_3^- flux at least under the conditions tested.

Moreover, my results also exclude the possibility of major contributions from any Cl^--dependent but HCO_3^--independent mechanism, such as a Cl^--OH^- exchanger (**Fig 3.4**). In fact, the stilbene disulfonate drug DBDS, a Cl^--OH^- exchange inhibitor (Sun, Leem & Vaughan-Jones, 1996), failed to inhibit the acid influx (see **Fig 4.4**).

II. HCO_3^--independent and Cl^--independent acid influx pathway: an unknown mechanism

Fig 3.9 shows that, under HCO_3^--free conditions, the acid influx induced by acid challenge was not affected by the application of 50 μM Hoe694. Since 50 μM Hoe694 completely inhibits Na^+-H^+ exchanger (for dose dependent inhibition of Na^+-H^+ exchanger by Hoe694, see Appendix 1), this result indicates Na^+-H^+ exchanger is almost totally inactive at pH_o 6.4, an observation consistent with other investigators (Vaughan-Jones & Wu, 1990). This inhibition of Na^+-H^+ exchanger by reducing pH_o may be caused by competition between Na^+_o and H^+_o ions for their binding site on Na^+-H^+ exchanger, as seen in other cell types (Aronson, Suhm & Nee, 1983), although a mixed inhibitory effect of H^+_o has been reported for Na^+-H^+ exchanger in cardiac tissue (Wu & Vaughan-Jones, 1997).

The application of an acid challenge in the presence of Hoe694 increases net acid loading, compared with that seen with Hoe694 alone. The acid loading rate recorded during Hoe694 treatment (J_H = 0.79±0.05 mequiv l^{-1} min^{-1}) can be regarded as the background acid loading unmasked by the inhibition of Na^+-H^+ exchanger. This rate increases about twofold to 1.99±0.39 mequiv l^{-1} min^{-1} as pH_o is reduced from 7.4 to 6.4 in the presence of Hoe694, suggesting the HCO_3^--independent and Cl^--independent acid influx pathway is an H^+_o-activated mechanism. My results also indicate this acid influx pathway is Na^+-independent, since removal of Na^+_o did not affect the acid loading in response to acid challenge (**Fig 3.10**).

At present, the exact nature of the HCO_3^--independent and Cl^--independent pathway is still not elucidated. Two possible candidates are considered here:

1. **H^+ channel**: After its discovery in snail neurones (Thomas & Meech, 1982), H^+ channels have also been identified in several mammalian cell types, including rat alveolar epithelial cells (DeCoursey, 1991), macrophages (Kapus, Romanek, Qu, Rotstein & Grinstein 1993) and neutrophils (DeCoursey & Cherny, 1993). Since the equilibrium potential for H^+ is $E_H = 2.3RT/F \times(pH_i-pH_o)$ (see **Equation 1.4**), a fall in pH_o increases the driving force for H^+ influx. It seems possible that an H^+ channel could be a candidate mechanism for the minor acid influx pathway. However, H^+ channels found so far in various cell types are voltage-gated. They open with depolarisation, and the voltage-dependence is strongly sensitive to pH_o and pH_i such that they only carry outward current (i.e. H^+ efflux) under physiological conditions (DeCoursey & Cherny 2000). In addition, in **Fig 3.7** and **Fig 3.8**, it has been shown that membrane depolarisation by high K^+ treatment

does not produce a significant change in acid influx, giving evidence against the involvement of an H^+ conductance pathway. It should be noted that experiments shown in **Fig 3.7** and **Fig 3.8** were carried out in CO_2/HCO_3^--buffered solutions, in which a small contribution to acid influx from the putative H^+ conductance may be difficult to detect due to the high value of CO_2/HCO_3^--dependent buffering. The effect of high K^+_o treatment was therefore further examined under CO_2/HCO_3^--free conditions (see Appendix 2), and there was still no evidence of acid influx through an H^+ channel. Nevertheless, for a comprehensive inspection of the existence and function of H^+ channel in the type I cell, further electrophysiological investigation will be needed.

2. **Ca^{2+}-ATPase**: Evidence for a plasmalemma Ca^{2+}-H^+ exchange activity has recently been reported in snail neurones (Schwiening, Kennedy & Thomas, 1993) and hippocampal neurones (Trapp, Lückermann, Kaila & Ballanyi, 1996), in which Ca^{2+} extrusion is coupled to H^+ influx via plasmalemmal Ca^{2+}-ATPase. An intracellular acidification mediated by Ca^{2+}-ATPase in response to Ca^{2+} influx was also reported in cerebellar granule cells (Wu, Chen, Chen, Chen & Chu, 1999). In addition, it was found the Ca^{2+}-H^+ ATPase activity increases at acidic pH_o (Schwiening *et al.* 1993; Valant & Haynes, 1993). Although a Ca^{2+}-H^+ ATPase has yet to be identified in type I cells, it is an attractive candidate for the novel H^+_o-activated acid influx pathway. Indeed, I have found that the application of high K^+_o induces a significant Ca^{2+}_o-dependent acid influx in HEPES-buffered solutions, an observation consistent with the involvement of Ca^{2+}-ATPase (hence Ca^{2+}-H^+ exchange). See Appendix 2 for further details.

CHAPTER 4

The Effect of DIDS upon Cl^--HCO_3^- Exchange in the Carotid Body Type I Cell

Introduction

As shown in Chapter 3, the majority of acid influx in response to extracellular acidosis in the type I cell is mediated by Cl^--HCO_3^- exchange operating as an acid loader. It has been established that stilbene disulphonates are specific inhibitors of the Cl^--HCO_3 exchanger (AE) (Cabantchik & Rothstein, 1972; 1974). The most commonly used stilbene disulphonates include DIDS (4,4'-diisothiocyano stilbene-2,2'-disulphonic acid), DBDS (4,4'-dibenzoyl stibene-2,2'-disulphonic acid) and H_2DIDS (4,4'-diisothiocyano dihydrostilbene-2,2'-disulphonic acid) (see Cabantchik & Greger, 1992 for review). Among them, DIDS is the most potent inhibitor of the Cl^--HCO_3^- exchanger, with IC_{50} values of 0.04 μM, 4 μM and 0.43 μM for AE1, AE2 and AE3, respectively (Funder, Toteson & Wieth, 1978; Lee, Gunn & Kopito, 1991; He, Wu, Knauf, Tabak & Melvin, 1993). Initially DIDS reversibly binds with the erythrocyte's band 3 protein (AE1). The reversible binding is sufficient for inhibition of Cl^--HCO_3^- exchange. DIDS then gradually forms an irreversible covalent bond with AE1 on a 1:1 basis, if treated continuously (Cabantchik & Rothstein, 1974; Lepke, Fasold, Pring & Passow, 1976). Structural studies have shown the covalent binding site is lysine 558 on mouse AE1. This covalent binding site, however, may not participate in the

reversible binding, since site-directed mutagenesis of lysine 558 on AE1 did not abolish its functional sensitivity to DIDS (Bartel, Lepke, Layh-Schmitt, Legrum & Passow, 1989; Wood, Müller, Sovak & Passow, 1992).

The kinetic mechanism of reversible inhibition of the Cl^--HCO_3 exchanger is presumably competitive inhibition, in which DIDS competes with Cl^-_o for the externally facing anion transport site (Shami, Carver, Ship & Rothstein, 1976; Jessen, Sjoholm & Hoffmann). There is also evidence that DIDS remains in an externally accessible position after binding, without entering the cell (Cabantchik & Rothstein, 1974). However, later studies using NMR techniques proposed that the binding sites of DIDS and Cl^- may not necessarily overlap, although the binding of DIDS indeed prevents subsequent Cl^- binding, possibly via steric hindrance (Falke & Chan, 1986; Bahar, Gunter, Wu, Kennedy & Knauf, 1999). Salhany and co-workers suggested DIDS binds at a different site on AE1 and interacts with Cl^- transport site allosterically (Salhany, Sloan, Cordes & Schopfer, 1994; Schofer & Salhany, 1995). Further structural studies are required to clarify the identity of DIDS and Cl^- binding sites.

Buckler *et al.* (1991b) demonstrated that DIDS inhibits the Cl^--free induced alkalosis mediated via the reverse transport mode of Cl^--HCO_3^- exchange in type I cells, evidence consistent with previous observations in other cell types, such as the cardiac Purkinje fibre (Vaughan-Jones, 1979) and smooth muscle (Aickin & Brading, 1984). In the present study, however, I find that although 200 μM DIDS is able to inhibit the reverse mode of Cl^--HCO_3^- exchange, it has no effect on the acid loading induced by isocapnic acidosis, which is presumably mediated via the forward mode of Cl^--HCO_3^- exchange. Possible explanations for this unexpected finding will be discussed.

Methods

General Methods

pH_i was recorded in isolated type I cells from the neonatal rats using carboxy-SNARF-1, as described in Chapter 2.

Solutions

Standard CO_2/HCO_3^--buffered solution, pH 6.4 CO_2/HCO_3^--buffered solution and sodium acetate solution were prepared as described in Chapter 2. Cl^--free solutions (CO_2/HCO_3^--buffered and HEPES-buffered) were prepared as described in Chapter 3.

Most experiments described in this chapter, excluding that shown in **Fig 4.11**, were carried out in CO_2/HCO_3^--buffered solution.

Drugs

The following drugs were used: 4,4'-diisothiocyano dihydrostilbene-2,2'-disulphonate, disodium salt (DIDS) was from Calbiochem (Nottingham, UK); 4,4'-dibenzoyl stibene-2,2'-disulphonate, disodium salt (DBDS) was from Molecular Probe (Eugene, Oregon, USA). Because isothiocyanates are unstable in water, DIDS was added as solid to the solutions immediately before use. As stilbene disulphonates are light-sensitive, containers in which solutions of DIDS and DBDS were kept were covered with aluminum foil during the experiment.

Results

Alkalosis induced by Cl^-_o-removal is inhibited by DIDS

Under resting conditions, Cl^--HCO_3^- exchange presumably operates in its forward mode transporting HCO_3 ions out of the cell in exchange for Cl^- ions, resulting in a net acid influx (see Chapter 1). When extracellular Cl^- (Cl^-_o) is removed, the large outward Cl^- gradients can force the net transport mode to reverse, leading to acid efflux (i.e. HCO_3^- influx). This phenomenon is demonstrated in **Fig 4.1**. In CO_2/HCO_3^--buffered solution, the abrupt Cl^-_o removal induced a reversible intracellular alkalosis in which pH_i increased by 0.49±0.05 pH units (n=4). This response was reversible and repeatable (data not shown).

The Cl^--free induced alkalosis was almost completely inhibited by Cl^--HCO_3^- exchange inhibitor DIDS, as shown in the later part of the experiment. The control net acid *efflux* was markedly reduced from 8.09±0.51 mequiv l^{-1} min^{-1} to 0.89±0.78 mequiv l^{-1} min^{-1} at pH_i=7.24±0.05 after DIDS treatment (n=5; P<0.01). This result is consistent with the observations of Buckler *et al.* (1991b).

Acid loading is insensitive to DIDS

I have shown that in CO_2/HCO_3^--buffered solution, acid influx induced by isocapnic acidosis is mainly mediated by Cl^--HCO_3^- exchange (see Chapter 3). It would therefore be expected that DIDS should inhibit such acid influx. **Fig 4.2**, however, shows that acid influx was unaffected by 200 μM DIDS, the same concentration that blocked the reversed mode of Cl^--HCO_3^- exchange in **Fig 4.1**. There is no statistical

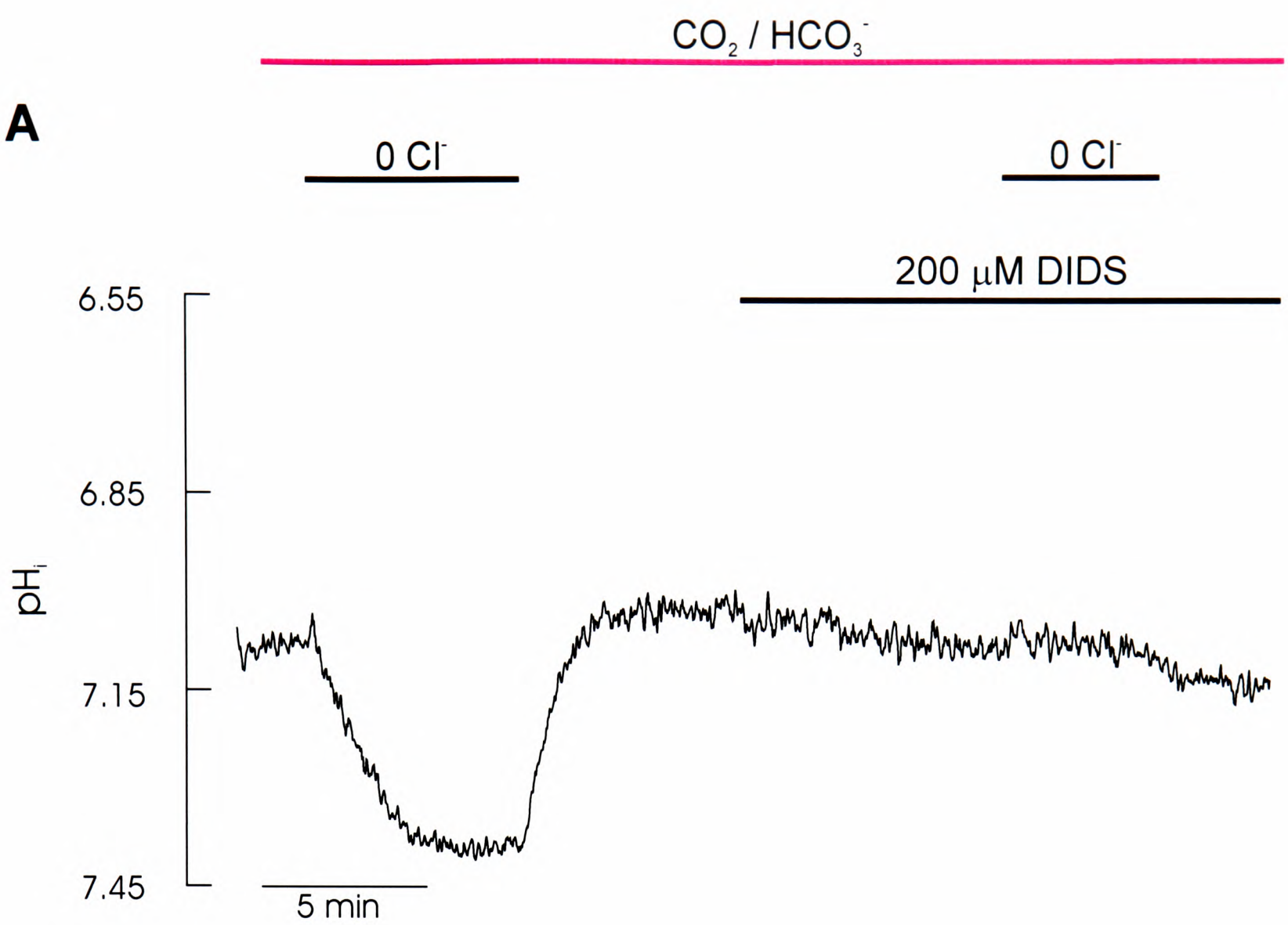


Figure 4.1

A, Effect of Cl^-_o removal upon pH_i in CO_2/HCO_3^--buffered solution. Cl^--free solution caused intracellular alkalosis, suggesting the existence of Cl^--$HCO3^-$ exchanger. 200 μM DIDS almost completely blocked this alkalosis. ***B***, Histogram shows mean acid efflux rate measured at pH_i 7.24±0.05 using data from 5 experiments similar to that shown in ***A***. Columns represent mean±S.E.M. ** significant difference, $P<0.01$.

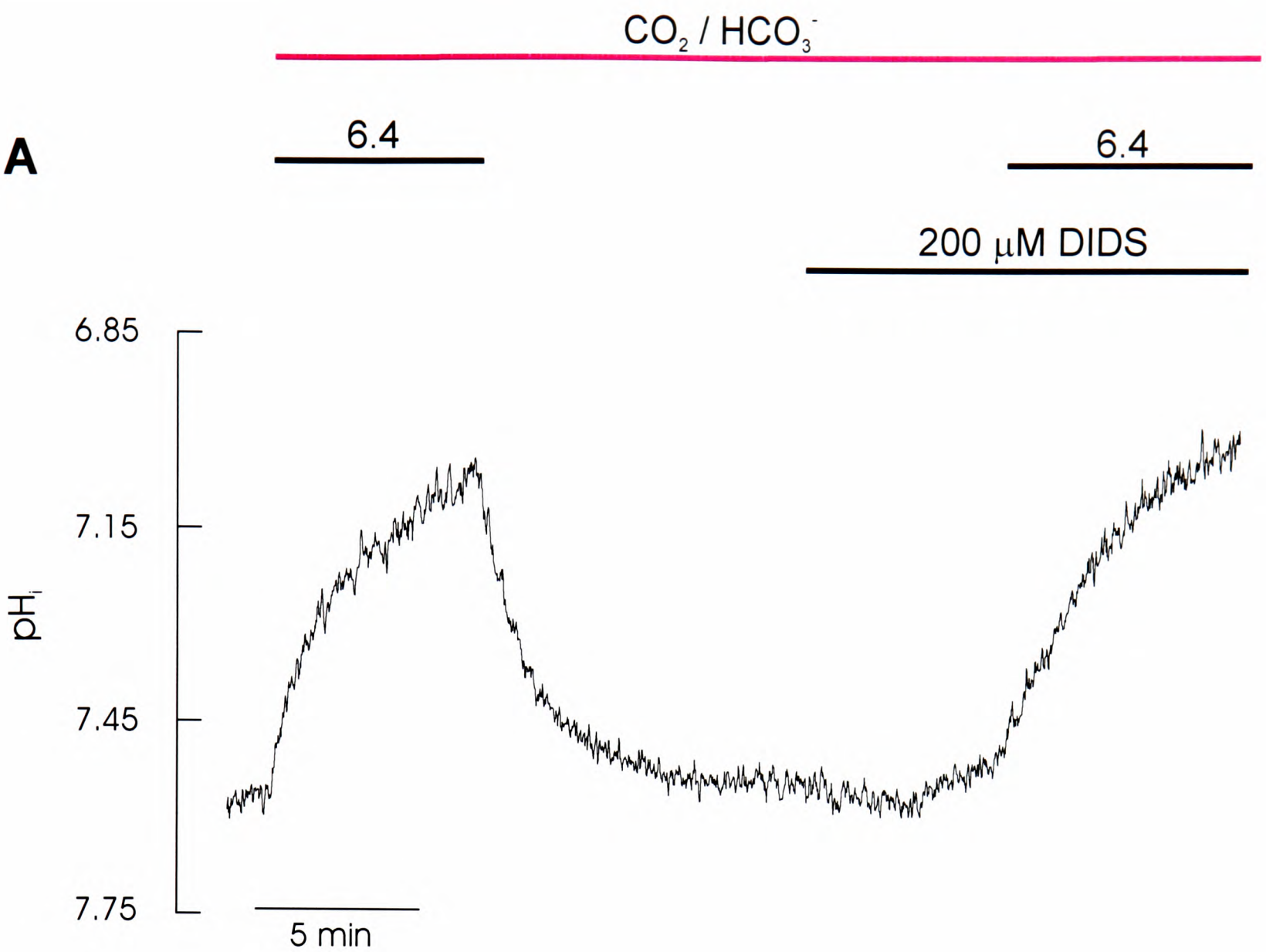


Figure 4.2

A, Effect of DIDS upon acid loading in CO_2/HCO_3^--buffered solution. Although 200 μM DIDS blocked Cl^--free induced alkalosis, as shown in **Fig.4.1**, the same concentration of DIDS did not have significant effect upon acid loader. ***B***, Histogram shows mean acid influx rate measured at pH_i 7.22±0.02 using data from 5 experiments similar to that shown in ***A***. Columns represent mean±S.E.M. No significant difference, P>0.5.

difference between acid influx before (5.41±0.73 mequiv l^{-1} min^{-1}) and after (4.56±0.47 mequiv l^{-1} min^{-1}) DIDS treatment ($P>0.5$; $n=5$ at pH_i 7.16±0.02).

The effect of DIDS upon acid loading was further examined in **Fig 4.3**. In this experiment, the acid influx rates were measured under Cl^--free conditions in the absence and presence of DIDS. Similar to **Fig 3.3** in Chapter 3, the acid loading in Cl^--free solution is about 30% of the control response. Furthermore, DIDS had no effect on the remaining Cl^--independent acid influx. The Cl^--independent acid influx rates were 4.02±0.73 mequiv l^{-1} min^{-1} and 5.41±0.73 mequiv l^{-1} min^{-1} at pH_i 7.31±0.12, in the absence and presence of DIDS, respectively ($n=3$; $P>0.1$).

Combining the above results, it is known that the total acid influx pathway (comprising major and minor acid influx pathways, as revealed in **Fig 4.2**) and the minor acid influx pathway (mediated by a Cl^--independent and HCO_3 -independent mechanism, as revealed in **Fig 4.3**) are both insensitive to DIDS. I therefore conclude that the major acid influx pathway, which is mediated by the forward transport mode of Cl^--HCO_3^- exchange, must also be insensitive to DIDS. Surprisingly, this is in contrast to the result of **Fig 4.1**, which demonstrates that the reversed transport mode of Cl^--HCO_3^- exchange is *sensitive* to DIDS.

DBDS, another stilbene disulphonate, has been reported to inhibit anion exchangers, including Cl^--HCO_3^- exchanger and Cl^--OH^- exchanger (Falke & Chan, 1986; Sun, Leem & Vaughan-Jones, 1996). Nevertheless, 200 μM DBDS had no effect on acid loading (**Fig 4.4**). The acid influx rates were 5.11±0.91 mequiv l^{-1} min^{-1} and

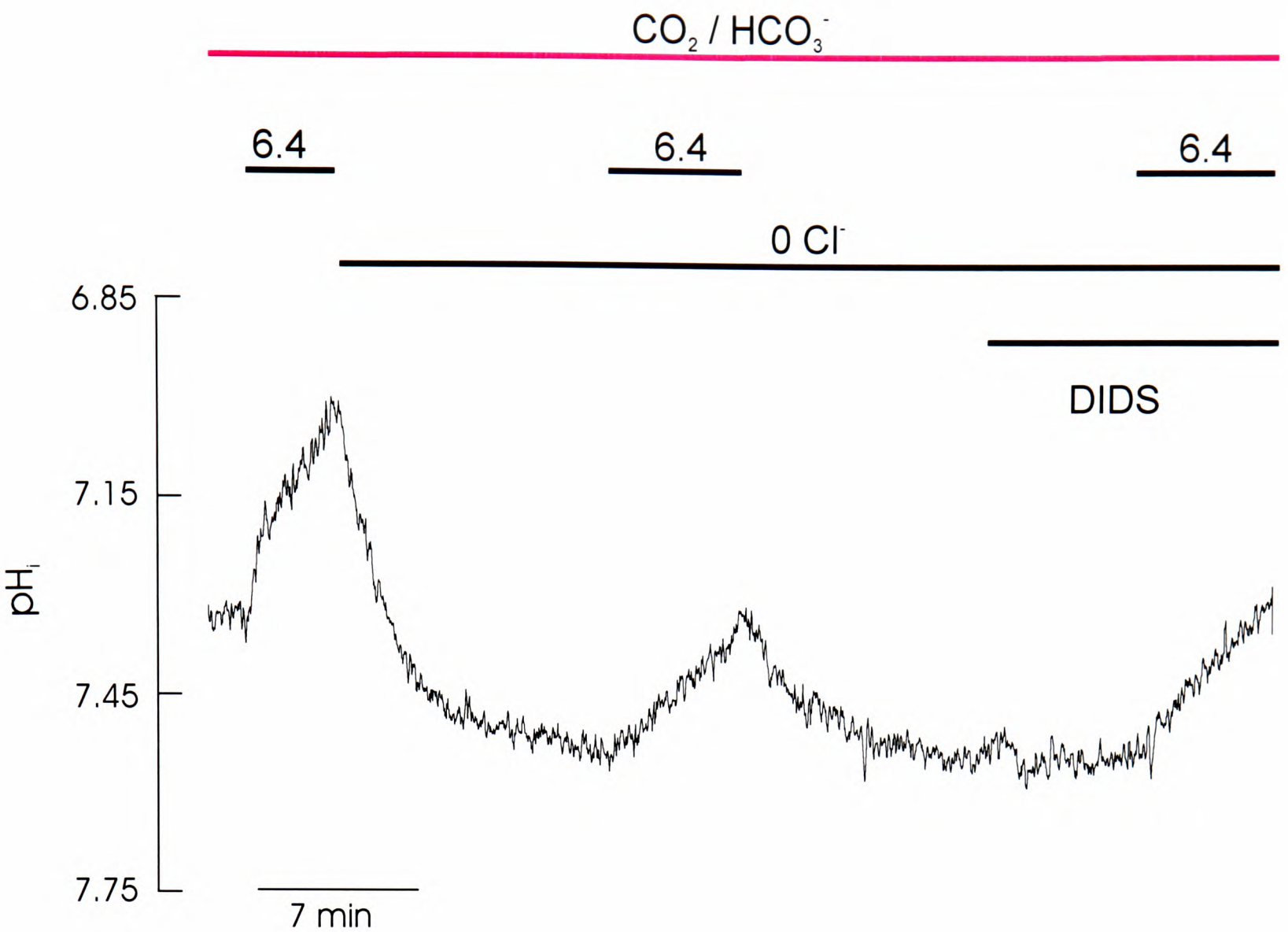


Figure 4.3

Effect of DIDS upon Cl^--independent acid loading in CO_2/HCO_3^--buffered solution. Acid challenge was applied in Cl^--free solution, in the absence and presence of 200 μM DIDS, so that the effect of DIDS upon Cl^--independent component of the acid loading can be seen. DIDS did not have significant effect upon Cl^--independent acid loading. This is a typical pH_i record from 3 similar experiments.

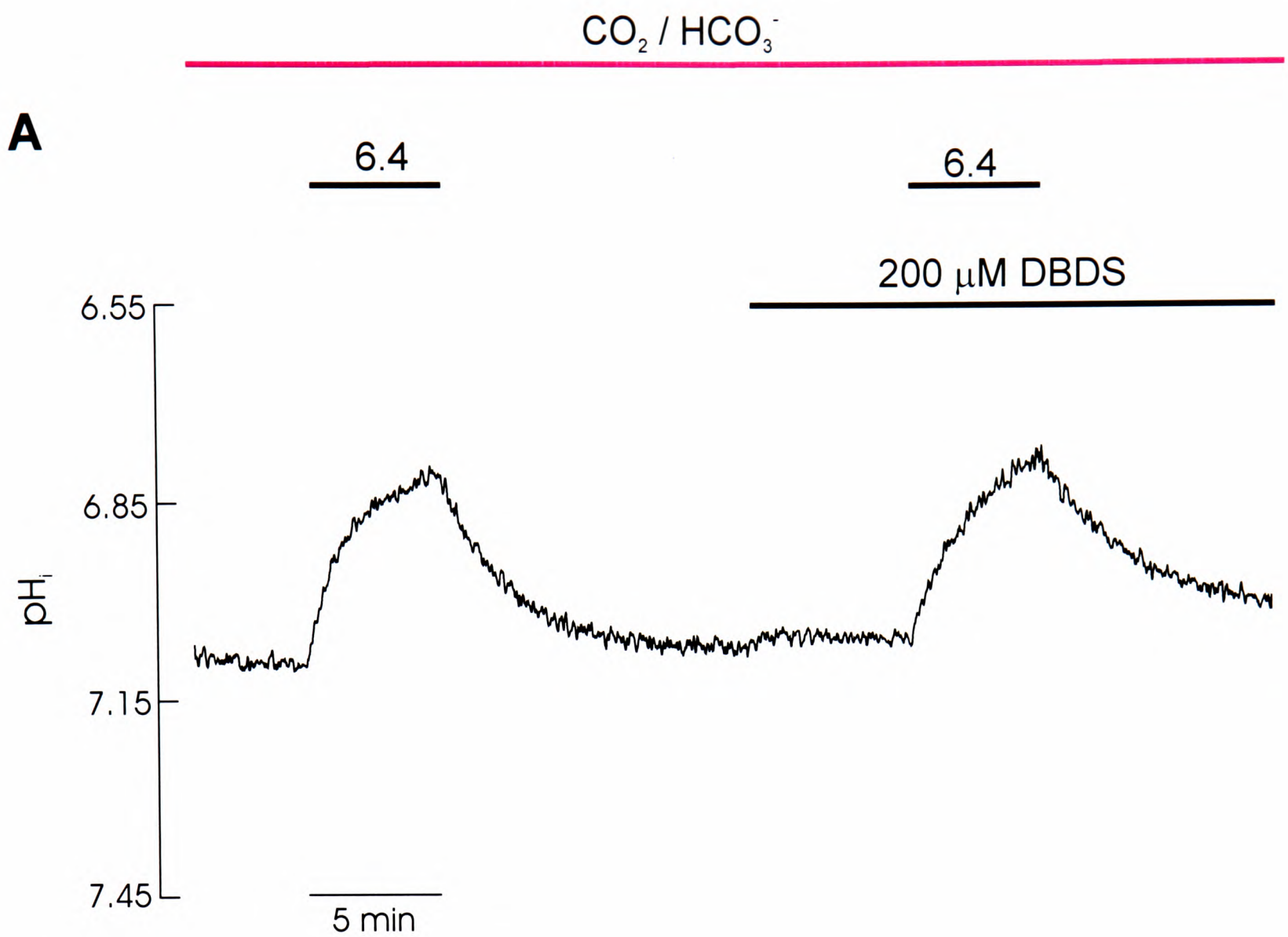


Figure 4.4

A, Effect of DBDS upon acid loading in CO_2/HCO_3^--buffered solution. 200 μM DBDS did not have significant effect upon acid loader. ***B***, Histogram shows mean acid influx rate measured at pH_i 7.20±0.02 using data from 5 experiments similar to that shown in ***A***. Columns represent mean±S.E.M. No significant difference, P>0.1.

4.82±0.36 mequiv l^{-1} min^{-1} at pH_i 7.20±0.02, in the absence and presence of DBDS, respectively (n=5; P>0.5).

DIDS insensitivity of acid loading is not caused by acidic pH_o

So far, my evidence shows that the acid loading induced by reducing pH_o is insensitive to DIDS. However, it is possible that the extracellular binding of DIDS to the Cl^--HCO_3^- exchanger and/or the inhibitory effect of DIDS is dependent on pH_o, i.e. at acidic pH_o (pH_o 6.4), the binding and/or inhibition of DIDS may be weakened. If such an effect were occurring, this could explain the difference in DIDS sensitivity of Cl^--free induced alkalosis at pH_o 7.4 (see **Fig 4.1**) and acid loading at pH_o 6.4 (see **Fig 4.2**). To test this possibility, I carried out the experiment illustrated in **Fig 4.5**. Type I cells were initially perfused with pH_o 6.4 solution, then the effect of DIDS on Cl^--induced alkalosis was examined at pH_o 6.4. It is evident that even at pH_o 6.4, DIDS still inhibited the reversed mode of Cl^--HCO_3^- exchange. The acid efflux rates were 4.09±1.27 mequiv l^{-1} min^{-1} and 1.27±0.61 mequiv l^{-1} min^{-1} at pH_i 6.61±0.22, in the absence and presence of DIDS, respectively (n=5; P<0.05). Nevertheless, the later part of this experiment demonstrates the acid loading induced by pH_o 6.4 treatment remained insensitive to DIDS. This result proves the DIDS insensitivity of acid loading is not the result of a pH_o dependency of its binding.

DIDS insensitivity of acid loading is not caused by the presence of Cl^-_o

Fig 4.1 demonstrated the inhibition of Cl^--free induced alkalosis by DIDS. In **Fig 4.6**, DIDS was added in Cl^--free solution after the initial alkalosis, and its effect on pH_i recovery after Cl^-_o re-addition was observed. It is obvious that while DIDS significantly reduced acid *influx* rate during the recovery, the inhibition was not

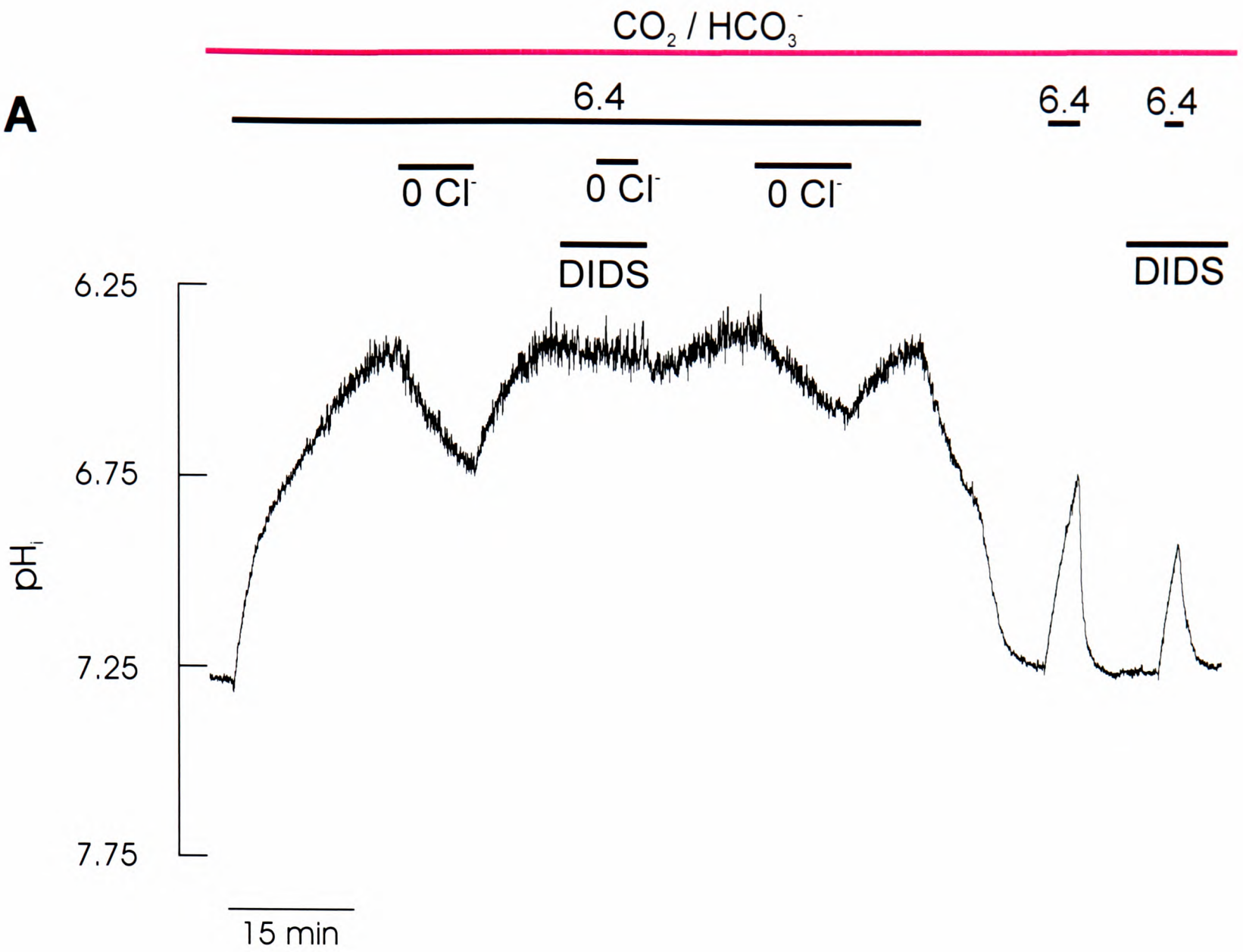


Figure 4.5

A, Effect of acid pH_o (pH_o 6.4) upon DIDS inhibition of Cl^--free induced alkalosis in CO_2/HCO_3^--buffered solution. At pH_o 6.4, 200 μM DIDS can still inhibit Cl^--free induced alkalosis, suggesting the effect of DIDS was not lost at pH_o 6.4. ***B***, Histogram shows mean acid efflux rate measured at pH_i 6.40±0.08 using data from 5 experiments similar to that shown in ***A***. Columns represent mean±S.E.M. ** significant difference, P<0.01.

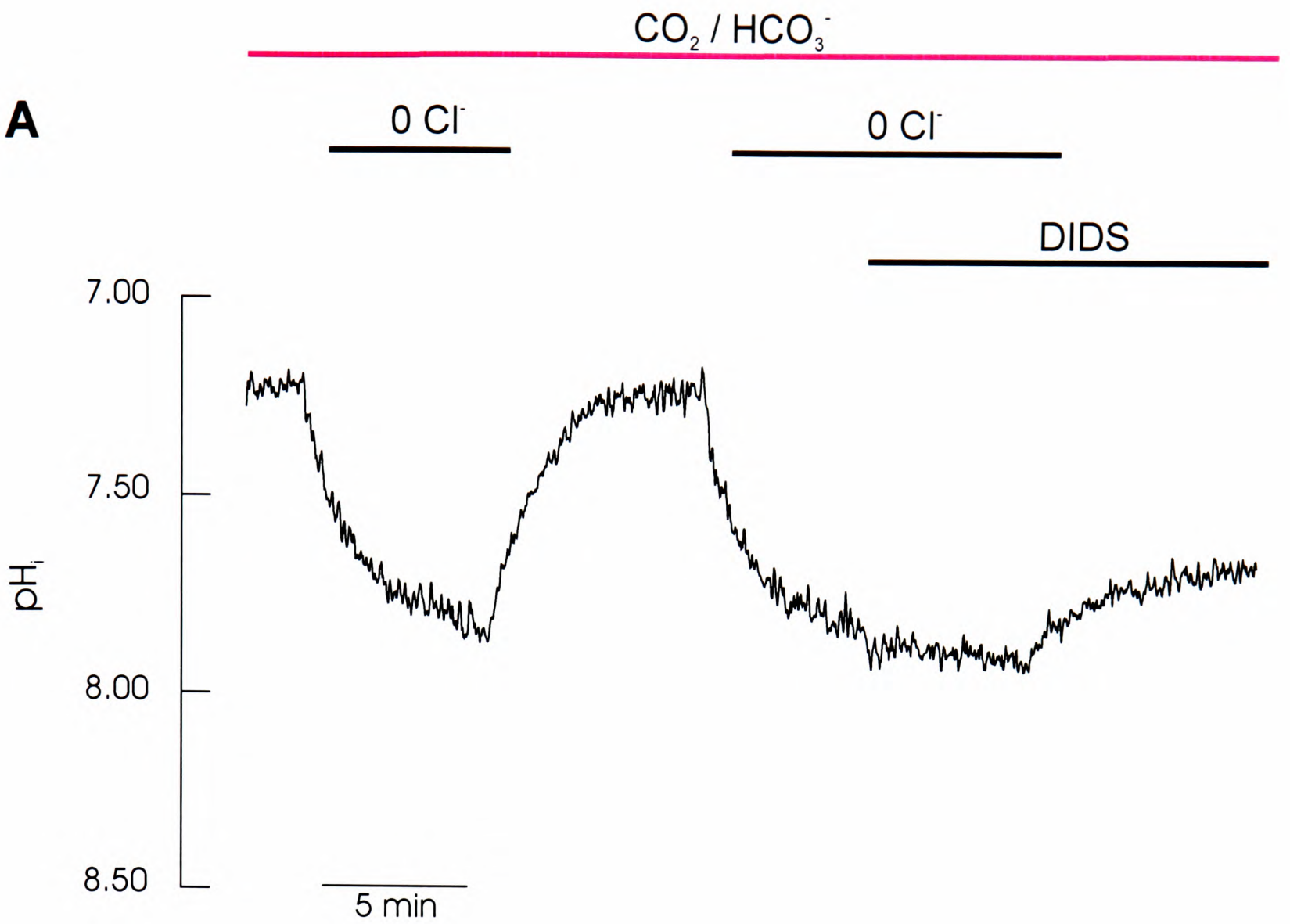


Figure 4.6

A, Effect of DIDS upon pH_i recovery from Cl^--free induced alkalosis in CO_2/HCO_3^--buffered solution. Although 200 μM DIDS largely reduced the recovery, there was still a small acid influx in the presence of DIDS. ***B***, Histogram shows mean acid efflux rate measured at pH_i 7.55±0.02 using data from 6 experiments similar to that shown in ***A***. Columns represent mean±S.E.M. ** significant difference, $P<0.01$.

complete. The acid influx rates were reduced from 10.78±2.90 mequiv l^{-1} min^{-1} to 1.98±0.02 mequiv l^{-1} min^{-1} at pH_i 7.55±0.02, before and after DIDS treatment, respectively (n=5; P<0.01).

It is commonly believed that DIDS inhibits Cl^--HCO_3^- exchanger by competing with Cl^- for binding (see Introduction). If there were a competition between DIDS and Cl^-_o, the presence of Cl^-_o might interfere with DIDS binding. In fact, DIDS inhibited about 80% of the recovery after Cl^- re-addition (see **Fig 4.6**), a little lower than the 90% inhibition of the Cl^--free induced acid efflux (see **Fig 4.1**). The difference in the extent of inhibition possibly reveals the competition between DIDS and Cl^-_o. Such a competition might also be able to explain the difference in DIDS sensitivity of Cl^--free induced alkalosis in the absence of Cl^-_o (see **Fig 4.1**) and acid loading in the presence of Cl^-_o (see **Fig 4.2**).

To investigate this possible explanation, I carried out the following two experiments. In **Fig 4.7**, a cell was pretreated with DIDS for over 5 minutes under Cl^--free conditions, allowing DIDS binding to the Cl^--HCO_3^- exchanger without the possible competition from Cl^-_o. In the continuous presence of DIDS, a standard acid challenge was then given simultaneously with the re-addition of Cl^-_o. This protocol was to ensure there was some DIDS bound to the transporter at the onset of the acid challenge. Even so, the subsequent acid loading was unaffected, with the rates of 4.22±0.74 mequiv l^{-1} min^{-1} and 3.76±0.59 mequiv l^{-1} min^{-1} at pH_i 7.08±0.02, in the absence and presence of DIDS, respectively (n=6; P>0.1). This evidence suggests the DIDS insensitivity of acid loading is not caused by competition from Cl^-_o.

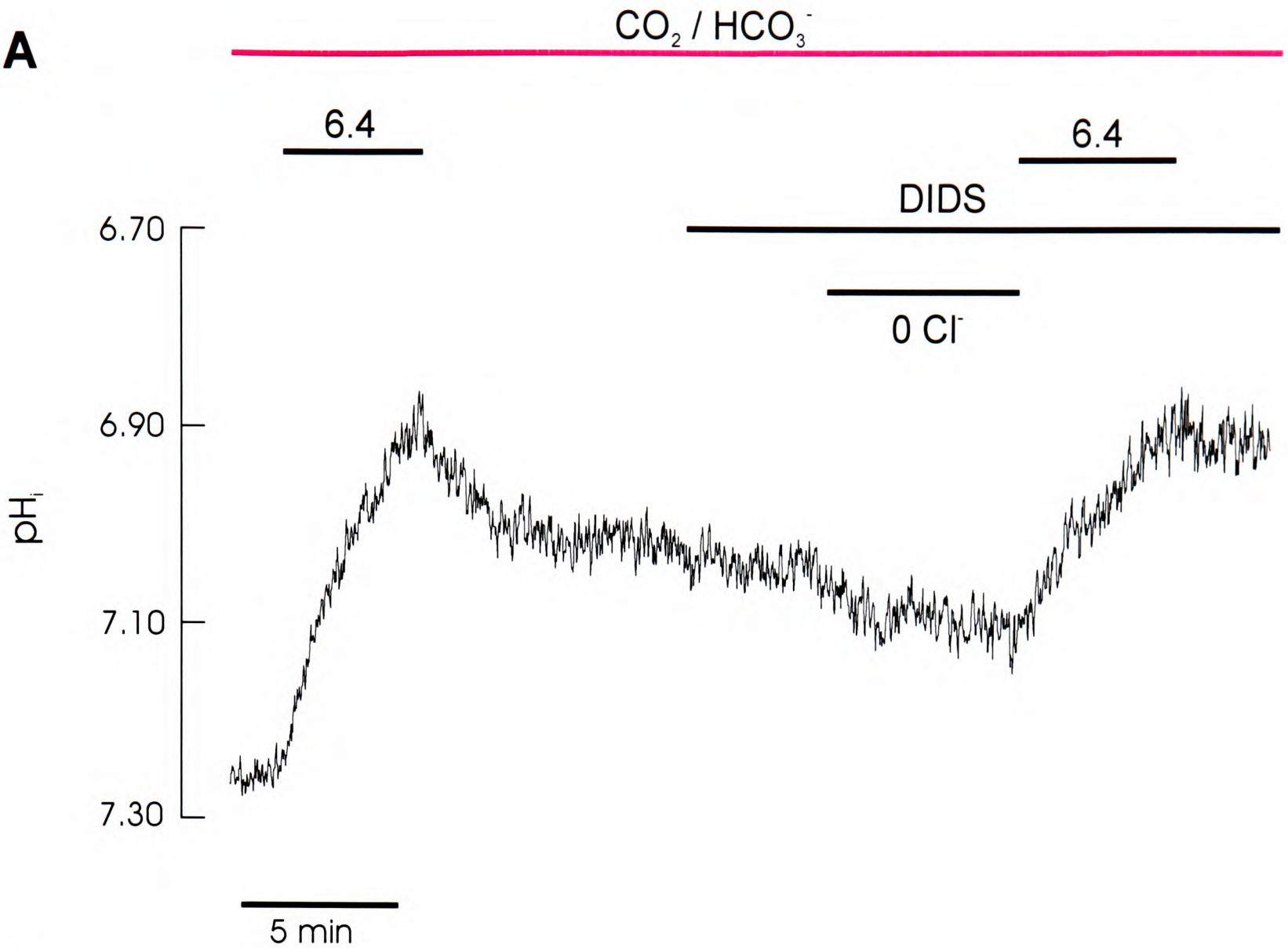


Figure 4.7

A, Effect of DIDS upon acid loading after a period of Cl^--free pre-treatment in CO_2/HCO_3^--buffered solution. Although 200 μM DIDS was initially applied in the absence of Cl_o^-, it did not have significant effect upon acid loader. This suggests that the insensitivity of acid loading process to DIDS is not due to competition from Cl_o^-. ***B***, Histogram shows mean acid efflux rate measured at pH_i 7.08±0.02 using data from 6 experiments similar to that shown in ***A***. Columns represent mean±S.E.M. No significant difference, P>0.1.

It is plausible that competition from Cl^-_o may be sufficiently strong that re-addition of Cl^-_o displaces all previously bound DIDS, hence abolishing DIDS inhibition (see **Fig 4.7**). I tested for this possibility in the experiment shown in **Fig 4.8**. Initially a cell was pretreated with DIDS for around 5 minutes under Cl^--free conditions, then Cl^-_o was re-added in the presence of DIDS for another 6 minutes. If the re-added Cl^-_o ions competed with and displaced all bound DIDS, then one would expect there to be no inhibition remaining after the 6 minute period in the presence of Cl^-_o. However, the rate of acid efflux induced by Cl^--free treatment after this period was markedly reduced from 7.32±1.85 mequiv l^{-1} min^{-1} to 2.81±0.25 mequiv l^{-1} min^{-1} after DIDS treatment (n=4 at pH_i 7.45±0.03; $P<0.01$). So it is safe to conclude that the re-addition of Cl^-_o did not displace the majority of bound DIDS.

DIDS insensitivity of acid loading is not caused by combined high H^+_o and normal Cl^-_o

The experiments shown in **Fig 4.5**, **Fig 4.7** and **Fig 4.8** exclude either acidic pH_o or competition from Cl^-_o being the causes of DIDS insensitivity of acid loading. However, there is still a final possibility that, during the acid challenge, the combination of high $[H^+]_o$ (pH_o 6.4) and normal $[Cl^-]_o$ (142.5 mM) conditions may reduce the DIDS sensitivity of the anion exchanger. The experiment shown in **Fig 4.9** was designed to test this possibility. After the control response of Cl^-_o-free induced alkalosis, two test episodes were performed. In each episode, the cell was treated with DIDS for 5 minutes, followed by a brief 45-60 second perfusion of pH_o 7.4 (period ***a***) or pH_o 6.4 (period ***b***) normal Tyrode solution. This latter brief perfusion allows low pH_o and Cl^-_o to be present simultaneously, therefore the possible combined effect of the two ions can be revealed. Cl^-_o was then removed again and the resulting acid

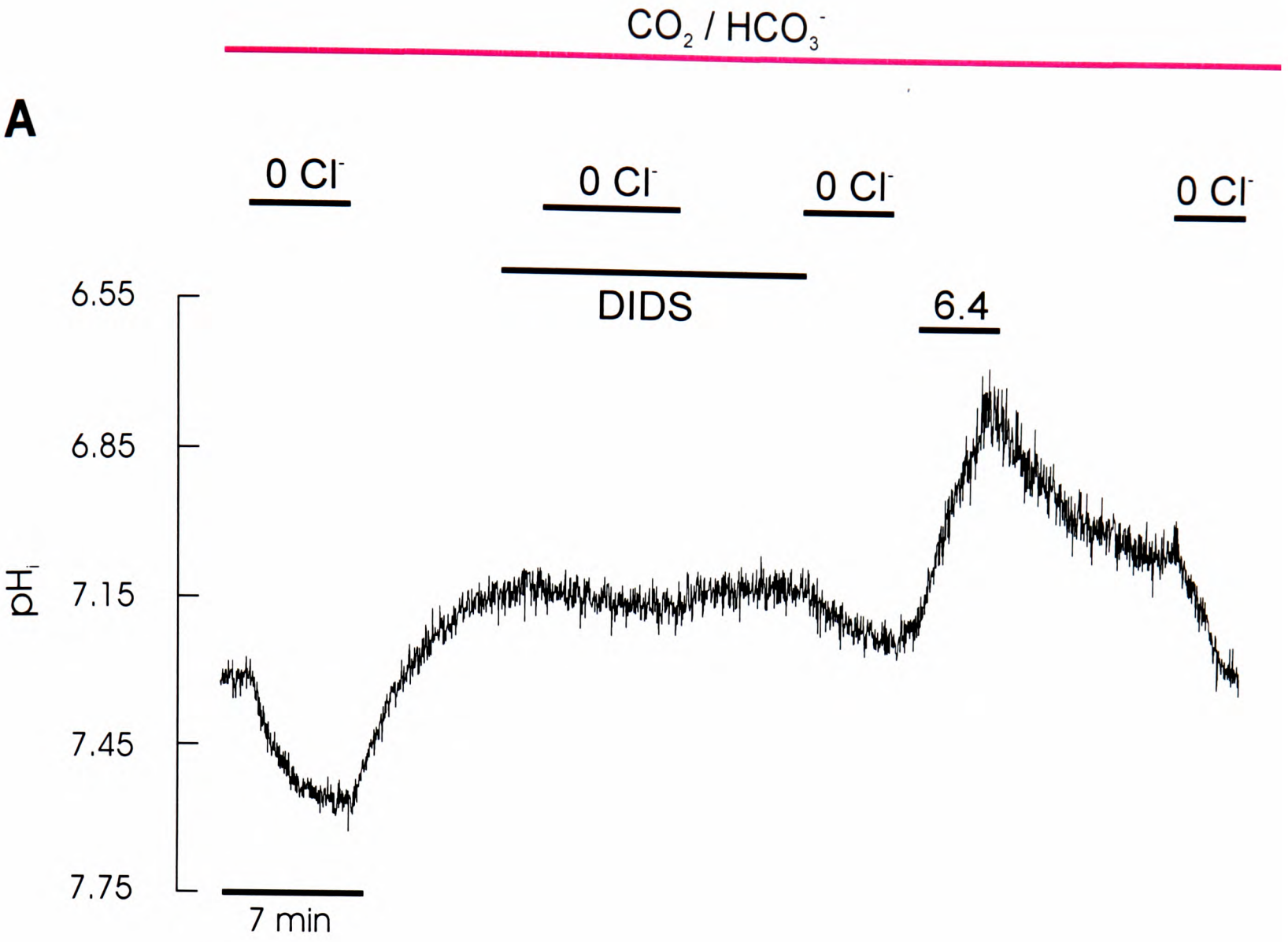


Figure 4.8

A, Effect of DIDS upon Cl^--free induced alkalosis after a period of Cl^--free pre-treatment in CO_2/HCO_3^--buffered solution. After the re-addition of Cl_o^-, the Cl^--free induced alkalosis was still reduced, even in the absence of DIDS. This suggests that the re-addition of Cl_o^- did not knock out previously bound DIDS. ***B***, Histogram shows mean acid efflux rate measured at pH_i 7.24±0.04 using data from 5 experiments similar to that shown in ***A***. Columns represent mean±S.E.M. * significant difference,

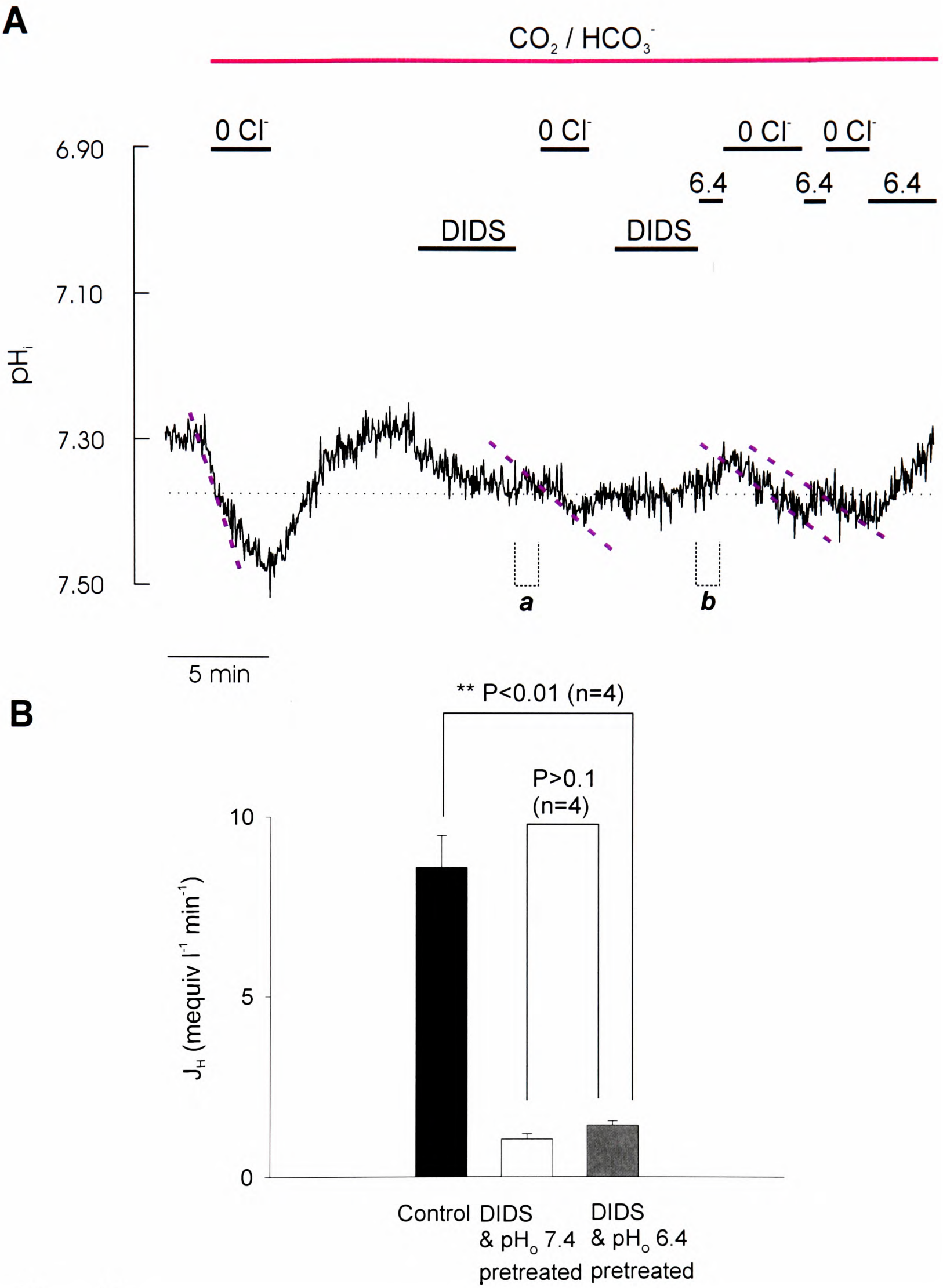


Figure 4.9

A, Combined effect of pH_o 6.4 and Cl^-_o upon DIDS inhibition of Cl^--free induced alkalosis in CO_2/HCO_3^-buffered solution. After DIDS pre-treatment, the cell was perfused with pH_o 7.4 (period ***a***) and pH_o 6.4 (period ***b***) solutions, followed by Cl^--free treatment. The whole experiment is under CO_2/HCO_3^- conditions. In both cases, the Cl^--free-induced alkalosis was similarly reduced. This result suggests the combination of Cl_o^- and low pH_o did not knock out previously bound DIDS. ***B***, Histogram shows mean acid efflux rate measured at pH_i 7.38±0.01 using data from 4

efflux was measured at pH_i 7.32±0.04 (n=4). The acid efflux rate of Cl^--free induced alkalosis after brief perfusion of pH_o 7.4 and 6.4 solutions was, 1.04±0.15 mequiv l^{-1} min^{-1} and 1.44±0.11 mequiv l^{-1} min^{-1}, respectively (P>0.1, no statistical difference). It is therefore evident that the combination of high $[H^+]_o$ and normal $[Cl^-]_o$ does not cause the DIDS insensitivity.

In summary, it can be concluded that the failure of DIDS to block acid influx via Cl^--HCO_3^- exchange is not due to a lack of drug binding.

The rate of pH_i recovery from alkali load is reduced by DIDS

In previous experiments, acid influx was induced by a fall in pH_o. Here the effect of DIDS on acid loading induced by an alkali load at pH_o 7.4 was examined in **Fig 4.10**. A 40 mM acetate prepulse (see Chapter 2) was used to produce an alkali load, which increased pH_i from resting level to 7.48±0.02 (n=5). The cells were allowed to recover towards resting pH_i in the absence and presence of DIDS. The acid influx rates were 5.53±0.74 mequiv l^{-1} min^{-1} and 1.47±0.13 mequiv l^{-1} min^{-1}, respectively, suggesting DIDS *does* block the acid loading under this condition (n=4; P<0.01; at pH_i 7.28±0.07). This result is apparently in contrast to that shown in **Fig 4.2**: the acid loading induced by acid challenge (pH_o 6.4) is insensitive to DIDS, while in this experiment the acid loading induced by alkali load (pH_i 7.4-7.5) is inhibited by DIDS. This difference of DIDS effect on acid loading will be considered later (see Discussion).

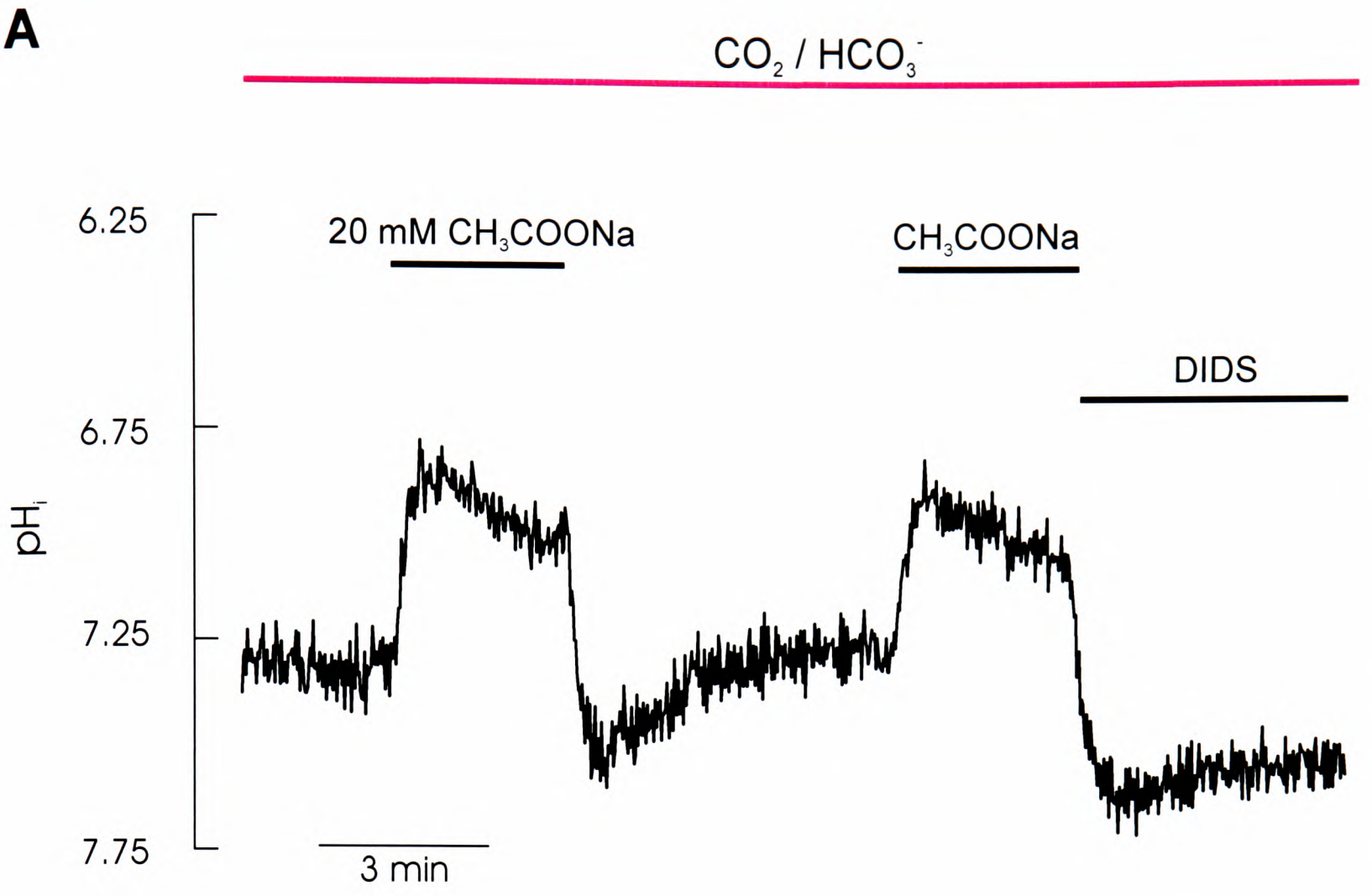


Figure 4.10

A, Effect of DIDS upon pH_i recovery from acetate prepusle in CO_2/HCO_3^--buffered solution. 200 μM DIDS reduced the recovery by 80%. ***B***, Histogram shows mean acid efflux rate measured at pH_i 7.25±0.03 using data from 4 experiments similar to that shown in ***A***. Columns represent mean±S.E.M. * significant difference, $P<0.05$.

Cl^--free induced alkalosis is still present under HCO_3^--free conditions

The Cl^--free-induced alkalosis seen in **Fig 4.1**, presumably due to reversed mode of Cl^--dependent transporter, was also tested in HEPES-buffered solution (**Fig 4.11A**). Although a direct comparison with the control response in HCO_3^--buffered solution is not always possible in the same cell, acid *efflux* rate induced by Cl^--free treatment in HCO_3^--buffered solution can still be measured from other cells, around the similar pH_i range (pH_i = 7.7). As **Fig 4.11A** shows, after changing to HEPES solution, alkalosis can still be induced by Cl^--free treatment. Nevertheless, the acid efflux rate was greatly reduced from 10.06±2.22 mequiv l^{-1} min^{-1} (estimated at pH_i 7.7±0.02 in different cells) to 0.63±0.12 mequiv l^{-1} min^{-1} (n=6; P<0.01, *unpaired t*-test). Again, 200 μM DIDS almost completely abolished (>92%) this Cl-induced alkalosis in HEPES-buffered solution (n=4; **Fig 4.11B**).

The effect of DIDS on the modes of transport of the Cl^--HCO_3 exchanger under various conditions tested is summarized in **Table 4.1**.

Discussion

DIDS insensitivity of acid loading

In this study I have demonstrated that 200 μM DIDS completely inhibits the Cl^--free induced alkalosis (protocol ① in **Table 4.1**), which is mediated by the reversal of Cl^--HCO_3^- exchange transporting Cl^- ions out of the cell in exchange for HCO_3 ions. This observation is consistent with that of Buckler *et al.* (1991b) and other cell types, such as Purkinje fibre (Vaughan-Jones, 1979), bladder epithelium (Fischer, Husted &

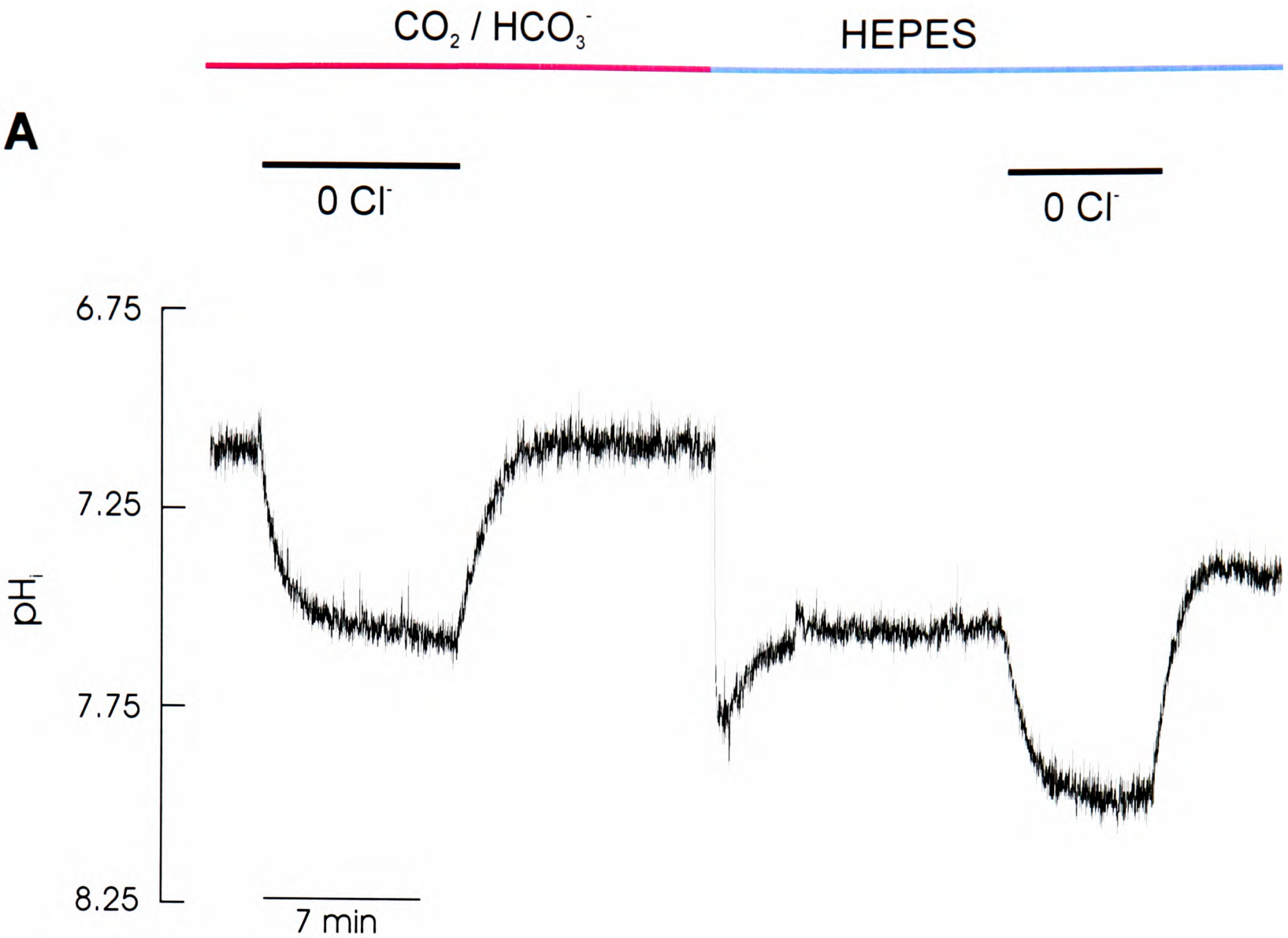


Figure 4.11

A, Effect of Cl^-_o removal upon pH_i, in the presence and absence of HCO_3^- ion. Cl^-_o removal also induced alkalosis in HEPES-buffered solution as in CO_2/HCO_3^--buffered solution, although the acid influx rate was greatly reduced. This is a typical pH_i record from 6 similar experiments. ***B***, Effect of DIDS upon Cl^--free-induced alkalosis in HEPES-buffered Tyrode solution. 200 μM DIDS almost completely blocked this alkalosis. This is a typical pH_i record from 4 similar experiments.

Table 4.1

Summary of DIDS sensitivity of Cl^--HCO_3^- exchange under various conditions tested in Chapter 4.

	Experimental protocol	Figure	pH_o	pH_i	$[Cl^-]_o$ (mM)	Presumed transport mode	Remaining acid flux in the presence of DIDS (% of control)
①	Acid efflux induced by Cl_o^--free (pH_o 7.4)	**4.1**	7.4	7.24±0.05	0	Reverse	*11%
②	Acid efflux induced by Cl_o^--free (pH_o 6.4)	**4.5**	6.4	6.40±0.08	0	Reverse	*17%
③	Acid influx induced by acid challenge (pH_o 6.4)	**4.2**	6.4	7.22±0.02	142.5	Forward	89%
④	Acid influx during Cl_o^- re-addition	**4.6**	7.4	7.55±0.02	142.5	Forward	*18%
⑤	Acid influx induced by alkali load after acetate pre-pulse	**4.10**	7.4	7.28±0.07	142.5	Forward	*19%

*significant difference ($P<0.05$) compared with control flux in the absence of DIDS.

Steinmetz, 1983), smooth muscle (Aickin & Brading, 1984), and liver cells (Meier, Knickelbein, Moseley, Dobbins & Boyer, 1985). However, the same concentration of DIDS unexpectedly failed to reduce the acid influx stimulated by acid challenge (protocol ③ in **Table 4.1**), which has been shown in Chapter 3 to be mediated by the forward mode of Cl^--HCO_3^- exchange mediating Cl^- influx in exchange for HCO_3^- efflux. The different sensibility to DIDS depending on the mode of operation of the Cl^--HCO_3^- exchanger has not been reported in previous studies. For example, in ventricular myocytes DIDS blocks both the Cl^--free induced alkalosis and low pH_o-induced acid loading on Cl^--HCO_3^- exchanger, hence there is no significant difference between DIDS sensitivity (Lagadic-Gossmann, Buckler & Vaughan-Jones, 1992; Sun, Leem & Vaughan-Jones, 1996).

DIDS inhibition of Cl^-_o-induced alkalosis is irreversible

Previous studies showed that DIDS binds with AE1 reversibly within few seconds, possibly through ionic interactions of its anionic groups, i.e. sulphonic acid group and carboxylic group (Lepke, Fasold, Pring, Passow, 1976; Cabantchik & Greger, 1992). In the continuous presence of DIDS, an irreversible covalent adduct is further formed between reversibly bound DIDS and the AE1 protein, although it has been suggested that the reversible binding of DIDS is sufficient for the inhibition of Cl^--HCO_3^- exchange. It is estimated that at 38 °C, the half time for this covalent binding is 80-90 sec, that is, over 80% of the AE1 is covalently bound with DIDS within 5 min (Janas, Bjerrum, Brahm & Wieth, 1989). For all experiments shown in this chapter, DIDS was applied for more than 5 min prior to acid challenge or Cl^-_o-free treatment. If the results obtained from previous studies are applicable to the Cl^--HCO_3^- exchanger in type I cells, it can be said that in these experiments, most of the acid loader protein

should have covalently bonded with DIDS. In fact, the Cl^-_o-induced alkalosis was significantly reduced, even after the washout of DIDS, indicating some extent of irreversible inhibition (**Fig 4.5**, **Fig 4.8**, **Fig 4.9**). However, the same or longer period of DIDS treatment did not affect acid influx during acid challenge (**Fig 4.2**, **Fig 4.3**, **Fig 4.5**, **Fig 4.7**). Thus the lack of effect of DIDS on acid influx is not caused by insufficient treatment time.

DIDS insensitivity of acid influx on the Cl^--HCO_3^- exchanger

I have confirmed the lack of sensitivity to DIDS of acid loading induced by acidic pH_o is not due to either an effect of increased H^+_o on DIDS binding or a competition between DIDS and Cl^-_o for binding to the exchanger. In **Fig 4.5**, even at acidic pH_o (pH_o 6.4), DIDS was still able to block the alkalosis induced by Cl^--free treatment (also see protocol ② in **Table 4.1**), suggesting that acidic pH_o *per se* did not prevent the binding and/or inhibitory effect of DIDS on the reversed transport mode of Cl^--HCO_3^- exchange. In **Fig 4.7**, DIDS was previously applied in the absence of Cl^-_o, so that DIDS would have bound to the exchanger prior to the subsequent acid challenge, without any interference from Cl^-_o. However, the acid loading was still not affected by DIDS, even though a parallel experiment showed that during this period the Cl^-_o-free induced alkalosis was significantly reduced by the drug (**Fig 4.8**).

One possibility is that, the increased H^+_o during acid challenge may, in some way, weaken the DIDS binding, so that Cl^-_o ion may compete with and rapidly displace DIDS at acidic pH_o. In effect, this hypothesis assumes that the combined effect of high $[H^+]_o$ and normal $[Cl^-]_o$ somehow causes the DIDS insensitivity of acid influx. As shown in **Fig 4.9**, after DIDS pre-treatment, the acid efflux induced by Cl^-_o removal

was reduced, indicating DIDS had bound to the exchanger. Nevertheless, after a period (~45 sec) of perfusion with high $[H^+]_o$ and normal $[Cl^-]_o$, the inhibition persisted. This experiment therefore indicates that the simultaneous presence of high $[H^+]_o$ and normal $[Cl^-]_o$ does not lead to loss of DIDS effect. Thus the DIDS insensitivity observed during acid influx is probably a genuine phenomenon.

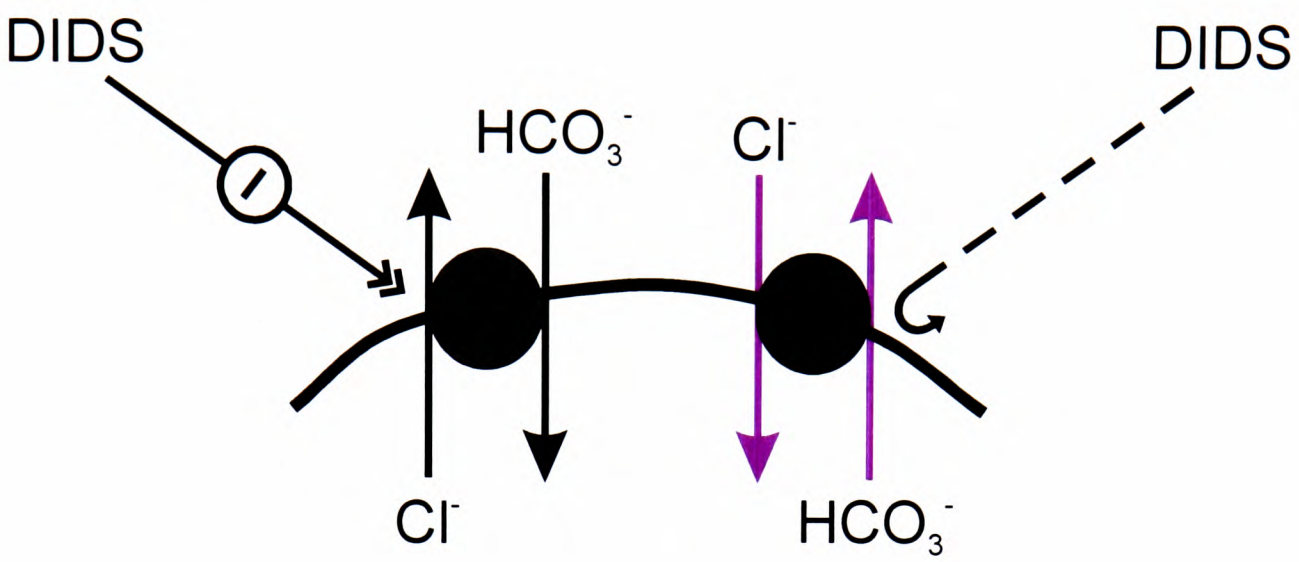
Possible explanations for the DIDS insensitivity of acid influx

Two possible explanations must initially be considered for DIDS insensitivity, as illustrated in **Fig 4.12**.

1. **Two distinct exchanger populations**: There may be two pharmacologically distinct Cl^--HCO_3^- exchangers, both of which would rectify with respect to acid flux, but in opposite directions. One of these exchangers would be an acid efflux rectifier, which would only function efficiently under thermodynamic conditions favouring Cl^- efflux and HCO_3^- influx (i.e. net acid efflux). The other exchanger would be an acid influx rectifier that only functions efficiently under conditions allowing Cl^- influx and HCO_3^- efflux (i.e. net acid influx). Of these two independent transporters, only the former, which mediates acid efflux, would be DIDS sensitive.

2. **Unidirectional inhibition of DIDS**: DIDS acts in some way to selectively inhibit forward mode (i.e. acid efflux) of the anion exchange, but not reversed mode (i.e. acid influx). Such a unidirectional inhibition of ion exchanger is not unprecedented: in the original reports of Na^+-Ca^{2+} exchanger inhibitor, KB-R7943, it is found that 0.3–2.4 mM KB-R7943 preferentially inhibits the reversed mode

A



B

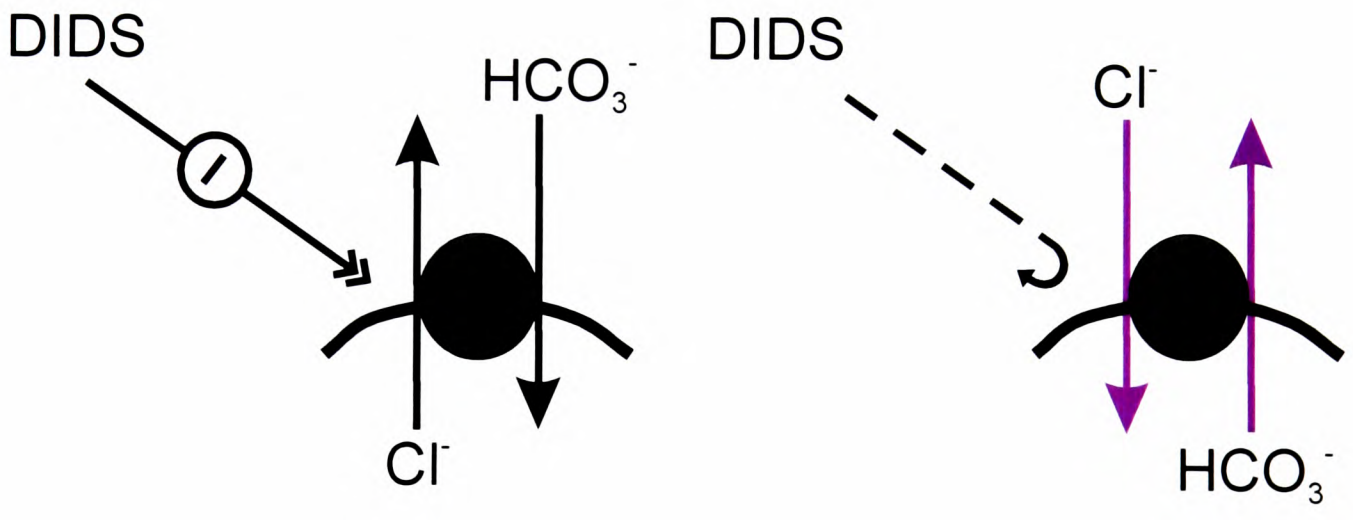


Figure 4.12

The two possible explanations for the failure of DIDS to block acid influx via Cl^--HCO_3^- exchange ***A***, There are two distinct, rectifying Cl^--HCO_3^- exchangers in type I cells. ***B***, DIDS may induce an unidirectional inhibition of Cl^-- HCO_3^- exchange. See text for more details.

(Na^+ efflux and Ca^{2+} influx) of Na^+-Ca^{2+} exchange, while the inhibition of forward mode (Na^+ efflux and Ca^{2+} influx) required 10-50 times higher concentrations (Watano, Kimura, Morita, Nakanishi, 1996; Iwamoto, Watano, Shigekawa, 1996). So far, the nature and cause of this transport mode-selective inhibition remains controversial (Elias *et al.* 2001; see Shigekawa, M. & Iwamoto, 2001 for review).

Neither of these explanations, however, can fully accommodate all of the experimental results listed in **Table 4.1**. In **Fig 4.6** and **Fig 4.10**, DIDS *does* block the acid loading mediated by the forward mode of Cl^--HCO_3^- exchange after Cl^-_o re-addition and acetate pre-pulse protocol (protocol ④ and ⑤ in **Table 4.1**). This evidence is not compatible with either of the above explanations, since both predict that DIDS would not block forward mode of Cl^--HCO_3^- exchange.

Hypothesis: two distinct Cl^--HCO_3^- exchangers with different DIDS and pH sensitivity

In **Table 4.1**, it is noted that among the five protocols tested, only the acid influx induced by external acid challenge is not inhibited by DIDS (protocol ③). All other acid fluxes on Cl^--HCO_3^- exchange are inhibited by >80% by 200 μM DIDS (protocol ① ② ④ ⑤), irrespective of their directionality of transport. That is, only acid influx stimulated by low pH_o (6.4) at normal pH_i level is DIDS-insensitive (protocol ③), while acid influx stimulated by high pH_i (> ~7.3) at normal pH_o level (7.4) is DIDS-sensitive (protocol ⑤). Based on these observations, I propose there are two distinct populations of Cl^--HCO_3 exchangers. One is DIDS-insensitive and active at low pH_o, while the other is DIDS-sensitive and active at normal or high pH_i. This hypothesis is

summarised in **Fig 4.13**. The molecular identity of those two Cl^--HCO_3^- exchangers is discussed as follows.

The AE2 isoform of Cl^--HCO_3^- exchanger is stimulated by alkaline pH_i and sensitive to DIDS, with an IC_{50} value of 4-13 μM (Lee, Gunn & Kopito, 1991; He, Wu, Knauf, Tabak & Melvin, 1993; Humphreys, Jiang, Chernova & Alper, 1994). Although the threshold of pH_i for AE2 activation varies among different cell types, generally its activity increases significantly when pH_i is higher than 7.3-7.4 (Jiang, Stuart-Tilley, Parkash & Alper, 1994). Therefore DIDS-sensitive acid influx induced by an acetate pre-pulse (**Fig 4.10**; protocol ⑤) is probably mediated by AE2.

The transporter protein responsible for low pH_o-activated and DIDS-insensitive Cl^--HCO_3^- exchange is still unidentified. Tsuganezawa *et al.* (2001) cloned a novel HCO_3^--dependent transporter, designated as AE4. It was found that 200 μM DIDS failed to inhibit AE4 activity, probably because AE4 lacks the consensus motif for covalent binding of DIDS (Kopito *et al.* 1989). Although AE4-mediated Na^+-independent Cl^--HCO_3^- exchange was shown in the original report, the Na^+-dependency of its function is disputed. In fact, the sequence of AE4 is highly homologous with other Na^+-HCO_3^- cotransporters, leading to speculations that AE4 is probably another NBC isoform (Soleimani, 2002). So AE4 is unlikely to be responsible for DIDS-insensitive acid influx in type I cells.

Nevertheless, among the newly found SLC26 anion exchangers (see Everett & Green, 1999, for review), many are much less sensitive to DIDS than AE1-3 proteins. It has been reported that 500 μM DIDS and 1 mM DIDS inhibited anion exchange on

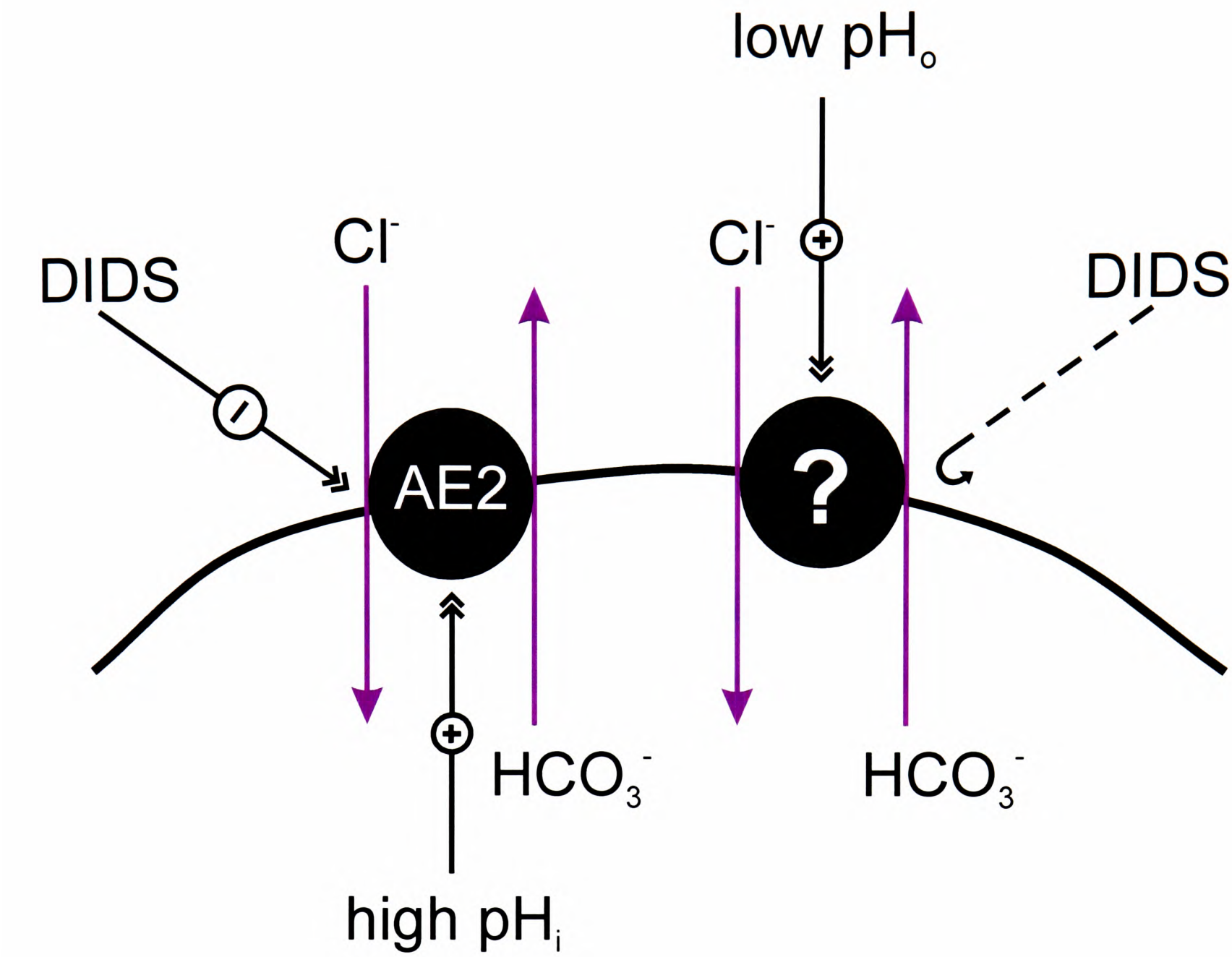


Figure 4.13

Hypothesis for DIDS-sensitive and DIDS-insensitive acid influx via Cl^--HCO_3^- exchange. There are two distinct Cl^--HCO_3^- exchangers in the type I cell. One Cl^--HCO_3^- exchanger (probably AE2) is DIDS-sensitive and activated at high pH_i, while another Cl^--HCO_3^- exchanger (possibly a member of SLC26 family) is DIDS-insensitive and activated at low pH_o. See text for more details.

SLC26A3 (also named DRA, for Down-Regulated in Adenoma) by only 26% and 24%, respectively (Melvin, Park, Richardson, Schultheis & Shull, 1999; Chernova *et al.* 2003). In another study, 1 mM DIDS inhibited 62% of the $^{36}Cl^-$ uptake mediated by SLC26A4 (also named PDS, for PenDred Syndrome) (Scott, Wang, Kreman, Sheffield & Karniski, 1999). Both anion exchangers have been shown to mediate Cl^--HCO_3^- exchange (Melvin *et al.* 1999; Soleimani *et al.* 2001). Although Chernova *et al.* (2003) reported $^{36}Cl^-$ efflux on SLC26A3 was not affected when pH_o decreased from 7.4 to 5.0, it is possible that other SLC26 proteins could be activated by acidic pH_o. Furthermore, SLC26A8 (also named TAT-1, for Testis Anion Exchanger-1), SLC26A9 and SCL26A11 are all modestly sensitive to DIDS. Previous studies showed 1 mM DIDS reduced sulfate transport via these transporters by 60-70% (Touré, Morin, Pineal, Bacid, Foresail & Garcon, 2001; Lohi *et al.* 2002; Vincourt, Jullien, Amalric & Girard, 2003). They are also possible candidates for DIDS-insensitive Cl^--HCO_3^- exchange observed in type I cells. At the moment, it is not known whether these sulfate transporters also mediate Cl^--HCO_3^- exchange.

CHAPTER 5

Characterisation of pH_i and pH_o Sensitivity of Acid Influx in the Carotid Body Type I Cell

Introduction

The pH_i of the type I cell is sensitive to changes of pH_o. Hence a fall in pH_o induces a parallel decrease in pH_i. Buckler *et al.* (1991b) reported the sensitivity of pH_i to pH_o ($\Delta pH_i/\Delta pH_o$) in type I cells is 0.6-0.7 (see Chapter 1). In previous chapters, I showed that the decrease in pH_i is due to an increased acid influx. I also concluded that the acid influx is mediated by at least two separate acid loading mechanisms: one of them is Cl^--HCO_3^- exchange system[1], of which there may be more than one type operating on the cell membrane. The other is an unidentified HCO_3^--independent and Cl^--independent mechanism.

Since both types of acid loading mechanism mediate acid-equivalent influx, it is plausible that their activity may be regulated differently by pH_i and pH_o levels. In order to characterise the pH_o-dependency and pH_i-dependency of both mechanisms, measurement of acid influx rates at different pH_o and pH_i are required. In the type I

[1] In Chapter 4 it was proposed that two distinct Cl^--HCO_3^- exchangers may exist in the type I cell, therefore in the present study the term "Cl^--HCO_3^- exchange system" is used to include all Cl^--HCO_3^- exchangers.

cell, quantification of acid loading fluxes has been preliminary. Richmond (1993) measured the background acid loading fluxes in the pH_i range 7.0-7.6 under normal pH_o (7.4) conditions. However, at present, there has been no measurement of acid loading fluxes in the type I cell either in the more acidic pH_i range (below 7.0) or at values of pH_o other than 7.4. In this chapter, the acid influx rates at different values of pH_o and pH_i are measured, in CO_2/HCO_3^--buffered and HEPES-buffered solutions, respectively. The pH_i and pH_o sensitivity of the combined Cl^--HCO_3^- exchange system and of the HCO_3^--independent mechanism has been determined. Results indicate that the activity of the combined Cl^--HCO_3^- exchangers is strongly dependent on pH_i and pH_o, being markedly activated by high pH_i and low pH_o, while the HCO_3^--independent mechanism is virtually pH_i-independent and moderately pH_o-dependent. The implication of these results in relation to the nature of the acid loaders is discussed. The characterisation of pH_i and pH_o sensitivity of acid influx pathways can be used to estimate their roles in determining the pH_i-sensitivity of pH_o in type I cells.

Methods

General Methods

pH_i was recorded in isolated type I cells from the neonatal rats using carboxy-SNARF-1, as described in Chapter 2.

Solutions

Standard CO_2/HCO_3^--buffered solution and HEPES-buffered solution were prepared as described in Chapter 2. Na^+-free solutions (CO_2/HCO_3^--buffered and HEPES-buffered) were prepared as described in Chapter 3.

Determination of Acid Influx at Different pH_i During Acid Loading

The principle of calculating net acid fluxes has been described in Chapter 2. For convenience, the recording of acid loading was divided into 50 s intervals, and the acid influx rate in each interval was computed, so was the corresponding mean pH_i. Then the computed acid influx rates from all similar experiments were pooled, and averaged over successive 0.1 pH_i ranges, to cover the whole course of pH_i change during acid loading. The final results of acid influx rates were expressed as mean±S.E.M at the midpoint pH_i of each 0.1 pH_i interval.

Curve Fitting and Data Handling

The curves drawn in **Fig 5.7** were the best-fit sigmoid curves using a least square difference method, based on original experimental data (Cornish-Bowden, 1995a). The curve fitting and parameter values were calculated by GraphPAD InPlot software. Original data of HCO_3^--dependent component of acid influx (J_{HCO3}) and its corresponding acid-equivalent concentration (either $[H^+]_i$ or $[H^+]_o$) was fitted to the 3-parameter sigmoid curve (modified from Hill, 1910),

$$J_{HCO3} = \frac{J_{HCO3}^{max} \cdot [H^+]^h}{K_a{}^h + [H^+]^h} = \frac{J_{HCO3}^{max}}{1 + 10^{h \cdot (pH - pK_a)}} \qquad \textbf{[Eqn. 5.1]}$$

Where J_{HCO3}^{max} is the maximal value of J_{HCO3}, h is Hill coefficient, while pK_a can be either $pK_a{}^i$ or $pK_a{}^o$, depending on the acid-equivalent data (pH_i or pH_o) being used.

The curves drawn in **Fig 5.9** were the best-fit regression lines using a least square difference method, based on original experimental data (Bland, 2000). The curve fitting and parameter values were calculated by GraphPAD InPlot software (San Diego, California, USA). Original data of HCO_3 -independent component of acid influx (J_H) and its corresponding pH (either pH_i or pH_o) was fitted to the linear relationship:

$$J_H = b \times pH + a \qquad \textbf{[Eqn. 5.2]}$$

Results

Effect of pH_o on acid loading in CO_2/HCO_3^--buffered solution

In order to examine the effect of pH_o on total acid influx, which is mainly mediated by Cl^--HCO_3 exchange (see Chapter 3), experiments were carried out in CO_2/HCO_3^--buffered solution. Initially, pH_i was increased from its resting level to 7.72±0.06 (n=6) by perfusing with a pH_o 7.9 solution. The purpose of inducing this alkali load was to allow subsequent acid loading to start from a more alkaline level (pH_i 7.6-7.7), thus extending the range of pH_i over which acid influx could be analysed (**Fig 5.1A**). Na^+_o was then removed, followed by reducing pH_o to different values (pH_o 7.7, 7.4, 7.1 and 6.4). The removal of Na^+_o was intended to inhibit all Na^+-dependent acid extruders, i.e. Na^+-H^+ exchange and Na^+-dependent Cl^--HCO_3^- exchange, in order to reveal the full extent of acid influx via the acid loading mechanisms (see Discussion). Using this protocol, the time course of acid loading at different pH_o values could be and compared. The results show that acid loading is enhanced at acidic pH_o (**Fig 5.1B**).

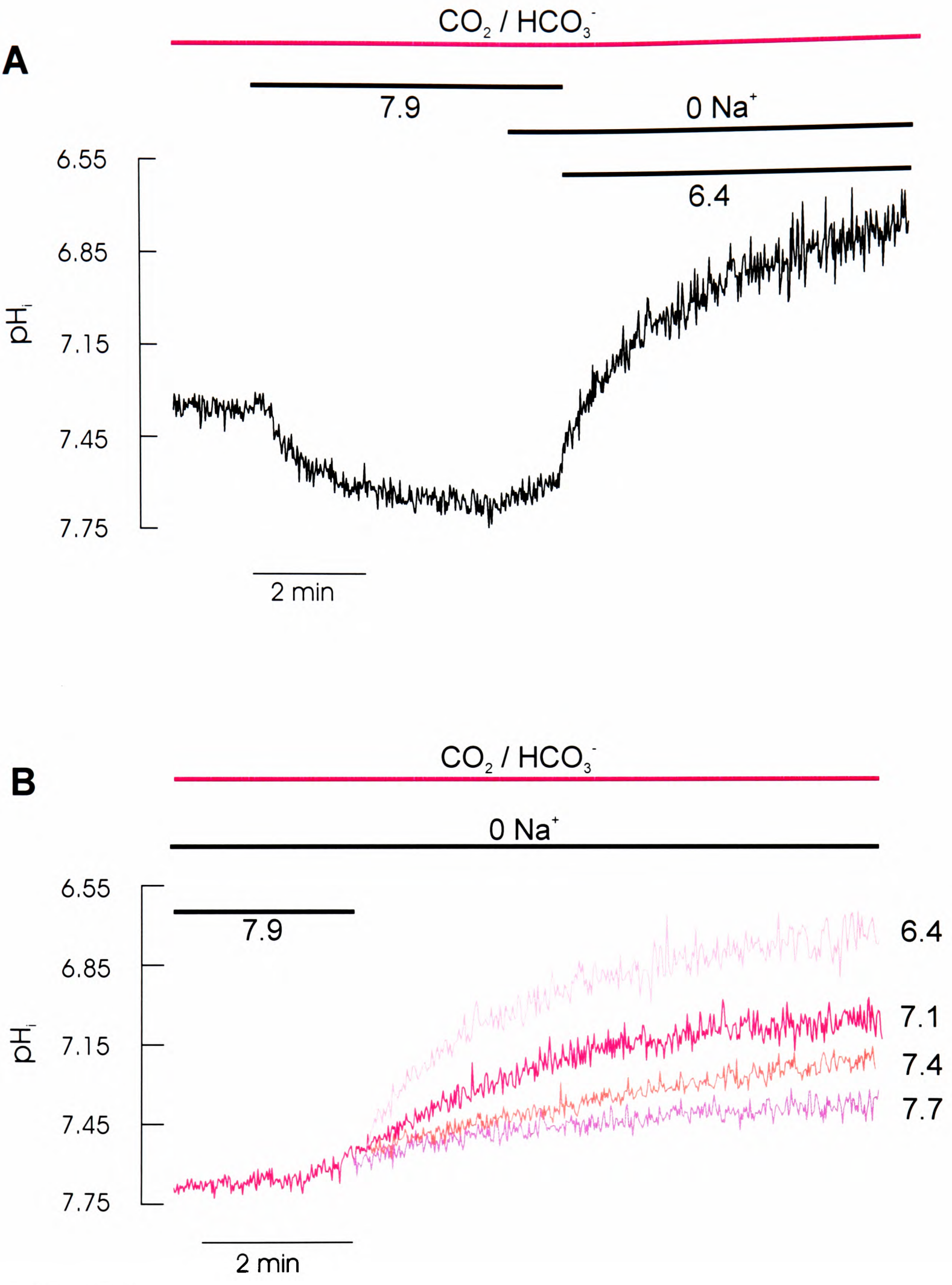


Figure 5.1

A, A typical recording of acid loading induced by pH_o 6.4 acid challenge in CO_2/HCO_3^--buffered solution. Initially, cells were pretreated with pH_o 7.9 solution, in order to allow the subsequent acid loading to start from a more alkali pH_i. ***B***, Effect of varying pH_o on acid loading in CO_2/HCO_3^--buffered solution. pH_i traces of acid loading from four separate experiments were superimposed, each being treated with different pH_o (7.7, 7.4, 7.1, 6.4) acid challenge. The first part of trace showing pH_o 7.9 pretreatment was taken from the experiment subsequently treated with pH_o 7.1 soultion.

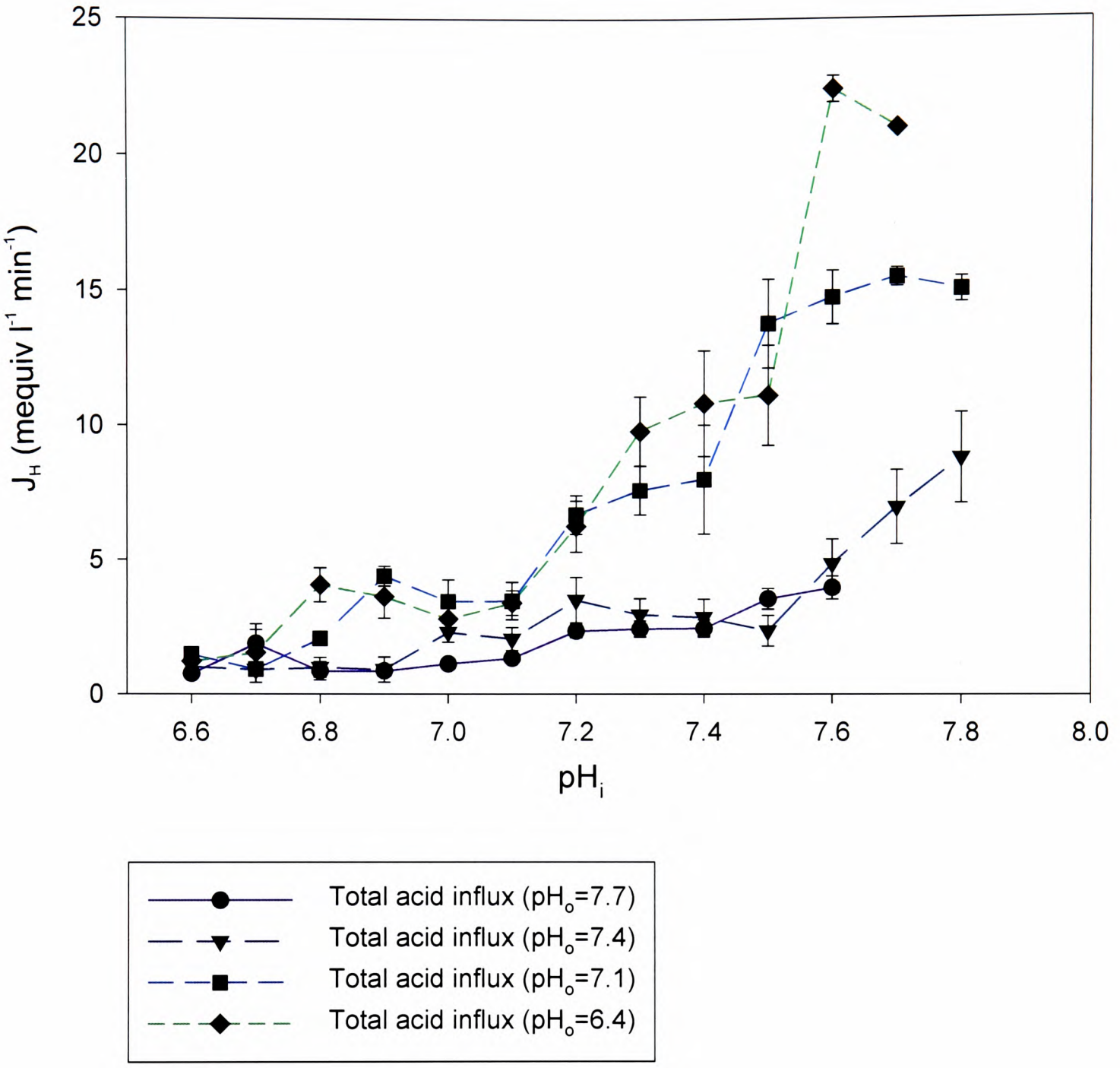


Figure 5.2

pH_i dependence of total acid influx at different pH_o measured in CO_2/HCO_3^--buffered solution. Data were derived from 62 cells exposed to experimental protocols like those shown in **Fig 5.1**. Acid influx rates were averaged over successive 0.1 pH ranges. Points represent mean±S.E.M.

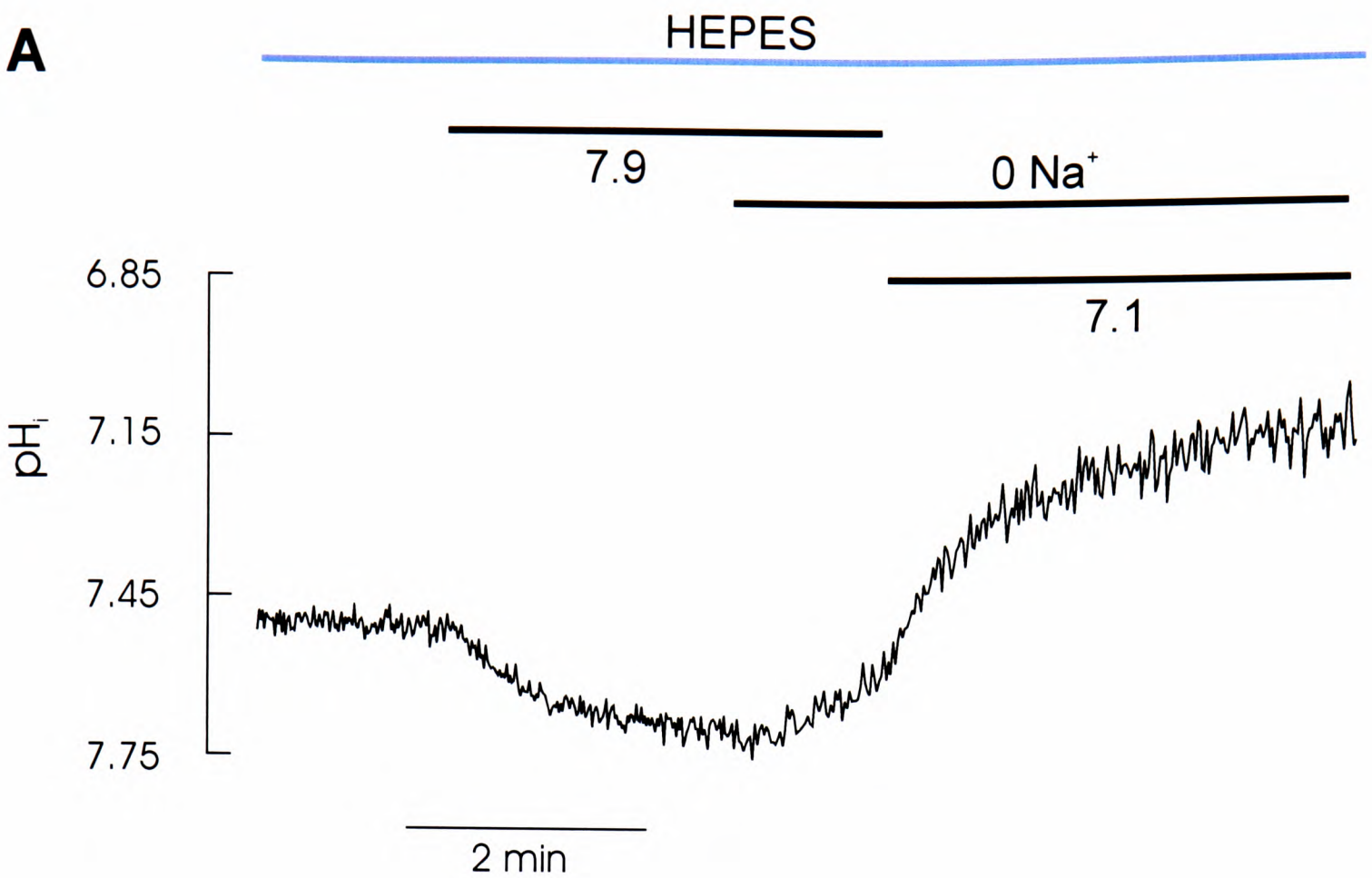
Acid loading under different pH_o, as seen in **Fig 5.1B**, can be further analysed over the whole course of its pH_i change (see Methods). **Fig 5.2** shows the average rates of total acid influx measured over a wide range of pH_i values (mainly 6.6-7.8) in solutions at different pH_o. For each pH_o condition, the total acid influx rate increases, in a non-linear fashion, as pH_i rises. In addition, more acidic pH_o values induce larger total acid influx at the same pH_i.

Effect of pH_o upon acid loading in HEPES-buffered solution

About 30% of the total acid influx induced by a pH_o 6.4 acid challenge is mediated by a HCO_3^--independent and Cl^--independent mechanism (see Chapter 3). To investigate the effect of pH_o on this acid loading pathway, the same protocol shown in **Fig 5.1** was repeated while using HEPES-buffered superfusates. Cells were initially perfused with pH_o 7.9 HEPES-buffered solution, hence the resting pH_i increased to 7.75±0.07 (n=6) (**Fig 5.3A**). Following removal of Na^+_o, pH_o was reduced to 7.7, 7.4, 7.1 and 6.4. The time course of HCO_3^--independent acid loading in different pH_o solutions was then recorded. Generally, a faster acid loading was associated with a more acidic pH_o (**Fig 5.3B**).

The average HCO_3^--independent acid loading at different pH_o values was measured over a range of pH_i values (mainly 6.6-7.8). The results are summarised in **Fig 5.4**, showing that while acid influx increases at low pH_o, it is relatively insensitive to changes of pH_i.

Effect of pH_o upon Cl^--HCO_3^- exchange-mediated acid loading



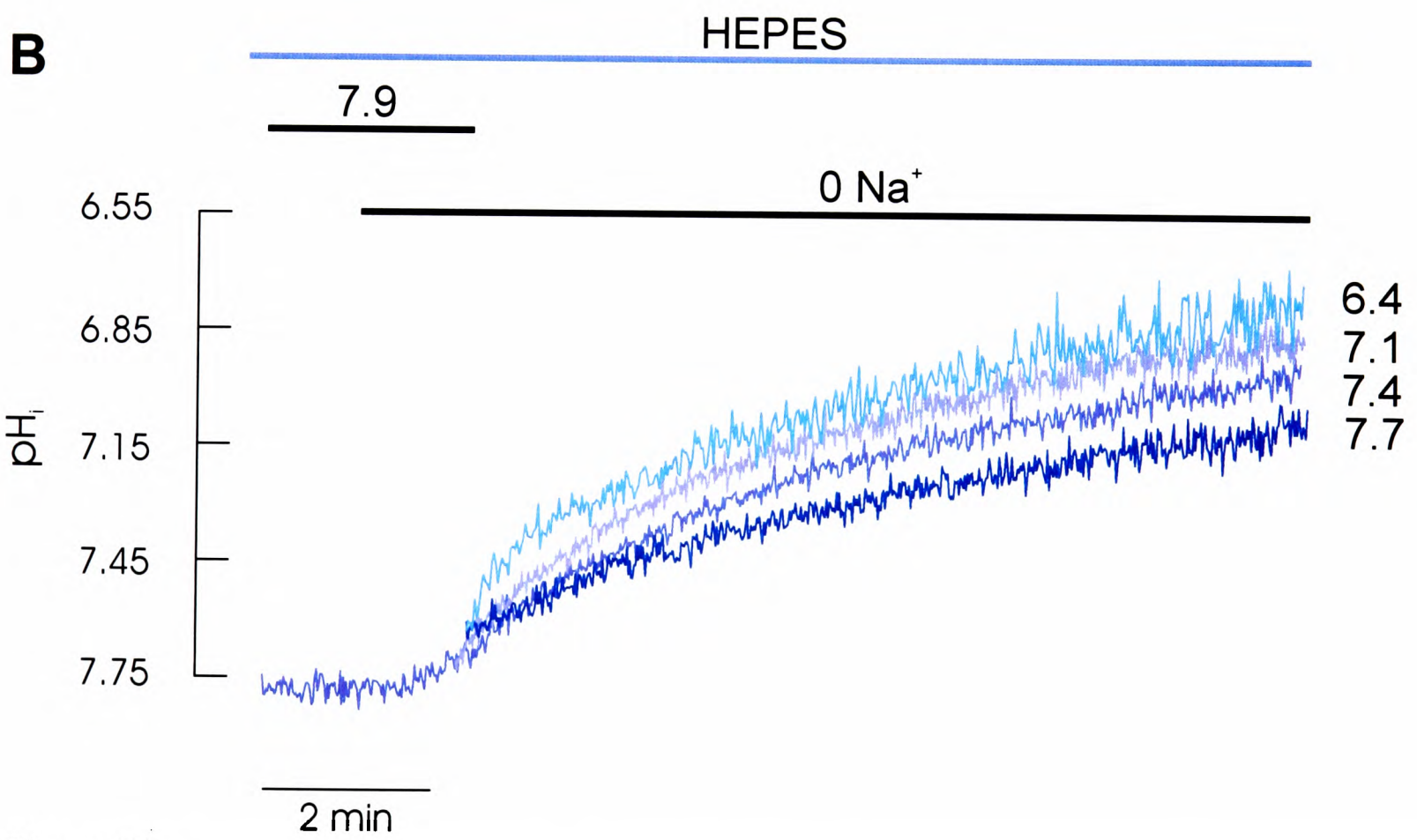


Figure 5.3

A, A typical recording of acid loading induced by pH_o 7.1 acid challenge in HEPES-buffered solution. Initially, cells were pretreated with pH_o 7.9 solution, in order to allow the subsequent acid loading to start from a more alkali pH_i. ***B***, Effect of varying pH_o on acid loading in HEPES-buffered solution. pH_i traces of acid loading from four separate experiments were superimposed, each being treated with different pH_o (7.7, 7.4, 7.1, 6.4) acid challenge. The first part of trace showing pH_o 7.9 pretreatment was taken from the experiment subsequently treated with pH_o 7.4 soultion.

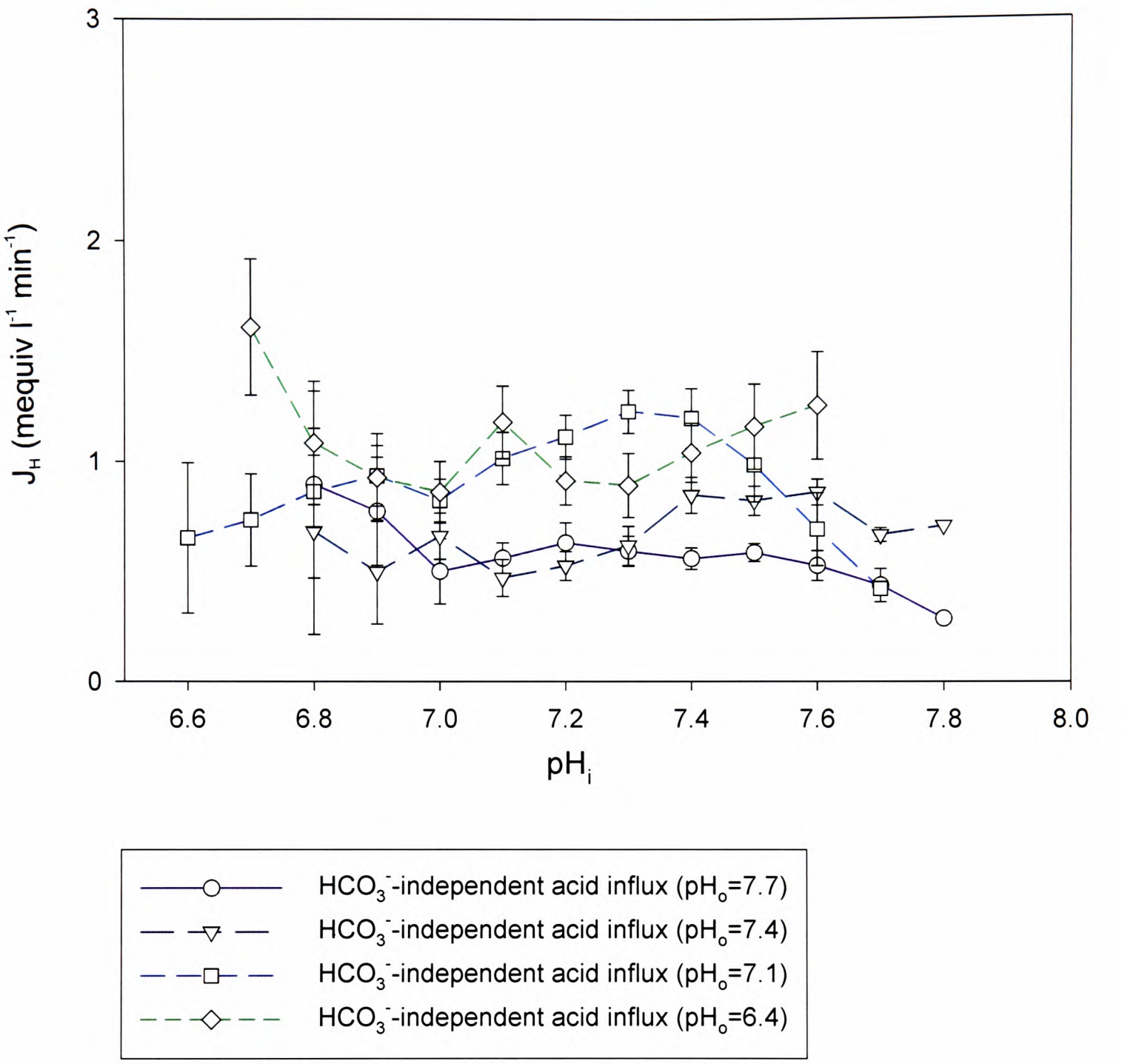


Figure 5.4

pH_i dependence of HCO_3^--independent acid influx at different pH_o measured in HEPES-buffered solution. Data were derived from 45 cells exposed to experimental protocols like that shown in **Fig 5.3**. Acid influx fluxes were averaged over successive 0.1 pH ranges. Points represent mean±S.E.M.

Once the pH_i dependency of total acid influx and HCO_3^--independent acid influx in different pH_o solutions were measured, the data could be used to estimate the pH_i sensitivity of HCO_3^--*dependent* acid influx at different pH_o levels. For each pH_o and pH_i condition, the HCO_3^--independent acid influx was subtracted from the corresponding total acid influx, to obtain the HCO_3 -dependent component of acid influx, which is presumably mediated by the Cl^--HCO_3^- exchange system. The results are summarised in **Fig 5.5**, representing the acid loading via Cl^--HCO_3 exchange at different pH_o values as a function of pH_i.

In addition, **Fig 5.6** plots HCO_3^--dependent acid influx as a function of pH_o for four different values of pH_i (7.0, 7.2, 7.4 and 7.6) to demonstrate the pH_o dependency of acid influx mediated by the Cl^--HCO_3^- exchange system.

pH_i and pH_o sensitivity of Cl^--HCO_3^- exchange activity

Fig 5.5 and **Fig 5.6** show that acid influx on the Cl^--HCO_3^- exchange system is both pH_i and pH_o dependent, such dependency being highly non-linear. However, this non-linearity could be simply the outcome of Cl^--HCO_3 exchange obeying Michalis-Menton kinetics with respect to its substrate, intracellular HCO_3 ($HCO_{3\,i}^-$) and extracellular HCO_3^- ($HCO_{3\,o}$)[2] (Michaelis & Menten, 1913; Stein, 1986). To examine further this non-linearity, data in **Fig 5.5** and **Fig 5.6** were fitted by a 3-parameter sigmoid curve, respectively (see Methods for details). The results of curve-fitting are shown in **Fig 5.7A** and **Fig 5.7B**, and the estimated parameters are listed in **Table 5.1**. If the data conformed to Michalis-Menton kinetics perfectly, their Hill coefficient with

[2] In isocapnic acidosis, P_{CO2} is kept constant. $[HCO_3^-]_i$ and $[HCO_3^-]_o$ are related exponentially to pH_i and pH_o in accordance with Handerson-Hasselbalch equation (**Equation 1.2**).

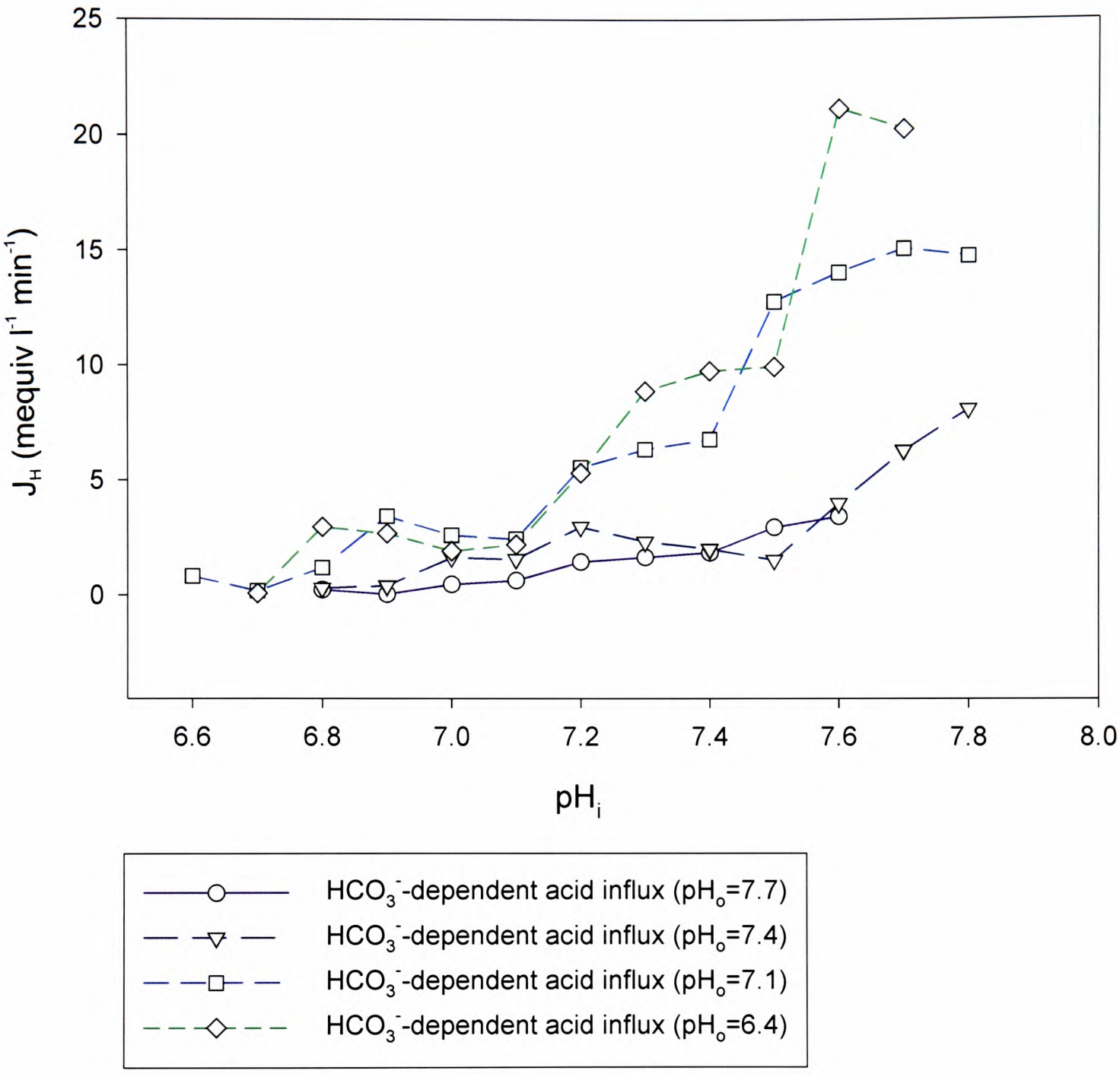


Figure 5.5

pH_i dependence of HCO_3^--dependent acid influx at different pH_o. Data were derived from substracting HCO_3^--independent acid influx (see **Fig 5.4**) from the corresponding total acid influx (see **Fig 5.2**) at different pH_o and pH_i.

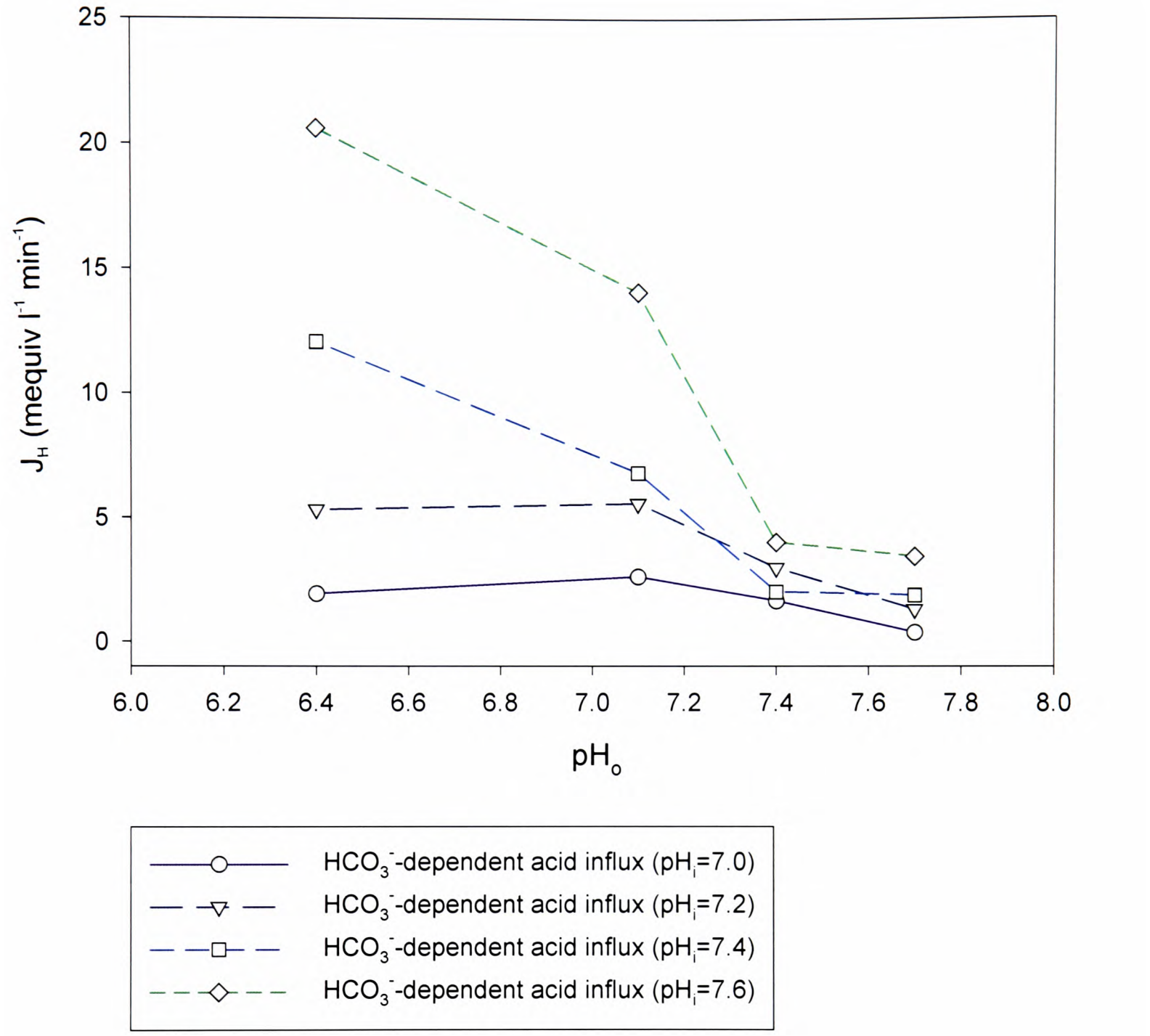


Figure 5.6

pH_o dependence of HCO_3^--dependent acid influx at different pH_i. The same data in **Fig 5.5** were used here, but plotted as acid influxes at different pH_i versus pH_o.

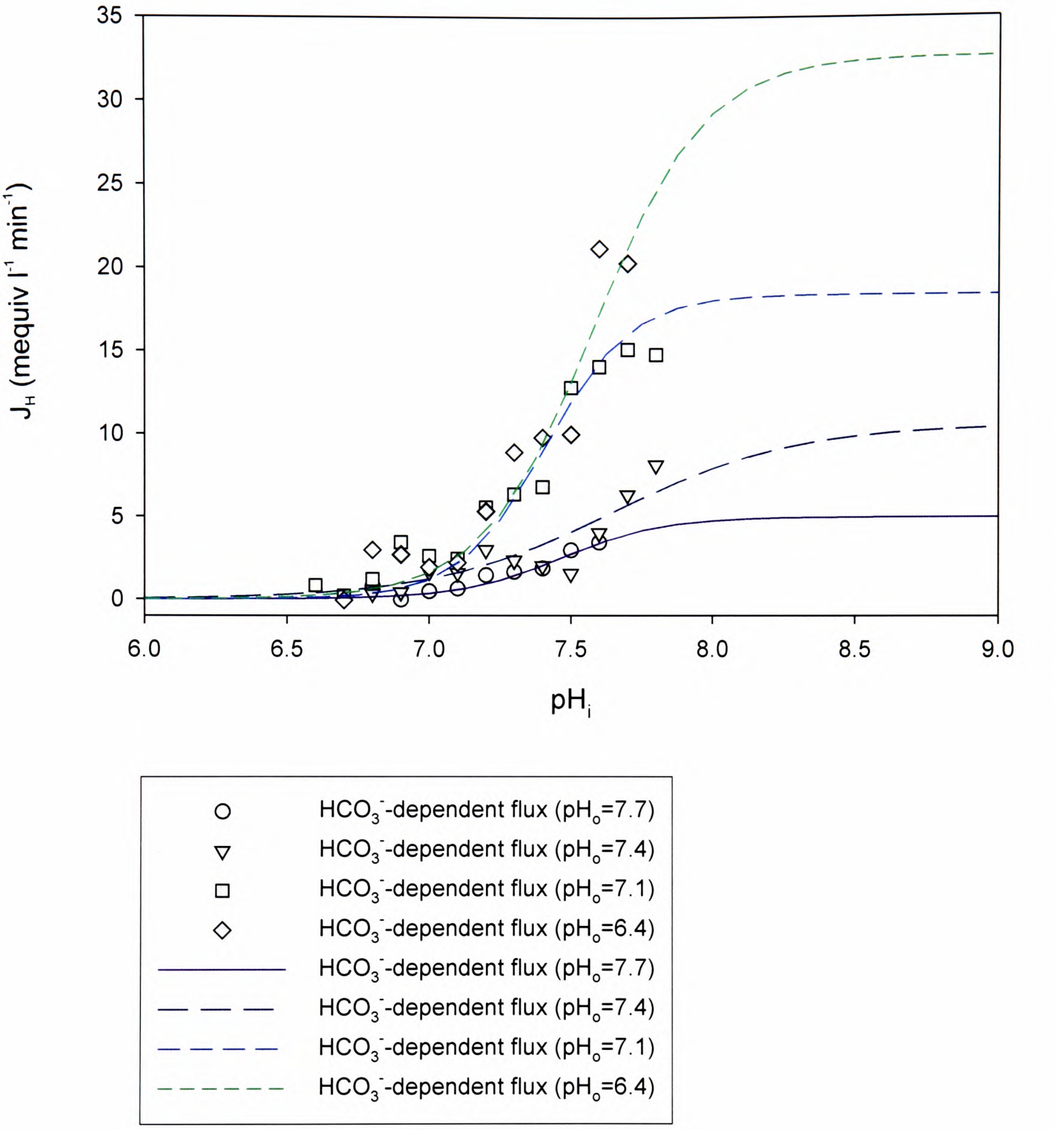


Figure 5.7

Analysis of pH_i and pH_o dependence of HCO_3^--dependent acid influx. ***A***, Analysis of pH_i dependence of HCO_3^--dependent acid influx at different pH_o. Data in **Fig 5.5** were fitted with 3-parameter sigmoid curve. The curve fitting parameters were estimated in **Table 5.1**.

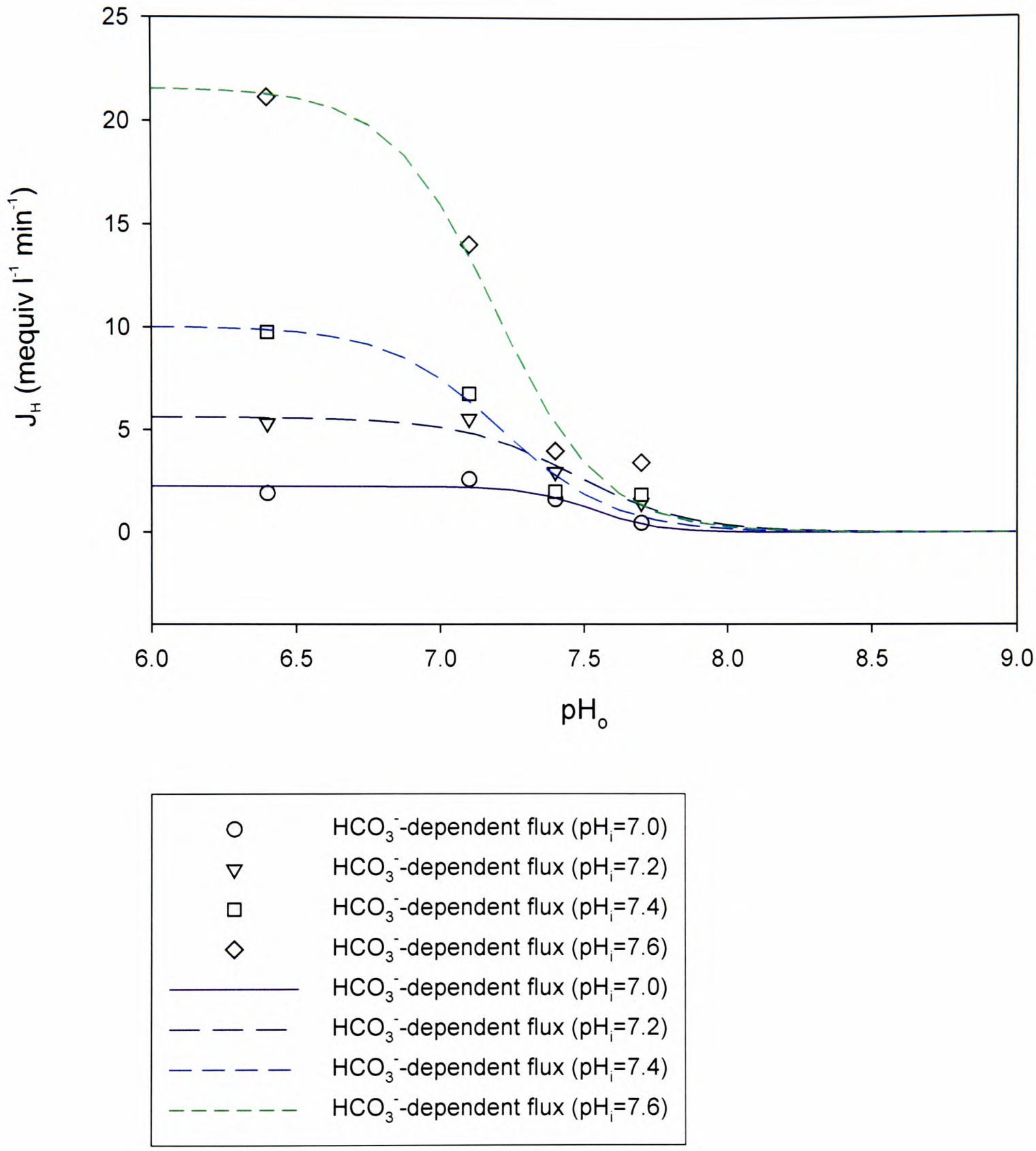


Figure 5.7 (continued)

B, Analysis of pH_o dependence of HCO_3^--dependent acid influx at different pH_i. Data in **Fig 5.6** were fitted with 3-parameter sigmoid curve. The curve fitting parameters were estimated in **Table 5.1**.

Table 5.1

Non-linear regression analysis of pH_i and pH_o dependency of HCO_3^--dependent acid influx (J_{HCO3}). Data in **Fig 5.5** and **Fig 5.6** were fitted with the 3-parameter sigmoid (see Methods),

$$J_{HCO3} = \frac{J^{max}_{HCO3}}{1+10^{h\cdot(pH-pK_a)}} \qquad \textbf{[Eqn. 5.1]}$$

The results are shown in **Fig 5.7A** and **Fig 5.7B**. Parameters of each curve were estimated as below.

pH_i dependency of HCO_3^--dependent acid influx
Parameters of sigmoid curve in **Fig 5.7A**

Condition (pH_o)	J^{max}_{HCO3}	pK_a^i	Hill coefficient	R^2*	Standard error
7.7	4.9571	7.4679	-2.4592	0.9367	0.3672
7.4	10.5103	7.6506	-1.3657	0.8974	0.9595
7.1	18.3740	7.4089	-2.8702	0.9631	1.2497
6.4	32.6332	7.5788	-2.2331	0.9291	2.3107

pH_o dependency of HCO_3^--dependent acid influx
Parameters of sigmoid curve in **Fig 5.7B**

Condition (pH_i)	J^{max}_{HCO3}	pK_a^o	Hill coefficient	R^2*	Standard error
7.0	2.2564	7.5316	3.8399	0.8812	0.5328
7.2	5.6178	7.4689	2.2197	0.9483	0.7754
7.4	10.0211	7.2138	2.2296	0.9569	1.3912
7.6	21.5809	7.1948	2.3645	0.9696	2.5749

* R^2 is the square of correlation coefficient

respect to acid-equivalent should be -1 (for $[H^+]_i$) or 1 (for $[H^+]_o$). However, the analysis shows that for most of the pH_i and pH_o conditions, the absolute value of their corresponding Hill coefficients for fluxes-pH (pH_i and pH_o, respectively) relationship are significantly larger than 1, mostly in the range of 2-3. These results therefore suggest that the activity of Cl^--HCO_3^- exchange system is probably sensitive to pH_i and pH_o changes, in addition to any substrate binding effects. **Table 5.1** also indicates the pH_i and pH_o levels for half-maximal activity of Cl^--HCO_3^- exchange, i.e. pK_a^i and pK_a^o, respectively. For most of pH_o and pH_i conditions, the corresponding pK_a^i and pK_a^o values are around 7.2-7.6. These values are close to physiological values of pH_i and pH_o, implying that the Cl^--HCO_3^- exchange system in the type I cell is physiologically regulated by both pH_o and pH_i. The implications of this finding are discussed below.

pH_i and pH_o sensitivity of HCO_3^- -independent acid loading

As indicated above, **Fig 5.4** shows pH_i dependency of HCO_3^--independent acid loading. In order to demonstrate pH_o dependency of the same acid loading mechanism, HCO_3^--independent acid influx was plotted as a function of pH_o at five representative pH_i levels (6.8, 7.0, 7.2, 7.4 and 7.6) in **Fig 5.8**. In both cases, data were analysed by linear regression for pH_i and pH_o dependency, respectively (see Methods for details). The estimated parameters are listed in **Table 5.2**.

Although **Table 5.2** shows the general relationship of HCO_3^--independent acid influx *versus* pH_i and pH_o, it is difficult to determine pH_i and pH_o sensitivity of acid influx due to the relatively small values of influx rate in relation to their variance. To reduce the variability of acid influx rates among individual cells, the acid influx rate induced

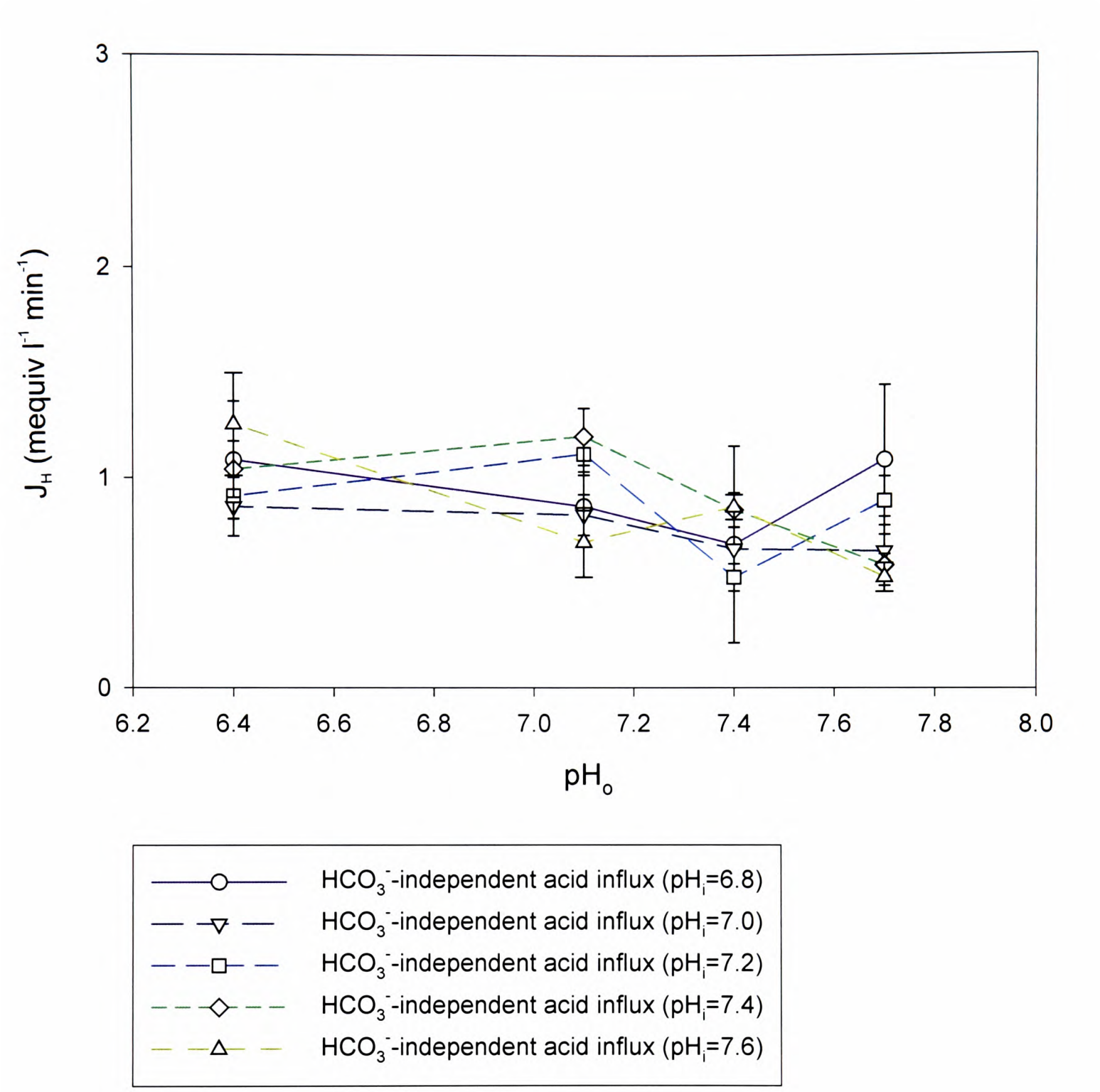


Figure 5.8

pH_o dependence of HCO_3^--independent acid influx at different pH_i. The same data in **Fig 5.4** were used here, but plotted as acid influxes at different pH_i versus pH_o.

Table 5.2

Linear regression analysis of pH_i and pH_o dependency of HCO_3^--independent acid influx (J_H). Data in **Fig 5.4** and **Fig 5.8** were fitted with regression line (see Methods),

$$J_H = b \times pH + a \qquad \textbf{[Eqn. 5.2]}$$

Parameters of each regression line are estimated as below.

* R^2 is the square of correlation coefficient

pH_i dependency of HCO_3^--independent acid influx
Parameters of regression line in **Fig 5.4**

Condition (pH_o)	b	a	R^2*	Standard error
7.7	-0.3954	3.4644	0.6682	0.1115
7.4	0.2202	-0.9379	0.2878	0.1211
7.1	0.0192	0.7519	0.0008	0.3114
6.4	-0.1383	2.0823	0.0342	0.2360

pH_o dependency of HCO_3^--independent acid influx
Parameters of regression line in **Fig 5.8**

Condition (pH_i)	b	a	R^2*	Standard error
7.6	-0.5066	4.4570	0.8149	0.1646
7.4	-0.3456	3.3823	0.4893	0.2408
7.2	-0.1276	1.7739	0.2904	0.2866
7.0	-0.1764	2.0112	0.8146	0.0574
6.8	-0.2070	2.2650	0.3163	0.2075

by acid challenge in each cell was normalised by dividing it with the background acid loading (under pH_o 7.9 and Na^+-free condition) measured immediately before acid challenge. After this normalisation treatment, the relationship between normalised HCO_3^--independent acid influx and pH_i is shown in **Fig 5.9A**. There is no clear pH_i dependency of normalised acid influx. When data were analysed by linear regression, the values of square of correlation coefficient (R^2) for these regression lines are all below 0.5 (**Table 5.3**). This suggests that acid influx via the HCO_3^--independent pathway is essentially pH_i insensitive.

Since pH_i does not significantly affect HCO_3 -independent acid influx, all normalised acid influx rates at all pH_i were pooled together for subsequent analysis of the pH_o sensitivity of the HCO_3 -independent acid influx pathway, which is explored by plotting normalised acid influx *versus* pH_o at five representative pH_i levels (6.8, 7.0, 7.2, 7.4 and 7.6) in **Fig 5.9B**. The correlation between pH_o and normalised acid fluxes was analysed by linear regression. As shown in **Table 5.3**, the value of square of correlation coefficient (R^2) for the regression line is 0.7376, with slope (b) of -1.0843 (negative value represents negative correlation). These results suggest that the HCO_3 -independent acid influx pathway is sensitive to pH_o. Thus it is concluded that at all pH_i levels, normalised acid influx increases 1.5 to 2 fold as pH_o falls from 7.4 to 6.4.

Discussion

The pH_i in carotid body type I cell represents a net balance of acid influx and acid efflux, therefore any change in either acid influx or efflux will lead to a change in pH_i.

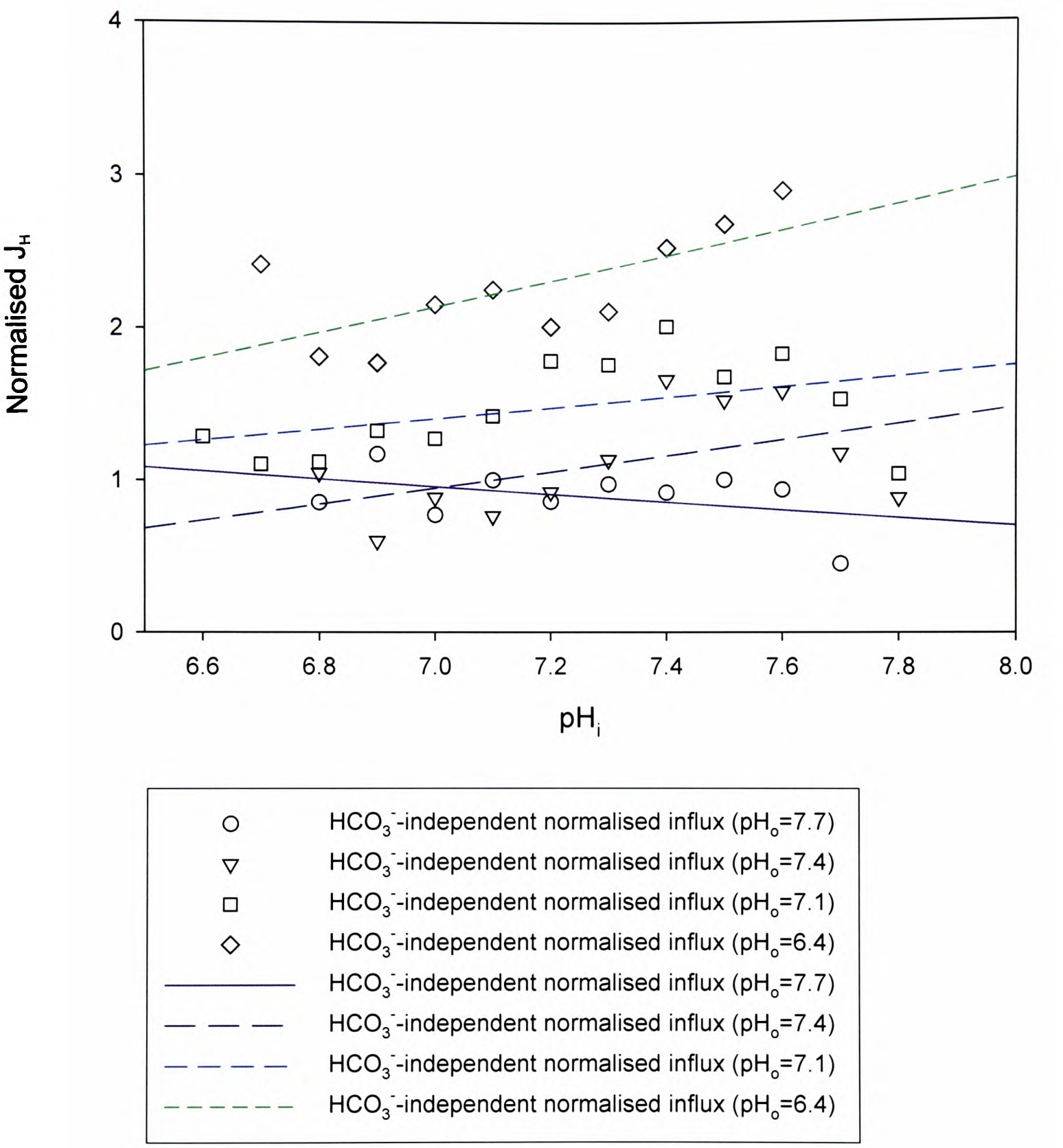


Figure 5.9

Analysis of pH_i and pH_o dependence of normalised HCO_3^--independent acid influx. ***A***, Analysis of pH_i dependence of normalised HCO_3^--independent acid influx at different pH_o. Acid influx rates were normalised by taking ratio of acid influx rate to background acid loading prior to acid challenge, then fitted with regression line. The regression parameters were estimated in **Table 5.3**.

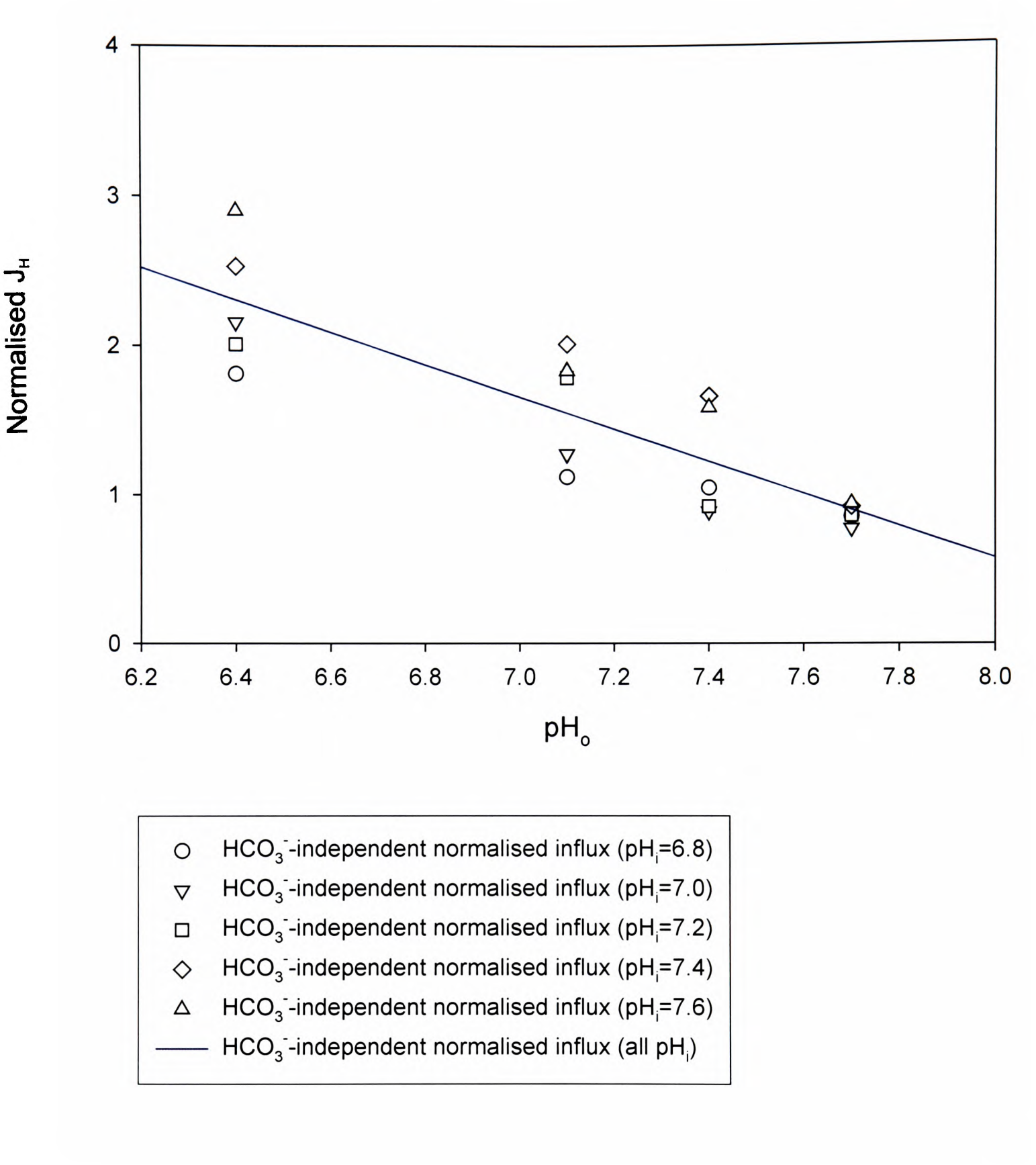


Figure 5.9 (continued)

B, Analysis of pH_o dependence of normalised HCO_3^--independent acid influx at all pH_i. Acid influx rates were normalised by taking ratio of acid influx rate to background acid loading prior to acid challenge, then fitted with regression line. Normalised HCO_3^--independent acid influx at all pH_i were pooled together for analysis. The regression parameters were estimated in **Table 5.3**.

Table 5.3

Linear regression analysis of pH_i and pH_o dependency of normalised HCO_3^--independent acid influx (J_H). Data in **Fig 5.9A** and **Fig 5.9B** were fitted with regression line (see Methods),

$$J_H = b \times pH + a \qquad \textbf{[Eqn. 5.2]}$$

Parameters of each regression line are estimated as below.

pH_i dependency of normalised HCO_3^--independent acid influx
Parameters of regression line in **Fig 5.9A**

Condition (pH_o)	b	a	R^2*	Standard error
7.7	-0.2563	2.7527	0.1679	0.1832
7.4	0.5317	-2.7736	0.2535	0.3189
7.1	0.3508	-1.0506	0.1885	0.2961
6.4	0.8396	-3.7386	0.4765	0.2826

pH_o dependency of normalised HCO_3^--independent acid influx
Parameters of regression line in **Fig 5.9B**

Condition (pH_i)	b	a	R^2*	Standard error
6.8-7.6	-1.0843	9.2461	0.7376	0.3287

* R^2 is the square of correlation coefficient

In the present study, I have focused on the regulation of acid influx. A fall in pH_o stimulates the dual acid influx pathways in the type I cell (i.e. the Cl^--HCO_3^- exchange system and the HCO_3^--independent mechanism), which, in combination with decreased acid efflux, lead to a fall of pH_i (see Chapter 3). Conversely, it is plausible to infer that total acid influx rate is decreased at lower pH_i, since acid influx progressively decreases as pH_i falls during an acid challenge (**Fig 3.1**). In order to clarify the acid loading process in response to isocapnic acidosis, I have attempted to characterise the effect of pH_i and pH_o upon acid loading pathways, including HCO_3^--dependent and HCO_3^--independent mechanisms.

Determination of acid influx rates

To measure the acid-equivalent flux during acid loading, the concomitant acid extrusion has to be inhibited, this can be achieved by removing extracellular Na^+ from the CO_2/HCO_3^--buffered solution since all known acid extruders in type I cells are Na^+_o-dependent, i.e. Na^+-H^+ exchanger and Na^+-HCO_3^--dependent acid extruder (probably Na^+-dependent Cl^--HCO_3^- exchanger, see Richmond 1993). However, it could be argued that, in the absence of Na^+_o these acid extruders operate in reversed transport mode exporting Na^+_i in exchange for the entry of acid-equivalents. In this case, the observed acid influx may be overestimated. The extent of such overestimation is discussed here.

For the measurement of total acid influx, cells had been perfused with pH_o 7.9 Na^+-free CO_2/HCO_3^--buffered solution for around 2 minutes before the start of acid challenge (**Fig 5.1**). The acid influx rate during this period was 2.37±0.44 mequiv l^{-1} min^{-1} at pH_i 7.7. It is difficult to decide how much of this was due to reversed

transport of acid extruders, as Na^+-free treatment also reveals background acid loading. But it is likely that acid influx mediated via reversal of acid extruders was lower than this value. Firstly, Boron and colleagues point out that, Na^+-dependent Cl^--HCO_3^- exchanger NDCBE1 found in human brain is very difficult to reverse (Grichtchenko, Choi, Zhong, Bray-Ward, Russell & Boron, 2001). Secondly, acid influx mediated by reversal of Na^+-H^+ exchange is estimated to be less than 0.5 mequiv l^{-1} min^{-1} at pH_o 7.9 (see Appendix 1), and this value would be expected to be even less at more acidic pH_o levels, given that low pH_o inhibits the activity of Na^+-H^+ exchanger (Vaughan-Jones & Wu, 1990). Thus, even allowing for the possibility of some reversed transport, the overestimation may not influence the total flux measurement significantly. Thirdly, given that resting $[Na^+]_i$ is probably about 10 mM, reversed transport of acid extruders, if any, is likely to decline after few minutes of Na^+_o–free treatment because of Na^+_i loss. Therefore, after the initial period of pH_o 7.9, Na^+–free perfusion, there may be very little reversed transport of acid extruders during the acid loading process (see **Fig 5.1** and **Fig 5.3**).

Comparing acid influx measured by the method described in this chapter with those values determined in Na^+-containing solutions also tends to confirm this conclusion. For example, the acid influx rate for pH_o 6.4 acid challenge in the presence and absence of Na^+ was 6.09±0.79 mequiv l^{-1} min^{-1} and 6.38±0.95 mequiv l^{-1} min^{-1} at pH_i 7.27, respectively; while for pH_o 7.1 the corresponding rates were 3.27±0.68 mequiv l^{-1} min^{-1} and 3.91±0.70 mequiv l^{-1} min^{-1} at pH_i 7.13 (original pH_i recordings not shown). The small difference is presumably due to Na^+-dependent acid efflux. Therefore, we conclude that the measurements of acid influx in this chapter actually reflect fluxes through the acid loading mechanisms.

pH_i and pH_o sensitivity of Cl^--HCO_3^- exchange system in type I cells

As concluded in Chapter 3, the major acid loading mechanism in the type I cell is Cl^--HCO_3^- exchange, which mediates transmembrane exchange of Cl^-_o with $HCO_3^-_i$. I also proposed in Chapter 4 that there could be two distinct Cl^--HCO_3^- exchangers in the type I cell, one is DIDS-sensitive and active at high pH_i (probably AE2) while the other is DIDS-insensitive and active at low pH_o (possibly a member of SLC26A protein). Thus it is expected that pH_i and pH_o may have different effects on the two types of Cl^--HCO_3^- exchangers. However, in this chapter the combined function of these Cl^--HCO_3 exchangers will be treated collectively as a Cl^--HCO_3 exchange system, in order to examine the physiological response of major acid influx pathway in the type I cell under different pH_i and pH_o conditions.

Since $[HCO_3^-]_i$ is determined by pH_i in a system open to CO_2, the acid loading may expected to be faster at more alkaline pH_i when pH_o is kept constant, due to more substrate $HCO_3^-_i$ for the anion exchange, provided $HCO_3^-_i$ is not saturated at Cl^--HCO_3^- exchanger (currently K_M^{HCO3-} for Cl^--HCO_3 exchanger in type I cells is still unknown). In this sense, the activity of anion exchange should be dependent on pH_i. It is not clear, however, whether pH_i changes have a direct effect on Cl^--HCO_3 exchange, i.e. allosteric modulation of anion transport by H^+ (or OH^- or HCO_3^-). This question could be investigated by Cl^- uptake experiment, in which the uptake of radioactive $^{36}Cl^-$, representing the Cl-Cl self-exchange via the anion exchanger, is assayed at different pH_i (Olsnes, Tonnessen & Sandvig, 1986; Mason, Smith, Garcia-Soto & Grinstein, 1989). In this way the effect of pH_i could be evaluated independent of changes in substrate (Cl^-_i and Cl^-_o). Another approach is to calculate the Hill

coefficient of Cl^--HCO_3^- exchange activation *versus* pH_i. Since saturation activity points were not observed on any of the curves shown in **Fig 5.5**, it is not possible to obtain a proper Hill plot. Instead, all curves were fitted with 3-parameter sigmoid, in order to estimate their respective Hill coefficient. Clearly, the estimated Hill coefficient for all curves is larger than 1, mostly between 2 and 3 (**Fig 5.7A** and **Table 5.1**). This result suggests more than one intracellular acid-equivalent ion ($HCO_3^-{}_i$ or $H^+{}_i$ or $OH^-{}_i$) interact with the exchanger. One explanation is that H^+ (or HCO_3^- or OH^-) has an allosteric modulation effect upon the exchanger molecule. The result of this modulation is an increase in exchange activity at higher pH_i.

Similarly, the dependence of Cl^--HCO_3 exchange system activity on pH_o is also examined by the same approach. The transport activity is higher at more acidic pH_o when pH_i is fixed. Nevertheless, this phenomenon cannot be fully explained by the increased acid influx as a result of larger transmembrane HCO_3^- gradient, since estimated Hill coefficients for all curves are between –2 and –4 (**Fig 5.7B** and **Table 5.1**). This implies extracellular H^+ (or HCO_3^- or OH^-) interact with the exchanger molecule in a manner that the Cl^--HCO_3^- exchange activity is enhanced at lower pH_o.

pH_i and pH_o sensitivity of Cl^--HCO_3^- exchange in other cell types

The above results show that in the type I cell, pH (both pH_i and pH_o) has a direct influence on Cl^--HCO_3^- exchange system. In addition, the effect of this influence is opposite for pH_i and pH_o: acid flux into the type I cell is activated at low pH_i, while inhibited at low pH_o. Combined with my hypothesis of two distinct Cl^--HCO_3^- exchangers proposed in Chapter 4, it is plausible to suggest that one Cl^--HCO_3^-

exchanger (probably AE2) is activated by a rise of H^+_o, while the other Cl^--HCO_3^- exchanger is inhibited by a rise of H^+_i (**Fig 5.10**).

Similar dependence of anion exchange activity on pH_i has also been reported in various other cell types, including mammalian Vero cell line (Olsnes, Tonnessen & Sandvig, 1986), cardiac Purkinje fibres (Vaughan-Jones, Eisner, and Lederer, 1987), mesangial cells (Boyarsky, Ganz, Sterzel & Boron, 1988), lymphocytes (Mason, Smith, Garcia-Soto & Grinstein, 1989) and ventricular myocytes (Leem & Vaughan-Jones, 1998). In some of these and other cell types, such as Vero cell line (Tonnessen, Aas, Ludt, Blomhoff & Olsnes, 1990), lymphocytes (Alper, Kopito, Libresco & Lodish, 1988) and thick ascending limb cells (Dominique *et al.*, 1998), AE2 has also been suggested to be responsible for the pH_i sensitivity of anion exchange. In contrast to pH_i sensitivity, the pH_o sensitivity of cloned AE proteins has not been thoroughly investigated. Partly this is because a change in pH_o inevitably results in a change in pH_i, thus complicating the analysis of pH_o effect on anion exchange activity (Stewart, Chernova, Kunes & Alper, 2001). In this regard, the purely extracellular pH effect on Cl^--HCO_3^- exchange (at fixed pH_i) shown in this study may have particular significance. Recently, Wilson & Vaughan-Jones (2001) reported that, in cardiomyocytes the Hill coefficient for the curve of Cl^--HCO_3^- exchange activity *versus* H^+_o is close to unity, suggesting there is only one acid-equivalent binding site (presumably for HCO_3 transport) on cardiac AE protein. Their result is very different from my finding that Cl^--HCO_3 exchange system in type I cells is strongly modulated by H^+_o. Such a difference in pH_o sensitivity may reflect different roles of Cl^--HCO_3^- exchange in these two cell types.

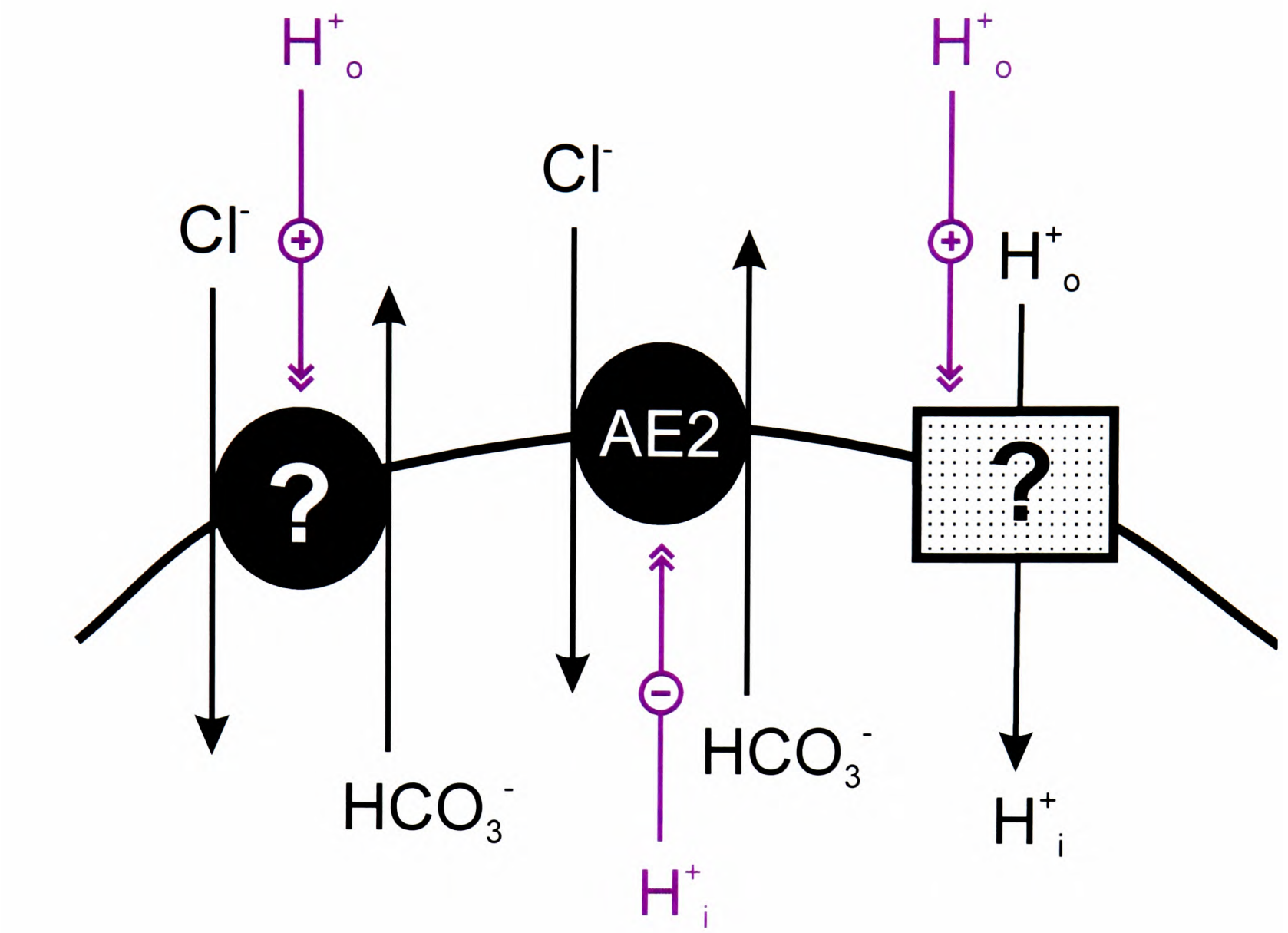


Figure 5.10

Schematic diagram showing the pH_i and pH_o sensitivity of acid influx mechanism in the type I cell. One Cl^--HCO_3^- exchanger (probably AE2) is inhibited as pH_i falls, while another Cl^--HCO_3^- exchanger is activated as pH_o rises. One possibility is these exchangers are allosterically modulated by H_o^+ and H_i^+. In addition, there is an unknown H_o^+-activated HCO_3^--independent mechanism.

pK_a^i and pK_a^o for Cl^--HCO_3^- exchanger and its physiological significance

In addition to the Hill coefficient, the pK_a^i and pK_a^o for Cl^--HCO_3^- exchange system, which represent the pH_i and pH_o values for half-maximal activation of the system, were also estimated. As shown in **Table 5.1**, all estimated values for pK_a^i and pK_a^o at different pH_o and pH_i conditions fall in the pH range of 7.1-7.6, indicating that the exchange system is normally operating at ~50% of its maximal activity. Furthermore, since pK_a of an activation curve represents the most sensitive point for regulation by pH, my results show the exchange system is subject to strong regulation by both pH_i and pH_o at resting conditions. Any shift of pH_i or pH_o from this normal resting range will produce significant changes in exchange activity. This observation is consistent with the physiological role of type I cells as the major acid chemoreceptor, in which Cl^--HCO_3^- exchange system is mainly responsible for transducing changes in pH_o into parallel changes in pH_i. For example, when pH_o is reduced from 7.4 to 6.4, the acid influx on the exchange system readily increases as a result of low pH_o activation, leading to a fall in pH_i. However, when pH_i decreases below the normal resting range of 7.1-7.3, the exchange system activity is reduced as a result of low pH_i inhibition, so the acid influx diminishes and finally stops. My results demonstrated that the pH_i and pH_o sensitivity of Cl^--HCO_3^- exchange system are both key factors in determining the steady-state pH_i. In this way, the exchange system maintains a tight link between pH_o and pH_i in the type I cell.

pH_i and pH_o sensitivity of HCO_3^--independent acid influx pathway in the type I cell

Unlike Cl^--HCO_3^- exchange, the HCO_3^--independent mechanism, which is responsible for the minor acid influx pathway, is virtually pH_i insensitive (**Fig 5.9A**). The plot of HCO_3 -independent acid influx *versus* pH_i can be fitted with almost horizontal regression lines. The normalised acid influx rate has little correlation with pH_i, a conclusion supported by its low correlation coefficient (**Table 5.3**). By contrast, the normalised HCO_3 -independent acid influx is enhanced by a fall in pH_o (**Fig 5.9B**), with correlation coefficient close to 1 (**Table 5.3**). For example, at pH_i 7.2 the HCO_3^--independent acid influx rate doubles when pH_o is reduced from 7.4 to 6.4. This result is consistent with my previous conclusion in Chapter 3, suggesting the unidentified acid loading mechanism is activated by H^+_o (**Fig 5.10**).

Modelling acid fluxes during acid loading

Having obtained the activation curves for both HCO_3 -dependent and HCO_3^--independent acid loading mechanism, we can use them to model the HCO_3^--dependent and HCO_3^--independent acid influxes during the time course of acid loading. As usual, a control response was recorded in **Fig 5.11A** when the type I cell was given a pH_o 6.4 acid challenge. Then the sigmoid and linear regression formula and parameters listed in **Table 5.1** and **Table 5.2** were used for calculating acid influxes via both mechanisms from the original pH_i data. So the individual fluxes and total acid flux can be plotted *versus* time before, during and after the acid challenge. As seen in **Fig 5.11B**, by switching the pH_o of the perfusate from 7.4 to 6.4, total acid influx

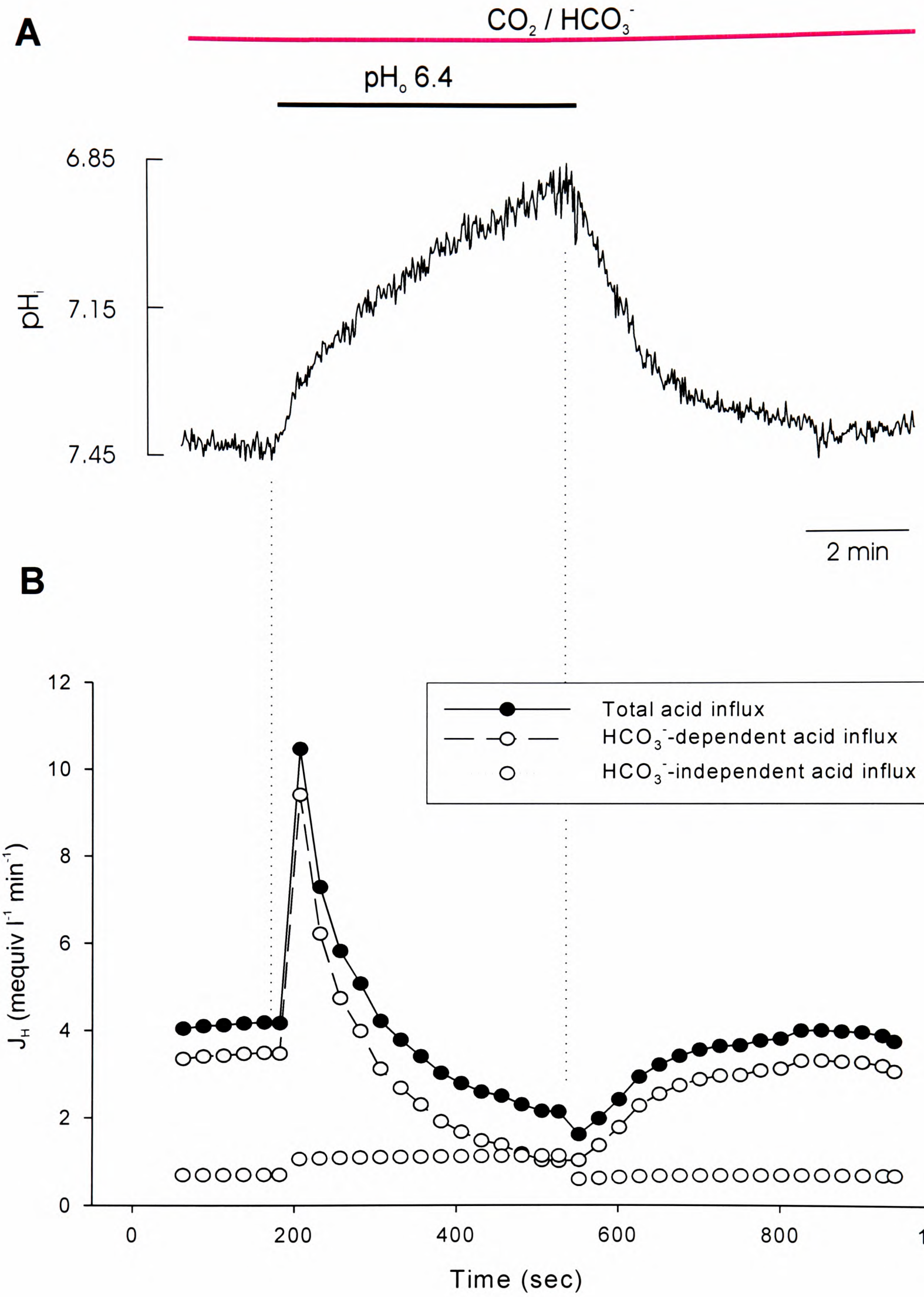


Figure 5.11

Modelling HCO_3^--dependent and HCO_3^--independent acid influxes during acid loading. ***A***, Control response of acid loading induced by pH_o 6.4 acid challenge. ***B***, The sigmoid and linear regression formula and parameters listed in **Table 5.1** and **Table 5.2** were used for calculating acid influxes via the dual acid influx pathways from the pH_i data shown in ***A***. So the individual fluxes and total acid flux can be plotted against time domain.

immediately surges from ~4 to ~10 mequiv l^{-1} min^{-1}, then gradually declines as pH_i decreases. At the end of acid loading (pH_o 6.4 and pH_i ~6.85), acid influx reaches as low as ~2 mequiv l^{-1} min^{-1}, followed by recovery to ~4 mequiv l^{-1} min^{-1} when pH_o is changed back to 7.4. Since the activity of HCO_3 -independent mechanism is moderately varied with pH_o but not with pH_i, this dramatic change in total acid influx is mainly caused by the pH_i and pH_o sensitivity of Cl^--HCO_3^- exchange system.

CHAPTER 6

General Discussion

The type I cell is the primary chemoreceptor in the carotid body, one of its physiological functions is to detect a reduction in arterial pH during acute metabolic (isocapnic) acidosis. In the type I cell, pH_i is tightly coupled to pH_o, hence pH_i decreases in response to a drop in pH_o. The reduction in both pH_i and pH_o causes K^+ channel inhibition on the cell membrane, leading to membrane depolarisation and neurosecretion. The chemoreflex eventually stimulates a ventilatory response. In this way, the carotid body induces respiratory compensation for metabolic acidosis (Rausch, Whipp, Wasserman & Huszczuk, 1991; Vovk, Duffin, Kowalchuk, Paterson & Cunningham, 2000). Although the basic mechanisms of pH_i regulation at normal pH_o (7.4) in type I cells have been examined previously (Wilding *et al.* 1992; Buckler *et al.* 1991a,b; Richmond, 1993), little is known about the nature and kinetics of acid influx mechanisms activated by isocapnic acidosis. Studies in this thesis have addressed these important questions, in the hope of providing an explanation for the high $\Delta pH_i/\Delta pH_o$ ratio of 0.6-0.7 observed in this cell type. The main conclusions are summarised and discussed below (see **Fig 6.1** for schematic diagram).

The major acid influx pathway: Cl^--HCO_3^- exchanger

In the carotid body type I cell, isocapnic acidosis stimulates two separate pathways, both of which transport acid-equivalents into the cell. In Chapter 3, it is shown that Cl^--HCO_3^- exchange is responsible for the major acid influx pathway. In response to a

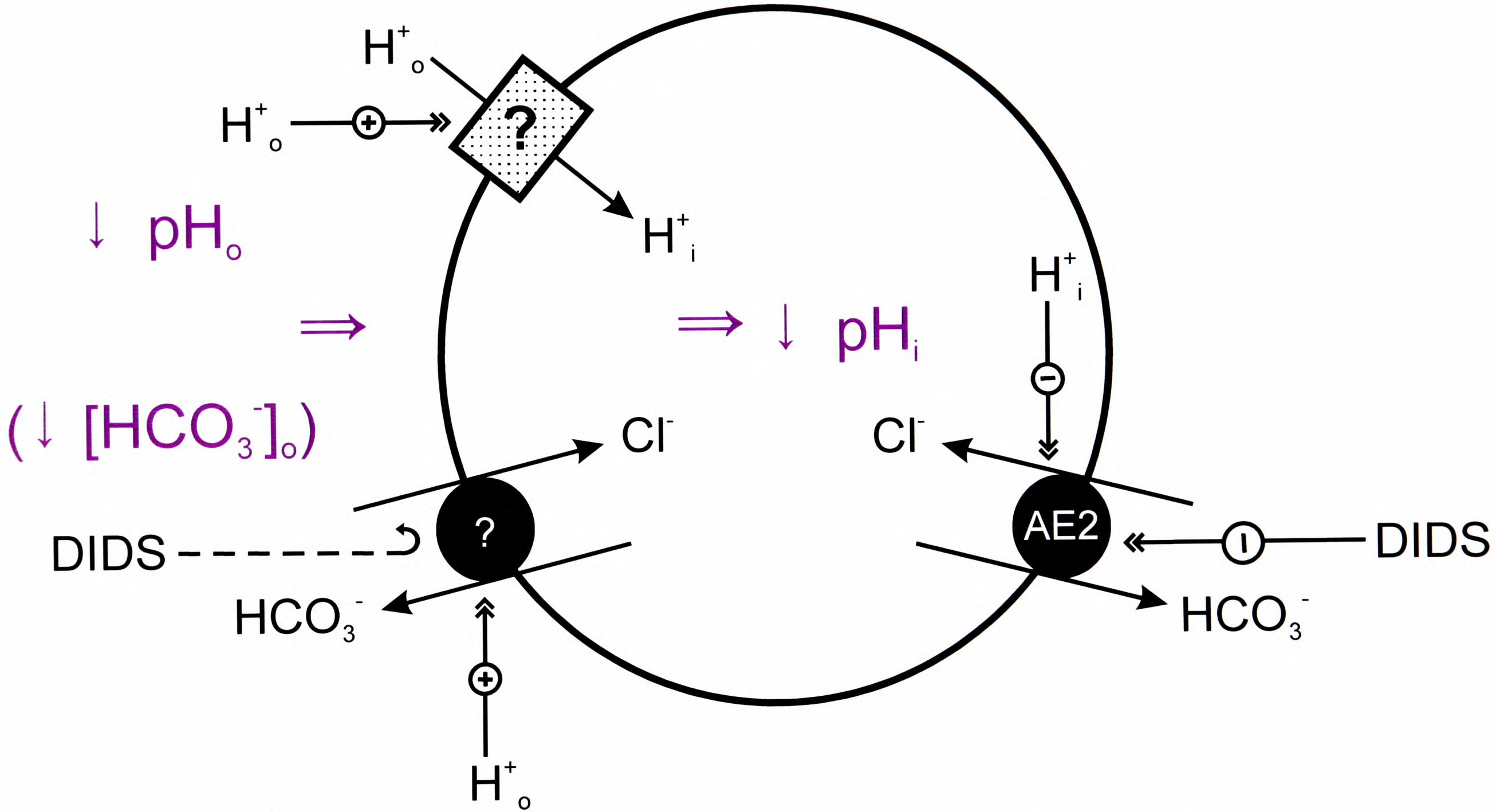


Figure 6.1
Schematic diagram showing major conclusions in this thesis. In response to extracellular acidosis, the majority of acid influx into type I cells is mediated via a DIDS-insensitive Cl^--HCO_3^- exchanger, which is activated by H^+_o. An unidentified H^+_o–activated mechanism contributes the remaining acid influx. Another DIDS-sensitive Cl^--HCO_3^- exchanger (probably AE2) is inhibited by H^+_i.

change of pH_o from 7.4 to 6.4 in physiological solutions (i.e. in the presence of CO_2/HCO_3^-), approximately 70% of total acid influx is mediated via this major pathway. Neither a HCO_3^- channel nor a Cl^--OH^- exchanger can account for this Cl^- or HCO_3^- dependence of acid influx. To clarify further the role played by this pathway in response to extracellular acidic stimuli, the kinetics of Cl^--HCO_3^- exchange system in the type I cell were characterised in Chapter 5. It was found that the acid loading activity of Cl^--HCO_3^- exchange is very sensitive to pH_i and pH_o. It is increased as pH_i rises and as pH_o falls, while is decreased as pH_i falls and pH_o rises. Preliminary analysis of the kinetic data also indicates that exchange activity is not a simple linear function of $[HCO_3^-]_i$ or $[HCO_3^-]_o$. The absolute value of Hill coefficients for the acid influx *versus* pH relationship (pH_i and pH_o) are mostly between 2-3, indicating the transporter binds more than one acid or base equivalent (H^+ or OH^- or HCO_3^-) on each side of the membrane. One possibility is that the transporter is activated allosterically by H^+_o and inhibited allosterically by H^+_i. In addition, pK_a^i and pK_a^o values for Cl^--HCO_3 exchange activity are within the range of 7.1-7.6, suggesting the Cl^--HCO_3^- exchange system in the type I cell will be subject to strong regulation by pH_i and pH_o under physiological conditions. In this way, the Cl^--HCO_3^- exchange system serves as a link for transducing acidic pH_o into a parallel acidification of pH_i.

DIDS insensitivity of acid influx

In the absence of Cl^-_o, Cl^--HCO_3^- exchange operates in reversed mode (i.e. acid efflux), resulting in Cl^--free induced alkalosis. This alkalosis is almost completely blocked by the anion exchanger inhibitor DIDS (200 μM), an observation that has been reported elsewhere (Vaughan-Jones, 1979; Aickin & Brading, 1984). Surprisingly, however, the acid influx induced by reducing pH_o to 6.4 is not affected

by the same concentration of DIDS in the type I cell (see Chapter 4). This intriguing finding cannot be explained in terms of H^+_o or Cl^-_o interference with DIDS binding. It is also unlikely that DIDS selectively blocks the reversed mode of Cl^--HCO_3^- exchange (acid efflux), but not the forward mode (acid influx), as DIDS blocks acid influx on Cl^--HCO_3^- exchange following Cl^-_o re-addition or after an acetate pre-pulse protocol. A remaining possibility is therefore that two types of Cl^--HCO_3^- exchange function in the type I cell, one is DIDS sensitive and stimulated by a rise of pH_i, the other DIDS insensitive and stimulated by a fall of pH_o (see below).

To my knowledge, the DIDS insensitivity of acid influx on Cl^--HCO_3^- exchange has not been reported. In cardiomyocytes, it has been shown that under CO_2/HCO_3^- conditions, Cl^--HCO_3^- exchanger is responsible for 40-50% of the acid influx stimulated by reducing pH_o (Sun, Leem & Vaughan-Jones, 1996). Unlike my results, in that research the acid influx mediated via Cl^--HCO_3^- exchanger is inhibited by DIDS. Elsewhere, although Cl^--HCO_3^- exchanger is generally recognised as DIDS-sensitive in many other nonerythroid cell types, it should be noted that in most of these studies the effect of DIDS was assessed either by the inhibition of Cl^-_o-free induced alkalosis or Cl^--Cl^- self-exchange in the absence of $HCO_3^-{}_o$. Both conditions are very different from the low pH_o-induced acid influx investigated in the present study, and not common in physiological systems. Because in most cell types Cl^--HCO_3 exchange functions as acid loader (i.e. in forward transport mode), my present finding of DIDS insensitive acid influx on Cl^--HCO_3^- exchange is physiologically important. It is likely that this insensitivity may exist in other cell types, but has not been properly investigated, since the effect of DIDS on acid influx was not assessed in previous studies.

Two types of Cl^--HCO_3^- exchanger in the type I cell

The molecular identity of the Cl^--HCO_3^- exchanger(s) in type I cells have not been investigated. In order to gauge the acid loader identity in type I cells, the evidence related to all 4 reported isoforms (AE1-4) is evaluated here. In erythrocyte, the inhibition of Cl^--HCO_3^- exchange on AE1 by DIDS is well documented (Lambert & Lowe, 1978; Kopito & Lodish, 1985), with IC_{50} value for Cl^--Cl^- self exchange of 0.04 μM (Funder, Toteson & Wieth, 1978). Previous studies showed that AE2 and AE3 are less sensitive to DIDS (Humphreys, Jiang, Chernova, Alper, 1994; Sterling & Casey, 1999), and IC_{50} values (estimated by the inhibition of Cl^-_o-free induced acid efflux) for AE2 and AE3 are 4 μM and 0.4 μM, respectively (Lee, Gunn & Kopito, 1991; He, Wu, Knauf, Tabak & Melvin, 1993). Based on these data, at the concentration of 200 μM used in the present study, all three isoforms should be almost completely inhibited. In respect of pH_i and pH_o sensitivity, AE1-mediated Cl^- transport is stable across a wide range of pH_o and pH_i (Zhang, Chernova, Stuart-Tilley, Jiang & Alper, 1996; Sterling & Casey, 1999). Previous studies showed that the activity of both AE2 and AE3 are pH_i-dependent and enhanced at higher pH_i (Lee, Gunn & Kopito, 1991; Humphreys, Jiang, Chernova & Alper, 1994; Stewart, Chernova, Kunes & Alper, 2001), although there is report suggesting AE3 protein is insensitive to pH_i change (Sterling & Casey, 1999). In addition, Stewart *et al.* (2001; 2002) reported that AE2 is not stimulated, and may even be inhibited at lower pH_o. Overall, based on the above evidence, it is likely that the Cl^--HCO_3^- exchanger(s) in type I cells include AE2 protein.

AE4, another novel HCO_3^--dependent transporter, was recently cloned (Tsuganezawa *et al.* 2001). It was reported to be DIDS insensitive. However, the Na^+-dependency of its function is disputed. In fact, AE4 is probably another NBC isoform (Soleimani, 2002), since the sequence of AE4 is highly homologous with other Na^+-HCO_3^- cotransporters. It seems therefore unlikely that AE4 mediates the DIDS insensitive acid influx in the type I cell.

It should be noted that, in addition to the classical AE proteins, there is another group of anion exchangers encoded by SLC26 gene family, among which over 10 proteins have been cloned recently (reviewed by Everett & Green, 1999; Vincourt, Jullien, Amalric & Girard, 2003). It is worth noting that these anion exchangers are generally less sensitive to DIDS than classical AE proteins. For instance, 1 mM DIDS reduced the anion exchange activity of SLC26A2 (also named DRA) and SLC26A4 (also named PDS) proteins by only 24% and 64%, respectively (Melvin, Park, Richardson, Schultheis & Shull, 1999; Scott, Wang, Kreman, Sheffield & Karniski, 1999). Both proteins have been shown to mediate Cl^--HCO_3^- exchange under physiological conditions (Melvin *et al.* 1999; Soleimani *et al.* 2001). In addition, Bissig *et al.* (1994) showed that SLC26A1 (also named SAT-1, for Sulphate Anion Transporter-1) is active at low pH_o. In the near future, more members of SLC26 transporters will be cloned and characterised, so it is plausible that some may turn out to be relatively DIDS insensitive and stimulated by low pH_o.

Combining evidence and observations stated above, I propose that there are two distinct populations of Cl^--HCO_3^- exchangers in the type I cell. One is DIDS sensitive and inhibited by H^+_i, the other is DIDS insensitive and activated by H^+_o. The

molecular identity of the former exchanger is possibly AE2, while the latter one is still unknown, although a member of the SLC26 transporter family is a feasible candidate. This hypothesis explains my data well, since it has been shown that acid influx induced by acetate pre-pulse (high pH_i and normal pH_o condition) is inhibited by DIDS, while acid influx induced by acid challenge (normal pH_i and low pH_o condition) is DIDS insensitive (see Chapter 4). It also incorporates the findings of pH_i and pH_o sensitivity of Cl^--HCO_3^- exchange system (see Chapter 5). Although the molecular identity of the Cl^--HCO_3^- exchanger(s) in type I cells remains to be found, this hypothesis provides a useful framework for future investigation.

The minor acid influx pathway: an unknown mechanism

The second pathway for acid-equivalent transport, which is independent of both Cl^-_o and $HCO_3^-_o$, accounts for about 30% of the acid influx as pH_o is reduced from 7.4 to 6.4. Although the exact nature of this second mechanism is still unknown, the present work indicates it is an acid influx enhanced by a fall in pH_o, in addition to the existing background acid loading unmasked by the inhibition of an acid extruder (e.g. Na^+-H^+ exchanger). Its activity is virtually pH_i independent, while it nearly doubles when pH_o is lowered from 7.4 to 6.4. Since this mechanism mediates relatively little acid influx, in comparison with the Cl^--HCO_3^- exchanger it makes a smaller contribution to the coupling of pH_i to pH_o under physiological conditions (i.e. in CO_2/HCO_3^--buffered solutions). Even so, it will play a role in determining the final steady-state pH_i in the type I cell. It is noteworthy that, as reported by Vaughan-Jones and co-workers, in cardiomyocytes where acid loading is mainly mediated by Cl^--HCO_3^- exchanger and Cl-OH exchangers, about 15-20% of total acid influx remains in Cl^--free solution. The

mechanism responsible for this Cl^--independent acid loading is also unknown (Sun *et al.* 1996).

In type I cells, the following candidates for the unidentified acid loading mechanism are proposed:

1. **H^+ channel**: Recently, H^+ channels have been identified in mammalian tissues, including alveolar epithelial cells (DeCoursey, 1991), macrophages (Kapus, Romanek, Qu, Rotstein & Grinstein, 1993), and neutrophils (DeCoursey & Cherny, 1993). Since a fall in pH_o increases the driving force for H^+ ion across cell membrane, H^+ channel could be a possible mechanism for this minor pathway. However, H^+ channels found in various cell types so far are all strongly voltage-gated and only carry outward current (i.e. H^+ efflux). These properties are incompatible with its role in mediating acid influx (DeCoursey & Cherny, 2000).

2. **Ca^{2+}-ATPase**: A significant $Ca^{2+}{}_o$-depedent acid influx is present in high $K^+{}_o$ solution (see Appendix 2), suggesting the possibility of a plasmalemma Ca^{2+}-H^+ exchange activity. In fact, in snail neurones (Schwiening, Kennedy & Thomas, 1993) and hippocampal neurones (Trapp, Lückermann, Kaila & Ballanyi, 1996), Ca^{2+}-ATPase is responsible for H^+ influx in exchange for Ca^{2+} extrusion. Such a mechanism would also mediate acid influx into type I cells during extracellular acidosis.

Further investigation is required for the identification of this unknown mechanism.

Integrated kinetic model for pH_i-pH_o relationship in the type I cell

A striking feature of the type I cell is its unusually high $\Delta pH_i/\Delta pH_o$ ratio, which appropriately suits its physiological role in monitoring pHa changes. Given the foregoing conclusions, an integrated kinetic model for the pH_i-pH_o relationship in the type I cell is proposed. The basic concept of the model is illustrated in **Fig 6.2**. The pH_i-dependent acid influxes at pH_o 7.4 and 6.4 are taken from the activation curves shown in **Fig 5.7**. The activation curve of acid effluxes at pH_o 7.4 is based on data obtained in type I cells (Richmond, 1993). Although the pH_o dependency of acid efflux is not yet determined in type I cells, it is plausible to assume that the acid efflux on Na^+-H^+ exchange (and probably on Na^+-dependent Cl^--HCO_3^- exchanger) at pH_o 6.4 is also a sigmoid function of pH_i, similar to those observed elsewhere (Vaughan-Jones & Wu, 1990; Boron & Knakal, 1992; Mellergard, Ouyang & Siesjo, 1994). Thus the activation curve of acid efflux at pH_o 6.4 is expected to be symmetrically opposite to that of acid influx. **Fig 6.2** outlines how pH_o may influence steady-state pH_i in type I cells. At normal pH_o of 7.4, a steady-state pH_i of about 7.2 is maintained when acid loaders and acid extruders counteract each other (point ***a***). When an acid challenge is applied (pH_o 6.4), acid influx increases, mainly due to the enhanced Cl^--HCO_3^- exchange system activity. Conversely, there is a decrease in acid efflux, assuming the activity of acid extruders is inhibited at lower pH_o. Such a change in both acid fluxes leads to accumulation of H^+_i (i.e. reduction in pH_i) until a new steady-state is reached, presumably around 6.6 (point ***b***), where Cl^--HCO_3^- exchange system activity is inhibited by low pH_i so that acid influx and acid efflux counteract each other again. As a result, it can be deduced that, the greater influence of pH_o on the activation curves of acid loaders and acid extruders, the larger the change in steady-state pH_i would be. In the present study, since Cl^--HCO_3^- exchange system has a

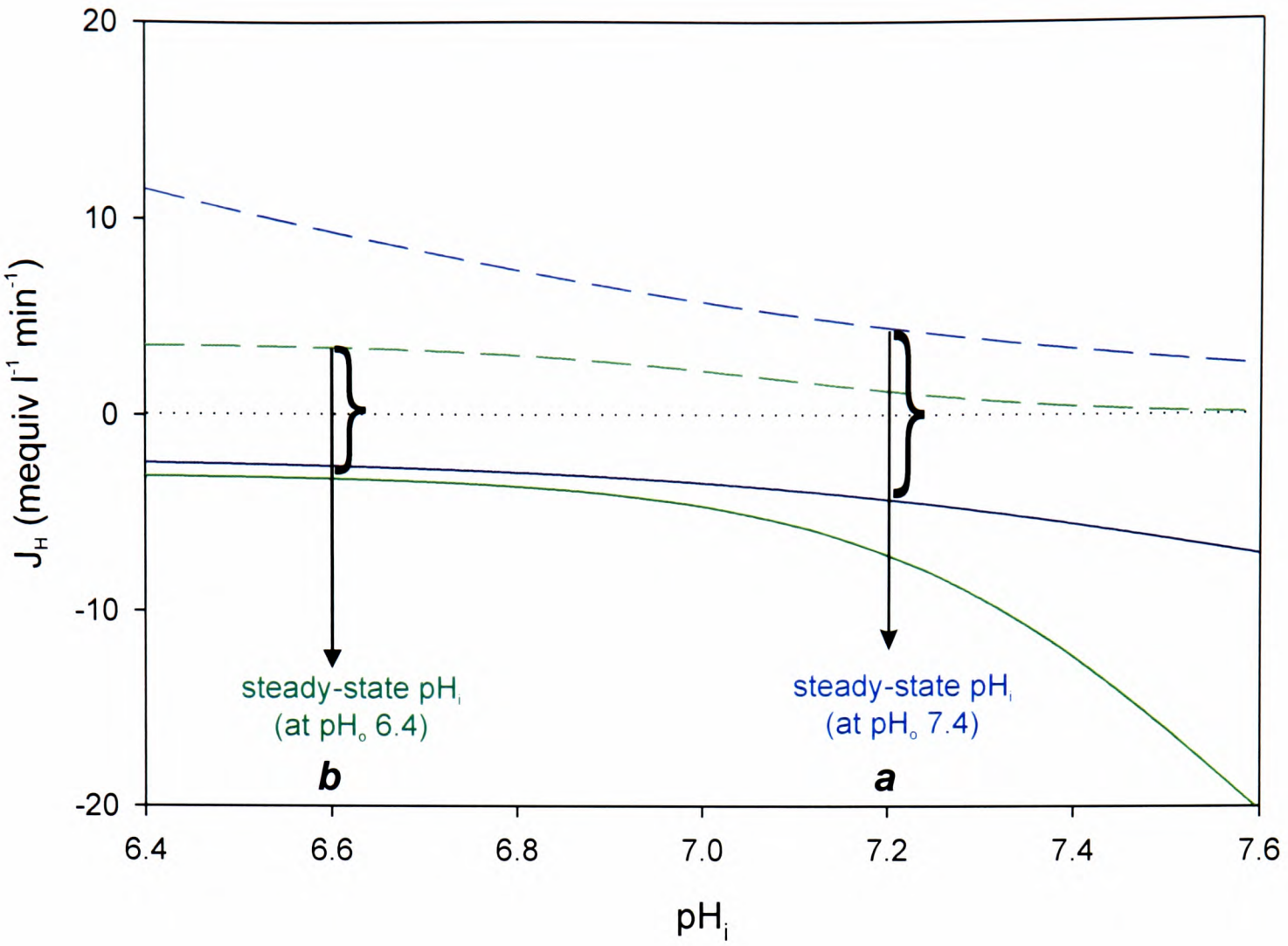


Figure 6.2
A proposed integrated model for the pH_o-pH_i relationship in the carotid body type I cell. The total acid influx is transported via Cl^--HCO_3^- exchange and the unknown HCO_3^--independent mechanism, while both Na^+-H^+ exchange and Na^+-dependent HCO_3^--dependent transporter (probably Na^+-dependent Cl^--HCO_3^- exchange) mediate acid efflux. At pH_o 7.4, total acid efflux counteracts total acid influx around pH_i 7.2, therefore maintaining a balance at point ***a***. When pH_o falls to 6.4, acid influx increases and acid efflux decreases, leading to a fall in pH_i. The new steady-state balance is re-established at pH_i 6.6 (point ***b***).

strong pH_o dependency, which is manifested by its rather high Hill coefficient of 2-3 (see Chapter 5), the unusually high $\Delta pH_i/\Delta pH_o$ ratio in the type I cell can be explained. More precise quantitative modelling of the close pH_o-pH_i relationship will require more detailed knowledge of the pH_i and pH_o sensitivity of acid extruders, plus their kinetics, similar to the characterisation of acid loaders presented in this thesis.

Comparison with other acid sensing cells

As described above, the $\Delta pH_i/\Delta pH_o$ ratio in type I cells is 0.6-0.7. Such a high value of $\Delta pH_i/\Delta pH_o$ is unusual, since in most cell types $\Delta pH_i/\Delta pH_o$ is normally 0.2-0.3. The only exceptions are putative chemosensitive neurones in brainstem and taste reporter cells in lingual epithelium: chemosensitive neurones in ventrolateral medulla and locus coeruleus have a $\Delta pH_i/\Delta pH_o$ ratio of 0.6-0.8 and 0.5, respectively (Ritucci, Chambers-Kersh, Dean & Putnam, 1998; Filosa, Dean & Putnam, 2002), while in acid-sensing cells of taste bud the ratio is 0.8-1.2 (Lyall, Feldman, Heck & DeSimone, 1997). The common feature of these cell types is their physiological role as acid sensors, suggesting that a tight coupling between pH_i and pH_o is essential in acid sensing. Therefore, my results in the present study, including the identification and characterisation of acid influx pathways, may provide a general framework for investigating other acid sensing cells. In fact, Putnam and colleagues suggested that in chemosensitive neurones from ventrolateral medulla, pH_i falls during hypercapnic acidosis with little recovery because the acid extruder Na^+-H^+ exchanger is particularly sensitive to inhibition by low pH_o (see Putnam, 2001 for review). However, in their work the involvement of Cl^--HCO_3^- exchanger during acidosis was not examined. It will be of interest to see the role of Cl^--HCO_3^- exchanger in acid sensing in these chemosensitive neurones.

Future directions of investigation

So far, the pH_o sensitivity of acid extrusion (either on Na^+-H^+ exchanger or Na^+-dependent Cl^--HCO_3^- exchanger) in the type I cell has not been characterised. As pH_i is determined by the balance of acid influx and acid efflux, these data must be incorporated once available, in order to complete an integrated kinetic model for the pH_o-pH_i relationship in the type I cell. The HCO_3^--independent acid loading mechanism also demands further investigation. Particularly, it is desirable to test whether pH_o 6.4 treatment induces acid loading in Ca_o^{2+}-free HEPES-buffered solution. If not, this evidence would favour the idea that Ca^{2+}-H^+ ATPase is responsible for the minor acid influx pathway.

Although in Chapter 3 I have concluded that the HCO_3^--dependent acid influx is not mediated by a HCO_3^- channel, this conclusion does not rule out the existence of such a channel in type I cells. In theory, HCO_3^- current through anion channel could still be important in the modulation of membrane depolarisation and neurosecretion response, even if the acid-equivalent flux is too small to cause significant change in pH_i. Electrophysiological studies are required to investigate this possibility.

At present, there has been no report on the cloning of acid-equivalent transporters in type I cells. As indicated in Chapter 4, based on the discrepancy of DIDS effect on acid influx and acid efflux, a hypothesis was proposed that there could be more than one Cl^--HCO_3^- exchanger population, possibly including member(s) of SLC26 gene family. This hypothesis would be scrutinised by the cloning of Cl^--HCO_3^- exchanger(s) from type I cells. Particularly, it would be of interest to see whether any

of SLC26 transporters are expressed. Once the molecular identity of these transporters is known, a complete study of their kinetic and pharmacological properties would be possible.

APPENDIX 1

Effect of Hoe694 on Na^+-H^+ Exchanger in the Carotid Body Type I Cell

Introduction

Na^+-H^+ exchanger (NHE) is the major acid extruder under CO_2/HCO_3 -free condition in type I cells (Buckler *et al.* 1991a). A novel NHE inhibitor Hoe694 (3-methylsulphonyl-4-piperidinobenzoyl guanidine methane-sulphonate) was synthesised by Scholtz *et al.* (1993). This compound has a highly selective inhibition for NHE1 isoform, over two orders of magnitude more effective than for the isoforms 2 and 3 (Counillon, Scholz, Lang & Pouyssengur, 1993). It has been shown to inhibit NHE in erythrocytes, platelets, endothelial cells and cardiomyocytes (Scholtz *et al.* 1993; Loh, Sun & Vaughan-Jones, 1996). By comparing the differential inhibitory effects of Hoe694 with other more classical amiloride-derived NHE inhibitors with lower selectivity for different NHE isoforms, Counillon *et al.* (1993) suggested the pharmacological properties of these inhibitors may be used to identify particular NHE isoforms. In this thesis, Hoe694 was used in various experiments to inhibit NHE activity (see Chapter 3 and Appendix 2). This appendix aims to establish a preliminary survey on the dose dependent inhibition by Hoe694 of NHE in type I cells. I conclude that NHE activity should be completely inhibited by 50 μM Hoe694, a concentration I used in all experiments to inhibit acid extrusion on NHE. In addition, the estimated

apparent K_i value for Hoe694 suggests NHE1 is the predominant isoform in type I cell.

Methods

General Methods

pH_i was recorded in isolated type I cells from the neonatal rats using carboxy-SNARF-1, as described in Chapter 2.

Solutions

All solutions used in this study were nominal CO_2/HCO_3^--free, HEPES-buffered solution. HEPES-buffered HCO_3^--free standard Tyrode solution and 20 mM sodium acetate solution were prepared as described in Chapter 2. Na^+-free HEPES-buffered solution was prepared as described in Chapter 3. For solutions containing Hoe694, the drug was added at required concentrations immediately before use.

(1) pH_o 7.9 Na^+-free HEPES-buffered solution

Composition	Concentration (mM)
NMDG	140
KCl	4.5
$MgCl_2$	1
$CaCl_2$	2.5
HEPES	20
Glucose	11
Adjust pH with HCl to 7.9 at 37 °C	

Drugs

Hoe694 (3-methylsulphonyl-4-piperidinobenzoyl guanidine methane-sulphonate) was used (see Methods in Chapter 3 for more information about Hoe694).

Curve Fitting and Data Handling

The dose-response curves drawn in **Fig Ai.1B** and **Fig Ai.2B** were the best-fit Michaelis-Menten curves using least square difference method, based on original experimental data (Cornish-Bowden, 1995a). The curve fitting and apparent K_i value was calculated by GraphPAD InPlot software.

Results

Dose-dependent inhibition of Na^+-H^+ exchanger by Hoe694

All experiments in this appendix were executed in HEPES-buffered solutions in order to investigate NHE activity. **Fig Ai.1A** illustrates a typical experimental protocol to measure the inhibitory effect of Hoe694 at different concentrations. Since the resting pH_i in type I cell is significantly alkaline (about 7.6-7.8) in the absence of CO_2/HCO_3 buffer, in order to measure the inhibition of Hoe694 in the pH_i range of 6.5-7.0, freshly isolated type I cells were bathed in HEPES-buffered solution for 4-6 hours, as reported by Buckler *et al.* (1991a). For each experiment, the recovery rates from acid load induced by ammonium pre-pulse technique (20 mM NH_4Cl, see Chapter 2) at different Hoe694 concentrations were measured. Since the recovery is mediated by NHE, the percentage inhibition of NHE activity by Hoe694 can be calculated. Results are summarised in **Fig Ai.1B**, showing the dose inhibition curve of Hoe694. The acid

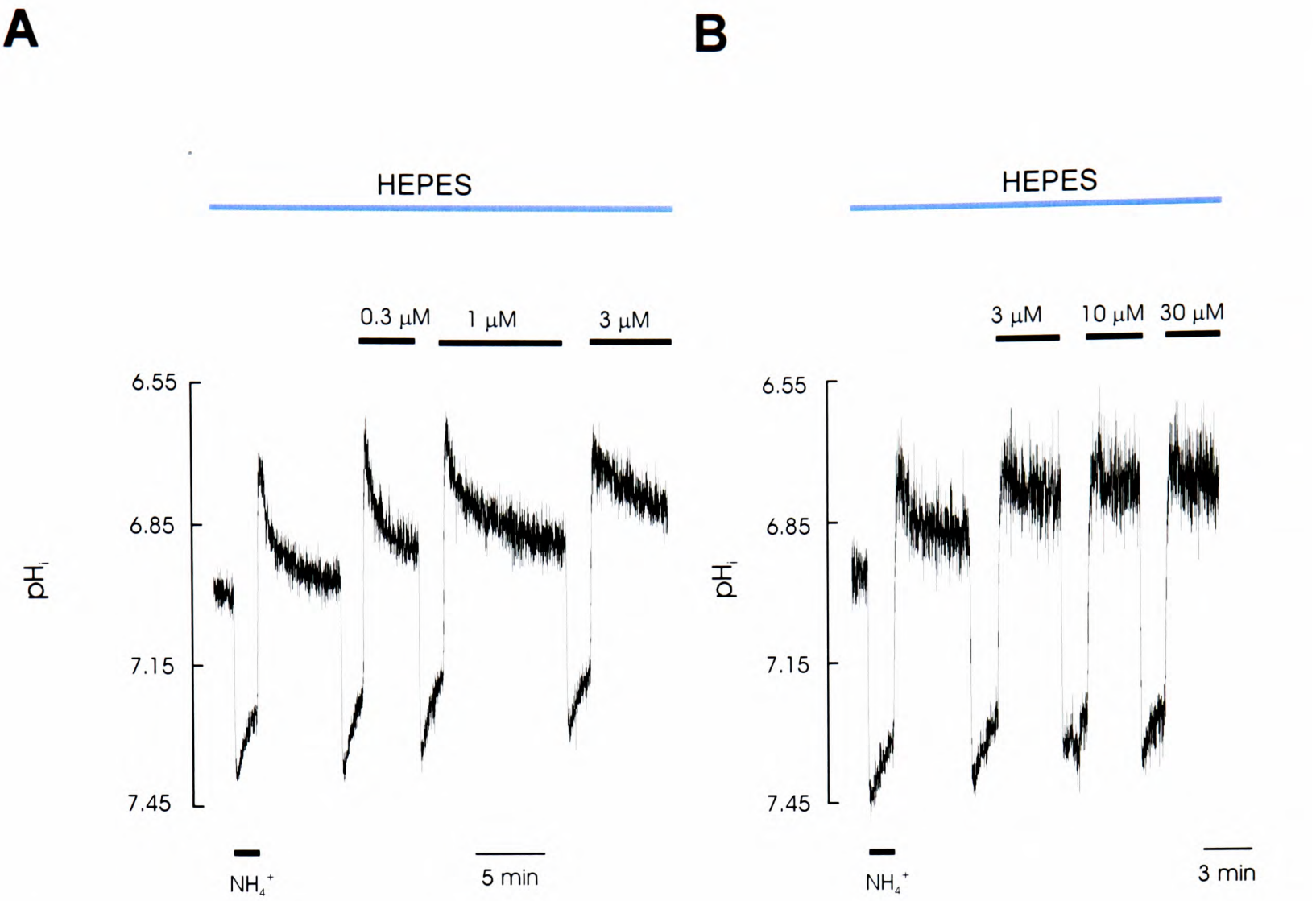


Figure Ai.1

A and ***B***, Experimental protocol showing effects of different doses of Hoe694 upon NHE activity, which was measured from pH_i recovery rate from acid load induced by 20 mM NH_4Cl pre-pulse. Note 30 μM Hoe694 almost completely inhibited the recovery. All experiment performed in HEPES-buffered solutions. ***C***, Normalised dose response curve plotted as a function of log_{10} [Hoe694 concentration], showing percentage inhibition of pH_i recovery measured at pH_i 6.96±0.03. Each point represents mean±S.E.M, with the sample n shown near to it. Curve drawn through points are best-fit Michaelis-Menten curves.

recovery rates were measured at pH_i = 6.96±0.03 (n = 4-6 for various Hoe694 concentrations, see **Fig Ai.1B**). The curve drawn through data points is the best-fit Michaelis-Menten curve (see Method), with a square of correlation coefficient (R^2) of 0.9821. The apparent K_i value, corresponding to 50% inhibition concentration, is 0.638 μM.

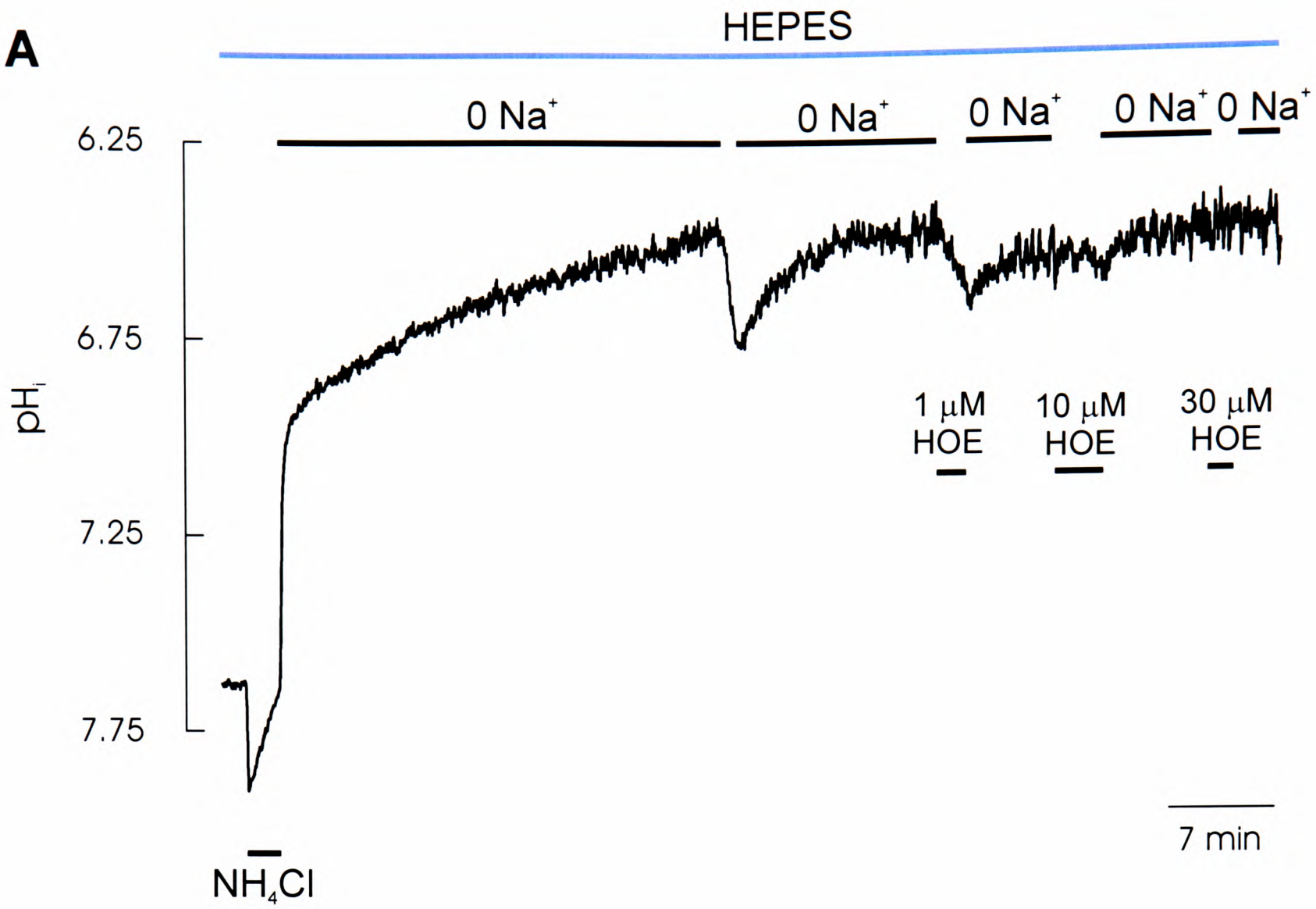
This apparent K_i, however, is not the real Michaelis inhibition constant, or "absolute K_i", for Hoe694. The value of absolute K_i is expected to be significantly smaller than apparent K_i because of the competition between Na^+_o and Hoe694 for binding to NHE (Counillon *et al.* 1993). Assuming a simple competition model between Na^+_o and Hoe694 for NHE, we have the following relationship (Cornish-Bowden, 1995b):

$$K_i^{app} = K_i^{abs} \times \left(1 + \frac{[Na^+]_o}{K_{0.5}^{Na}}\right) \qquad \textbf{[Eqn. Ai.1]}$$

Where K_i^{app} and K_i^{abs} are apparent and absolute K_i for Hoe694, respectively, $K^{Na}_{0.5}$ is the apparent Michaelis constant for extracellular Na^+.

Wilding, Chen & Roos (1992) reported that NHE in type I cells has a $K^{Na}_{0.5}$ of 58 mM. Taking normal $[Na^+]_o$ of 140 mM, the absolute K_i is determined to be 0.1871 μM according to **Equation Ai.1**.

As shown in **Fig Ai.1B**, 30 μM Hoe694 almost completely blocks NHE activity, with an percentage inhibition of over 98%. To further confirm this, the inhibitory effect of Hoe694 was examined in a different way in **Fig Ai.2**. Type I cells were perfused with



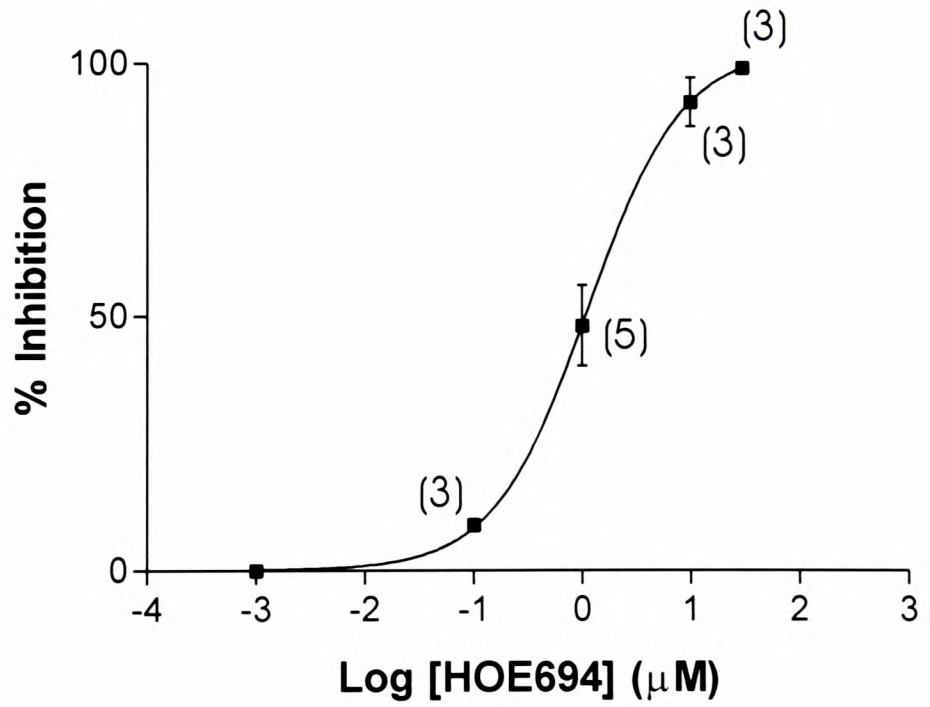


Figure Ai.2

A, Experimental protocol showing effects of different doses of Hoe694 upon NHE activity. Cells were given Na^+-free treatment after the initial acid load induced by 20 mM NH_4Cl, then the acid extrusion rates were measured when Na^+ was re-added in the superfusate, with different doses of Hoe694. All experiment performed in HEPES-buffered solutions. ***B***, Normalised dose response curve plotted as a function of $\log_{10}$ [Hoe694 concentration], showing percentage inhibition of pH_i recovery measured at $pH_i = 6.74 \pm 0.04$. Each point represents mean±S.E.M, with the sample n shown near to it. Curve drawn through points are best-fit Michaelis-Menten curves.

Na^+-free solution after the initial acid load, then Na^+_o was added back to the superfusate, causing immediate acid extrusion on NHE. By repetitive Na^+_o re-addition and removal, the acid extrusion was tested at different Hoe694 concentrations, from 0.1 μM to 30 μM. My result clearly proved that, the acid extrusion of NHE was completely abolished by 30 μM Hoe694 (n=3). In **Fig Ai.2A**, the acid extrusion recovery rates were measured at pH_i = 6.74±0.04 (n = 3-5 for various Hoe694 concentrations). Similar to **Fig Ai.1B**, a best-fit Michaelis-Menten curve was generated (see **Fig Ai.2B**). The apparent K_i value is 1.134 μM, not far from the value obtained in **Fig Ai.1B**.

Does NHE operate in reverse mode in when Na^+_o is removed?

In pH_o 7.9 HEPES-buffered solution, the removal of Na^+_o induced a sustained acid influx (**Fig Ai.3**). As explained in Chapter 3, this acid influx contains the background acid loading exposed by the inhibition of NHE due to lack of Na^+_o. But does it also include some acid influx due to reversed transport of NHE? When 50 μM Hoe694 was added to this Na^+-free solution, there was a small but significant reduction in the acid influx. The influx rate before and after adding Hoe694 was 1.05±0.25 mequiv l^{-1} min^{-1} and 0.55±0.16 mequiv l^{-1} min^{-1}, respectively ($P<0.05$, n=5 at pH_i = 7.37±0.10), indicating NHE probably operates as an *acid loader* in its reversed transport mode under Na^+_o-free conditions (see Discussion).

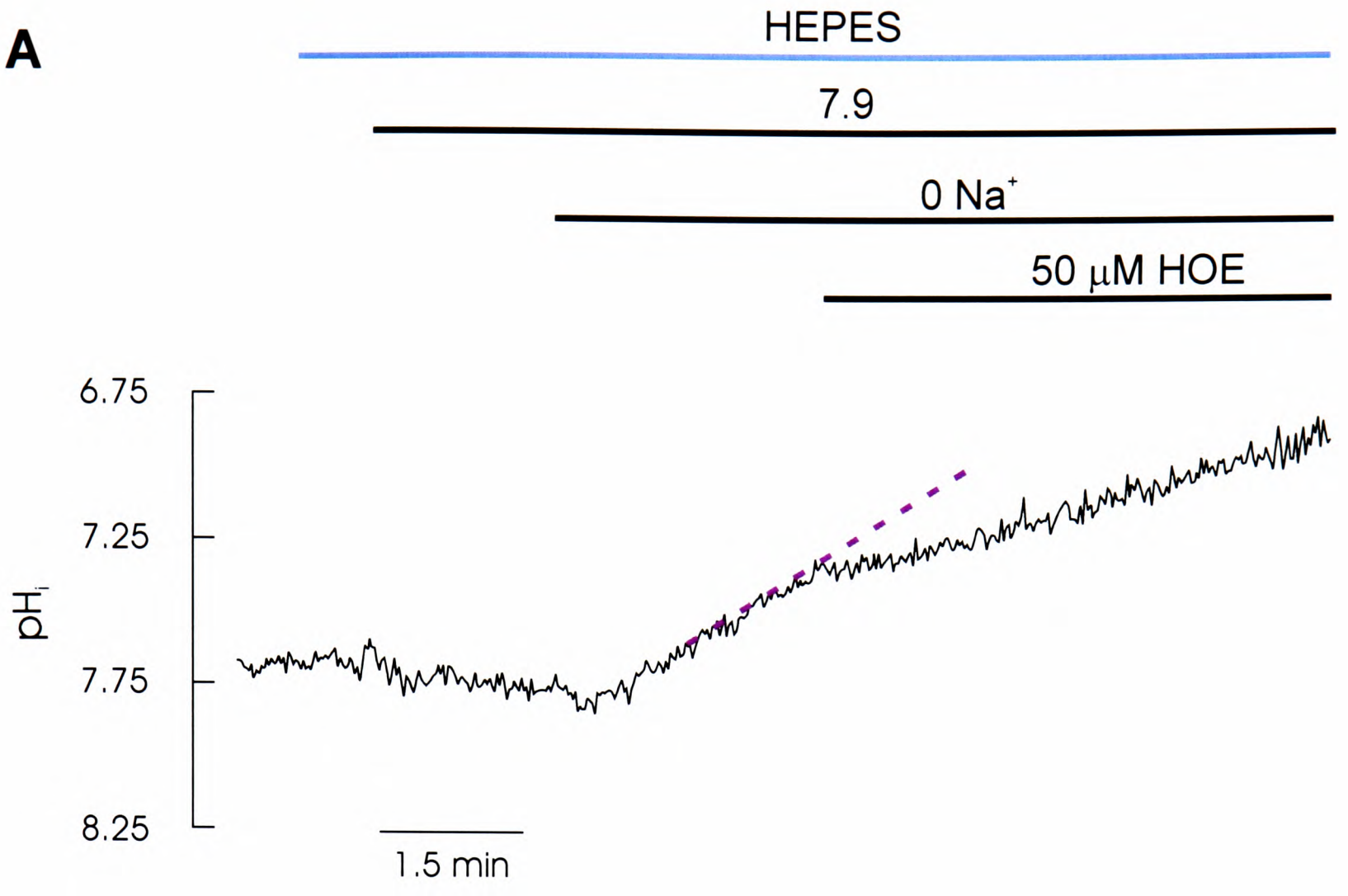


Figure Ai.3

A, Effect of Hoe694 on Na^+-free induced intracellular acidification. Cells were given Na^+-free treatments in pH_o 7.9 HEPES-buffered Tyrode solution, then 50 μM Hoe694 was added in the superfusate. The acid influx rates before and after the addition of Hoe694 were compared. Acid influx was decreased in the latter case. ***B***, Histogram shows mean acid influx rate measured at pH_i 7.41±0.05 using data from 5 experiments similar to that shown in ***A***. Columns represent mean±S.E.M. *significant difference, $P<0.05$.

Discussion

The evidence presented in **Fig Ai.1** and **Fig Ai.2** clearly demonstrate that nearly all NHE activity is blocked by 30 μM Hoe694. Therefore we can be sure that, by further raising Hoe694 concentration to 50 μM, no remaining NHE activity could be detected in the type I cell. This conclusion is important, since it guarantees that for all experiments requiring blockade of NHE, the concentration used (50 μM Hoe694) is enough to completely inhibit all NHE activity (see experiments in **Fig 3.10** and **Fig 3.11**, for example).

Counillon *et al.* (1993) expressed NHE isoforms NHE1-3 in mutant fibroblasts and measured their absolute K_i in extra-low $[Na^+]_o$ levels (100 μM). They estimated absolute K_i values of Hoe694 for NHE1, NHE2 and NHE3 as 0.16, 5 and 650 μM, respectively. Using a $K^{Na}_{0.5}$ value of 58 mM obtained in type I cells (Wilding, Chen & Roos, 1992), I calculate the absolute K_i as 0.1871 μM. This is very close to the value determined for NHE1 (0.16) by Counillon and colleagues. It is worth noting that, this $K^{Na}_{0.5}$ value of NHE (58 mM) is higher than those reported elsewhere. For example, in sheep Purkinje fibre, $K^{Na}_{0.5}$ of NHE is 13.7 mM (Wu & Vaughan-Jones, 1997). If the latter value is substituted in **Equation Ai.1**, the new estimated absolute K_i would be 0.057 μM. In either case, no matter which $K^{Na}_{0.5}$ is being used, the estimated absolute K_i values are within the same order of magnitude. So it can be concluded that the NHE1 is the predominant isoform in type I cells.

Appendix 1. Effect of Hoe694 on Na^+-H^+ Exchange

Results in **Fig Ai.3** suggest in Na^+-free conditions Na^+-H^+ exchange may operate in reverse mode mediating Na^+ efflux / H^+ influx. Although this is consistent with the prediction from thermodynamics, kinetically it might not happen in all cell types. In cardiomyocytes, for example, there is no statistical difference between the acid loading revealed by Na^+_o-free treatment and by 30 mM Hoe694, a dose blocking all NHE activity (Loh, 1998). In this study, I showed that at pH_o 7.9, about 50% of acid influx induced by Na^+_o-free treatment in HEPES-buffered solution is presumably due to the reverse transport of H^+ on NHE. It is arguable that the more alkaline pH environment (pH_o 7.9) in that experiment might enhance the acid loader activity of the transporter, so in normal pH_o 7.4 solution such a reverse transport might not be so large. In fact, my results in Chapter 3 show that the acid influx induced by Na^+_o-free and Hoe694 treatment are 1.15±0.27 at pH_i 7.29±0.02 and 0.79±0.05 at pH_i 7.17±0.07, respectively. This data indicate a small difference between the two acid influx rates at pH_o 7.4, although I was not able to compare acid influx rates at the same pH_i level. In any case, however, caution should be taken while using Na^+_o-free treatment as an alternative to inhibit NHE activity in type I cells (cf. **Fig 3.10**).

APPENDIX 2

Ca^{2+}_o-dependent Intracellular Acidosis Induced by High K^+_o in the Carotid Body Type I Cell

Introduction

In Chapter 3 it was concluded that an unidentified HCO_3^--independent and Cl^--independent mechanism is responsible for 20-30% of the total acid influx under physiological conditions. It was also suggested that the Ca^{2+}-H^+ exchange activity of Ca^{2+}-ATPase could be a possible candidate for that unknown mechanism (see Discussion of Chapter 3). Such an acid loading mechanism has been reported in snail neurones (Schwiening, Kennedy & Thomas, 1993), hippocampal neurones (Trapp, Lückermann, Kaila & Ballanyi, 1996), and cerebellar granule cells (Wu, Chen, Chen & Chu, 1999). A preliminary examination of this possible mechanism is summarised in this appendix. I observed a high K^+_o-induced intracellular acidification under CO_2/HCO_3^--free conditions. Such high K^+_o-induced acidification reduced by over 80% in the absence of Ca^{2+}_o, suggesting a similar mechanism of Ca^{2+}-H^+ exchange could be involved in type I cells.

Methods

General Methods

pH_i was recorded in isolated type I cells from the neonatal rats using carboxy-SNARF-1, as described in Chapter 2.

Solutions

All solutions used in this study were nominal CO_2/HCO_3 -free, HEPES-buffered solution. HEPES-buffered HCO_3 -free standard Tyrode solution was prepared as described in Chapter 2.

For Ca^{2+}-free solutions, $CaCl_2$ was omitted, and EGTA (ethylene glycol-bis(β-aminoethyl ether)-N,N,N',N'-tetraacetic acid) was added as the chelator for any residual Ca^{2+} ions. For solutions containing Hoe694, the drug was added immediately before use.

(1) Ca^{2+}-free HEPES-buffered Tyrode solution

Composition	Concentration (mM)
NaCl	140
KCl	4.5
$MgCl_2$	1
HEPES	20
Glucose	11
EGTA	1
Adjust pH with NaOH to 7.4 at 37 °C	

(2) Na^+-free HEPES-buffered solution

Composition	Concentration (mM)
NMDG	140
KCl	4.5
$MgCl_2$	1
$CaCl_2$	2.5
HEPES	20
Glucose	11
Adjust pH with HCl to 7.4 at 37 °C	

For Ca^{2+}-free solution, $CaCl_2$ was omitted, and 1 mM EGTA was added.

(3) Na^+-free high K^+ HEPES-buffered solution

Composition	Concentration (mM)
KCl	144.5
$MgCl_2$	1
$CaCl_2$	2.5
HEPES	20
Glucose	11
Adjust pH with HCl to 7.4 at 37 °C	

For Ca^{2+}-free solution, $CaCl_2$ was omitted, and 1 mM EGTA was added.

Drugs

Hoe694 (3-methylsulphonyl-4-piperidinobenzoyl guanidine methane-sulphonate) was used (see Methods in Chapter 3 for more information about Hoe694).

Results

High K^+_o-induced acid loading

All experiments in this appendix were carried out in HEPES-buffered solutions. **Fig Aii.1** demonstrates the pH_i response of carotid body type I cells when in response to high K^+ treatment. In this experiment, the acid influx rate in Na^+-free normal K^+ ($[K^+]_o$ 4.5 mM) and Na^+-free high K^+ ($[K^+]_o$ 144.5 mM) solutions was 3.54±0.79 mequiv l^{-1} min^{-1} and 0.58±0.08 mequiv l^{-1} min^{-1}, respectively, at pH_i 7.39±0.01. The high K^+_o treatment significantly increased the acid loading ($P<0.01$; $n=5$). All acid influx rates in this study were measured in the presence of 50 μM Hoe694 in order to inhibit possible acid uptake via reversed transport mode of Na^+-H^+ exchange (see Appendix 1).

Ca^{2+}_o dependency of High K^+_o-induced acid loading

Buckler and colleagues have shown that the application of high K^+_o (30–50 mM) evoked rapid rise in $[Ca^{2+}]_i$ in type I cells, with a maximal $[Ca^{2+}]_i$ elevation of 800-900 nM (Buckler & Vaughan-Jones 1994b; Dasso, Buckler & Vaughan-Jones, 1997). They concluded that this $[Ca^{2+}]_i$ elevation is due to Ca^{2+} influx via voltage-gated Ca^{2+} channel activated by membrane depolarisation. To examine whether the high K^+_o-induced acidification is also dependent on extracellular Ca^{2+} (Ca^{2+}_o), a similar experiment to that shown in **Fig Aii.1A** was repeated in Ca^{2+}–free conditions (**Fig Aii.2A**). In the absence of Ca^{2+}_o, no difference in acid influx rates can be found between Na^+-free normal K^+ (1.01±0.26 mequiv l^{-1} min^{-1}) and Na^+-free high K^+

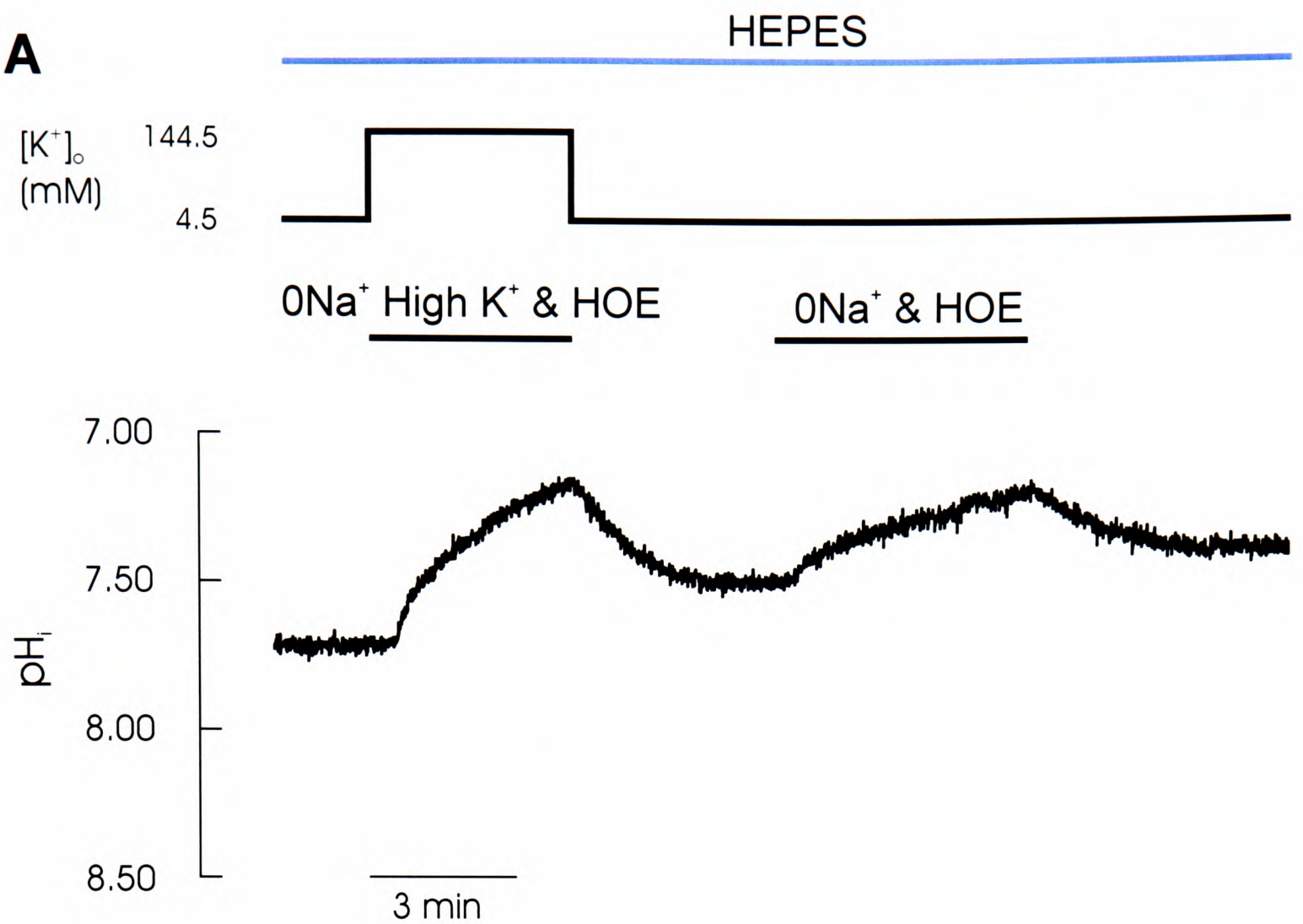


Figure Aii.1

A, Effect of high K^+ treatment upon acid influx in HEPES-buffered solution. Cells were given Na^+-free high K^+ and Na^+-free normal K^+ treatments in HEPES-buffered Tyrode solution (both containing normal Ca^{2+} and 50 μM Hoe694). The acid influx rate was decreased by 80% in the latter case. ***B***, Histogram shows mean acid influx rate measured at pH_i 7.39±0.01 using data from 5 experiments similar to that shown in ***A***. Columns represent mean±S.E.M. **significant difference, $P<0.01$.

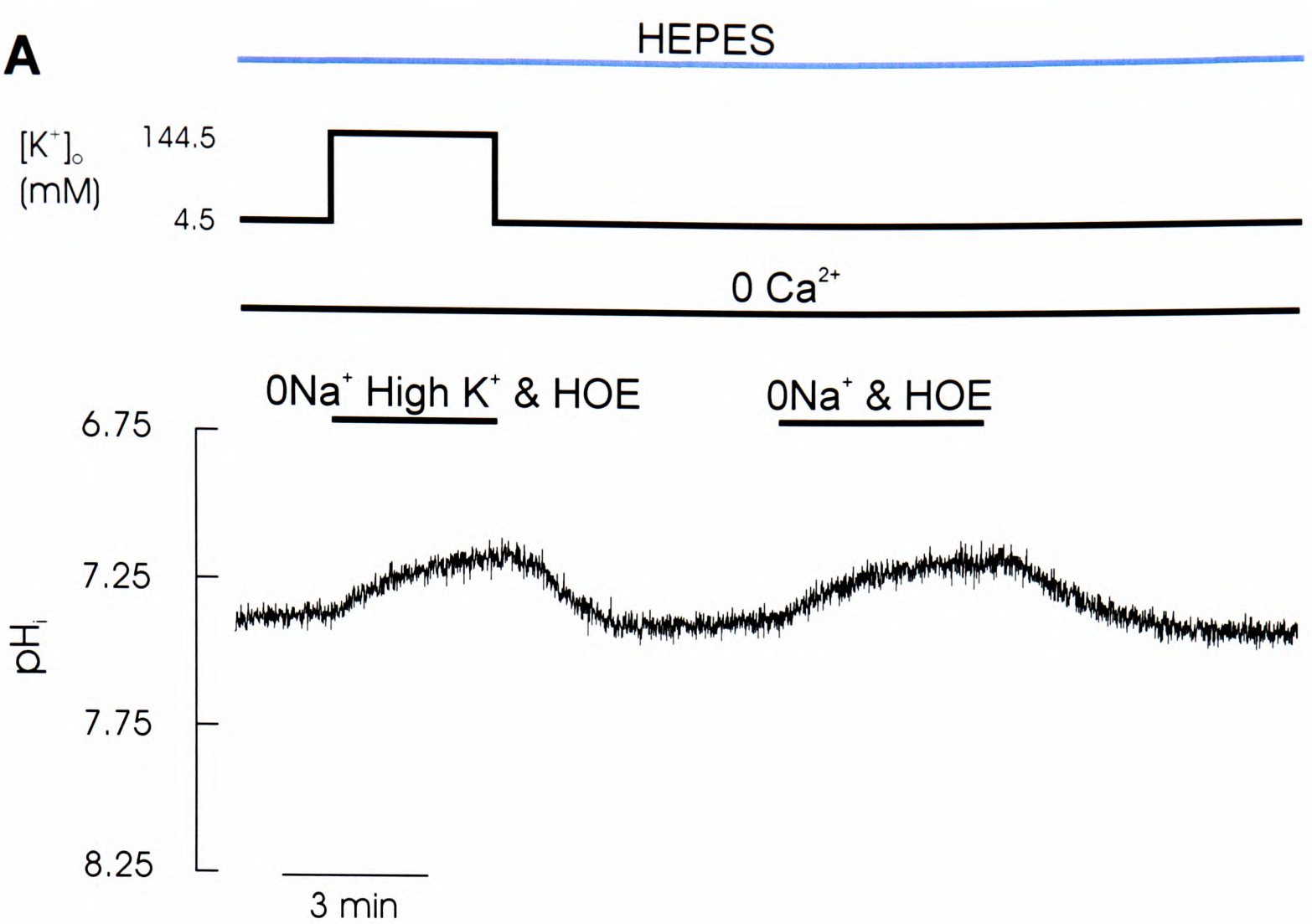


Figure Aii.2

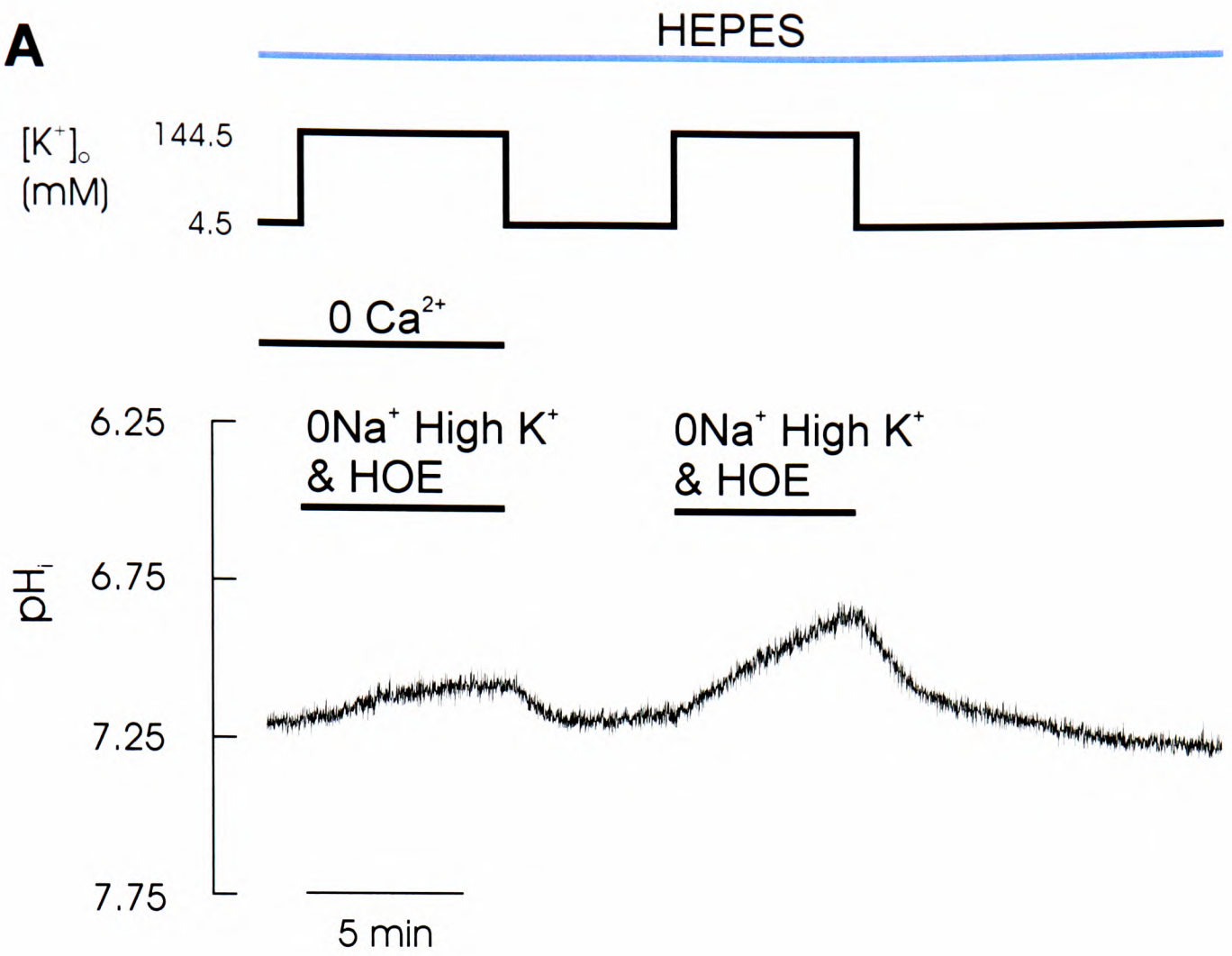
A, Effect of high K^+ treatment upon acid influx in Ca^{2+}-free HEPES-buffered solution. Cells were given Na^+-free high K^+ and Na^+-free normal K^+ treatments in Ca^{2+}-free HEPES-buffered Tyrode solution (both containing 50 μM Hoe694). The acid influx rates were the same. ***B***, Histogram shows mean acid influx rate measured at pH_i 7.23±0.17 using data from 5 experiments similar to that shown in ***A***. Columns represent mean±S.E.M.

(1.07±0.04 mequiv l^{-1} min^{-1}) treatments ($P>0.5$; $n=5$ at pH_i 7.23±0.17). Since the $[Ca^{2+}]_i$ elevation evoked by high K^+_o was abolished in Ca^{2+}–free solution, as reported by Buckler & Vaughan-Jones (1994b), this result indicates that there is a link between high K^+_o-induced acidification and $[Ca^{2+}]_i$ elevation.

To further confirm the Ca^{2+}_o dependency of high K^+_o-induced acidification, the acid loading rates during high K^+_o treatment in the absence and presence of Ca^{2+}_o were compared in **Fig Aii.3**. The result showed the acid influx in normal Ca^{2+} ($[Ca^{2+}]_o$ 2.5 mM) solution is significantly faster than that in Ca^{2+}-free solution, with influx rates of 2.85±0.60 mequiv l^{-1} min^{-1} and 0.50±0.09 mequiv l^{-1} min^{-1}, respectively ($P<0.05$; $n=4$ at pH_i 7.29±0.13). Similar decrease in acid influx can also be achieved by removing all Ca^{2+}_o from the superfusate during high K^+_o treatment. The fast acid influx seen in normal Ca^{2+} solution was abruptly reduced to about 20% of the original value as soon as Ca^{2+}_o was removed (data not shown).

Discussion

A high K^+_o-induced intracellular acidification was observed in type I cells perfused with HEPES-buffered solution. My results showed this pH_i response requires Ca^{2+}_o since it was abolished under Ca^{2+}_o-free conditions. Taking into account of the voltage-dependent Ca^{2+} influx evoked by membrane depolarisation, which was reported in previous studies by Buckler *et al.* (1994b), the present data suggest the high K^+_o-induced acid influx is simultaneously accompanied with Ca^{2+} influx and $[Ca^{2+}]_i$ elevation.



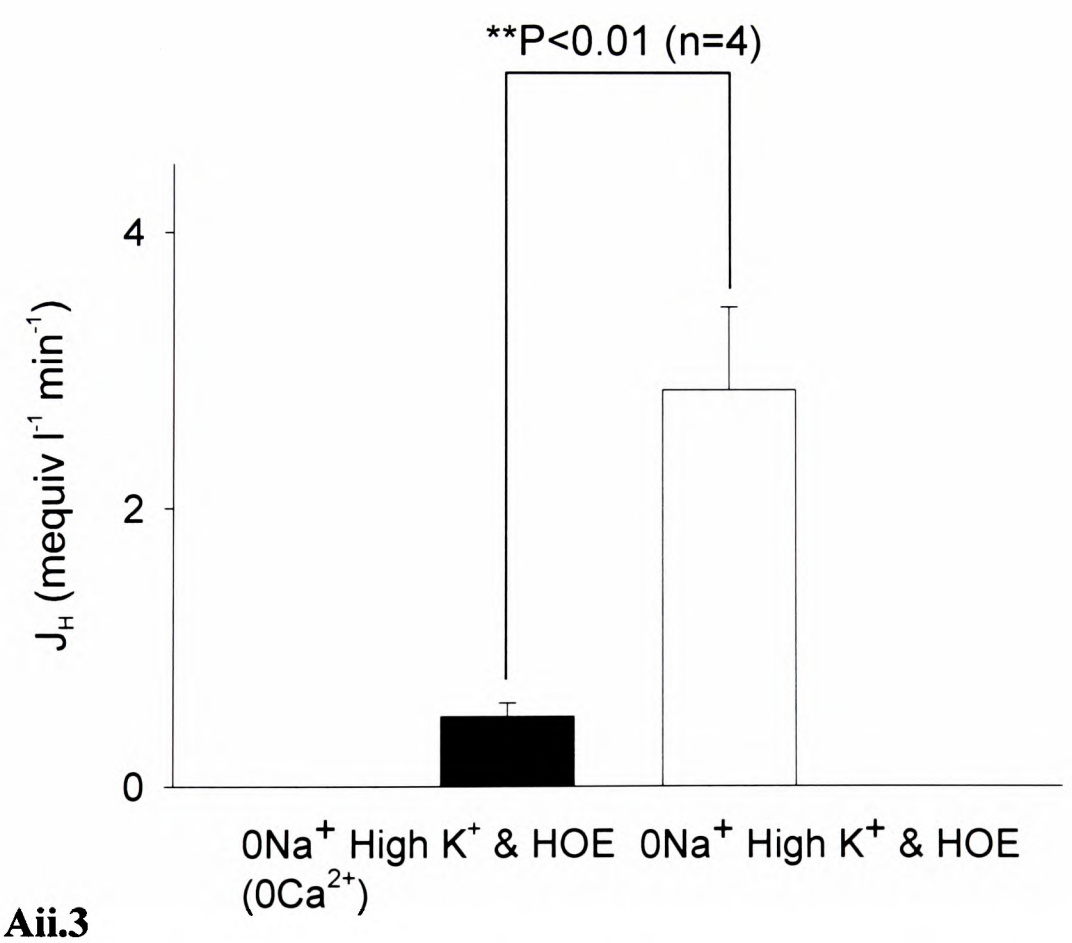


Figure Aii.3

A, Effect of Ca^{2+}_o upon acid influx in high K^+ HEPES-buffered solution. Cells were given Na^+-free high K^+ treatment in the absence and presence of Ca^{2+} in HEPES-buffered Tyrode solution (both containing 50 μM Hoe694). The acid influx rate during the former treatment was only 20% of the latter. ***B***, Histogram shows mean acid influx rate measured at pH_i 7.29±0.13 using data from 4 experiments similar to that shown in ***A***. Columns represent mean±S.E.M. *significant difference, $P<0.05$.

Appendix 2. High K^+- induced acidification

The above results are in agreement with similar observations of high K^+_o (membrane depolarisation)-induced intracellular acidification reported in hippocampal neurones (Trapp *et al.* 1996) and cerebellar granule cells (Wu *et al.* 1999), in which it has been proved to be caused by plasmalemmal Ca^{2+}-ATPase transporting H^+_o into the cell as Ca^{2+}_i is pumped out. The purpose of the activation of Ca^{2+}-ATPase in response to high K^+_o treatment is to rapidly remove excess Ca^{2+}_i generated by Ca^{2+} influx. The stoichiometry of such a Ca^{2+}-H^+ exchange has been determined to be electroneutral with a Ca^{2+} : H^+ coupling ratio of 1:2 (Niggli, Sigel & Carafoli, 1982).

In carotid body type I cells, acidic stimuli also causes membrane depolarisation, leading to Ca^{2+} influx and $[Ca^{2+}]_i$ elevation (Buckler *et al.* 1994b). Buckler and Vaughan-Jones (1993) showed that an isocapnic acidosis of pH_o 7.0 induced an increase of $[Ca^{2+}]_i$ around 200 nM. Therefore, it is expected that plasmalemmal Ca^{2+}-ATPase may also play an important role in $[Ca^{2+}]_i$ regulation in response to acidic stimuli in type I cells. Furthermore, as demonstrated in snail neurones (Schwiening *et al.* 1993) and platelets (Valant & Haynes, 1993), plasmalemmal Ca^{2+}-ATPase (hence Ca^{2+}-H^+ exchange) activity is raised in acidic pH_o, allowing it to mediate *more* acid influx when removing excess Ca^{2+}_i. This would result in a secondary acid influx due to the activity of Ca^{2+}-H^+ exchange. If such a mechanism also exists in the type I cell, it could serve as a candidate for the unidentified HCO_3^--independent and Cl^--independent acid influx pathway, which is also enhanced by H^+_o (see Chapter 3). It would be of interest to further investigate this possibility.

Appendix 2. High K^+- induced acidification

In addition to plasmalemmal Ca^{2+}-ATPase, the excess $Ca^{2+}{}_i$ could also be removed from cytosol by endoplasmic reticulum (ER) Ca^{2+}-ATPase, which uptakes $Ca^{2+}{}_i$ into intracellular calcium stores in ER. In fact, Vicario *et al.* showed ER Ca^{2+}-ATPase in type I cells contributes to maintain the resting $[Ca^{2+}]_i$ in neonatal rabbit type I cells (Vicario, Obeso, Rocher, López-López & González, 2000). Since the sarcoplasmic reticulum (SR, a subcellular structure similar to ER in skeletal muscle cells) Ca^{2+}-ATPase also mediates Ca^{2+}-H^+ exchange (Madeira, 1978; Levy, Seigneuret, Bluzat & Rigaud, 1990), ER Ca^{2+}-ATPase in type I cells may as well involve in the high $K^+{}_o$-induced intracellular acidification.

My results also demonstrated that, in Na^+-free normal K^+ solution containing 50μM Hoe694, there is no $Ca^{2+}{}_o$-dependent acid influx (see **Fig Aii.1** and **Fig Aii.2**). The slow acid influx under this condition (around 0.5-1 mequiv l^{-1} min^{-1}) is regarded as the unmasked background acid loading (see Chapter 3 and Appendix 1). It should be noted that although Na^+-free treatment does induce Ca^{2+} influx via reversed mode of Na^+-Ca^{2+} exchange in some cell types such as cardiomyocytes (Allen, Eisner, Lab & Orchard, 1983), however, Buckler *et al.* (1994b) found the same treatment failed to produce any significant increase in $[Ca^{2+}]_i$ in type I cells. Their observation is in agreement with the lack of increase in Ca^{2+}-H^+ exchange activity (hence lack of increased acid influx) during Na^+-free treatment shown in the present study.

It should be noticed that, when $Ca^{2+}{}_o$ was removed, the acid influx rates in both Na^+-free normal K^+ and Na^+-free high K^+ solutions were the same. In the absence of $Ca^{2+}{}_o$, high K^+ treatment had no effect on acid loading (**Fig Aii.2**). This suggests that H^+ channels make no contribution to acid influx at the resting pH_i (7.2-7.4) and normal

pH_o (7.4) being examined (cf. Chapter 3), since the equilibrium potential for H^+ (E_H) is -12 mV under this condition, H^+ channels would be expected to mediate acid efflux during high K^+_o-induced membrane depolarisation.

References

1. Abuladze, N., Lee, I., Newman, D., Hwang, J., Boorer, K., Pushkin, K. & Kurtz, I. (1998). Molecular cloning, chromosomal localization, tissue distribution, and functional expression of the human pancreatic sodium bicarbonate cotransporter. *Journal of Biological Chemistry* **273**: 17689-17695.

2. Acker, H., Dufau, E., Huber, J. & Sylvester, D. (1989). Indications to an NADPH oxidase as a possible P_{O2} sensor in the rat carotid body. *FEBS Letters* **256**: 75-78.

3. Adams, W. E. (1958). *The Comparative Morphology of Carotid Sinus*. Charles C. Thomas Publisher, Springfield, Illinois.

4. Aickin, C. C. (1994). Regulation of intracellular pH in the smooth muscle of guinea-pig ureter: HCO_3^- dependence. *Journal of Physiology* **479**: 317-329.

5. Aickin, C. C. & Brading, A. F. (1984). The role of chloride-bicarbonate exchange in the regulation of intracellular chloride in guinea-pig vas deferens. *Journal of Physiology* **349**: 587-606.

6. Aickin, C. C. & Thomas, R. C. (1977). An investigation of the ionic mechanism of intracellular pH regulation in mouse soleus muscle fibres. *Journal of Physiology* **273**: 295-316.

7. Al-Hashem, F., Barbe, C. & Kumar, P. (2001). Interaction of ATP and CO_2 upon carotid body chemosensitivity *in vitro*. *Journal of Physiology* **536**: 142P.

8. Allen, D. G., Eisner, D. A., Lab, M. J. & Orchard, C. H. (1983). The effects of low sodium solutions on intracellular calcium concentration and tension in ferret ventricular muscle. *Journal of Physiology* **345**: 391-407.

9. Alper, S. L., Kopito, R. R., Libresco, S. M. & Lodish, H. F. (1988). Cloning and characterization of a murine band 3-related cDNA from kidney and from a lymphoid cell line. *Journal of Biology Chemistry* **263**: 17092-17099.

10. Alper, S. L. (1991). The band 3-related anion exchanger (AE) gene family. *Annual Review of Physiology* **53**:549-64.

11. Alper, S. L., Darman, R. B., Chernova, M. N., Dahl, N. K. (2002). The AE gene family of Cl^-/HCO_3^- exchangers. *Journal of Nephrology* **15**: S41-S53.

12. Amlal, H., Burnham, C. E. & Soleimani, M. (1999). Characterization of Na^+/HCO_3 cotransporter isoform NBC-3. *American Journal of Physiology* **276**: F903-F913.

13. Anichcov, S. V. & Belenk'ii, M. L. (1963). *Pharmacology of the Carotid Body Chemoreceptors*. Macmillan Publishing, New York.

14. Aronson, P. (1985). Kinetic properties of the plasma membrane Na^+/H^+ exchanger. *Annual Review of Physiology* **47**: 545-560.

15. Aronson, P. S., Nee, J. & Suhm M. A. (1982). Modifier role of internal H^+ in activating the Na^+-H^+ exchanger in renal microvillus membrane vesicles. *Nature* **299**: 161-163.

16. Aronson, P. S., Suhm M. A. & Nee, J. (1983). Interaction of external H^+ with the Na^+-H^- exchanger in renal microvillus membrane vesicles. *Journal of Biological Chemistry* **258**: 6767-6771.

17. Baird, N. R., Orlowski, J., Szabo, E. Z., Zaun, H. C., Schultheis, P. J., Menon, A. G., Shull, G. E. (1999). Molecular cloning, genomic organization, and functional expression of Na^+/H^+ exchanger isoform 5 (NHE5) from human brain. *Journal of Biological Chemistry* **274**: 4377-4382.

18. Bahar, S., Gunter, C. T., Wu, C., Kennedy, S. D. & Knauf, P. A. (1999). Persistence of external chloride and DIDS binding after chemical modification of Glu-681 in human band 3. *American Journal of Physiology* **277**: C791-C799.

19. Ballantyne, D. & Scheid, P. (2000). Mammalian brainstem chemosensitive neurons: linking them to respiration *in vitro*. *Journal of Physiology* **525**: 567-577.

20. Bánfi, B., Maturana, A., Jaconi, S., Arnaudeau, S., Laforge, T., Sinha, B., Ligeti, E., Demaurex, N., Krause, K.-H. (2000). A mammalian H^+ channel generated through alternative splicing of the NADPH oxidase homolog NOH-1. *Science* **287**: 138-142.

21. Barbé, C., Al-Hashem, F., Conway, A. F., Dubuis, E., Vandier, C. & Kumar, P. (2002). A possible dual site of action for carbon monoxide-mediated chemoexcitation in the rat carotid body. *Journal of Physiology* **543**: 933–945.

22. Barish, M. E. & Baud, C. (1984). A voltage-gated hydrogen ion current in the oocyte membrane of the axolotl, *Ambystoma*. *Journal of Physiology* **352**: 243-63.

23. Bartel, D., Lepke, S., Layh-Schmitt, G., Legrum, B. & Passow H. (1989). Anion transport in oocytes of *Xenopus laevis* induced by expression of mouse erythroid band 3 protein-encoding cRNA and of a cRNA derivative obtained by site-directed mutagenesis at the stilbene disulfonate binding site. *EMBO Journal* **8**: 3601-3609.

24. Bevensee, M. O., Apkon, M. & Boron, W. F., (1997). Intracellular pH regulation in cultured astrocytes from rat hippocampus. II. Electrogenic Na/HCO_3 cotransport. *Journal of General Physiology* **110**: 467-83.

25. Bianchi, A. L., Denavit-Saubie, M. & Champagnat, J. (1995). Central control of breathing in mammals: neuronal circuitry, membrane properties, and neurotransmitters. *Physiological Reviews* **75**: 1-45.

26. Biscoe, T. J., Duchen, M. R., Eisner, D. A., O'Neill, S. C. & Valdeolmillos, M. (1989). Measurements of intracellular Ca^{2+} in dissociated type I cells of the rabbit carotid body. *Journal of Physiology* **416**: 421-434.

27. Biscoe, T. J., Lall, A. & Sampson, S. R. (1970). Electron microscopic and electrophysiological studies on the carotid body following intracranial section of the glossopharyngeal nerve. *Journal of Physiology* **208**: 133-152.

28. Biscoe, T. J., Purves, M. J. & Sampson, S. R. (1970). The frequency of nerve impulses in single carotid body chemoreceptor afferent fibres recorded *in vivo* with intact circulation. *Journal of Physiology* **208**: 121-131.

29. Bissig, M., Hagenbuch, B., Stieger, B., Koller, T. & Meier, P. J. (1994). Functional expression cloning of the canalicular sulfate transport system of rat hepatocytes. *Journal of Biological Chemistry* **269**: 3017-3021.

30. Bland, M. (2000). *An Introduction to Medical Statistics*, 3rd edn., pp. 185-209. Oxford University Press, Oxford, UK.

31. Bock, P. (1980). Adenine nucleotides in the carotid body. *Cell Tissue Research* **206**: 279–290.

32. Bonanno J. A. (1991). Two distinct HCO_3^--dependent H^+ efflux pathways in human vascular endothelial cells. *American Journal of Physiology* **277**: H28-H32.

33. Boron, W. F. (1985). Intracellular pH-regulating mechanism of the squid axon: relation between the external Na^+ and HCO_3^- dependences. *Journal of General Physiology* **85**: 325-345.

34. Boron, W. F. & Boulpaep, E. L. (1983). Intracellular pH regulation in the renal proximal tubule of the salamander. Basolateral HCO_3^- transport. *Journal of General Physiology* **81**: 53-94.

35. Boron, W. F. & Boulpaep, E. L. (1989). The electrogenic Na/HCO_3 cotransporter. *Kidney International* **36**: 392-402.

36. Boron, W. F. & Knakal, R. C. (1992). Na^+-dependent Cl^--HCO_3^- exchange in the squid axon. Dependence on extracellular pH. *Journal of General Physiology* **99**: 817-837.

37. Bowman, E. J., Tenney, K. & Bowman, B. J. (1988). Isolation of genes encoding the *Neurospora* vacuolar ATPase. *Journal of Biological Chemistry* **263**: 13994–14001.

38. Boyarsky, G., Ransom, B. Schlue, W. R., Davis, M. B. E. & Boron, W. F. (1993). Intracellular pH regulation in single cultured astrocytes from rat forebrain. *Glia* **8**: 241-248.

39. Brett, C. L., Wei, Y., Donowitz, M. & Rao, R. (2002). Human Na^+/H^+ exchanger isoform 6 is found in recycling endosomes of cells, not in mitochondria. *American Journal of Physiology* **282**: C1031-C1041.

40. Brown, D., Gluck, S. & Hartwig, J. (1987). Structure of the novel membrane-coating material in proton-secreting epithelial cells and identification as an H^+ ATPase. *Journal of Cell Biology* **105**: 1637–1648.

41. Buckler, K. J. (1997). A novel oxygen-sensitive potassium current in rat carotid body type I cells. *Journal of Physiology* **498**: 649-662

42. Buckler, K. J. (1998). Oxygen sensing in arterial chemoreceptors: role of a novel oxygen-dependent potassium channel. In *Oxygen Regulation of Ion Channels and Gene Expression*, ed. López-Barneo & Weir, E. K., pp. 145-155. Futura Publishing Company, Armonk, New York, USA.

43. Buckler, K. J., Nye, P. C. G., Peers, C. & Vaughan-Jones, R. D. (1990). Effects of simulated respiratory and metabolic acidosis/alkalosis on pH_i in isolated type-I carotid body cells from neonatal rat. *Journal of Physiology* **426**: 66P.

44. Buckler, K. J. & Vaughan-Jones, R. D. (1990). Application of a new pH-sensitive fluoroprobe (carboxyl-SNARF-1) for intracellular pH-measurement in small isolated cells. *Pflügers Archiv* **412**: 234-239.

45. Buckler, K. J. & Vaughan-Jones, R. D. (1993). Effects of acidic stimuli on intracellular calcium in isolated type I cells of the neonatal rat carotid body. *Pflügers Archiv* **425**: 22-27.

46. Buckler, K. J. & Vaughan-Jones, R. D. (1994a). Effects of hypoxia on membrane potential and intracellular calcium in rat carotid body type I cells. *Journal of Physiology* **476**: 423-428.

47. Buckler, K. J. & Vaughan-Jones, R. D. (1994b). Effects of hypercapnia on membrane potential and intracellular calcium in rat carotid body type I cells. *Journal of Physiology* **487**: 157-171.

48. Buckler, K. J. & Vaughan-Jones, R. D. (1994c). Role of intracellular pH and $[Ca^{2+}]_i$ in acid chemoreception in type-I cells of the carotid body. In *Arterial Chemoreceptors: Cell to System*, ed. O'Regan, R. *et al.*, pp. 41-54. Plenum Press, New York, USA.

49. Buckler, K. J. & Vaughan-Jones, R. D. (1998). Effects of mitochondrial uncouplers on intracellular calcium, pH and membrane potential in rat carotid body type I cells. *Journal of Physiology* **513**: 819-833.

50. Buckler, K. J., Vaughan-Jones, R. D., Peers, C., Lagadic-Gossmann, D. & Nye, P. C. G. (1991a). Effects of extracellular pH, P_{CO2} and HCO_3 on intracellular pH in isolated type I cells of the neonatal rat carotid body. *Journal of Physiology* **444**: 703-721.

51. Buckler, K. J., Vaughan-Jones, R. D., Peers, C. & Nye, P. C. G (1991b). Intracellular pH and its regulation in isolated type I carotid body cells of the neonatal rat. *Journal of Physiology* **436**: 107-129.

52. Buckler K. J., Williams, B. A. & Honoré, E. (2000) An oxygen-, acid- and anaesthetic-sensitive TASK-like background potassium channel in rat arterial chemoreceptor cells. *Journal of Physiology* **525**: 135–142.

53. Burton, R. F. (1975). *Ringer Solutions and Physiological Salines*. pp. 43-54. John Wright & Sons, Bristol, UK.

54. Cabantchik, Z. I. & Greger, R. (1992). Chemical probes for anion transporters of mammalian cell membranes. *American Journal of Physiology* **262**: C803-C827.

55. Cabantchik, Z. I. & Rothstein A. (1972). The nature of the membrane sites controlling anion permeability of human red blood cells as determined by studies with disulfonic stilbene derivatives. *Journal of Membrane Biology* **10**: 311-330.

56. Cabantchik, Z. I. & Rothstein, A. (1974). Membrane proteins related to anion permeability of human red blood cells. I. Localization of disulfonic stilbene binding sites in proteins involved in permeation. *Journal of Membrane Biology* **15**: 207-226.

57. Camilion de Hurtado, M. C., Perez, N. G. & Cingolani, H. E. (1995). An electrogenic sodium-bicarbonate cotransport in the regulation of myocardial intracellular pH. *Journal of Molecular and Cellular Cardiology* **27**: 231-242.

58. Carpenter, E. & Peers, C. (1997). Swelling- and cAMP- activated Cl^- currents in isolated rat carotid body type I cells. *Journal of Physiology* **503**: 497-511.

59. Chatterjee, D., Chakraborty, M., Leit, M., Neff, L., Jamsakellokumpu, S., Fuchs, R. & Baron, R. (1992). Sensitivity to vanadate and isoforms of subunit-a and subunit-b distinguish the osteoclast proton pump from other vacuolar H^+ ATPases. *Proceedings of the National Academy of Science USA* **89**: 6257–6261.

60. Chernova, M. N., Jiang, L., Shmukler, B. E., Schweinfest, C. W., Blanco, P., Freedman, S. D., Stewart, A. K. & Alper, S. L. (2003). Acute regulation of the SLC26A3 congenital chloride diarrhoea anion exchanger (DRA) expressed in *Xenopus* oocytes. *Journal of Physiology* **549**: 3-19.

61. Cherny, V. V. & DeCoursey, T. E. (1999). pH-dependent inhibition of voltage-gated H^+ currents in rat alveolar epithelial cells by Zn^{2+} and other divalent cations. *Journal of General Physiology* **114**: 819–838.

62. Chesler, M. & Kaila, K. (1992). Modulation of pH by neuronal activity. *Trends in Neurosciences* **15**: 396-402.

63. Chiocchio, S. R., Biscardi, A. M. & Tramezzani, J. H. (1966). Catecholamines in the carotid body of the cat. *Nature* **212**: 834-835.

64. Chiocchio, S. R., Biscardi, A. M. & Tramezzani, J. H. (1967). 5-Hydroxytrptamine in the carotid body of the cat. *Science* **158**: 790-791.

65. Chitravanshi, V. C., Kachroo, A. & Sapru, H. N. (1994). A midline area in the nucleus commissuralis of NTS mediates the phrenic nerve responses to carotid chemoreceptor stimulation. *Brain Research* **662**: 127-133.

66. Choi, I., Aalkjaer, C., Boulpaep, E. L. & Boron, W. F. (2000). An electroneutral sodium/bicarbonate cotransporter NBCn1 and associated sodium channel. *Nature* **405**: 571-575.

67. Choi, I., Romero, M. F., Khandoudi, N., Bril, A. & Boron, W. F. (1999). Cloning and characterization of a human electrogenic Na^+-HCO^-_3 cotransporter isoform (hhNBC). *American Journal of Physiology* **276**: C576-C584.

68. Cidon, S. & Nelson, N. (1983). A novel ATPase in the chromaffin granule membrane. *Journal of Biological Chemistry* **258**: 2892–2898.

69. Collins, J. F., Honda, T., Knobel, S., Bulus, N. M., Conary, J., DuBois, R. & Ghishan, F. K. (1993). Molecular cloning, sequencing, tissue distribution, and functional expression of a Na^+/H^+ exchanger (NHE-2*). Proceeding of National Academy Science of the USA* **90**: 3938-3942.

70. Cornish-Bowden, A. (1995a). *Analysis of Enzyme Kinetic Data*, pp. 3-36. Oxford University Press, Oxford, UK.

71. Cornish-Bowden, A. (1995b). *Fundamentals of Enzyme Kinetics*, 2nd edn, pp. 94-128. Portland Press, London, UK.

72. Comroe, J. H. (1939). The location and function of the chemoreceptors of the aorta. *American Journal of Physiology* **127**: 176-191.

73. Cougnon, M., Planelles, G., Crowson, M. S., Shull, G. E., Rossier, B. C. & Jaisser, F. (1996). The rat distal colon P-ATPase subunit encodes a ouabain-sensitive H^+,K^+-ATPase. *Journal of Biological Chemistry* **271**: 7277-7280.

74. Counillon, L. & Pouyssegur, J. (2000). The expanding family of eucaryotic Na^+/H^+ exchangers. *Journal of Biological Chemistry* **275**: 1-4.

75. Counillon, L., Scholz, W., Lang, H.-J. & Pouyssengur, J. (1993). Pharmacological characterization of stably transfected Na^+/H^+ antiporter isoforms using amiloride analogs and a new inhibitor exhibiting anti-ischemic properties. *Molecular Pharmacology* **44**: 1041-4045.

76. Cuello, A. C. & McQueen, D. S. (1980). Substance P: a carotid body peptide. *Neuroscience Letters* **17**: 215-219.

77. Cunningham, D. J. C., Robbins, P. A. & Wolff, C. B. (1986). Integration of respiratory response to changes in alveolar partial pressures of CO_2 and O_2 and arterial pH. In *Hand Book of Physiology,* Sec. III, *The Respiratory System,* Vol. 2, *Control of Breathing,* ed. Cherniack, N. S. & Widdicombe, J. G., pp. 475-528. American Physiological Society, Bethesda, Maryland, USA.

78. Dart, C. & Vaughan-Jones, R. D. (1992). Na^+-HCO_3^- symport in the sheep cardiac Purkinje fibre. *Journal of Physiology* **451**: 365-385.

79. Dasso, L. T., Buckler, K. J. & Vaughan-Jones, R. D. (1997). Muscarinic and nicotinic receptors raise intracellular Ca^{2+} levels in rat carotid body type I cells. *Journal of Physiology* **498**: 327-338.

80. Davies, R. O. & Edwards, M. W. Jr. (1975). Medullary relay neurons in the carotid-body chemoreceptor pathway of cats. *Resapiration Physiology* **24**:69-79.

81. De Castro, F. (1926). Sur la structure et l'innervation de la glande intercarotidienne (glomus caroticum) de l'homme et des mammifères, et sur un nouveau système d'innervation autonome du nerf glossopharyngien. Ètudes anatomiques et experimentales. *Trabajos del Labpratorio de Investigaciones Biologicas de la Univerrsidad de Madrid* **24**: 365-432.

82. De Castro, F. (1928). Sur la structure et l'innervation du sinus carotidien de l'homme et des mammifères. Nouveaux faits sur l'innervation et la fonction du glomus caroticum. Études anatomiques et physiologiques. *Trabajos del Labpratorio de Investigaciones Biologicas de la Univerrsidad de Madrid* **25**: 331-380.

83. De Castro, F. (1951). Sur la structure de la synapse dans les chemorecepteurs: leur mechanisme d'excitation et role dans la circulation sanguine locale. *Acta Physiologica Scandinavica* **22**: 14-43.

84. DeCoursey, T. E. (1991). Hydrogen ion currents in rat alveolar epithelial cells. *Biophysical Journal* **60**: 1243-1253.

85. DeCoursey, T. E. & Cherny, V. V. (1993). Potential, pH and arachidonate gate hydrogen ion currents in human neutrophils. *Biophysical Journal* **65**: 1590-1598.

86. DeCoursey, T. E. & Cherny, V. V. (2000). Common themes and problems of bioenergetics and voltage-gated proton channels. *Biochimica et Biophysica Acta* **1458**: 104-119.

87. De Kock, L. L. & Dunn, A. E. G. (1966). An electron microscope study of the carotid body. *Acta Anatomica* **64**: 163-178.

88. Deitmer, J. W. & Schlue, W. R. (1989). An inwardly directed electrogenic sodium-bicarbonate co-transport in leech glial cells. *Journal of Physiology* **411**: 179-194.

89. Deitmer, J. W. & Schneider, H. P. (1995). Voltage-dependent clamp of intracellular pH of identified leech glial cells. *Journal of Physiology* **485**: 157-166.

90. Deitmer, J. W. & Szatkowski, M. S. (1990). Membrane potential dependence of intracellular pH regulation by identified glial cells in the leech central nervous system. *Journal of Physiology* **421**: 617-631.

91. Deitmer, J. W. & Rose, C. R. (1996). pH regulation and proton signaling by glial cells. *Progress in Neurobiology* **48**: 73-103.

92. Demuth, D. R., Showe, L. C., Ballantine, M., Palumbo, A., Fraser, P. J., Cioe, L., Rovera, G. & Curtis, P. J. (1986). Cloning and structural characterization of a human non-erythroid band 3-like protein. *EMBO Journal* **5**: 1205-1214.

93. Docherty, R. J. & McQueen, D. S. (1978). Inhibitory action of dopamine on cat carotid chemoreceptors. *Journal of Physiology* **279**: 425-436.

94. Douglas, W. W. (1952). The effect of a ganglionic blocking-drug, hexamethonium, on the response of the cat's carotid body to various stimuli. *Journal of Physiology* **118**: 373-383.

95. Doyle, T. P. & Donnelly, D. F. (1994). Effect of Na^+ and K^+ channel blockade on hypoxia-induced catecholamine release from rat carotid body in vitro. *Journal of Applied Physiology* **77**: 2606-2611.

96. Duchen, M. R., Caddy, K. W., Kirby, G. C., Patterson, D. L., Ponte, J. & Biscoe, T. J. (1988). Biophysical studies of the cellular elements of the rabbit carotid body. *Neuroscience* **26**: 291-311.

97. Duchen, M. R. & Biscoe, T. J. (1992). Relative mitochondrial membrane potential and $[Ca^{2+}]_i$ in type I cells isolated from the rabbit carotid body. *Journal of Physiology* **450**: 33-61.

98. Duprat, F., Lesage, F., Fink, M., Reyes, R., Heurteaux, C. & Lazdunski, M. (1997). TASK, a human background K^+ channel to sense external pH variations near physiological pH. *EMBO Journal* **16**: 5464-5471.

99. Edsall, J. T. (1969). Carbon dioxide, carbonic acid, and bicarbonic ion: physical properties and kinetics of interconversion. In *CO2: Chemical, Biological and Physiological Aspects*, ed. Forster, R. E. *et al.*, pp. 15-27. NASA, Washington, USA.

100. Eladari, D., Blanchard, A., Leviel, F., Paillard, M., Stuart-Tilley, A. K., Alper, S. L. & Podevin, R. A. (1998). Functional and molecular characterization of luminal and basolateral Cl^-/HCO^-_3 exchangers of rat thick limbs. *American Journal of Physiology* **275**: F334-F342.

101. Elias, C. L., Lukas, A., Shurraw, S., Scott, J., Omelchenko A., Gross, G. J., Hnatowich, M. & Hryshko, L. V. (2001). Inhibition of Na^+/Ca^{2+} exchange by KB-R7943: transport mode selectivity and antiarrhythmic consequences. *American Journal of Physiology* **281**: H1334-H1345.

102. von Euler, U. S., Liljestrand, G. & Zotterman, Y. (1939). The excitation mechanism of the chemoreceptors in rabbit carotid body. *Skand. Arch. Physiol.* **83**: 132-152, 1939.

103. Everett, L. A. & Green, E. D. (1999). A family of mammalian anion transporters and their involvement in human genetic diseases. *Human Molecular Genetics* **8**: 1883-1891.

104. Eyzaguirre, C. & Lewin, J. (1961). Effect of different oxygen tensions of the carotid body *in vitro*. *Journal of Physiology* **159**: 238-250.

105. Eyzaguirre, C. & Koyano, H. (1965a). Effects of hypoxia, hypercapnia, and pH on the chemoreceptor activity of the carotid body *in vitro*. *Journal of Physiology* **178**: 385-409.

106. Eyzaguirre, C. & Koyano, H. (1965b). Effects of some pharmacological agents on chemoreceptor discharges. *Journal of Physiology* **178**: 410-437.

107. Eyzaguirre, C., Koyano, H. & Taylor, J. R. (1965). Presence of acetylcholine and transmitter release from carotid body chemoreceptors. *Journal of Physiology* **178**: 463-476.

108. Eyzaguirre, C. & Zapata, P. (1968a). Pharmacology of pH effects on carotid body chemoreceptors in vitro. *Journal of Physiology* **195**: 557-588.

109. Eyzaguirre, C. & Zapata, P. (1968b). The release of acetylcholine from carotid body tissues. Further study on the effects of acetylcholine and cholinergic blocking agents on the chemosensory discharge. *Journal of Physiology* **195**: 589-607.

110. Eyzaguirre, C., Leitner, L. M., Nishi, K. & Fidone, S. J. (1970). Depolarisation of chemosensory nerve endings in carotid body of the cat. *Journal of Neurophysiology* **33**: 156-169.

111. Eyzaguirre, C. & Fidone, S. J. (1980). Transduction mechanisms in carotid body: glomus cells, putative neurotransmitters, and nerve endings. *American Journal of Physiology* **239**: C135-C152.

112. Eyzaguirre, C. & Zapata, P. (1984). Perspectives in carotid body research. *Journal of Applied Physiology* **57**: 931-957.

113. Fairbanks, G., Steck, T. L. & Wallach, D. F. H. (1971). Electrophoretic analysis of the major polypeptides of the human erythrocyte membrane. *Biochemistry* **10**: 2606-2617.

114. Falke, J. J. & Chan, S. I. (1985). Evidence that anion transport by band 3 proceeds via a ping-pong mechanism involving a single transport site. A ^{35}Cl NMR study. *Journal of Biological Chemistry* **260**: 9537-9544.

115. Falke, J. J. & Chan, S. I. (1986). Molecular mechanisms of band 3 inhibitors. 1. Transport site inhibitors. *Biochemistry* **25**: 7888-7894.

116. Falke, J. J., Kane, K. J. & Chan, S. I. (1985). The kinetic equation for the chloride transport cycle of band 3. A ^{35}Cl and ^{37}Cl NMR study. *Journal of Biological Chemistry* **260**: 9545-9551.

117. Fafournoux, P., Demigne, C. & Remesy, C. (1985). Carrier-mediated uptake of lactate in rat hepatocytes. Effects of pH and possible mechanisms for L-lactate transport. *Journal of Biological Chemistry* **260**: 292-299.

118. Feldman, J. L. & Smith, J. C. (1994). Neural control of respiratory pattern in mammals: an overview. In *Regulation of Breathing*, 2nd edn., ed. Dempsey, J. A., pp. 39-68. Marcel Dekker, Inc., New York, USA.

119. Fidone, S. J. & González, C. (1982). Catecholamine synthesis in rabbit carotid body *in vitro*. *Journal of Physiology* **333**: 69-79.

120. Fidone, S. J. & González, C. (1986). Initiation and control of chemoreceptor activity in the carotid body. In *Hand Book of Physiology,* Sec. III, *The Respiratory System,* Vol. 2, *Control of Breathing,* ed. Cherniack, N. S. & Widdicombe, J. G., pp. 247-312. American Physiological Society, Bethesda, Maryland, USA.

121. Fidone, S. J., González, C. & Yoshizaki, K. (1982). Effects of low oxygen on the release of dopamine from the rabbit carotid body *in vitro*. *Journal of Physiology* **333**: 93-110.

122. Fidone, S. J., Weintraub, S. T. & Stavinoha, W. B. (1976). Acetylcholine content of normal and denervated cat carotid bodies measured by pyrolysis gas chromatography/mass fragmentometry. *Journal of Neurochemistry* **26**:1047-1049.

123. Fidone, S. J., Zapata, P. & L. J. Stensaas. (1977). Axonal transport of labelled material into sensory nerve endings of cat carotid body. *Brain Research* **124**: 9-28.

124. Fieber, L. A. & McCleskey, E. W. (1993). L-type calcium channels in type I cells of the rat carotid body. *Journal of Neurophysiology* **70**: 1378-1384.

125. Filosa, J. A., Dean, J. B. & Putnam, R. W. (2002). Role of intracellular and extracellular pH in the chemosensitive response of rat locus coeruleus neurones. *Journal of Physiology* **541**: 493-509.

126. Finley, J. C. W. & Katz, D. M. (1992). The central organization of carotid body afferent projections to the brainstem of the rat. *Brain Research* **572**: 108-116.

127. Fischer, J. L., Husted, R. F. & Steinmetz, P. R. (1983). Chloride dependence of the HCO_3^- exit step in urinary acidification by the turtle bladder. *American Journal of Physiology* **245**: F564-F568.

128. Fitzgerald, R. S. (2000). Oxygen and carotid body chemotransduction: the cholinergic hypothesis – a brief history and new evaluation. *Resapiration Physiology* **120**: 89-104.

129. Fitzgerald, R. S. & Dehghani, G. A. (1982). Neural responses of the cat carotid and aortic bodies to hypercapnia and hypoxia. *Journal of Applied Physiology* **52**: 596-601.

130. Fitzgerald, R. S. & Lahiri, S. (1986). Reflex responses to chemoreceptor stimulation. In *Hand Book of Physiology*, Sec. III, *The Respiratory System,* Vol. 2, *Control of Breathing,* ed. Cherniack, N. S. & Widdicombe, J. G., pp. 313-362. American Physiological Society, Bethesda, Maryland, USA.

131. Fitzgerald, R. S. & Lahiri, S. (1996). The history of chemoreceptors. In *Respiratory Physiology: People and Ideas*, ed. West, J. B., pp. 289–318. Oxford University Press, New York, USA.

132. Fitzgerald, R. S., Shirahata. M. & Ide, T. (1997). Further cholinergic aspects of carotid body chemotransduction of hypoxia in cats. *Journal of Applied Physiology* **82**: 819-827.

133. Funder, J., Tosteson, D. C. & Wieth, J. O., (1978). Effects of bicarbonate on lithium transport in human red cells. *Journal of General Physiology* **71**: 721-746.

134. Ganfornina, M. D. & López-Barneo, J. (1991). Single K^+ channels in membrane patches of arterial chemoreceptor cells are modulated by O_2 tension. *Proceedings of the National Academy of Sciences of the United States of America* **88**: 2927-2930.

135. Geers, C. & Gros, G. (2000). Carbon dioxide transport and carbonic anhydrase in blood and muscle. *Physiological Review* **80**: 681-715.

136. Gevers, W. (1977). Generation of protons by metabolic processes in heart cells. *Journal of Molecular and Cellular Cardiology* **9**: 867-874.

137. Gluck, S. & Al-Awqati, Q. (1984). An electrogenic proton-translocating adenosine triphosphatase from bovine kidney medulla. *Journal of Clinical Investigation* **73**:1704–1710.

138. Goldstein, S. A. N., Bockenhauer, D., O'Kelly, I. & Zilberberg, N. (2001). Potassium leak channels and the KCNK family of two-P-domain subunits. *Nature Reviews Neuroscience* **2**: 175-184.

139. Gómez, L. P. (1908). The anatomy and pathology of the carotid gland. *American Journal of Medical Sciences* **136**: 98-111.

140. González, C., Almaraz, L., Obeso, A. & Rigual, R. (1994a). Oxygen and acid chemoreception in the carotid body chemoreceptors. *Trends in Neuroscience* **15**: 146-153.

141. González, C., Almaraz, L., Obeso, A. & Rigual, R. (1994b). Carotid body chemoreceptor: from natural stimuli to sensory discharges. *Physiological Review* **74**: 829-898.

142. González, C. & Fidone, S. J. (1977). Increased release of 3H-dopamine during low O2 stimulation of rabbit carotid body *in vitro*. *Neuroscience Letters* **6**: 95-99.

143. Goodman, N. W. & McCloskey, D. I. (1972). Intracellular potential in the carotid body. *Brain Research* **39**: 501-504.

144. Goyal, S., Vanden Heuvel, G. B. & Aronson, P. S. (2003). Renal expression of novel Na^+/H^+ exchanger isoform NHE8. *American Journal of Physiology* **284**: F467-F473.

145. Gozal, D., Gozal, E. & Simakajornboon, N. (2000). Signaling pathways of the acute hypoxic ventilatory response in the nucleus tractus solitarius. *Respiration Physiology* **121**: 209–221.

146. Graber, M. & Pastoriza-Munoz, E. (1993). Regulation of cell pH by K^+/H^+ antiport in renal epithelial cells. *American Journal of Physiology* **265**: F773-F783.

147. Gray B.A. (1968). Response of the perfused carotid body to changes in pH and P_{co2}. *Respiration Physiology* **4**: 229-245.

148. Gray, B. A. (1971). On the speed of the carotid chemoreceptor response in relation to the kinetics of CO_2 hydration. *Respiration Physiology* **11**: 235-246.

149. Grichtchenko, I. I., Choi, I., Zhong, X., Bray-Ward, P., Russell, J. M. & Boron, W. F. (2001). Cloning, characterization, and chromosomal mapping of a human electroneutral Na^+-driven Cl^--HCO_3^- exchanger. *Journal of Biological Chemistry* **276**: 8358-8363.

150. Grinstein, S., Cohen, S. & Rothstein, A. (1984). Cytoplasmic pH regulation in thymic lymphocytes by an amiloride-sensitive Na^+/H^+ antiport. *Journal of General Physiology* **83**: 341-369.

151. Gronblad, M., Akerman, K. E. & Eranko, O. (1979) Induction of exocytosis from glomus cells by incubation of the carotid body of the rat with calcium and ionophore A23187. *Anatomical Record* **195**: 387-395.

152. Gross, E., Hawkins, K., Abuladze, N., Pushkin, A., Cotton, C. U., Hopfer, U. & Kurtz, I. (2001). The stoichiometry of the electrogenic sodium bicarbonate cotransporter NBC1 is cell-type dependent. *Journal of Physiology* **531**: 597-603.

153. Grynkiewicz, G., Poenie, M. & Tsien, R. Y. (1985). A new generation of Ca^{2+} indicators with greatly improved fluorescence properties. *Journal of Biological Chemistry* **260**: 3440-3450.

154. Guz, A., Noble, I. M., Widdicombe, J. G., Trenchard, D. & Mushin, W. W. (1966). The effect of bilateral block of vagus and glossopharyngeal nerves on the ventilatory response to CO_2 of conscious man. *Respiration Physiology* **1**: 206-210.

155. Haldane, J. S. & Priestley, J. G. (1905). The regulation of the lung-ventilation. *Journal of Physiology* **32**: 225-266.

156. Halestrap, A. P. & Price, N. T. (1999). The proton-linked monocarboxylate transporter (MCT) family: structure, function and regulation. *Biochemical Journal* **343**: 281-299.

157. Hanson, M. A., Nye, P. C. G. & Torrance, R. W. (1971). The exodus of an extracellular bicarbonate theory of chemoreception and the genesis of an intracellular one. In *Arterial Chemoreceptors*, ed. Belmonte, C., Palloy, D. J., Acker, H. & Fidone, S. J., pp. 403-416. Leicester University Press, Leicester, UK.

158. Hasselbalch, K. A. (1916). Die Berechnung der Wasserstoffzahl des blutes auf der freien und gebundenen Kohlensaure desselben, und die Sauerstoffbindung des Blutes als Funktion der Wasserstoffzahl. *Biochemische Zeitschrift* **78**: 112-144.

159. He, S. F., Wei, J. Y. & Eyzaguirre, C. (1991). Intracellular pH and some membrane characteristics of cultured carotid body glomus cells. *Brain Research* **547**: 258-266.

160. He, X., Wu, X., Knauf, P. A., Tabak, L. A. & Melvin, J. E. (1993). Functional expression of the rat anion exchanger AE2 in insect cells by a recombinant baculovirus. *American Journal of Physiology* **264**: C1075–C1079.

161. Henderson, L. J. (1908). The theory of neutrality regulation in the animal organism. *American Journal of Physiology* **21**: 427-428.

162. Henderson, L. M., Chappell, J. B. & Jones, O. T. G. (1987). The superoxide-generating NADPH oxidase of human neutrophils is electrogenic and associated with an H^+ channel. *Biochemical Journal* **246**: 325-329.

163. Hess, A. & Zapata, P. (1972). Innervation of the cat carotid body; normal and experimental studies. *Federation Proceedings* **31**: 1365-1382.

164. Heymans, C., Bouckaert J. J. & Dautrebande, L. (1930). Sinus réflexes de l'acidôse, de l'alcalôse, de l'anhydride carbonique, de l'ion hydrogène et de l'anoxémie: sinus carotidiens et échanges respiratoires dans les poumons et au delà des poumons. *Archives Internationales de Pharmacodynamie et de Therapie*. **39**: 400-408.

165. Heymans, C., Bouckaert J. J. & Dautrebande, L. (1931). Sinus carotidien et réflexes respiratoires; sensibilité des sinus carotidiens aux substances chimiques. Action stimulante respiratoire reflexe du sulfure de sodium, du cyanure de potassium, de la nicotine et de la lobeline. *Archives Internationales de Pharmacodynamie et de Therapie*. **40**: 54-91.

166. Heymans, C. & Neil, E. (1958). *Reflexogenic Areas of the Cardiovascular System*. Churchill, London, UK.

167. Hill, A. V. (1910). The possible effects of the aggregation of the molecules of haemoglobin on its dissociation curves. *Journal of Physiology* **40**: iv-vii.

168. Hochachka, P. W. & Mommsen, T. P. (1983). Protons and anaerobiosis. *Science* **219**: 1391-1397.

169. Hofer, A. M. & Machen, T. E. (1992). K-induced alkalinization in all cell types of rabbit gastric glands: a novel K/H exchange mechanism. *Journal of Membrane Biology* **126**: 245-256.

170. Honda, Y. & Tani, H. (1999). Chemical control of breathing. In *Control of Breathing in Health and Disease*, ed. Altose, M. & Kawakami, Y., pp. 41-86. Marcel Dekker, Inc., New York, USA.

171. Honda, Y., Watanabe, S., Hashizume, I., Hasegawa, S., Satomura, Y., Hata, N., Sakakibara, Y., Severinghaus, J. W. (1979). Hypoxic chemosensitivity in asthmatic patients two decades after carotid body resection. *Journal of Applied Physiology* **46**: 632-638.

172. Humphreys, B. D., Jiang, L., Chernova, M. N. & Alper, S. L. (1994). Functional characterization and regulation by pH of murine AE2 anion exchanger expressed in *Xenopus* oocytes. *American Journal of Physiology* **267**: C1295-C1307.

173. Ishibashi, K., Sasaki, S., & Marumo, F. (1998). Molecular cloning of a new sodium bicarbonate cotransporter cDNA from human retina. *Biochemical Biophysical Research Communications* **246**: 535-538.

174. Ishiguro, H., Steward, M. C., Lindsay, A. R. & Case, R. M., (1996). Accumulation of intracellular HCO_3^- by Na^+-HCO_3^- cotransport in interlobular ducts from guinea-pig pancreas. *Journal of Physiology* **495**: 169-178.

175. Iwamoto, T., Watano, T. & Shigekawa, M. (1996). A novel isothiourea derivative selectively inhibits the reverse mode of Na^+/Ca^{2+} exchange in cells expressing NCX1. *Journal of Biological Chemistry* **271**: 22391-22397.

176. Jaisser, F. & Beggah, A. T. (1999). The nongastric H^+-K^+-ATPases: molecular and functional properties. *American Journal of Physiology* **276**: F812-F824.

177. Janas, T., Bjerrum, P. J., Brahm, J. & Wieth, J. O. (1989). Kinetics of reversible DIDS inhibition of chloride self exchange in human erythrocytes. *American Journal of Physiology* **257**: C601-C606.

178. Jarisch, A., Landgren, S., Neil, E. & Zotterman, Y. (1952). Impulse activity in the carotid sinus nerve following intra-carotid injection of potassium chloride, veratrine, sodium citrate, adenosine-triphosphate and alpha-dinitrophenol. *Acta Physiologica Scandinavica* **25**: 195-211.

179. Jentsch, T. J., Keller, S. K., Koch, M. & Wiederholt, M. (1984). Evidence for coupled transport of bicarbonate and sodium in cultured bovine corneal endothelial cells. *Journal of Membrane Biology* **81**: 189-204.

180. Jentsch, T.J., Gunther, W., Pusch, M. & Schwappach, B. (1995). Properties of voltage-gated chloride channels of the ClC gene family. *Journal of Physiology* **482**: 19S-25S.

181. Jennings, M. L. (1989). Structure and function of the red blood cell anion transport protein. *Annual Review of Biophysics and Biophysical Chemistry* **18**: 397-430.

182. Jessen, F., Sjoholm, C. & Hoffmann, E. K. (1986). Identification of the anion exchange protein of Ehrlich cells: a kinetic analysis of the inhibitory effects of 4,4'-diisothiocyano-2,2'-stilbene-disulfonic acid (DIDS) and labelling of membrane proteins with ^{3}H-DIDS. *Journal of Membrane Biology* **92**: 195-205.

183. Jiang, L., Stuart-Tilley, A., Parkash, J. & Alper, S. L. (1994). pH_i and serum regulate AE2-mediated Cl^-/HCO_3^- exchange in CHOP cells of defined transient transfection status. *American Journal of Physiology* **267**: C845-C856.

184. Jones, J. F. X. & Daly, M. de B. (1997). Reflex cardiac dromotropic responses to stimulation of the carotid and aortic chemoreceptors in the anaesthetised cat. *Journal of Physiology* **502**: 461-467.

185. Kaila, K. & Voipio, J. (1987). Postsynaptic fall in intracellular pH induced by GABA-activated bicarbonate conductance. *Nature* **330**: 163-5.

186. Kaila, K., Saarikoski, J. & Voipio, J. (1990). Mechanism of action of GABA on intracellular pH and on surface pH in crayfish muscle fibres. *Journal of Physiology* **427**: 241-260.

187. Kaila, K., Voipio, J., Paalasmaa, P., Pasternack, M. & Deisz, R. A. (1993). The role of bicarbonate in $GABA_A$ receptor-mediated IPSPs of rat neocortical neurones. *Journal of Physiology* **464**: 273-289.

188. Kakinuma, Y., Ohsumi, Y. & Anraku, Y. (1981). Properties of H^+-translocating adenosine triphosphatase in vacuolar membranes of *Saccharomyces cerevisiae*. *Journal of Biological Chemistry* **256**: 10859–10863.

189. Kameda, Y., Nishimaki, T., Takeichi, M. & Chisaka, O. (2002). Homeobox gene *Hoxa3* is essential for the formation of the carotid body in the mouse embryos. *Developmental Biology* **247**: 197–209.

190. Kapus, A., Romanek, R., Qu, A. Y., Rotstein, O. D. & Grinstein, S. (1993). A pH-sensitive and voltage-dependent proton conductance in the plasma membrane of macrophages. *Journal of General Physiology* **102**: 729-760.

191. Keeling, D. J., Fallowfield, C. & Underwood, A. H. (1987). The specificity of omeprazole as an H^+-K^+-ATPase inhibitor depends upon the means of its activation. *Biochemical Pharmacology* **36**: 339-344.

192. Kenyon, J. L. & Gibbons, W. R. (1977). Effects of low chloride solutions on action potentials of sheep cardiac Purkinje fibres. *Journal of General Physiology* **70**: 635-660.

193. Kim, Y., Bang, H. & Kim, D. (1999). TBAK-1 and TASK-1, two-pore K^+ channel subunits: kinetic properties and expression in rat heart. *American Journal of Physiology* **277**: H1669–H1678.

194. Kinsella, J. L. & Aronson, P. S. (1980). Properties of the Na^+-H^+ exchanger in renal microvillus membrane vesicles. *American Journal of Physiology* **238**: F461-F469.

195. Kinsella, J. L. & Aronson, P. S. (1981). Amiloride inhibition of the Na^+-H^+ exchanger in renal microvillus membrane vesicles. *American Journal of Physiology* **241**: F374-F379.

196. Kirshner, N. (1962) Uptake of catecholamines by a particular fraction of the adrenal medulla. *Journal of Biological Chemistry* **237**: 2311–2317.

197. Klanke, C. A., Su, Y.-R., Callen, D. F., Wang, Z., Meneton, P., Baird, N., Kandasamy, R. A., Orlowski, J., Otterud, B. E. & Leppert, M. (1995). Molecular cloning and physical and genetic mapping of a novel human Na^+/H^+ exchanger (NHE5/SLC9A5) to chromosome 16q22.1. *Genomics* **25**: 615-622.

198. Kondo, H. (1975). A light and electromicroscopic study on the embryonic development of the rat carotid body. *American Journal of Anatomy* **144**: 275-294.

199. Kondo, H., Iwanaga, T. & Nakajima, T. (1982). Immunocytochemical study on the localisation of neuron-specific enolase and S-100 protein in the carotid body of rats. *Cell and Tissue Research* **144**: 275-294.

200. Kopito, R. R., Lee, B. S., Simmons, D. M., Lindsey, A. E., Morgans, C. W. & Schneider, K. (1989). Regulation of intracellular pH by a neuronal homolog of the erythrocyte anion exchanger. *Cell* **59**: 927-937.

201. Kopito, R. R. & Lodish, H. F. (1985). Primary structure and transmembrane orientation of the murine anion exchange protein. *Nature* **316**: 234-238.

202. Kummer, W. & Acker, H. (1995). Immunohistochemical demonstration of four subunits of neutrophil NAD(P)H oxidase in type I cells of carotid body. *Journal of Applied Physiology* **78**: 1904-1909, 1995.

203. Lagadic-Gossmann, D., Buckler, K. J., Vaughan-Jones, R. D. (1992). Role of bicarbonate in pH recovery from intracellular acidosis in the guinea pig ventricle myocyte. *Journal of Physiology* **458**: 361-384.

204. Lahiri, S. (1980) Chemical modification of carotid body chemoreception by sulfhydryls. *Science* **212**: 1065-1066.

205. Lahiri, S. & Delaney, R. (1975). Stimulus interaction in the responses of carotid body chemoreceptor single afferent fibers. *Respiration Physiology* **24**: 249-266.

206. Lahiri, S., Mokashi, A., Mulligan, E. & Nishino, T. (1981). Comparison of aortic and carotid chemoreceptor responses to hypercapnia and hypoxia. *Journal of Applied Physiology* **51**: 55-61.

207. Lahiri, S., Nishno, T., Mokashi A. & Mulligan, E. (1980a). Relative responses of aortic and carotid body chemoreceptors to hypotension. *Journal of Applied Physiology* **48**: 781-788.

208. Lahiri, S., Nishino, T., Mokashi, A. & Mulligan, E. (1980b) Interaction of dopamine and haloperidol with O_2 and CO_2 chemoreception in carotid body. *Journal of Applied Physiology* **49**: 45-51.

209. Lahiri, S., Roy, A., Rozanov, C. & Mokashi, A. (1998). K^+-current modulated by P_{O2} in type I cells in rat carotid body is not a chemosensor. *Brain Research* **794**: 162-165.

210. Lambert, A. & Lowe, A. G. (1978). Chloride/bicarbonate exchange in human erythrocytes. *Journal of Physiology* **275**: 51-63.

211. Lee, B. S, Gunn, R. B. & Kopito, R. R. (1991). Functional differences among nonerythroid anion exchangers expressed in a transfected human cell line. *Journal of Biological Chemistry* **266**: 11448-11454.

212. Leem, C. H., Lagadic-Gossmann, D. & Vaughan-Jones, R. D. (1999). Characterization of intracellular pH regulation in the guinea-pig ventricular myocyte. *Journal of Physiology* **517**: 159-180.

213. Leem, C. H. & Vaughan-Jones, R. D. (1997). Chloride-hydroxyl exchange in the guinea-pig ventricular myocyte: no role for bicarbonate. *Journal of Molecular and Cellular Cardiology* **29**: 2483-2489.

214. Leem, C. H. & Vaughan-Jones, R. D. (1998). Sarcolemmal mechanisms for pH_i recovery from alkalosis in the guinea-pig ventricular myocyte. *Journal of Physiology* **509**: 487-496.

215. Le Lièvre, C. S. & Le Douarin, N. M. (1975). Mesenchymal derivatives of the neural crest: Analysis of chimaeric quail and chick embryos. *Journal of Embryology and Experimental Morphology* **34**: 125–154.

216. Lepke, S., Fasold, H., Pring, M. & Passow, H. (1976). A study of the relationship between inhibition of anion exchange and binding to the red blood cell membrane of 4,4'-diisothiocyano stilbene-2,2'-disulfonic acid (DIDS) and its dihydro derivative (H_2DIDS). *Journal of Membrane Biology* **29**: 147-177.

217. Lesage, F., Guillemare, E., Fink, M., Duprat, F., Lazdunski, M., Romey, G. & Barhanin J. (1996). TWIK-1, a ubiquitous human weakly inward rectifying K^+ channel with a novel structure. *EMBO Journal* **15**: 1004-1011.

218. Lesage, F. & Lazdunski, M. (2000). Molecular and functional properties of two-pore-domain potassium channels. *American Journal of Physiology* **279**: F793–F801.

219. Lever, J. D. & Boyd, J. D. (1957). Osmiophile granules in the glomus cells of the rabbit carotid body. *Nature* **179**: 1082-1083.

220. Lever, J. D., Lewis, P. R. & Boyd, J. D. (1959). Observations on the fine structure and histochemistry of the carotid body in the cat and rabbit. *Journal of Anatomy* **93**: 478-490.

221. Levy, D., Seigneuret, M., Bluzat, A. & Rigaud, J. L. (1990). Evidence for proton countertransport by the sarcoplasmic reticulum Ca^{2+}-ATPase during calcium transport in reconstituted proteoliposomes with low ionic permeability. *Journal of Biological Chemistry* **265**: 19524-19534.

222. Linn, S. C., Kudrycki, K. E. & Shull, G. E. (1992). The predicted translation product of a cardiac AE3 mRNA contains an N-terminus distinct from that of the brain AE3 Cl^-/HCO_3^- exchanger. Cloning of a cardiac AE3 cDNA, organization of the AE3 gene, and identification of an alternative transcription initiation site. *Journal of Biological Chemistry* **15**: 7927-7935.

223. Lishajko, F. (1970). Release and uptake of dopamine in isolated granules from a human carotid body tumour. *Acta Physiologica Scandinavica* **79**: 533-536.

224. Liu, S., Piwinca-Worms, D. & Lieberman, M. (1990). Intracellular pH regulation in cultured embryonic chick heart cells: Na^+-dependent Cl^-/HCO_3^- exchange. *Journal of General Physiology* **96**: 1247-1269.

225. Loeschcke, H. H. (1982). Central chemosensitivity and the reaction theory. *Journal of Physiology* **332**: 1-24.

226. Loh, S.-H. (1998). Pharmacology and Physiology of H^+-eqivalent membrane transport in the mammalian ventricular myocyte. *D. Phil. Thesis.* University of Oxford, UK.

227. Loh, S.-H., Sun, B. & Vaughan-Jones, R. D. (1996). Effect of Hoe694, a novel Na^+-H^+ exchange inhibitor, on intracellular pH regulation in the guinea-pig ventricular myocyte. *British Journal of Pharmacology* **118**: 1905-1912.

228. Lohi, H., Kujala, M., Kerkela, E., Saarialho-Kere, U., Kestilä, M. & Kere, J. (2000). Mapping of five new putative anion transporter genes in human and characterization of SLC26A6, a candidate gene for pancreatic anion exchanger. *Genomics* **70**: 102-112.

229. Lohi, H., Kujala, M., Mäkelä, S., Lehtonen, E., Kestilä, M., Saarialho-Kere, U., Markovich, D. & Kere, J. (2002). Functional characterization of three novel tissue-specific anion exchangers SLC26A7, -A8, and -A9. *Journal of Biological Chemistry* **277**: 14246–14254.

230. López-Barneo, J. (1996). Oxygen-sensing by ion channels and the regulation of cellular functions. *Trends in Neuroscience* **19**: 435-440.

231. López-Barneo, J., López-López J. R., Urena J. & González C. (1988). Chemotransduction in the carotid body: K^+ current modulated by P_{O2} in type I chemoreceptor cells. *Science* **241**: 580-582.

232. López-López J. R., González C., Urena J. & López-Barneo, J. (1989). Low pO_2 selectively inhibits K^+ channel activity in chemoreceptor cells of the mammalian carotid body. *Journal of General Physiology* **93**: 1001-1015.

233. Lückermann, M., Trapp, S. & Ballanyi, K. (1997). GABA- and glycine-mediated fall of intracellular pH in rat medullary neurons *in situ*. *Journal of Neurophysiology* **77**: 1844-1852.

234. Lukacs, G. L., Kapus, A., Nanda, A., Romanek, R. & Grinstein, S. (1993). Proton conductance of the plasma membrane: properties, regulation, and functional role. *American Journal of Physiology* **265**: C3-C14.

235. Lyall V., Feldman G. M., Heck, G. L. & DeSimone, J. A. (1997). Effects of extracellular pH, P_{CO2}, and HCO_3^- on intracellular pH in isolated rat taste buds. *Journal of American Physiology* **273**: C1008-C1019.

236. Madeira, V. M. (1978). Proton gradient formation during transport of Ca^{2+} by sarcoplasmic reticulum. *Archives of Biochemistry and Biophysics* **185**: 316-325.

237. Mason, M. J., Smith, J. D., Garcia-Soto, J. J. & Grinstein, S. (1989). Internal pH-sensitive site couples Cl^--HCO_3^- exchange to Na^+-H^+ antiport in lymphocytes. *American Journal of Physiology* **256**: C428-433.

238. McDonald, D. M. (1981). Peripheral chemoreceptors. Structure-function relationships of carotid body. In *Regulation of Breathing*, Part I, ed. Hornbein, T. F., pp. 105-319. Marcel Dekker, New York, USA.

239. McQueen, D. S. (1977). A quantitative study of the effects of cholinergic drugs on carotid chemoreceptors in the cat. *Journal of Physiology* **273**: 515-532.

240. Meier, P. J., Knickelbein, R., Moseley, R. H., Dobbins, J. W. & Boyer, J. L. (1985). Evidence for carrier-mediated chloride/bicarbonate exchange in canalicular rat liver plasma membrane vesicles. *Journal of Clinical Investigation* **75**: 1256-63.

241. Mellergard, P., Ouyang, Y. B. & Siesjo, B. K. (1994). The regulation of intracellular pH is strongly dependent on extracellular pH in cultured rat astrocytes and neurons. *Acta Neurochirurgica Supplement* **60**:34-37.

242. Melvin, J. E., Park, K., Richardson, L., Schultheis, P. J. & Shull, G. E. (1999). Mouse down-regulated in adenoma (DRA) is an intestinal Cl^-/HCO_3^- exchanger and is up-regulated in colon of mice lacking the NHE3 Na^+/H^+ exchanger. *Journal of Biological Chemistry* **274**: 22855-22861.

243. Metz, B. (1969). Release of acetylcholine from the carotid body by hypoxia and hypoxia plus hypercapnia. *Resapiration Physiology* **6**: 386-394.

244. Michaelis, L. & Menten, M. L. (1913). The kinetics of invertin action. *Biochemische Zeitschrift* **49**: 333-69.

245. Mills, E. & Jöbsis, F. F. (1972). Mitochondrial respiratory chain of carotid body and chemoreceptor response to changes in oxygen tension. *Journal of Neurophysiology* **35**: 405-328.

246. Mitchell, P. (1961). Coupling of phosphorylation to electron and hydrogen transfer by a chemiosmotic type of mechanism. *Nature* **191**: 144–148.

247. Mitchell, R. A. (1966). Cerebrospinal Fluid and the Regulation of Respiration. In *Advances in Respiratory Physiology*, ed. Caro, C. G., pp. 1-47. Edward Arnold, London, UK.

248. Mitchell, R. A., Loceschcke, H. H., Massion, W. H. & Severinghaus, J. W. (1963). Respiratory responses mediated through superficial chemosensitive areas on the medulla. *Journal of Applied Physiology* **18**: 523-533.

249. Monti-Bloch, L., Abudara, V. & Eyzaguirre, C. (1993) Electrical communication between glomus cells of the rat carotid body. *Brain Research* **622**: 119-131.

250. Morris, K. F., Arata, A., Shannon, R. & Lindsey, B. G. (1996). Inspiratory drive and phase duration during carotid chemoreceptor stimulation in the cat: medullary neurone correlations. *Journal of Physiology* **491**: 241-259.

251. Mulligan, E., Lahiri, S. & Storey, B. T. (1981). Carotid body O_2 chemoreception and mitochondrial oxydative phosphorylation. *Journal of Applied Physiology* **51**: 438–446.

252. Munson, K., Lambrecht, N., Shin, J. M. & Sachs, G. (2000). Analysis of the membrane domain of the gastric H^+/K^+-ATPase. *Journal of Experimental Biology* **203**: 161-170.

253. Murer H, Hopfer U, Kinne R. (1976). Sodium/proton antiport in brush-border-membrane vesicles isolated from rat small intestine and kidney. *Biochemical Journal* **154**: 597-604.

254. Nattie, E. (1999). CO_2, brainstem chemoreceptors and breathing. *Progress in Neurobiology* **59**: 299-331.

255. Nelson, H. & Nelson, N. (1989). The progenitor of ATP synthases was closely related to the current vacuolar H^+-ATPase. *FEBS Letters* **247**: 147–153.

256. Niggli, V., Sigel, E. & Carafoli, E. (1982). The purified Ca^{2+} pump of human erythrocyte membranes catalyses an electroneutral Ca^{2+}-H^+ exchange in reconstituted liposomal systems. *Journal of Biological Chemistry* **257**: 2350-2356.

257. Numata, M., Petrecca, K., Lake, N. & Orlowski, J. (1998). Identification of a mitochondrial Na^+/H^+ exchanger. *Journal of Biological Chemistry* **273**: 6951-6959.

258. Numata, M. & Orlowski, J. (2001). Molecular cloning and characterization of a novel $(Na^+,K^+)/H^+$ exchanger localized to the trans-Golgi network. *Journal of Biological Chemistry* **276**: 17387-17394.

259. Numata, M., Petrecca, K., Lake, N. & Orlowski J. (1998). Identification of a Mitochondrial Na^+/H^+ Exchanger. *Journal of Biological Chemistry* **273**: 6951-6959.

260. Obeso, A., Gómez-Niño, A., & González, C. (1999). NADPH oxidase inhibition does not interfere with low P_{O2} transduction in rat and rabbit CB chemoreceptor cells. *American Journal of Physiology* **276**: C593–C601.

261. Olsnes, S., Tonnessen, T. I. & Sandvig, K. (1986). pH-regulated anion antiport in nucleated mammalian cells. *Journal of Cell Biology* **102**: 967-971.

262. O'Regan, R. G. (1982). Role of peripheral chemoreceptors and central chemosensitivity in the regulation of respiration and circulation. *Journal of Experimental Biology* **100**: 23-40.

263. Oren, A., Whipp, B. J. & Wasserman, K. (1982). Effect of acid-base status on the kinetics of the ventilatory response to moderate exercise. *Journal of Applied Physiology* **52**: 1013-1017.

264. Orlowski J. (1993). Heterologous expression and functional properties of amiloride high affinity (NHE-1) and low affinity (NHE-3) isoforms of the rat Na/H exchanger. *Journal of Biological Chemistry* **268**: 16369-16377.

265. Orlowski, J., Kandasamy, R. A. & Shull, G. E. (1992). Molecular cloning of putative members of the Na/H exchanger gene family: cDNA cloning, deduced amino acid sequence, and mRNA tissue expression of the rat Na/H exchanger NHE-1 and two structurally related proteins. *Journal of Biological Chemistry* **267**: 9331-9339.

266. Overholt, J. L. & Prabhakar, N. R. (1997). Ca^{2+} current in rabbit carotid body glomus cells is conducted by multiple types of high voltage-activated Ca^{2+} channels. *Journal of Neurophysiology* **78**: 2467-2474.

267. Oyama, Y., Walker, J. L. & Eyzaguirre, C. (1986). The intracellular chloride activity of glomus cells in the isolated rabbit carotid body. *Brain Research* **368**: 167-169.

268. Paintal, A. S. (1966). Mechanical transmission of sensory information at chemoreceptors. In *The Proceedings of the Wates Foundation Symposium on Arterial Chemoreceptors*, ed. Torrance, R. W., pp. 121-130. Blackwell Scientific Publications, Oxford, UK.

269. Paintal, A. S. & Riley, R. L. (1966). Responses of aortic chemoreceptors. *Journal of Applied Physiology* **21**: 543-548, 1966.

270. Pauling, L. (1970). *General Chemistry*, 3rd edn, pp. 479-507. W.H Freeman and Company, San Francisco, USA.

271. Peers, C. (1990). Hypoxic suppression of K^+ currents in type I carotid body cells: selective effect on the Ca^{2+}-activated K^+ current. *Neuroscience Letters* **119**: 253-256.

272. Peers, C. & Green, F. K. (1991) Inhibition of Ca^{2+}-activated K^+ currents by intracellular acidosis in isolated type I cells of the neonatal rat carotid body. *Journal of Physiology* **437**: 589-602.

273. Petrovic, S., Ju, X., Barone, S., Seidler, U., Alper, S. L., Lohi, H., Kere, J. & Soleimani, M. (2003). Identification of a basolateral Cl^-/HCO_3^- exchanger specific to gastric parietal cells. *American Journal of Physiology* **284**: G1093–G1103.

274. Pineda, J. & Aghajanian, G. K. (1997). Carbon dioxide regulates the tonic activity of locus coeruleus neurons by modulating a proton- and polyamine-sensitive inward rectifier potassium current. *Neuroscience* **77**: 723-743.

275. Pitts, R. F., Ayer, J. L. & Schiess, W. A. (1949). Renal regulation of acid-base balance in man: reabsorption and excretion of bicarbonate. *Journal of Clinical Investigation* **28**: 35-44.

276. Planelles, G., Thomas, S. R. & Anagnostopoulos, T. (1993). Change of apparent stoichiometry of proximal-tubule Na^+-HCO_3 cotransport upon experimental reversal of its orientation. *Proceedings of the National Academy of Science USA* **90**: 7406-7410.

277. Poole, R. C. & Halestrap, A. P. (1993). Transport of lactate and other monocarboxylates across mammalian plasma membranes. *American Journal of Physiology* **264**: C761-C782.

278. Prabhakar, N. R. (2000). Oxygen sensing by the carotid body chemoreceptors. *Journal of Applied Physiology* **88**: 2287-2295.

279. Prasad, M., Fearon, I. M., Zhang, M., Laing, M., Vollmer, C. & Nurse, C. A. (2001). Expression of P2X2 and P2X3 receptor subunits in rat carotid body afferent neurones: role in chemosensory signaling. *Journal of Physiology* **537**: 667–677.

280. Pucéat, M. (1999). pH_i regulatory ion transporters: an update on structure, regulation and cell function. *Cellular and Molecular Life Sciences* **55**: 1216-1229.

References

281. Pushkin, A., Abuladze, N., Newman, D., Lee, I., Xu, G. & Kurtz, I. (2000). Cloning, characterization and chromosomal assignment of NBC4, a new member of the sodium bicarbonate cotransporter family. *Biochimica et Biophysica Acta* **1493**: 215-218.

282. Putnam, R. W. (1998). Intracellular pH regulation. In *Cell Physiology Sourcebook*, 2nd edn., ed. Sperelakis, N., pp. 293-311. Academic Press, San Diego, USA.

283. Putnam, R. W. (2001). Intracellular pH regulation of neurons in chemosensitive and nonchemosensitive areas of brain slices. *Respiration Physiology* **129**: 37–56.

284. Putnam, R. W. & Roos, A. (1991). Which value for the first dissociation constant of carbonic acid should be used in biological work? *American Journal of Physiology* **260**: C1113-C1116.

285. Rausch, S. M., Whipp, B. J., Wasserman, K. & Huszczuk, A. (1991). Role of the carotid bodies in the respiratory compensation for the metabolic acidosis of exercise in humans. *Journal of Physiology* **444**: 567-578.

286. Reusch, H. P., Lowe, J. & Ives, H. E. (1995). Osmotic activation of a Na^+-dependent Cl^-/HCO_3 exchanger. *American Journal of Physiology* **268**: C147-C153.

287. Richmond, P. H. (1993). The regulation of intracellular pH (pH_i) and its role in chemoreception in the carotid body type-1 cell of the neonatal rat. *D. Phil. Thesis.* University of Oxford, UK.

288. Richmond, P.H. & Vaughan-Jones, R. D. (1997). Assessment of evidence for K^+-H^+ exchange in isolated type-I cells of neonatal rat carotid body. *Pflügers Archiv* **434**: 429-437.

289. Ridderstrale, Y. & Hanson, M. A. (1984). Histochemical localisation of carbonic anhydrase in the carotid body. *Annals of the New York Academy of Sciences* **429**: 398-400.

290. Riesco-Fagundo, A. M., Pérez-García, M. T., González, C. & López-López, J. R. (2001). O_2 modulates large conductance Ca^{2+}-dependent K^+ channels of rat chemoreceptor cells by a membrane-restricted and CO-sensitive mechanism. *Circulation Research* **89**: 430–436.

291. Rigual, R., López-López, J. R. & González, C. (1991). Release of dopamine and chemoreceptor discharge induced by low pH and high P_{CO2} stimulation of the cat carotid body. *Journal of Physiology* **433**: 519-531.

292. Ritucci, N. A., Chambers-Kersh, L., Dean, J. B. & Putnam, R. W. (1998). Intracellular pH regulation in neurons from chemosensitive and nonchemosensitive areas of the medulla. *American Journal of Physiology* **275**: R1152–R1163.

293. Rocher, A., Obeso, González, C. & Herreros, B. (1991). Ionic mechanisms for the transduction of acid stimuli in rabbit carotid body glomus cells. *Journal of Physiology* **433**: 533-548.

294. Romero, M. F. & Boron, W. F. (1999). Electrogenic Na^+/HCO_3^- cotransporters: cloning and physiology. *Annual Reviews of Physiology* **61**: 699-723.

295. Romero, M. F., Hediger, M. A., Boulpaep, E. L. & Boron, W. F. (1997). Expression cloning and characterization of a renal electrogenic Na^+/HCO_3^- cotransporter. *Nature* **387**: 409-413.

296. Romero, M. F., Henry, D., Nelson, S., Harte, P. J., Dillon, A. K. & Sciortino, C. M. (2000). Cloning and characterization of a Na^+-driven anion exchanger (NDAE1). A new bicarbonate transporter. *Journal of Biological Chemistry* **275**: 24552-24559.

297. Roos, A. & Boron, W. F. (1981). Intracellular pH. *Physiological Review* **61**: 296-434.

298. Rose C. R. & Deitmer, J. W. (1995). Stimulus-evoked changes of extra- and intracellular pH in the leech central nervous system. I. Bicarbonate dependence. *Journal of Neurophysiology* **73**: 125-131.

299. Rose C. R. & Deitmer, J. W. (1995). Stimulus-evoked changes of extra- and intracellular pH in the leech central nervous system. II. Mechanisms and maintenance of pH homeostasis. *Journal of Neurophysiology* **73**: 132-140.

300. Russell, J. M. & Boron, W. F. (1976). Role of choloride transport in regulation of intracellular pH. *Nature* **264**: 73-74.

301. Sabolic, I., Brown, D., Gluck, S. L. & Alper, S. L. (1997). Regulation of AE1 anion exchanger and H^+-ATPase in rat cortex by acute metabolic acidosis and alkalosis. *Kidney International* **51**: 125-137.

302. Sachs, G., Chang, H. H., Rabon, E., Schackman, R., Lewin, M. & Saccomani, G. (1976). A nonelectrogenic H^+ pump in plasma membranes of hog stomach. *Journal of Biological Chemistry* **251**: 7690-7698.

303. Salhany, J. M., Sloan, R. L., Cordes, K. A. & Schopfer, L. M. (1994). Kinetic evidence for ternary complex formation and allosteric interactions in chloride and stilbene disulfonate binding to band 3. *Biochemistry* **33**: 11909-11916.

304. Sampson, S. R. (1971). Effects of mecamylamine on responses of carotid body chemoreceptors *in vivo* to physiological and pharmacological stimuli. *Journal of Physiology* **212**: 655-666.

305. Sampson, S. R., Aminoff, M. J., Jaffe, R. A. & Vidruk, E. H. (1976). Analysis of inhibitory effect of dopamine on carotid body chemoreceptors in cats. *American Journal of Physiology* **230**:1494-1498.

306. Sardet, C., Franchi, A. & Pouyssegur, J. (1989). Molecular cloning, primary structure, and expression of the human growth factor-activatable Na^+/H^+ antiporter. *Cell* **56**: 271-280.

307. Satoh, H., Susaki, M., Shukunami, C., Iyama, K., Negoro, T. & Hiraki, Y. (1998). Functional analysis of diastrophic dysplasia sulfate transporter. Its involvement in growth regulation of chondrocytes mediated by sulfated proteoglycans. *Journal of Biological Chemistry* **273**: 12307-12315.

308. Schmitt, B. M., Berger, U. V., Douglas, R. M., Bevensee, M. O., Hediger, M. A., Haddad, G. G. & Boron, W. F. (2000). Na/HCO_3 cotransporters in rat brain: expression in glia, neurons and choroid plexus. *Journal of Neuroscience* **20**: 6839-6848.

309. Schopfer, L. M. & Salhany, J. M. (1995). Characterization of the stilbene disulfonate binding site on band 3. *Biochemistry* **34**: 8320-8329.

310. Scholz, W., Albus, U., Lang, H.-J., Linz, W., Martorana, P. A., Englert, H. C. & Scholkens, B. A. (1993). Hoe 694, a new Na^+/H^+ exchange inhibitor and its effects in cardiac ischaemia. *British Journal of Pharmacology* **109**: 562-568.

311. Schrenzel, J., Serrander, L., Bánfi, B., Nüsse, O., Fouyouzi, R., Lew, D. P., Demaurex, N. & Krause, K.-H. (1998). Electron currents generated by the human phagocyte NADPH oxidase. *Nature* **392**: 734-737.

312. Schweitzer, A. & Wright, S. (1938). Action of prostigmine and acetylcholine on respiration. *Quarterly Journal of Experimental Physiology* **28**: 33-47.

313. Schwiening, C. J. & Boron, W. F. (1994). Regulation of intracellular pH in pyramidal neurones from the rat hippocampus by Na^+-dependent Cl^--HCO_3^- exchange. *Journal of Physiology* **475**: 59-67.

314. Schwiening, C. J., Kennedy, H. J. & Thomas, R. C. (1993). Calcium-hydrogen exchange by the plasma membrane Ca-ATPase of voltage-clamped snail neurons. *Proceedings of Royal Society B* **253**: 285-289.

315. Scott, D. A., Wang, R., Kreman, T. M., Sheffield, V. C. & Karniski, L. P. (1999). The Pendred syndrome gene encodes a chloride-iodide transport protein. *Nature Genetics* **21**: 440-443.

316. Shami, Y., Carver, J., Ship, S. & Rothstein, A. (1976). Inhibition of C1- binding to anion transport protein of the red blood cell by DIDS (4, 4'-diisothiocyano-2, 2'-stilbene disulfonic acid) measured by ^{35}C1 NMR. *Biochemical and Biophysical Research Communications* **76**: 429-436.

317. Shigekawa, M. & Iwamoto, T. (2001). Cardiac Na^+-Ca^{2+} exchange: molecular and pharmacological aspects. *Circulation Research* **88**: 864-876.

318. Shirahata, M., Ishizawa, Y., Rudisill, M., Schofield, B. & Fitzgerald, R. S. (1998). Presence of nicotinic acetylcholine receptors in cat carotid body afferent system. *Brain Research* **814**: 213-217.

319. Shrode L. D. & Putnam R. W. (1994). Intracellular pH regulation in primary rat astrocytes and C_6 glioma cells. *Glia* **12**: 196-210.

320. e Silva, M. J. & Lewis, D. L. (1995). L- and N-type Ca^{2+} channels in adult rat carotid body chemoreceptor type I cells. *Journal of Physiology* **489**: 689-699.

321. Silver, R. B. & Soleimani, M. (1999). H^+-K^+-ATPases: regulation and role in pathophysiological states. *American Journal of Physiology* **276**: F799-F811.

322. Soleimani, M. (2002). Na^+:HCO_3^- cotransporters (NBC): expression and regulation in the kidney. *Journal of Nephrology* **15**: S32-S40.

323. Soleimani, M., Greeley, T., Petrovic, S., Wang, Z., Amlal, H., Kopp, P. & Burnham, C. E. (2001). Pendrin: an apical $Cl^-/OH^-/HCO_3^-$ exchanger in the kidney cortex. *American Journal of Physiology* **280**: F356–F364.

324. Spergel, D. & Lahiri, S. (1993). Differential modulation by extracellular ATP of carotid chemosensory responses. *Journal of Applied Physiology* **74**: 3052-3056.

325. Stea, A. & Nurse, C. A. (1989). Chloride channels in cultured glomus cells of the rat carotid body. *American Journal of Physiology* **257**: C174-C181.

326. Stein, W. D. (1986). *Transport and diffusion across cell membrane.* pp. 231-361. Academic Press, Orlando, USA.

327. Sterling, D. & Casey, J. R. (1999). Transport activity of AE3 chloride/bicarbonate anion-exchange proteins and their regulation by intracellular pH. *Biochemical Journal* **344**: 221-229.

328. Stewart, A. K., Chernova, M. N., Kunes, Y. Z. & Alper, S. L. (2001). Regulation of AE2 anion exchanger by intracellular pH: critical regions of the NH_2-terminal cytoplasmic domain. *American Journal of Physiology* **257**: C174-C181.

329. Stewart, A. K., Chernova, M. N., Shmukler, B. E., Wilhelm, S. & Alper, S. L. (2002). Regulation of AE2-mediated Cl^- transport by intracellular or by extracellular pH requires highly conserved amino acid residues of the AE2 NH2-terminal cytoplasmic domain. *Journal of General Physiology* **120**: 707–722.

330. Sun, B., Leem, C., & Vaughan-Jones, R. D. (1996). Novel chloride-dependent acid loader in the guinea-pig ventricular myocyte: part of a dual acid-loading mechanism. *Journal of Physiology* **495**: 65-82.

331. Sun, B., Vaughan-Jones, R. D. & Kambayashi, J. (1999). Two distinct HCO_3 -dependent H^+ efflux pathways in human vascular endothelial cells. *American Journal of Physiology* **277**: H28-H32.

332. Teppema, L. J., Barts, P. W. J. A., Folgering, H. T. & Evers, J. A. M. (1983). Effects of respiratory and (isocapnic) metabolic arterial acid-base disturbance on medullary extracellular fluid pH and ventilation in cats. *Respiration Physiology* **53**: 379-395.

333. Thomas, J. A., Bushsbaum, R. N. & Racker, E. (1979). Intracellular pH measurements in Ehrlich Ascites tumour cells utilising spectroscopic probes generated in situ. *Biochemistry* **18**: 2210-2218.

334. Thomas, R. C. (1976). The effect of carbon dioxide on the intracellular pH and buffering power of snail neurones. *Journal of Physiology* **255**:715-735.

335. Thomas, R. C. (1977). The role of bicarbonate, chloride and sodium ions in the regulation of intracellular pH in snail neurones. *Journal of Physiology* **273**: 317-338.

336. Thomas, R. C. & Meech, R. W. (1982). Hydrogen ion currents and intracellular pH in depolarised voltage-clamped snail neurones. *Nature* **299**: 826-828.

337. Thomas, R. C. (1984). Experimental displacement of intracellular pH and the mechanism of its subsequent recovery. *Journal of Physiology* **354**: 3P-22P.

338. Tolkovsky, A. M. & Richards, C. D. (1987). Na^+/H^+ exchange is the major mechanism of pH regulation in cultured sympathetic neurons: measurements in single cell bodies and neurites using a fluorescent pH indicator. *Neuroscience* **22**:1093-1102.

339. Tonnessen, T. I., Aas, A. T., Ludt, J., Blomhoff, H. K. & Olsnes, S. (1990). Regulation of Na^+/H^+ and Cl^-/HCO_3^- antiports in Vero cells. *Journal of Cellular Physiology* **143**: 178-187.

340. Torrance, R. W. (1968). Prolegomena. In *Arterial Chemoreceptors*, ed. Torrance, R. W., Blackwell, Oxford, UK.

341. Torrane, R. W. (1974). Arterial chemoreceptors. In *Respiratory Physiology I*, ed. Widdicombe, J. G., University Park, Baltimore, USA.

342. Torrance, R. W. (1977). Convergence of stimuli in arterial chemoreceptors. *Advanced Experimental Medical Biology* **78**: 203-207.

343. Touré, A., Morin, L., Pineau, C., Becqi, F., Dorseuil, O. & Gacon, G. (2001). Tat1, a Novel Sulfate Transporter Specifically Expressed in Human Male Germ Cells and Potentially Linked to RhoGTPase Signaling. *Journal of Biological Chemistry* **276**: 20309–20315.

344. Trapp, S., Lückermann, M., Kaila, K. & Ballanyi, K. (1996). Acidosis of hippocampal neurones mediated by a plasmalemmal Ca^{2+}/H^+ pump. *Neuroreport* **7**: 2000-2004.

345. Tsuganezawa, H., Kobayashi, K., Iyori, M., Araki, T., Koizumi, A., Watanabe, S., Kaneko, A., Fukao, T., Monkawa, T., Yoshida, T., Kim, D. K., Kanai, Y., Endou, H., Hayashi, M. & Saruta T. (2001). A new member of the HCO_3^- transporter superfamily is an apical anion exchanger of β-intercalated cells in the kidney. *Journal of Biological Chemistry* **276**: 8180-8189.

346. Urena, J., López-López, J., González, C. & & López-Barneo, J. (1989). Ionic currents in dispersed chemoreceptor cells of the mammalian carotid body. *Journal of General Physiology* **93**: 979-999.

347. Valant, P. A. & Haynes, D. H. (1993). The Ca^{2+}-extruding ATPase of the human platelet creates and responds to cytoplasmic pH changes, consistent with a 2 Ca^{2+}/nH^+ exchange mechanism. *Journal of Membrane Biology* **136**: 215-230.

348. Van Slyke, D. D. (1922). On the measurement of buffer values and the relationship of buffer value to the dissociation constant of the buffer solution. *Journal of Biological Chemistry* **52**: 525-570.

349. Varas, R., Alcayaga, J. & Iturriaga, R. (2003). ACh and ATP mediate excitatory transmission in cat carotid identified chemoreceptor units *in vitro*. *Brain Research* **988**: 154–163.

350. Vaughan-Jones, R. D. (1979). Regulation of chloride in quiescent sheep-heart Purkinje fibres studied using intracellular chloride and pH-sensitive microelectrodes. *Journal of Physiology* **295**: 111-137.

351. Vaughan-Jones, R. D. (1982). Chloride activity and its control in skeletal and cardiac muscle. *Philosophical Transactions of the Royal Society B* **299**: 537-548.

352. Vaughan-Jones, R. D. (1986). An investigation of chloride-bicarbonate exchange in the sheep cardiac Purkinje fibre. *Journal of Physiology* **379**: 377-406.

353. Vaughan-Jones, R. D., Eisner, D. A. and Lederer, W. J. (1987). Effects of changes in intracellular pH on contraction in sheep cardiac Purkinje fibres. *Journal of General Physiology* **89**:1015-1032

354. Vaughan-Jones, R. D. & Wu, M.-L. (1990). Extracellular H^+ inactivation of Na^+/H^+ exchanger in the sheep cardiac Purkinje fibre. *Journal of Physiology* **425**: 429-448.

355. Verna, A., Roumy, M. & Leitner, L. M. (1975). Loss of chemoreceptive properties of the rabbit carotid body after destruction of the glomus cells. *Brain Research* **100**: 13-23.

356. Verna, A., Talib, N., Roumy, M. & Pradet, A. (1990). Effects of metabolic inhibitors and hypoxia on the ATP, ADP and AMP content of the rabbit carotid body in vitro: the metabolic hypothesis in question. *Neuroscience Letters* **116**: 156–161.

357. Vicario, I., Obeso, A., Rocher, A., López-López, J. R. & González, C. (2000). Intracellular Ca^{2+} stores in chemoreceptor cells of the rabbit carotid body: significance for chemoreception. *American Journal of Physiology* **279**: C51-C61.

358. Vidruk, E. H., Olson, J. E. B., Ling, L. & Mitchell, G. S. (2001). Responses of single-unit carotid body chemoreceptors in adult rats. *Journal of Physiology* **531**: 165-170.

359. Vincourt, J.-B., Jullien, D., Amalric, F. & Girard, J.-P. (2003). Molecular and functional characterization of SLC26A11, a sodium-independent sulfate transporter from high endothelial venules. *FASEB Journal*; DOI: 10.1096/fj.02-0787fje.

360. Virkki, L. V., Wilson, D. A., Vaughan-Jones, R. D. & Boron, W. F. (2002). Functional characterization of human NBC4 as an electrogenic Na^+-$HCO3^-$ cotransporter (NBCe2). *American Journal of Physiology* **282**: C1278–C1289.

361. Voipio, J. & Ballanyi, K. (1997). Interstitial P_{CO2} and pH, and their role as chemostimulants in the isolated respiratory network of neonatal rats. *Journal of Physiology* **499**: 527-542.

362. Vovk, A., Duffin, J. Kowalchuk, J. M., Paterson, D. H. & Cunningham, D. A. (2000). Changes in chemoreflex characteristics following acute carbonic anhydrase inhibition in humans at rest. *Experimental Physiology* **85**: 847-856.

363. Wakabayashi S., Shigekawa, M. & Pouyssegur, J. (1997). Molecular physiology of vertebrate Na^+/H^+ exchangers. *Physiological Reviews* **77**: 51-74.

364. Wallmark, B., Briving, C., Fryklund, J., Munson, K., Jackson, R., Mendlein, J., Rabon, E. & Sachs, G. (1987). Inhibition of gastric H^+,K^+-ATPase and acid secretion by SCH 28080, a substituted pyridyl(1,2a)imidazole. *Journal of Biological Chemistry* **262**: 2077-2084.

365. Wang, C.-Z., Yano, H., Nagashima, K. & Seino, S. (2000). The Na^+-driven Cl^-/HCO_3 exchanger. Cloning, tissue distribution, and functional characterization. *Journal of Biological Chemistry* **275**: 35486-35490.

366. Wang, Z., Orlowski, J. & Shull, G. E. (1993). Primary structure and functional expression of a novel gastrointestinal isoform of the rat Na/H exchanger. *Journal of Biological Chemistry* **268**:11925-11928.

367. Wasserman, K., Whipp, B. J., Koyal, S. N. & Cleary, M. G. (1975). Effect of carotid body resection on ventilatory and acid-base control during exercise. *Journal of Applied Physiology* **39**: 354-358.

368. Watano, T., Kimura, J., Morita, T. & Nakanishi, H. (1996). A novel antagonist, No. 7943, of the Na^+/Ca^{2+} exchange current in guinea-pig cardiac ventricular cells. *British Journal of Pharmacology* **119**: 555-563.

369. Whalen, W. J. & Nair, P. (1983). Oxidative metabolism and tissue P_{O2} of the carotid body. In *Physiology of the Peripheral Arterial Chemoreceptors*. pp. 117-132., Elsevier, Amsterdam, The Netherlands.

370. Wieczorek, H., Brown, D., Grinstein, S., Ehrenfeld, J. & Harvey, W. R. (1999). Animal plasma membrane energization by proton-motive V-ATPases. *Bioessays* **21**: 637-648.

371. Wilding, T. J., Cheng, B. & Roos, A. (1992). pH regulation in adult rat carotid body glomus cells. *Journal of General Physiology* **100**: 593-608.

372. Wilson, D. A. & Vaughan-Jones, R. D. (2001). Chloride-hydroxyl and chloride-bicarbonate exchangers in the guinea-pig ventricular myocyte exhibit different kinetic characteristics. In: XXXIV International Congress of Physiological Sciences, Christ Church, New Zealand.

373. Wilson, D. F., Rumsey, W. L., Green, T. J. & Vanderkooi, J. M. (1988). The oxygen dependence of mitochondrial oxidative phosphorylation measured by a new optical method for measuring oxygen concentration. *Journal of Biological Chemistry* **263**: 2712–2718.

374. Wood, P. G., Muller, H., Sovak, M. & Passow, H. (1992). Role of Lys 558 and Lys 869 in substrate and inhibitor binding to the murine band 3 protein: a study of the effects of site-directed mutagenesis of the band 3 protein expressed in the oocytes of *Xenopus laevis*. *Journal of Membrane Biology* **127**: 139-148.

375. Wu, M.-L., Chen, J.-H., Chen, W.-H., Chen, Y.-C. & Chu, K.-C. (1999). Novel role of the Ca^{2+}-ATPase in NMDA-induced intracellular acidification. *American Journal of Physiology* **277**: C717-C727.

376. Wu, M.-L. & Vaughan-Jones, R. D. (1997). Interaction between Na^+ and H^+ ions on Na-H exchange in sheep cardiac Purkinje fibers. *Journal of Molecular and Cellular Cardiology* **29**: 1131-1140.

377. Wyatt, C. N. & Buckler K. J. (2000). The effect of mitochondrial inhibitors on membrane currents in isolated neonatal rat carotid body type I cells. *Journal of Physiology* **527**: 121P-122P.

378. Wyatt, C. N., Weir, E. K. & Peers, C. (1994). Diphenyleneiodonium blocks K^+ and Ca^{2+} currents in type I cells isolated from neonatal rat carotid body. *Neuroscience Letters* **172**: 63–66.

379. Yannoukakos, D., Stuart-Tilley, A., Fernandez, H. A., Fey, P., Duyk, G. & Alper, S. L. (1994). Molecular cloning, expression, and chromosomal localization of two isoforms of the AE3 anion exchanger from human heart. *Circulation Research* **75**: 603-614.

380. Yoshitomi, K., Burckhardt, B. C. & Fromter, E. (1985). Rheogenic sodium-bicarbonate cotransport in the peritubular cell membrane of rat renal proximal tubule. *Pflügers Archiv* **405**: 360-366.

381. Zapata, P. (1975). Effects of dopamine on carotid chemo- and baroreceptors in vitro. *Journal of Physiology* **244**: 235-251.

382. Zeng, Y., Oberdorf, J. A. & Florman, H. M. (1996). pH regulation in mouse sperm: identification of Na^+-, Cl^--, and HCO_3^--dependent and arylaminobenzoate-dependent regulatory mechanisms and characterization of their roles in sperm capacitation. *Developmental Biology* **173**: 510-520.

383. Zhang, Y., Chernova, M. N., Stuart-Tilley, A. K., Jiang, L. & Alper, S. L. (1996). The cytoplasmic and transmembrane domains of AE2 both contribute to regulation of anion exchange by pH. *Journal of Biological Chemistry* **271**: 5741–5749.

384. Zhang, M., Zhong, H., Vollmer, C. & Nurse, C. A. (2000). Co-release of ATP and ACh mediates hypoxic signalling at rat carotid body chemoreceptors. *Journal of Physiology* **525**: 143-158.

385. Zhong, H., Zhang, M. & Nurse, C. A. (1997). Synapse formation and hypoxic signalling in co-cultures of rat petrosal neurones and carotid body type I cells. *Journal of Physiology* **503**: 599-612.